AD621074

ACCELERATED RELIABILITY TEST METHODS FOR MECHANICAL AND ELECTROMECHANICAL PARTS

William Yurkowsky
R. E. Schafer

TECHNICAL REPORT NO. RADC-TR-65-46
July 1965

ACCELERATED RELIABILITY TEST METHODS FOR MECHANICAL AND ELECTROMECHANICAL PARTS

William Yurkowsky
R. E. Schafer

AFLC, GAFB, N.Y., 20 Aug 65-176

DISCLAIMER NOTICE

FOREWORD

This report is the result of a study performed by Hughes Aircraft Company, Ground System Group, Fullerton, California, from December 1963 to January 1965. The research team was headed by W. Yurkowsky. R. E. Schafer developed the approach used in the statistical portions of the report. W.G. Johnson developed and supervised the test program on snap action switches, O-rings, and timing belts. B. Conway performed the tests on these parts. T.F. Odell developed the test method and performed the testing on relays. Data analysis was by Mrs. K.S. Tracey and K.R. Brock. Failure analysis was by H.R. Marker.

The study was performed for the Research and Technology Division of Rome Air Development Center under Contract Number AF30(602)-3268, System 760E, Project 5519, Task 551902. Contractor's Secondary report number is FR 65-10-16. The RADC Project Manager was Mr. Donald W. Fulton (EMERR).

The researchers wish to acknowledge the assistance, and active cooperation of Mr. Fulton throughout the course of the study. Gratitude is expressed also for the helpful suggestions received from Mr. S.F. Newman, General Motors Technical Center, Mr. E.J. Zulinski, Ford Motor Company, and Dr. J.N. Berrettoni, Chairman, Statistics Department, Western Reserve University.

This technical report has been reviewed and is approved.

Approved: DONALD W. FULTON
Reliability Engineering Section
Reliability Branch

Approved: WILLIAM F. BETHKE
Chief, Engineering Division

FOR THE COMMANDER: IRVING J. GABELMAN
Chief, Advanced Studies Group

ABSTRACT

This study addresses itself to the problem of the development of accelerated reliability test methods for mechanical and electromechanical parts. The expected life span of these classes of parts is extremely long when they are used under manufacturers' rated conditions. Therefore accelerated test methods are required to reduce the time period required for the verification of the reliability characteristics of these part types and to reduce the expenses associated with these tests.

The specific parts selected for study were:

1. Snap Action Switches - MS 25085-1, 5 ampere, 250 volt AC, single pole, double throw, subminiature

2. Crystal Can Relays - 3 ampere, 28 volt dc contacts; double pole, double throw; 675 ohm, 26.5 volt coil

3. Mechanical Seals (O-rings) - AN 6227B-11; OD - 3/4", ID-9/16", cross sectional width 3/32"; material: Buna-N rubber

4. Timing Belts - 1/5 pitch, 12 inch pitch length, 60 teeth, .037" width.

The parts selected were chosen because they represented large generic families of high usage rate.

The search for an accelerated reliability test method for each of the four parts included in the study were conducted by selecting a combination of operating and environmental stresses and by applying them at higher than manufacturer's rated level of suggested operation. Parts were also tested at manufacturer's rated conditions to create data for comparison on parts from the same manufacturing lot.

The physical test methods used were developed during the study and were designed to control the accelerating stresses being applied. The statistical test method employed was a full factorial experiment with replications. It was selected in order to be able to evaluate main effects and interactions in searching for the most efficient accelerated test method.

The mean life of snap action switches was affected by the application of various levels of contact load, actuation rate, and contact overtravel, and by the interactions between contact load and actuation rate and contact load and contact overtravel. The failure times of these parts fit Weibull distributions. The fits were made by calculating a linear regression line by the method of least squares. Tests for goodness of fit were performed to verify the Weibull fits. The cumulative failure distributions and hazard rates were calculated for the parts operated at manufacturer's rated conditions (Test Run 1) and for the parts operated at each of 26 combinations of accelerated conditions.

An analysis of the failed switches indicated that most of the parts failed by burning of the contacts. As contact load increased there was a tendency to experience a failure mode change in the form of welding of the contacts.

Based on the above mentioned analyses performed on switches, the most favorable stresses to be applied as an accelerated test method were: contact load-10 amps; contact overtravel-.010 inches, actuation rate-150 to 300 cycles/minute.

The mean life of crystal can relays is affected by contact load, ambient temperature, and by the interactions of contact load and temperature. The failure times of these parts are in most cases distributed according to the Weibull distribution. Cumulative failure distributions and hazard rates were calculated for each set of stresses applied in combination. The predominant failure mode in the relays was erosion and material transfer between the normally open contacts and blade. At higher contact loads contact welding occurred frequently.

From the analyses performed, desirable accelerated reliability test methods for crystal can relays were specified. They call for 6 amps contact load, 150°C ambient temperature, and 10 cycles per second actuation rate or 6 amps contact load, 25°C ambient temperature and 30 cycles per second actuation rate.

The life of O-rings was affected by both temperature, ultraviolet exposure and by the interactions of these two stresses. Temperature contributed most heavily to reducing part life. The temperature range studied was 200° to 275°F. The failure times were according to the Weibull distribution. The predominant failure mode observed was radial cracking with a lesser amount of circumferential cracking. In the case of O-rings it was not possible to run a test at normal operating conditions and observe any failures during the one year study period. Therefore it can only be said that the life of O-rings decreases over the stress ranges studied but with no reference to normal stress levels.

Timing belts were studied at normal and severe levels of load and pulley diameter in combination. Not enough failures were observed to arrive at any conclusions.

The test of whether or not the accelerated reliability test methods specified for switches and relays are truly valid depends on whether the results obtained from them can be translated to parts operated at normal conditions. In order to make this translation, five mathematical models are presented as possible representations of the failure laws operating when parts are operated at different levels of combined stresses. The five models are variations of time transformations on: the cumulative failure distribution, the hazard rate, and the ratio of the hazard rates. The validation as to which of these models best represents what happens in an accelerated test must await further study.

TABLE OF CONTENTS

		PAGE
Section 1.0	INTRODUCTION	1
1.1	Statement of the Reliability Testing Problem	1
1.2	Objectives of the Study	1
1.3	Definition of Accelerated Testing	3
1.4	Criteria for Selection of an Accelerated Reliability Test Method	4
1.5	Study Approach	5
1.5.1	Selection of Study Method	5
1.5.2	Selection of Parts for Study	5
1.5.3	Environments Applied in Combination and Sequentially	6
1.6	Outline of Report	7
Section 2.0	SNAP ACTION SWITCHES	8
2.1	Summary	8
2.2	Details of Investigation	9
2.2.1	Stress Selection	9
2.2.2	Statistical Experimental Design	11
2.2.3	Definition of Failure	13
2.3	Presentation of Test Results	13
2.3.1	Analysis of Variance	13
2.3.1.1	t Tests	16
2.3.1.2	Comparison of First Miss and Total Failure Results	23
2.3.2	Failure Analysis of Snap Action Switches	23
2.3.3	Analyses Related to Switch Life Distribution Functions	24
2.3.3.1	Weibull Plots	26
2.3.3.2	Tests for Goodness of Fit	26
2.3.3.3	Cumulative Failure Distributions	33
2.3.3.4	Calculation of Hazard Rates	34
2.3.3.5	Confidence Limits for Weibull Parameters	34
2.3.4	Analysis of Switch Operating Parameters	34
2.4	Selection of Accelerated Reliability Test Method (Switches)	38
Section 3.0	CRYSTAL CAN RELAYS	41
3.1	Summary	41
3.2	Details of the Investigation	42
3.2.1	Selection of Stresses	42
3.2.2	Statistical Experimental Design	44
3.2.3	Definition of Failure	45
3.3	Presentation of Test Results	45
3.3.1	Analysis of Variance	45
3.3.1.1	t Tests	50
3.3.1.2	Comparison of First Miss and Total Failure Results	53
3.3.2	Failure Analysis of Crystal Can Relays	53
3.3.3	Analyses Related to Relay Life Distribution Functions	54
3.3.3.1	Weibull Plots	56
3.3.3.2	Tests for Goodness of Fit	56

PAGE

3.3.3.3 Cumulative Failure Distributions 59
3.3.3.4 Calculation of Hazard Rates 59
3.3.3.5 Confidence Limits for Weibull Parameters 62
3.3.4 Analysis of Relay Operating Parameters 62
3.4 Selection of Accelerated Reliability Test Method (Relays) 62
3.5 Validation of Normal Test Conditions 66

Section 4.0 MATHEMATICAL MODELS 69
4.1 Summary 70
4.2 Relationship of the Failure Distribution Under Accelerated and Normal Conditions 70
4.3 Mathematical Model #1: For a True Accelerated Test When the Failure Distribution is Known to be Weibull both at Accelerated and Normal Conditions 72
4.4 Mathematical Model #2: The General Form 74
4.5 Mathematical Model #3: A Time Transfer Function on the Cumulative Distribution Function (TFC) 76
4.6 Mathematical Model #4: A Time Transfer Function of Hazard Rates (TFH) 77
4.7 Mathematical Model #5: Constant Ratio of Hazard Rates (CRH) 78
4.8 Conclusions on Mathematical Models 80

Section 5.0 MECHANICAL SEALS (O-RINGS) 81
5.1 Summary 81
5.2 Details of Investigation 81
5.2.1 Stress Selection 81
5.2.2 Statistical Experimental Design 83
5.2.3 Definition of Failure 84
5.3 Presentation of Test Results 84
5.3.1 Analysis of Variance 84
5.3.1.1 t Tests 84
5.3.2 Failure Analysis of O-Rings 87
5.3.3 Analysis Related to Life Distribution Functions 88
5.4 Selection of Accelerated Reliability Test Method (O-Rings) 88

Section 6.0 TIMING BELTS 90
6.1 Summary 90
6.2 Details of the Investigation 90
6.2.1 Selection of Stresses 90
6.2.2 Statistical Experimental Design 91
6.2.3 Failure Analysis of Timing Belts 92
6.2.4 Definition of Failure 92
6.3 Results of Test Program 92

Section 7.0 CONCLUSIONS 94

Section 8.0 RECOMMENDATIONS 97

		PAGE
APPENDIX I	Cumulative Failure Distributions (Switches)	99
APPENDIX II	Cumulative Failure Distributions (Relays)	109
APPENDIX III	Failure Analysis of Relays.	119
APPENDIX IV	Failure Analysis of O-Rings	127
APPENDIX V	Physical Test Methods	135
APPENDIX VI	Weibull Plots of Test Runs.	147
APPENDIX VII	Confidence Limits for Weibull Parameters.	214
APPENDIX VIII	Mathematical Models	216
APPENDIX IX	Bibliography	225

LIST OF FIGURES

FIGURE		PAGE
1-1	Two Cumulative Failure Distributions with F_A Always > F_N	2
1-2	Two Cumulative Failure Distributions with F_A Not Always > F_N	2
1-3	Most Desirable Relationship Between F_A and F_N	2
4-1	Failure Distribution Function (Weibull) Under Normal Conditions	71
4-2	Failure Distribution Function (Weibull) Under (Accelerated) Change y = 1/4x	71
I-1	Cumulative Failure Distribution for Switch Test Runs 1, 2, & 3 (First Miss)	100
I-2	Cumulative Failure Distribution for Switch Test Runs 4, 5, & 6 (First Miss)	101
I-3	Cumulative Failure Distribution for Switch Test Runs 7, 8, & 9 (First Miss)	102
I-4	Cumulative Failure Distribution for Switch Test Runs 10, 11, & 12 (First Miss)	103
I-5	Cumulative Failure Distribution for Switch Test Runs 13, 14, 15 (First Miss)	104
I-6	Cumulative Failure Distribution for Switch Test Runs 16, 17, 18 (First Miss)	105
I-7	Cumulative Failure Distribution for Switch Test Runs 19, 20, 21 (First Miss)	106
I-8	Cumulative Failure Distribution for Switch Test Runs 22, 23, 24 (First Miss)	107
I-9	Cumulative Failure Distribution for Switch Test Runs 25, 26, 27 (First Miss)	108
II-1	Cumulative Failure Distribution for Relay Test Runs 1, 2, 3 (First Miss)	110
II-2	Cumulative Failure Distribution for Relay Test Runs 4, 5, 6 (First Miss)	111
II-3	Cumulative Failure Distribution for Relay Test Runs 7, 8, 9 (First Miss)	112
II-4	Cumulative Failure Distribution for Relay Test Runs 10, 11, 12 (First Miss)	113
II-5	Cumulative Failure Distribution for Relay Test Runs 13, 14, 15 (First Miss)	114
II-6	Cumulative Failure Distribution for Relay Test Runs 16, 17, 18 (First Miss)	115
II-7	Cumulative Failure Distribution for Relay Test Runs 19, 20, 21 (First Miss)	116
II-8	Cumulative Failure Distribution for Relay Test Runs 22, 23, 24 (First Miss)	117
II-9	Cumulative Failure Distribution for Relay Test Runs 25, 26, 27 (First Miss)	118

FIGURE		PAGE
V-1	Schematic for Snap Action Switch Test Method	136
V-2	O-Ring Test Method	142
V-3	O-Ring Test Fixture	143
V-4	Schematic of Timing Belt Test Method	145
VI-1	Switch Test Run No. 1	149
VI-2	Switch Test Run No. 2	150
VI-3	Switch Test Run No. 3	151
VI-4	Switch Test Run No. 4	152
VI-5	Switch Test Run No. 5	153
VI-6	Switch Test Run No. 6	154
VI-7	Switch Test Run No. 7	155
VI-8	Switch Test Run No. 8	156
VI-9	Switch Test Run No. 9	157
VI-10	Switch Test Run No. 10	158
VI-11	Switch Test Run No. 11	159
VI-12	Switch Test Run No. 12	160
VI-13	Switch Test Run No. 13	161
VI-14	Switch Test Run No. 14	162
VI-15	Switch Test Run No. 15	163
VI-16	Switch Test Run No. 16	164
VI-17	Switch Test Run No. 17	165
VI-18	Switch Test Run No. 18	166
VI-19	Switch Test Run No. 19	167
VI-20	Switch Test Run No. 20	168
VI-21	Switch Test Run No. 21	169
VI-22	Switch Test Run No. 22	170
VI-23	Switch Test Run No. 23	171
VI-24	Switch Test Run No. 24	172
VI-25	Switch Test Run No. 25	173
VI-26	Switch Test Run No. 26	174
VI-27	Switch Test Run No. 27	175
VI-28	Relay Test Run No. 1	177
VI-29	Relay Test Run No. 2	178
VI-30	Relay Test Run No. 3	179
VI-31	Relay Test Run No. 4	180
VI-32	Relay Test Run No. 5	181
VI-33	Relay Test Run No. 6	182
VI-34	Relay Test Run No. 7	183
VI-35	Relay Test Run No. 8	184
VI-36	Relay Test Run No. 9	185
VI-37	Relay Test Run No. 10	186
VI-38	Relay Test Run No. 11	187
VI-39	Relay Test Run No. 12	188
VI-40	Relay Test Run No. 13	189
VI-41	Relay Test Run No. 14	190
VI-42	Relay Test Run No. 15	191
VI-43	Relay Test Run No. 16	192
VI-44	Relay Test Run No. 17	193
VI-45	Relay Test Run No. 18	194
VI-46	Relay Test Run No. 19	195

FIGURE		PAGE
VI-47	Relay Test Run No. 20	196
VI-48	Relay Test Run No. 21	197
VI-49	Relay Test Run No. 22	198
VI-50	Relay Test Run No. 23	199
VI-51	Relay Test Run No. 24	200
VI-52	Relay Test Run No. 25	201
VI-53	Relay Test Run No. 26	202
VI-54	Relay Test Run No. 27	203
VI-55	O-Ring Test Run No 1	205
VI-56	O-Ring Test Run No. 2	206
VI-57	O-Ring Test Run No. 3	207
VI-58	O-Ring Test Run No. 4	208
VI-59	O-Ring Test Run No. 5	209
VI-60	O-Ring Test Run No. 6	210
VI-61	O-Ring Test Run No. 7	211
VI-62	O-Ring Test Run No. 8	212
VI-63	O-Ring Test Run No. 9	213

LIST OF TABLES

TABLE		PAGE
1-1	Factors for Selecting Desirable Accelerated Reliability Test Methods	5
2-1	Factorial Experiment for Snap Action Switch Tests	12
2-2	Snap Action Switches: Cycles to First Miss	14
2-3	Snap Action Switches: Cycles to Total Failure	15
2-4	Analysis of Variance on Snap Action Switches (First Miss)	17
2-5	Analysis of Variance Table for Snap Action Switches (Total Failure)	18
2-6	Interactions Between Contact Load and Overtravel (First Miss-Switches)	19
2-7	Contact Load and Overtravel Interactions (Total Failure-Switches)	20
2-8	Contact Load and Actuation Rate Interactions (Total Failure-Switches)	22
2-9	Snap Action Switches: Failure Modes	25
2-10	Weibull Parameters for Switch Test Runs (First Miss)	27
2-11	F Tests for Goodness of Fit (Switches)	29
2-12	Comparison of $\bar{x}_i$ and $\tilde{\mu}_i$ for Switches	31
2-13	Hazard Rates for Snap Action Switches Where Failure Criterion is First Miss	35
2-14	Confidence Limits for β (Switches)	36
2-15	Confidence Limits for α_o (Switches)	37
2-16	Factors for Selecting Desirable Accelerated Reliability Test Methods (Snap Action Switches)	40
3-1	Factorial Experiment on Crystal Can Relays	44
3-2	Relays: Cycles to First Miss	46
3-3	Relays: Cycles to Total Failure	47
3-4	Analysis of Variance - Relays (First Miss)	48
3-5	Analysis of Variance - Relays (Total Failure)	49
3-6	Contact Load and Temperature Interactions - Relays (First Miss)	50
3-7	Contact Load and Temperature Interactions	52
3-8	Relays: Failure Modes	55
3-9	Weibull Parameters for Relays (First Miss)	57
3-10	F Test for Goodness of Weibull Fits (Relays)	58
3-11	Comparison of $\tilde{\mu}_i$ and $\bar{x}_i$ of Relay Test Runs	60
3-12	Hazard Rates for Relays Where First Miss Denotes Failure	61
3-13	Confidence Limits for β (Relays)	63
3-14	Confidence Limits for α_o (Relays)	64
3-15	Factors for Selecting Desirable Accelerated Reliability Test Method (Relays)	65
3-16	Comparison of Test Results With Field Data	68

TABLE		PAGE

4-1	Algorithms	79
4-2	Observed Weibull Parameters	79
5-1	Factorial Experiment for O-Rings.	83
5-2	O-Rings: Hours to Failure	85
5-3	Analysis of Variance - O-Rings	86
5-4	Temperature and Ultraviolet Interactions on O-Rings .	86
5-5	Summary of Weibull Parameters from O-Ring Tests .	88
6-1	Factorial Experiment for Timing Belts	92
6-2	Timing Belt Test Results.	93

Evaluation

The over-all objective of the program, of which this effort was a part, is to develop optimum techniques for the demonstration of the reliability of nonelectronic parts and components. This effort had as objectives the development of accelerated test methods which would reduce the time and cost associated with the testing of four specific components and the development of mathematical models to relate the reliability under accelerated stress conditions to the reliability under normal stress conditions. The components investigated were a subminiature snap-action switch, crystal can relay, "O" ring mechanical seal and a rubber timing belt. Emphasis was placed on the first two components.

A full 3x3x3 factorial experiment was performed on both switches and relays so that both the main effects and the interactions could be measured. Analysis of the results showed that the data for both components fits the Weibull distribution. A failure acceleration factor on the mean life of the switches of 75 and on the mean life of the relays of 25 was realized. Since the lives follow the Weibull cumulative distribution, the time transfer function cannot take the form of $y = cx$. Not only is there a compression of time, but the parameters of the Weibull distributions (normal vs accelerated) are not equal. The transfer functions developed take the preceding into consideration. The failure times of the O-rings under accelerated conditions were according to the Weibull distribution. No failures were developed under normal conditions and thus it can only be said that the lives decrease as the stresses increase. The experiment on the timing belts was intended only as a probing test. Few failures occurred and there appeared to be little decrease in life with increases in the stresses studied.

The results of this contract serve to orient the second phase of program which will determine the validity of these results as they pertain to functionally similar switches and relays manufactured and supplied by other companies.

Donald W. Fulton

DONALD W. FULTON
RADC Project Engineer

SECTION 1.0 INTRODUCTION

1.1 STATEMENT OF THE RELIABILITY TESTING PROBLEM.

In general, statistical theory shows quite clearly that the precision of the estimates of the parameters of life distributions depends on the degrees of freedom available to estimate them. Degrees of freedom, for all intents and purposes translates into sample size. It is here that problems peculiar to life testing occur:

1. Sample size for life testing is not the number of items tested necessarily but is the observed number of failures.

2. The observed number of failures usually depends on the reliability of the device in question.

Since the reliability of mechanical and electromechanical parts is often very high it requires a good deal of time/parts to obtain worthwhile reliability estimates. There are a number of approaches to overcome this objection. One of them consists of reducing the confidence level. This amounts to decreasing the precision required and is really begging the question. Sequential testing may afford an optimal approach in many cases but large test times/parts still result. Another approach which appears satisfactory but is in the too distant future is the use of prior information in the test. This is often referred to as Bayes sampling. If done carefully, one of the most useful approaches is that of accelerated testing. For particular parts this method is studied in some detail in this report.

Briefly, accelerated testing consists of actually changing the parameters of the failure distribution so the failures occur earlier and the required sample sizes become available much earlier and hence testing costs are lower. In using accelerated testing one must be careful that the mathematical model used to relate the normal and accelerated environments is indeed representative of the physical laws operating. This report presents some intuitively appealing mathematical models which will be validated during future study.

1.2 OBJECTIVES OF THE STUDY

The objectives of this study are:

1. To determine the effects on the lifetimes of relays, snap action switches, mechanical seals (O-rings) and timing belts of various combinations of operating and environmental stresses.

2. To determine the relative contributions of these factors and their interactions to part lifetime variability.

3. To determine the failure modes and mechanisms operating at each selected combination of operating and environmental stresses.

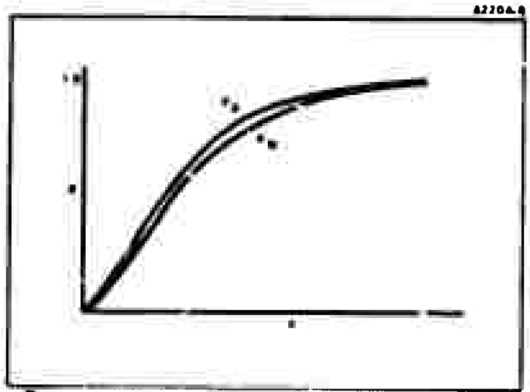

Figure 1-1. Two Cumulative Failure Distributions with F_A Always $> F_N$

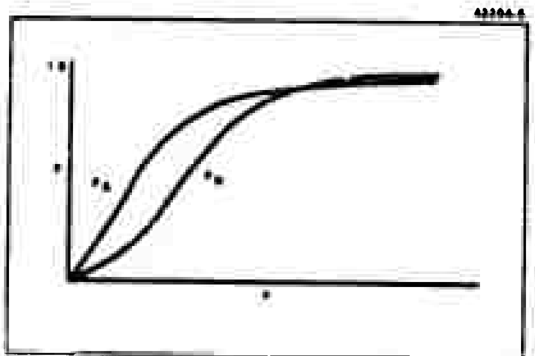

Figure 1-2. Two Cumulative Failure Distributions with F_A Not Always $> F_N$

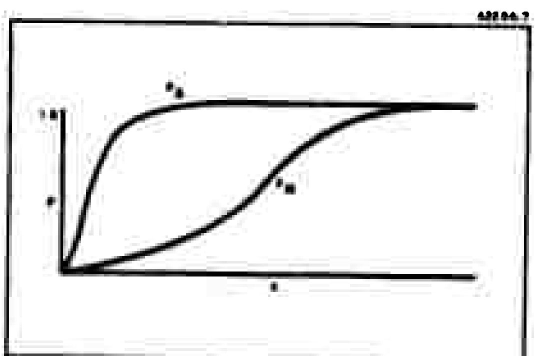

Figure 1-3. Most Desirable Relationship Between F_A and F_N

4. To develop an accelerated test method for each part under study which reduces test time and test expense and which, except for an acceleration factor, represents life under normal conditions.

5. To present methods that will allow normal lifetimes to be estimated from accelerated lifetimes.

1.3 DEFINITION OF ACCELERATED TESTING.

The definition of accelerated tests used in this report differs in several important respects from the common definition. The prevailing definition of accelerated tests can be grouped roughly into two classes.

1. A test is accelerated if the operating and/or environmental parameters exceed normal use conditions.

2. A test is accelerated if the cumulative distribution function (cdf) under normal conditions, $F_N(x)$, and the cdf under accelerated conditions, $F_A(x)$, are such that:

   a) $F_A(x) \geq F_N(x)$ for all x

   b) $F_A(x) > F_N(x)$ for at least one x.

Obviously definition 1 above may be necessary, but not sufficient, i.e., rapid failures always occur in both extreme operating and environmental stresses. Accelerated conditions do not necessarily mean rapid failures. Definition 2 is too restrictive in one sense and too loose in another. It is too restrictive because it may be unrealistic to require $F_A(x) \geq F_N(x)$ for all x. In fact it may be sufficient to require $F_A(x) \geq F_N(x)$ for $x < x^*$, x^* large.

It is too loose because if $F_A(x) = F_N(x)$ for all x and $F_A(x) > F_N(x)$ for a set of x on which it is large, then definition 2 is satisfied but the acceleration is certainly not rapid. These ideas are shown in Figure 1-1. Figure 1-2 shows a situation where definition 2 is not satisfied but yet it may well be satisfactory as an accelerated test if x^* is large enough. Of course, Figure 1-3 represents the most desirable relationship between F_A and F_N.

Also the present definitions fail to account for the importance of the hazard rate and mean life. It is after all, mean life that reflects the expected length of test and hazard rate reflects the "kill rate" as a function. For this report then an accelerated test will be defined as: A test conducted at some combination of operating and/or environmental loads which:

1. Preserves the modes of failure experienced at normal conditions.

2. Results in significantly lower (than normal) mean lives so that expected test times are lower.

3. Has the property that $F_A(x) > F_N(x)$ for all $x < x^*$, x^* large.

4. Has the property that the hazard rate $h_N(x)$ and $h_A(x)$ are such that $h_A(x) > h_N(x)$ for all $x < x^*$, x^* large.

Once such a definition has been selected, it is then possible to accomplish the following tasks:

1. Select an accelerated test.

2. Develop mathematical models to reflect the physical laws operating between accelerated and normal conditions so that normal testing can be eliminated.

3. Validate Models.

The remainder of this report is concerned primarily with 1 and 2 above. Step 3 will be studied in future efforts.

1.4 CRITERIA FOR SELECTION OF AN ACCELERATED RELIABILITY TEST METHOD

The factors to be considered in the specification of an accelerated reliability test method are that it must:

- result in a shorter mean life than that of parts operated at normal stress levels.

- require the use of accelerating stresses that are easily applied, controlled, and measured. They should be stresses that have been proven in their ability to reduce the life of the part of interest.

- not result in a failure mode different from that observed in parts operated at normal conditions.

- impart to the devices tested, a cumulative failure distribution that results in failure more quickly over a given range of test time than other potential accelerated test methods.

- produce a hazard rate in the parts tested that is higher at all points over a given range of interest than that of parts operated at normal conditions.

- be adaptable to the simultaneous application of more than one accelerating stress.

- be described by the same general failure distribution function as parts tested at normal conditions. The requirement is not that the parameters be the same but that its life characteristics must be expressable in the same mathematical terms as those of parts operated at normal stress levels.

- result in the shortest possible test in terms of calendar time.

- result in an economical test method with regard to test equipment required, monitoring procedures needed, and the data collection and analysis system.

- produce test results from the accelerated test that are translatable back to how the parts would have performed had they been operated at normal stress levels.

The matrix shown in Table 1-1 is a checklist to be applied to accelerated reliability test methods that are developed in this study in order to select those that appear to have the most merit.

TABLE 1-1. FACTORS FOR SELECTING DESIRABLE ACCELERATED RELIABILITY TEST METHODS

Factor	Test Run	1	2	3	4	5	6	7 -------- 27
Short Mean Life								
Controllable Accelerating Stresses								
Constant Failure Mode								
Cumulative Failure Distribution								
Hazard Rate								
Same Failure Distribution								
Short Calendar Time								
Economical								

There is no attempt to weight the factors for purposes of tradeoff studies, but it is expected that a specified accelerated reliability test method in order to be considered, should possess positive attributes in each of the above factors.

1.5 STUDY APPROACH

1.5.1 SELECTION OF STUDY METHOD

In deciding the methodology to follow in searching for accelerated reliability test methods it was apparent that there was a need for the generation of data on the life of parts when operated at several different operating and/or environmental stress levels. In addition to requiring knowledge of reliability characteristics at different levels, information was needed regarding the interactions taking place when two or more accelerating stresses were operating on a given part, in order to take advantage of any synergistic effects which might result in reduced test times. This requirement dictated the use of a factorial experimental design which allows the evaluation of each main effect and all interactions.

Another requirement of the study was to make observations that would lead to an estimation of the life distribution functions. Hence a number of replications in each test cell of the matrix was specified.

1.5.2 SELECTION OF PARTS FOR STUDY

One of the stated objectives of the study is to develop accelerated reliability test methods for mechanical and electromechanical parts. There are thousands of parts and hundreds of thousands of applications to which the study could therefore apply. In order to direct the study into specific channels, two electromechanical and two mechanical parts were selected. The parts selected were ones that are widely used and are representative of large generic parts groups to which the study results might possibly apply.

The specific parts selected for inclusion in the study program were as follows:

1. Snap Action Switches MS25085-1

   Contact rating is 5 amps and up to 250 volts AC; single pole double throw, subminiature type. Actuation is by means of a roller leaf spring.

2. Crystal Can Relays

   The relays are double pole, double throw, with a contact rating of 3 amps, 28 volts DC. The temperature range is -65°C to +125°C. The coil is rated at 675 ohms, 26.5 volts.

3. O-Rings AN6227-B-11

   The parts are of Buna N type rubber, with an OD of 3/4" and an ID of 9/16". The cross-sectional width is 3/32".

4. Timing Belts

   These parts are 1/5 pitch, 12 inch pitch length, 60 teeth, .037 inch width. The teeth are of neoprene with nylon facing. The tension member is steel cable with neoprene backing.

1.5.3 ENVIRONMENTS APPLIED IN COMBINATION AND SEQUENTIALLY.

The factorial experimental design used in this study provides for environments applied in combination. In order that the selection of a factorial design will not appear arbitrary and because of the "apparent" popularity of sequentially applied environments some remarks comparing the two methods of testing will be made.

It would appear that the submission of units to a sequentially applied environment say first shock, then vibration, then temperature, etc., is hard to justify on any except economic grounds. Certainly environments are not so "nice" that they occur sequentially during actual use. In fact it is to be expected that environments occur in combination under normal use conditions. Moreover the synergistic (interaction) effects which may be caused by environments acting together are immeasurable by sequentially applied tests. A great number of these effects were observed in this study. As part qualification tests then, the sequential tests fail to measure up UNLESS IT HAS BEEN PREVIOUSLY DEMONSTRATED THAT THE PARTICULAR TEST CYCLE USED WELL REPRESENTS HOW THE DEVICES BEHAVE UNDER USE CONDITIONS. Actually this is, theoretically, not an insurmountable objection. However, the sequentially applied environments test as an accelerated test suffers from more serious objections. First it may be inefficient from the standpoint of requiring too much time because the environments are applied sequentially and because any additional "killing" effects due to interactions are lost. Secondly, and very importantly, it is often very difficult to interpret physically (i.e., in terms of physical laws) what is happening to a device when subjected to sequential environments. Since normal use conditions cannot be described in terms of a sequentially applied environment it is difficult to relate normal and accelerated conditions.

1.6 OUTLINE OF REPORT

The remainder of this report is a presentation of the data generated during this study together with the conclusions and results based on the analysis of the data. The results pertaining to snap action switches are presented in Section 2, to crystal can relays in Section 3, to O-rings in Section 5 and timing belts in Section 6. Each section begins with a summary of the findings. This is followed by a table of times to failure for each part. An analysis of variance was then performed to identify the stresses and interactions of stresses which had a significant effect on the mean lives of parts tested under each of 27 combinations of different stress levels.

The times to failure of all groups of parts tested were analyzed to estimate their underlying life distribution functions. The life distributions were plotted on Weibull probability paper and goodness of fit tests were performed. Cumulative failure distributions and hazard rates were calculated for the parts tested at normal stress levels and for each of the other groups of parts tested at combinations of accelerated stresses. Included in each section is an analysis of the failure modes and mechanisms acting on parts operated at normal stress levels as compared to those found on parts operated at the various combinations of severe stresses. The final paragraph of each of the sections relating to the specific parts studied is a selection of the set of combined stress levels from among those studied which yields the most promise for use as an accelerated reliability test method.

Section 4 is devoted to a presentation of the mathematical models studied as possible representations of the physical effects caused by the application of combined accelerated stresses. This relationship between the mean life of a part operated at normal stresses and one operated at accelerated conditions must be established before an accelerated test method has meaningful value.

Section 6 contains Conclusions and Section 7 is titled Recommendations. The appendix contains a description of the test methods used, details of the failure analyses, and graphs relating to the life distributions of the parts included in the study program.

SECTION 2.0 SNAP ACTION SWITCHES

2.1 SUMMARY

There were 270 snap action switches subjected to life tests. Ten parts were tested at normal operating and environmental conditions (Test Run 1:5 amps contact load, 70 cycles/minute actuation rate, and 005 inches contact overtravel). Ten parts were also tested at each of 26 other combinations of stresses which were evaluated for utility as accelerated reliability test methods. The number of cycles to failure was recorded for each part at both first miss and at total failure.

An analysis of variance was performed on each set of data in order to determine those stresses and combinations of stresses that contributed significantly in reducing switch life.

The following stresses were found to affect switch life at their respective failure definitions:

	1st Miss	Total Failure
Contact Load	X	X
Actuation Rate	X	X
Contact Overtravel	X	X
Interactions (Contact Load & Overtravel)	X	X
Interactions (Contact Load & Actuation Rate)		X

The next step in the analysis was to estimate the magnitude of the contribution to variance of each of the significant effects. By far the greatest effect on switch life was exerted by contact load. With failure defined as first miss, contact load produced 74.6% of the total variance. Using the total failure definition it accounted for 67.4% of total variation. The other significant main effects and interactions were each responsible for from 1.1 to 7.0% of the total variation. Residual or unexplained variance was 13.3% for first miss and 17.1% for total failure.

Student's t test was used to group the test runs that could have come from populations with the same mean. The reason for this was to compare the mean life of the parts tested at normal conditions (Test Run 1) with those operated at accelerated stress levels. In general, all Test Runs which utilized a contact load of 5 amps, exhibited no differences in mean life from Test Run 1. Hence this level of contact load was not feasible for use as an accelerated test. The parts operated at 15 amps displayed a change in failure mode in the form of welding of the contacts. Also the test runs at 10 amps and .005 inches overtravel exhibited failure modes that changed to welded contacts from the burned and eroded contacts of Test Run 1. Hence none of these meet the criteria for accelerated test methods set down in Section 1.

The failure times of the switches tested at normal stress levels (Test Run 1) and those tested at combined accelerated stress levels were plotted on Weibull probability paper to ascertain if this was the life distribution function which best described the reliability characteristics of these parts. Several goodness of fit tests were used to verify that switches operated in this manner failed according to the Weibull distribution.

The Weibull shape parameter (β) and scale parameter (α) for each test run were calculated as well as the cumulative failure distributions and hazard rates for each set of stress levels included in the test. The Weibull location parameter (γ) was assumed to be zero.

In summary it is noted that the results obtained regarding significant stresses and interactions which affect the mean number of cycles to failure of snap action switches where failure is defined as first miss are quite similar to those found when the tests were continued until total failure of the parts. This fact is in itself a form of desirable accelerated test since test time can be reduced with high assurance of obtaining similar results.

A further measure of the agreement between the results of the analysis of life test data with the two different failure definitions was obtained by calculating the correlation coefficient. The .972 obtained shows that there is a high degree of agreement between the two sets of test results.

After evaluating all the data generated there were two test runs which exhibited desirable characteristics for use as an accelerated reliability test method. These were:

Test Run #14 (10 amps contact load, .010 inches contact overtravel, and 150 cycles/minute)

Test Run #15 (10 amps contact load, .010 inches contact overtravel and 300 cycles/minute)

2.2 DETAILS OF THE INVESTIGATION

2.2.1 STRESS SELECTION

The manufacturer's data and discussions with the manufacturer's representative indicated the following "normal" operating conditions for the single pole, double throw snap action, switch (MS 25085-1) selected for study:

Contact Load	5 amps
Temperature range	100°F to +180°F
Mechanical life	50,000 operations minimum
Operating force (at plunger)	3 to 5 oz. (85 to 142 grams)
Release force	1 oz min. (28.4 grams)

Overtravel --------------------	.005 inches minimum
Actuation rate------------------	up to 300 cycles/minute
Vibration --------------------	5-2000 cps, .03 double amplitude with no contact bounce
Shock ------------------------	50g, 11 sec. with no contact bounce

Not designed for application in humid, corrosive, or dust atmosphere.

The following test conditions were considered for inclusion as stress variables to be applied to the switches:

Actuation rate

Vibration

Temperature

Atmosphere (Oxygen rich, corrosive, other)

Overtravel

Contact load

Contamination

Criteria for selecting the stresses to be applied included:

1. probable effect of stress on life and/or test time
2. probable effect on failure mode
3. uniformity of application at various stress levels
4. test setup complexity
5. ease of control of stresses
6. accuracy of measurement of stresses

This resulted in the selection of:

Actuation rate

Overtravel

Contact load

as the variable stresses to be applied to the tests.

Experimental tests at actuation rates above 325 cpm resulted in a random early miss pattern resulting from actuator miss rather than switch malfunction. Therefore an upper limit of 300 cpm was established. The lower or "normal" limit was based primarily on the project calendar time available divided by the forcecast of switch life, times the number of switches. This resulted in a lower limit of 70 cpm. An intermediate value of 150 cpm was selected as one half the maximum and double the minimum actuation rate. The initial lot of switches was checked for maximum overtravel and was found to range from .014 to .025 inches. Based on these studies .015 and .010 inches overtravel were selected for comparison with a defined "normal" overtravel of .005 inches.

Exploratory tests were performed on switches under the following combinations of stresses:

No load, .007 inches overtravel, 160 cycles/minute
No load, .010 inches overtravel, 160 cycles/minute
5 amp load, .004 inches overtravel, 160 cycles/minute
28 amp load, .005 inches overtravel, 70 cycles/minute

At the no load conditions, not enough failures would have been observed during the study period. At 28 volts, failure occurred in from 10 to 144 cycles. This was extremely severe and failure mode changes were obviously occurring.

The rated load of 5 amps was chosen as the lowest value since it does represent "normal conditions." Screening tests at 10 and 15 amps yielded neither extremely short life nor strong indications of failure mode changes.

A summary of the overall stress selection is:

Applied Stress	Normal	Intermediate	Maximum
Actuation Rate	70 cpm	150 cpm	300 cpm
Overtravel	.005"	.010"	.015"
Current	5 amps	10 amps	15 amps

A complete description of the test method and test equipment used is detailed in Appendix V-1.

2.2.2 STATISTICAL EXPERIMENTAL DESIGN

The study to develop accelerated reliability test methods for snap action switches continued with the formulation of a 3^3 full factorial experiment with ten replications in each of the 27 test cells comprising the combined environments. Table 2-1 shows the operating and environmental stresses and stress levels used to study the life characteristics of these parts.

TABLE 2-1. FACTORIAL EXPERIMENT FOR SNAP ACTION SWITCH TESTS

Contact Load		5 amps			10 amps			15 amps		
Contact Overtravel		.005"	.010"	.015"	.005"	.010"	.015"	.005"	.010"	.015"
Actuation Rate (cycles per minute)	70	(1)	(4)	(7)	(10)	(13)	(16)	(19)	(22)	(25)
	150	(2)	(5)	(8)	(11)	(14)	(17)	(20)	(23)	(26)
	300	(3)	(6)	(9)	(12)	(15)	(18)	(21)	(24)	(27)

NOTE: The numbers in parentheses are designations used throughout the study to identify each of the 27 test runs. For example Test Run #14 consists of 10 switches which were tested at 10 amps contact load, .010" contact overtravel, and 150 cycles per minute. Each test run contained 10 switches.

For convenience in the discussion of results throughout this report, each cell representing 10 switches tested at a combination of environmental and/or operating stresses has been numbered as shown in the Table.

Test Run Number 1 was selected as a condition that represented manufacturer's rated operating conditions. The other test runs comprise different combinations of the stress levels being studied and they were selected for the purpose of measuring both the effects on switch life of each main effect and of all their interactions.

2.2.3 DEFINITION OF FAILURE

One of the objectives of the study was to determine whether the same information could be obtained by: (1) testing until the first signs of intermittent operation occurred and (2) by testing until the part was completely inoperable. This resulted in two separate definitions of what constituted failure. A record was maintained of the number of cycles at first miss for each switch. After first miss, the tests were continued until total failure. Total failure was defined as 100 consecutive misses. Two separate analyses of the data gathered during the tests are analyzed in the next section to determine if these two failure definitions result in similar conclusions.

2.3 PRESENTATION OF TEST RESULTS

The factorial experiment on switches consisted of 27 Test Runs each containing 10 parts. Test Run 1 (5 amps contact load, .005 inches contact overtravel, and 70 cycles/minute actuation rate) was defined as normal operation. The other 26 test runs consisted of combined stresses of 5, 10, and 15 amps contact load, .005, .010 and .015 inches overtravel, and 70, 150, and 300 cycles per minute actuation rate. The combined stresses were utilized to evaluate the effects on mean cycles to first miss of the main effect of the three stresses employed (i.e., contact load, overtravel, and actuation rate) and to investigate the significance of their interactions. The results of these tests are shown in Table 2-2. The mean life of each test run is designated as $\overline{x}$ and is located below the individual readings for each of the 10 switches in a test run. The test run numbers are in the upper right hand corner of each cell in the matrix.

The 270 switches tested and reported on for first miss data in the previous paragraph were continued on life test until total failure. This was defined as 100 consecutive misses. The cycles to total failure of each switch are presented in Table 2-3. The mean value ($\overline{x}$) of the 10 switches in each test run is included with the data.

2.3.1 ANALYSIS OF VARIANCE

The statistical method used for discovering the stresses or combinations of stresses which affect switch life was an analysis of variance. It is based on the assumption that there is equal variance in each cell of the factorial experiment and that the values in each cell are distributed approximately

TABLE 2-2. SNAP ACTION SWITCHES: CYCLES TO FIRST MISS

Contact Load	5 Amps			10 Amps			15 Amps		
Actuation Rate / Contact Overtravel	.005"	.010"	.015"	.005"	.010"	.015"	.005"	.010"	.015"
70 C. P. M.	207,800 #1	146,932 #4	12,715 #7	3,493 #10	2,431 #13	49,824 #16	873 #19	6,055 #22	600 #25
	172,490	154,168	41,031	43,585	4,054	57,206	3565	4,981	713
	191,373	180,272	99,701	2,005	69,398	62,953	1640	8,272	17,408
	176,025	154,498	274,442	20,454	19,168	73,623	1566	2,047	657
	206,998	256,057	185,660	4,490	11,502	91,810	1850	4,481	10,802
	249,102	215,594	152,245	2,253	7,363	78,042	4028	3,351	8,681
	106,425	161,711	206,074	1,995	24,888	57,546	3097	3,384	11,853
	165,052	186,794	153,191	4,437	7,255	65,348	4681	12,622	5,758
	282,409	128,807	172,059	3,239	10,964	62,662	4400	3,444	5,038
	219,474	158,994	218,655	6,918	21,132	54,567	2187	1,841	11,821
	$\tilde{x}$ = 197,715	$\tilde{x}$ = 174,383	$\tilde{x}$ = 151,577	$\tilde{x}$ = 9287	$\tilde{x}$ = 17,816	$\tilde{x}$ = 65,358	$\tilde{x}$ = 2791	$\tilde{x}$ = 5048	$\tilde{x}$ = 7333
150 C. P. M.	85,618 #2	120,825 #5	116,337 #8	3,183 #11	41,667 #14	33,147 #17	1687 #20	2,459 #23	5,258 #26
	92,120	82,916	77,873	3,623	20,684	41,714	5999	4,012	7,385
	89,933	187,270	49,612	7,425	12,504	61,533	4253	4,033	6,387
	176,440	146,935	34,616	2,937	7,190	68,240	7395	2,475	7,708
	107,142	244,239	156,613	1,874	6,212	29,041	2926	4,393	5,338
	197,655	159,918	142,214	4,366	12,798	38,241	1479	3,019	4,750
	89,513	202,172	81,063	3,605	5,530	40,173	4477	3,209	864
	97,754	148,310	53,394	7,737	4,798	52,683	6589	10,413	11,898
	133,430	26,690	213,118	3,919	17,691	8,645	7182	9,248	13,858
	199,312	103,592	155,471	2,045	8,934	68,561	6655	5,132	5,515
	$\tilde{x}$ = 126,892	$\tilde{x}$ = 142,287	$\tilde{x}$ = 108,031	$\tilde{x}$ = 4071	$\tilde{x}$ = 13,801	$\tilde{x}$ = 44,198	$\tilde{x}$ = 4864	$\tilde{x}$ = 4839	$\tilde{x}$ = 6896
300 C. P. M.	127,682 #3	122,215 #6	51,157 #9	4,706 #12	2,383 #15	8,906 #18	762 #21	2,529 #24	17,297 #27
	117,992	43,684	250,725	2,351	8,389	1,699	647	4,752	1,088
	54,932	59,548	83,391	6,069	10,574	1,870	1716	7,802	15,983
	68,062	29,670	140,070	3,661	10,401	23,802	365	7,648	997
	77,259	201,616	68,729	2,518	4,005	12,128	2498	1,241	9,523
	135,778	159,179	234,023	7,215	22,009	36,362	6050	467	2,508
	137,734	116,431	219,421	3,200	3,225	49,738	6981	587	2,235
	110,366	158,265	207,210	3,557	32,389	49,674	771	6,682	4,410
	30,164	186,129	161,420	3,114	2,541	66,796	2646	2,048	4,632
	99,247	241,635	203,674	3,526	41,337	57,607	3041	395	3,457
	$\tilde{x}$ = 95,922	$\tilde{x}$ = 131,837	$\tilde{x}$ = 161,982	$\tilde{x}$ = 3992	$\tilde{x}$ = 13,725	$\tilde{x}$ = 30,858	$\tilde{x}$ = 2548	$\tilde{x}$ = 3415	$\tilde{x}$ = 6213

TABLE 2-3. SNAP ACTION SWITCHES CYCLES TO TOTAL FAILURE

Contact Load	5 Amps			10 Amps			15 Amps		
Over Travel / Actuation Rate	.005"	.010"	.015"	.005"	.010"	.015"	.005"	.010"	.015"
70 C. P. M.	207,800 #1 172,490 258,594 176,100 229,827 249,102 228,855 165,052 282,409 219,474 x̄ = 218,970	231,620 #4 154,191 180,272 184,525 256,057 215,594 186,794 229,808 226,189 289,420 x̄ = 215,447	182,170 #7 261,280 246,980 294,070 208,480 261,755 206,074 163,440 195,923 218,655 x̄ = 223,883	22,644 #10 43,585 5,922 88,805 63,054 92,319 2,264 22,501 17,566 49,696 x̄ = 40,836	54,677 #13 57,971 81,799 62,711 70,758 56,274 82,159 24,863 75,414 98,732 x̄ = 66,536	49,824 #16 69,426 86,549 73,623 91,810 78,042 57,546 65,348 62,662 54,567 x̄ = 68,939	5,263 #19 5,951 2,347 3,503 2,831 4,684 4,881 4,681 9,073 13,765 x̄ = 5,698	35,864 #22 41,193 24,214 30,155 49,998 3,351 33,599 19,055 17,680 31,484 x̄ = 28,659	600 #25 1,176 17,408 17,642 10,802 10,266 28,502 30,658 29,689 20,060 x̄ = 16,680
155 C. P. M.	186,655 #2 172,227 183,825 182,147 107,576 220,337 159,891 189,512 201,914 199,987 x̄ = 188,407	120,825 #5 148,573 187,270 160,808 244,285 159,958 247,035 148,310 55,670 246,337 x̄ = 171,907	116,337 #8 181,038 172,174 147,007 156,613 142,214 81,063 210,973 213,118 1[illegible]7,267 x̄ = 158,780	13,201 #11 88,684 24,210 65,658 1,902 87,330 7,127 46,789 104,291 61,121 x̄ = 50,051	51,303 #14 95,855 58,178 57,230 64,306 53,386 87,765 96,580 17,691 65,116 x̄ = 64,741	77,451 #17 41,714 61,538 68,240 103,247 75,633 41,927 52,583 64,522 68,561 x̄ = 65,552	17,291 #20 15,546 11,222 22,422 2,987 1,553 11,658 26,589 34,289 12,144 x̄ = 15,570	31,941 #23 42,070 44,563 31,406 16,384 44,406 31,630 22,296 28,186 6,811 x̄ = 29,969	21,311 #26 25,489 47,263 41,034 42,901 51,897 17,118 29,942 20,683 39,720 x̄ = 33,736
300 C. P. M.	127,682 #3 117,992 126,892 227,819 97,288 135,778 148,101 110,366 94,204 99,247 x̄ = 128,537	122,315 #6 83,651 154,087 55,930 202,177 163,204 131,306 219,084 186,129 241,635 x̄ = 155,952	200,609 #9 250,725 83,391 190,361 199,152 234,047 214,421 207,210 220,974 203,674 x̄ = 200,456	7,431 #12 10,062 6,301 81,569 87,260 48,805 3,200 88,051 16,551 19,060 x̄ = 36,829	52,387 #15 81,001 73,209 98,600 40,442 61,354 62,471 66,817 73,093 41,338 x̄ = 65,071	72,965 #18 43,636 39,773 69,785 51,483 62,023 61,000 49,674 66,796 72,605 x̄ = 58,974	810 #21 817 1,716 365 2,898 14,049 11,251 6,570 2,646 3,041 x̄ = 4,416	14,758 #24 4,853 8,077 7,752 1,241 647 587 6,746 12,365 395 x̄ = 5,742	19,740 #27 1,760 15,983 2,162 9,713 19,981 5,224 13,424 17,037 10,864 x̄ = 11,589

normally. An inspection of the test data on cycles to first miss of switches indicated that this was not the case. However a method of dealing with this problem is suggested by Davies (Reference 14). It involves the use of a logarithmic transformation when the variance is proportional to the magnitude of the mean. The transformation was used prior to the performance of the analysis of variance.

The results of the analysis of variance on first miss are shown in Table 2-4. The same information based on total failure is in Table 2-5.

The asterisked numbers in the "F Ratio" column of these tables denote the sources of variance that significantly affect the lives of the switches included in this series of tests. The contact load, actuation rate, and contact overtravel main effects and the interactions between contact loads and overtravels are significant at the $F_{.05}$ level where the failure definition is first miss. Where it is total failure, the same effects are significant plus the interactions between contact load and actuation rate. The indication of significance of the interactions is a signal that a synergistic effect is taking place. In other words some phenomenon takes place when the two stresses are applied in combination that could not have been detected if the stresses had been applied individually or sequentially.

Knowledge of the significant effects and interactions affecting the mean number of cycles to first miss is important. However it is equally important to measure the magnitude of the contribution of each significant factor or interaction to the total variance observed. This was accomplished by calculating the Components of Variance. The results of these calculations are shown for the first miss as the % Contribution to Total Variance column in Table 2-4. It indicates that contact load is responsible for 74.6% of the observed variance. The interaction between Contact Load and Overtravel contributed 7.0%, Overtravel 4.0%, and Actuation Rate 1.1%. The residual amounted 13.3%.

The Components of Variance analysis for total failure is shown as the right hand column in the Analysis of Variance Table 2-5. The results obtained here are in basic agreement with the first miss data in that contact load is by far the largest contributor to variance (67.4%). The contact load and actuation rate interaction is 6.0%, while the contact load and overtravel interaction represents 2.2% of the variation. The residual term is 17.1%.

2.3.1.1 t TEST

The analysis of variance highlighted the main effects and the interactions that affect the life of switches. The components of variance indicated which of the significant effects and interactions exerted the greatest effect. The t test was used to indicate whether the stress caused the mean life to increase or to decrease.

TABLE 2-4. ANALYSIS OF VARIANCE ON SNAP ACTION SWITCHES (FIRST MISS)

Source of Variance	Sum of Squares	Degrees of Freedom	Mean Squares	F Ratio	$F_{.05}$	% Contribution To Total Variance
Between Contact Loads	114.14395	2	57.072	507.08*	3.03	74.6
Between Actuation Rates	1.87564	2	.938	8.33*	3.03	1.1
Interactions Between Contact Loads and Actuation Rates	.88489	4	.221	1.97	2.41	0
Between Contact Overtravels	6.35768	2	3.179	28.24*	3.03	4.0
Interactions Between Contact Loads and Overtravels	7.60480	4	1.901	16.89*	2.41	7.0
Interactions Between Actuation Rates and Overtravels	.06332	4	.016	.14	2.41	0
Interactions Between Contact Load, Actuation Rates, Overtravel	1.53079	8	.191	1.70	1.97	0
Residual	27.34974	243	.113			13.3
Total	159.81081	269				100.0

TABLE 2-5. ANALYSIS OF VARIANCE TABLE FOR SNAP ACTION SWITCHES (TOTAL FAILURE)

Source of Variance	Sum of Squares	Degrees of Freedom	Mean Squares	F Ratio	$F_{.05}$	% Contribution To Total Variance
Between Contact Loads	71.02939	2	35.51470	354.97*	3.03	67.4
Between Actuation Rates	3.68144	2	1.84072	18.40*	3.03	3.3
Interaction Between Contact Load and Actuation Rates	4.58418	4	1.14605	11.45*	2.41	6.0
Between Contact Overtravels	4.45402	2	2.22701	22.26*	3.03	4.1
Interactions Between Contact Loads and Overtravels	1.95891	4	.48973	4.89*	2.41	2.2
Interactions Between Actuation Rates and Overtravels	0.75826	4	.18957	1.89	2.41	0
Interaction Between Contact Loads, Actuation Rates, Overtravel	1.39789	8	.17474	1.75	1.98	0
Residual	24.31121	243	.10005			17.1
Total	112.17530	269				100.0

*Denotes significance at the $F_{.05}$ level.

Since the interaction of contact loads and overtravel was significant on the first miss data, it is valid to combine data across actuation rates in order to obtain a better estimate of the effects of the interaction. Table 2-6 is a matrix of the logarithmic mean values of contact load and overtravel. Each value in the matrix is the mean of the cycles to first miss of 30 switches.

TABLE 2-6. INTERACTIONS BETWEEN CONTACT LOAD AND OVER-TRAVEL (FIRST MISS-SWITCHES)

Contact Overtravel (Inches)	Contact Load		
	5 amps	10 amps	15 amps
.005	5.10	3.62	3.42
.010	5.12	4.01	3.53
.015	5.06	4.55	3.65

The t test is used to evaluate the differences between means. Using the residual error of .11255 from the analysis of variance and 243 degrees of freedom it is calculated that a difference of greater than .144 between means is required to denote significance at the $t_{.05}$ level.

Therefore it can be seen that the switches fall roughly into four groups based on their mean lives.

These are:

Load	Overtravel	
5 amps,	.010" = 5.12	Group 1
5 amps,	.005" = 5.10	Group 1
5 amps,	.015" = 5.06	Group 1
10 amps,	.015" = 4.55	Group 2
10 amps,	.010" = 4.01	Group 3
15 amps,	.015" = 3.65	Group 4
10 amps,	.005" = 3.62	Group 4
15 amps,	.010" = 3.53	Group 4
15 amps,	.005" = 3.42	Group 4

These groupings may be interpreted as follows. Group 1 consisting of Test Runs 1 through 9 all exhibited mean cycles to first miss which were not significantly different. Since Test Run 1 was defined as normal operating conditions and Test Runs 2 through 9 did not reduce the mean time to failure, it is obvious that none of these test runs qualify for use as accelerated reliability test methods.

Group 4 resulted in mean lives which were shorter than Test Run 1 (5 amps, .010 inches overtravel, and 70 actuations/minute), but they also introduced a changed failure mode in the form of welded contacts (See Table 2-9). Hence these test runs are deemed unsatisfactory for use as accelerated reliability test methods.

Groups 2 and 3 both exhibit shorter mean lives than Test Run 1 (normal conditions) and do not result in a change in failure mode. Hence from the standpoint of these two criteria the test runs included in these two groups (i.e., Test Runs 13 through 18) are candidates for consideration for use as accelerated test methods.

The analysis of the differences between the means of test runs where the failure definition was total failure was more complex since two first order interactions were significant in the analysis of variance.

The logarithmic observations were first summed over actuation rates to evaluate the contact load and overtravel interaction. This resulted in the matrix in Table 2-7.

TABLE 2-7. CONTACT LOAD AND OVERTRAVEL INTERACTIONS (TOTAL FAILURE-SWITCHES)

Overtravel	Contact Load		
	5 amps	10 amps	15 amps
.005	5.23	4.40	3.72
.010	5.23	4.79	4.10
.015	5.27	4.80	4.15

The interval between the means required for significance at the $t_{.05}$ level was calculated as follows:

$$\bar{X}_1 - \bar{X}_2 = t_{.05}\sqrt{\frac{\hat{\sigma}^2_x}{n_1} + \frac{\hat{\sigma}^2_x}{n_2}}$$

where: $\bar{X}_1$ and $\bar{X}_2$ = any two means from the matrix

$$\bar{X}_1 - \bar{X}_2 = 1.645 \sqrt{\frac{.100}{30} + \frac{.100}{30}}$$

$t_{.05}$ = Student t statistic for 243 degrees of freedom

$$\bar{X}_1 - \bar{X}_2 = .19$$

$\hat{\sigma}_r^2$ = the residual term from the analysis of variance

n_i = number of observations in each mean being compared

This interval when applied to the mean values in Table 2-7 separates the test runs into the following groups:

Load	Overtravel	
5 amps,	.015 = 5.27	Group 1
5 amps,	.005 = 5.23	
5 amps,	.010 = 5.23	
10 amps,	.015 - 4.80	Group 2
10 amps,	.010 = 4.79	
10 amps,	.005 = 4.40	Group 3
15 amps,	.015 = 4.15	Group 4
15 amps,	.010 = 4.10	
15 amps,	.005 = 3.72	Group 5

This separation of the test runs into groups having significantly different means lends itself to the same analysis as that used on the first miss data. Again Group 1 contains Test Run 1 (normal conditions) and therefore all other test runs included in this group are not suitable for accelerated test methods since they do not significantly reduce part life. As with the first miss data Groups 3, 4, and 5 while they reduce part life, also change the failure mode. As before the most promising accelerated test methods from the point of view of both mean life and failure mode are the test runs in Group 2 which is made up of Test Runs 13 through 18. Consequently the t tests on both first miss and total failure data result in exactly the same conclusions.

It is still important to evaluate the contact load and actuation rate interactions. The logarithmic means calculated when summing across all levels of overtravel produces the results shown in Table 2-8. The same $\bar{X}_1 - \bar{X}_2$ of .19 holds for evaluation of this matrix. The interactions of contact load and actuation rate form into 5 groups as follows:

TABLE 2-8. CONTACT LOAD AND ACTUATION RATE INTERACTIONS (TOTAL FAILURE-SWITCHES)

Actuation Rate (c.p.m.)	Contact Load 5 amps	10 amps	15 amps
70	5.33	4.68	4.03
150	5.22	4.69	4.33
300	5.18	4.63	3.61

5 amps,	70 cpm = 5.33	Group 1
5 amps,	150 cpm = 5.22	Group 1
5 amps,	300 cpm = 5.18	Group 1
10 amps,	150 cpm = 4.69	Group 2
10 amps,	70 cpm = 4.68	Group 2
10 amps,	300 cpm = 4.63	Group 2
15 amps,	150 cpm = 4.33	Group 3
15 amps,	70 cpm = 4.03	Group 4
15 amps,	300 cpm = 3.61	Group 5

These groupings indicate that actuation rates over the range of 70 to 300 cycles per minute do not result in different mean lives for switches at contact loads of either 5 amps or 10 amps. However when 15 amps are applied to the contacts, contact load interacts with actuation rate. At 300 cycles per minute the life is shortest; probably due to severe heat build up and then welding. On the other hand, 70 cycles also suffers from the same problem. It appears that 150 cycles per minute offers a compromise at 15 amps between heat buildup due to fast cycling and heat buildup due to long closure time of the contacts. In summary then it appears that from both sets of t tests performed on total failure data, and from the analysis of first miss results, the most logical candidate for an accelerated test is in the test runs at 10 amps and .010 inches overtravel. Actuation rate did not significantly affect mean life but obviously 300 cycles per minute results in a test that can be performed in the shortest calendar time. Test Run #15 was performed at 10 amps, .010 inches overtravel and 300 cycles/minute.

2.3.1.2 COMPARISON OF FIRST MISS AND TOTAL FAILURE RESULTS

The purpose of this section is to compare the results obtained by testing with the failure definition of snap action switches described as first miss and again as total failure (100 consecutive misses). The analyses of variance that were performed on both sets of data resulted in the selection of nearly similar sets of stresses as significant contributors to different mean lives of switches. The only exception was that total failure picked up the interaction of actuation rate and contact load which becomes a factor at 15 amps. The residual term of the analysis of variance of first miss data was .113, and it was .100 for the total failure results. Both analyses pointed to Test Run #15, (10 amps, .010 inches overtravel and 300 cycles per minute) as a suitable accelerated test for comparison with test run.

As another measure of the similarity of the results obtained by the two different failure criteria, a linear regression analysis was performed with the sample mean values of each test run at first miss as the dependent variable and the comparable values of total failure data as the independent variable. The correlation coefficient computed was .972. The two sets of results yield answers that are quite similar. On this basis it seems reasonable to suggest that a method of reducing test time is to test only until first miss.

2.3.2 FAILURE ANALYSIS OF SNAP ACTION SWITCHES

At the conclusion of the test to total failure, each switch was opened for inspection by making a small saw cut through an outside wall of the switch. This enabled a visual evaluation of the interior mechanism of the switch without disturbing the mechanical relationships of the parts.

Using a jewelers eye piece with 7X magnification, the interior parts were examined for specific failure mode. With only two exceptions, all switch failures fell into one or more of the following modes:

1. Leaf spring and/or common contact burned off. (Many cases of contact burn off permitted excessive leaf movement to a position such that the over center spring maintained the leaf in the normally open position.)

2. Leaf spring annealed and/or distorted (insufficient return force or distortion limits the movement).

3. Contacts welded (normally closed contact-to-common contact).

4. Leaf spring wedged by loose common contact (normally closed side of contact button burned off and permitted remainder of contact to loosen and fall from leaf spring. Contact then moved inside of the housing until the leaf spring was wedged).

5. Contact surface oxidized or foreign material insulated contact to extent that operating voltage didn't break thru surface.

The five numbers given above will be used as code numbers to designate each of the failure modes throughout this report.

The two exceptions to the above failure modes were:

#216 - switch apparently developed a short to ground and literally burned up.

#291 - leaf spring fractured.

Since the latter two failures were only one of a kind and definitely did not have any indication of a "normal" type pattern, they were classed as isolated cases and not to be considered in the overall pattern.

The results of the failure mode analysis are shown in Table 2-9. The two and three digit numbers in each cell of the matrix are the identifying serial numbers assigned to each switch tested. The numbers following each switch serial number represent the failure mode found on inspection of that part. The numbers used are 1 through 5 and these refer to the code numbers used in the failure mode definitions given above.

The findings based on the failure analysis that are apparent in Table 2-9 are as follows:

- The predominant failure mode observed at 5 amps was burned contacts. At 10 amps and .010" and .015" overtravel, this was also true.
- The predominant failure mode at 15 amps was welded contacts. This was also true at 10 amps and .005" overtravel.
- The effect of actuation rate on failure mode is most pronounced at 15 amps and the higher overtravel test conditions. Test runs #24 and 27 (300 cycles per minute) show a higher incidence of failure mode 3 (welded contacts) than did Test Runs #23 and 26 (150 cycles/minute) and Test Runs #22, and 25 (70 cycles/minute).
- The effect of overtravel as an accelerating factor was the reverse of what was originally expected. As overtravel increased so did mean life. The smaller overtravel and high currents resulted in more welded contacts. This is due to the fact that the higher overtravels produced a greater wiping action and also resulted in a greater breakaway force which would not result in failure if the contacts were only lightly welded.

2.3.3 ANALYSES RELATED TO SWITCH LIFE DISTRIBUTION FUNCTIONS

The analyses described up to this point have been related to the differences in mean cycles to failure when different combinations of stresses were applied. An equally important objective of the study is to estimate the characteristics of the life distribution functions of snap action switches operated at different levels of combined stresses of contact load, contact overtravel and actuation rate.

TABLE 2-9. SNAP ACTION SWITCHES: FAILURE MODES

Contact Load	5 Amps			10 Amps			15 Amps		
Contact Overtravel	.005"	.010"	.015"	.005"	.010"	.015"	.005"	.010"	.015"
Actuation Rate: 70 C. P. M.	#1 200-5 201-1 202-1 203-1 204-1 205-1 206-1 207-1 208-1 209-1	#4 132-1 133-1 148-1 149-1 172-1 173-1 174-5 175-1 176-1 177-1	#7 80-1&2 81-1 82-1 83-1 84-3 85-1 86-1 87-1 88-1 89-1	#10 134-1 135-2 136-1 137-1 138-1&3 139-1 140-3 141-3 142-3 143-1	#13 144-1 145-1 146-1 147-1 150-1 151-1 152-2 153-1 154-1 155-3	#16 122-2 123-2 124-1&2 125-1 126-1&2 127-1 128-4 129-1 130-1 131-1	#19 49-3 50-3 51-3 52-3 53-3 54-3 55-3 56-3&2 57-3 58-3	#22 166-1 168-1 169-4 170-4 171-3 178-3 179-1 180-1 181-5 182-1	#25 70-1 71-2 72-1&2 73-1&4 74-3 75-1&4 76-1&2 77-1&2 78-1&2 79-1&2
150 C. P. M.	#2 251-1 252-1 253-1 254-1 255-1 256-1 257-1 258-1 259-1 260-1	#5 275-1&4 276-1&4 277-1 278-1 279-1 280-1 281-1 282-1&4 283-3 284A-1	#8 285-3 286-1 287-1 288-1 289-5 290A-1&2 291 fractured leaf 292-1 293-1 294-1	#11 264-3 265-1 266-1 267-1 268-3 269-1 270-3 271-1 273-1 274-1	#14 244-1 245-1 246-1 247-1 248-1&2 249-1 250-1 261-1 262-1 263-1	#17 233-1 235-5 236-1 237-1 238-1 239-1 240-3 241-1 242-1 243-1	#20 223-3 224-3 225-3 226-1 227-3 228-3 229-3 230-3 231-3 232-1	#23 213-3 214-1 215-1 216-Burned Up 217-1 218-3 219-3 220-4 221-1 222-3	#26 193-1 295-3 195-3 196-1 197-1 198-1 199-3 210-3 211-3 212-1
300 C. P. M.	#3 59-1&2 60-1&2 61-1 62-1&2 63-1&2 64-1 65-1 66-1&2 67-1 68-1	#6 183-1 184-1 185-1 186-1 187-5 188-1 189-1 190-1 191-1 192-1	#9 90-1 91-1 92-1 93-1 94-1 95-1 96-1 97-1 99-1 100-1	#12 101-3 102-1 103-3 104-3&1 105-1 106-1 109-3 110-1&4 111-3 112-3	#15 156-1 157-1 158-1 159-1 160-1 161-2 162-1 163-1 164-1 165-1	#18 112A-1 113-1 114-1 115-1 116-1 117-1 118-1 119-1 120-1 121-1	#21 38-3&2 39-3 40-3&2 41-3 42-2 43-1 44-3 45-3&2 46-3&2 47-3&2	#24 18-3&2 19-2 20-3&2 21-3 22-1&2 23-3 24-3 26-3&2 27-3 35-3&2	#27 15-1 16-3 17-3 25-3&2 28-3&2 29-3&2 30-3 31-3&2 32-3 34-3&2

Due to the similarity of results between first miss and total failure data found thus far, this part of the analysis has been performed only on first miss failures.

2.3.3.1 WEIBULL PLOTS

The results of Test Run 1 (normal conditions) and each of the 26 test runs at accelerated conditions were plotted on Weibull probability paper. These plots are shown in Appendix VI-1 (Figures VI-1 through VI-27). The line of best fit was drawn through the plotted points based on calculations on a computer using the method of least squares. The abscissa on the Weibull plots is number of cycles to first miss. The scale is coded for maximum clarity in presenting information on the graph. The points are plotted on the ordinate at the median rank values for a sample size of 10 (Reference 13).

Included on each Weibull plot is the shape parameter (β) and the scale parameter (α). The α shown on each chart is a coded value which is dependent on the time scale used. A discussion of decoding to real time is included in Appendix VI-1.

Each of the Weibull plots is identified by a test run number and the level of each of the accelerating stresses which were used in combination.

In general the fit of the plotted points to the calculated line of best fit is quite good. There are instances where some form of mixed Weibull might have fit the data better. Test Run #2 is an example of this, although the failure analysis in the tested parts did not reveal any visual reason for the failure pattern. Test Run #7 (15 amps, .015 inches overtravel, and 70 cycles per minute) is also an example of a mixed Weibull in operation. However no reason for the early failures could be found in the failure analysis.

Test Runs 10 and 12 also contain several points that do not follow the expected line of best fit. In these two test runs there was a failure mode change occurring. Several parts failed due to welding and the remainder due to contact erosion and material transfer.

The Weibull shape parameters ($\tilde{\beta}$), the coded scale parameters ($\tilde{\alpha}_k$), and the uncoded scale parameters (α_o) for each of the 27 switch test runs are summarized in Table 2-10. They are located in matrix form for ease of associating the Weibull parameters calculated in each test run with the combined stresses applied during the test.

2.3.3.2 TESTS FOR GOODNESS OF FIT

A great deal of literature exists which claims the Weibull is a good fit for electromechanical device failure distributions. From a purely statistical standpoint, the Weibull distribution is quite versatile and able to describe a wide variety of physical phenomena. However, due to the fact that the methods of analysis and conclusions of this report depend heavily on the

TABLE 2-10 WEIBULL PARAMETERS FOR SWITCH TEST RUNS (FIRST MISS)

Contact Load	5 Amps			10 Amps			15 Amps		
Contact Overtravel	005"	010"	015"	005"	010"	015"	005"	010"	015"
Actuation Rate									
70 cpm	Run #1 $\tilde{\beta} = 4.07$ $\tilde{\alpha}_5 = 24.04$ $\tilde{\alpha}_o = 53,848 \times 10^{17}$	Run #4 $\tilde{\beta} = 5.12$ $\tilde{\alpha}_5 = 26.58$ $\tilde{\alpha}_o = 1058 \times 10^{24}$	Run #7 $\tilde{\beta} = .91$ $\tilde{\alpha}_5 = 1.95$ $\tilde{\alpha}_o = 66,066$	Run #10 $\tilde{\beta} = 1.01$ $\tilde{\alpha}_3 = 8.00$ $\tilde{\alpha}_o = 8576$	Run #13 $\tilde{\beta} = 1.12$ $\tilde{\alpha}_3 = 26.58$ $\alpha_o = 60,895$	Run #16 $\tilde{\beta} = 5.71$ $\tilde{\alpha}_4 = 69,564$ $\tilde{\alpha}_o = 461,243,752 \times 10^{19}$	Run #19 $\tilde{\beta} = 2.00$ $\tilde{\alpha}_3 = 10.38$ $\tilde{\alpha}_o = 1030 \times 10^4$	Run #22 $\tilde{\beta} = 1.79$ $\tilde{\alpha}_3 = 22.87$ $\tilde{\alpha}_o = 5,360,728$	Run #25 $\tilde{\beta} = .77$ $\tilde{\alpha}_3 = 5.16$ $\tilde{\alpha}_o = 1078$
150 cpm	Run #2 $\tilde{\beta} = 2.81$ $\tilde{\alpha}_5 = 2.83$ $\tilde{\alpha}_o = 3175 \times 10^{11}$	Run #5 $\tilde{\beta} = 1.70$ $\tilde{\alpha}_5 = 2.46$ $\tilde{\alpha}_o = 777,852 \times 10^3$	Run #8 $\tilde{\beta} = 1.84$ $\tilde{\alpha}_5 = 1.49$ $\tilde{\alpha}_o = 236,165 \times 10^4$	Run #11 $\tilde{\beta} = 2.26$ $\tilde{\alpha}_3 = 31.82$ $\tilde{\alpha}_o = 191,747,320$	Run #14 $\tilde{\beta} = 1.53$ $\tilde{\alpha}_3 = 66.69$ $\tilde{\alpha}_o = 2,594,241$	Run #17 $\tilde{\beta} = 1.74$ $\tilde{\alpha}_4 = 18.00$ $\tilde{\alpha}_o = 164,160 \times 10^3$	Run #20 $\tilde{\beta} = 1.80$ $\tilde{\alpha}_3 = 22.87$ $\tilde{\alpha}_o = 5,744,944$	Run #23 $\tilde{\beta} = 2.02$ $\tilde{\alpha}_3 = 31.87$ $\tilde{\alpha}_o = 36,586,760$	Run #26 $\tilde{\beta} = 1.38$ $\tilde{\alpha}_3 = 16.78$ $\tilde{\alpha}_o = 231,564$
300 cpm	Run #3 $\tilde{\beta} = 2.25$ $\tilde{\alpha}_5 = 1.73$ $\tilde{\alpha}_o = 4187 \times 10^9$	Run #6 $\tilde{\beta} = 1.33$ $\tilde{\alpha}_5 = 1.92$ $\tilde{\alpha}_o = 8,576,640$	Run #9 $\tilde{\beta} = 1.89$ $\tilde{\alpha}_5 = 3.06$ $\tilde{\alpha}_o = 862306 \times 10^4$	Run #12 $\tilde{\beta} = 2.91$ $\tilde{\alpha}_3 = 79.04$ $\tilde{\alpha}_o = 4,244,448 \times 10^4$	Run #15 $\tilde{\beta} = 1.00$ $\tilde{\alpha}_3 = 14.44$ $\tilde{\alpha}_o = 14,440$	Run #18 $\tilde{\beta} = .78$ $\tilde{\alpha}_4 = 2.61$ $\tilde{\alpha}_o = 3286$	Run #21 $\tilde{\beta} = 1.09$ $\tilde{\alpha}_3 = 3.00$ $\tilde{\alpha}_o = 5506$	Run #24 $\tilde{\beta} = .91$ $\tilde{\alpha}_3 = 3.25$ $\tilde{\alpha}_o = 1745$	Run #27 $\tilde{\beta} = 1.07$ $\tilde{\alpha}_3 = 7.46$ $\tilde{\alpha}_o = 12,100$

prevailing distribution function it was felt necessary to test the validity of the Weibull assumption. Three tests of the goodness of fit were used:

1. F test

2. Kolmogorov - Smirnov test

3. Comparison of test run sample means with the means estimated from the Weibull

It would have been preferable to use a X^2 goodness of fit test, but only ten observations per test run were available. To use this test, the data must be divided into cells containing a minimum of five observations. Therefore only 2 cells per test run could be formed from the 10 observations available. The X^2 test requirement of n-3 degrees of freedom where n equals the number of cells demonstrates the impossibility of using a X^2 test.

Since, for the Weibull distribution ln ln $1/1-F(x)$ is a straight line in log(x), Weibull data plotted on Weibull paper results in a straight line. These various lines for the test runs were fitted by least squares using as an estimate of $F(X_i)$ the order statistic the median rank. The regression line was then used to estimate α, β, y_0 and μ. (The estimates of these quantities are denoted by $\tilde{\alpha}$, $\tilde{\beta}$, $\tilde{y}_0$, $\tilde{\mu}$.)

It should be kept in mind that none of the three tests used (or any test for that matter) has a great deal of sensitivity for the small number (per test run) of observations available.

1. The F Test.

This test involves testing for the significance of the regression in the Weibull plot by analyzing the variance of the lifetimes (for each test run) into its component parts and forming the ratio

$$F_{1,n-2} = \frac{\text{Mean Square Due to Regression}}{\text{Residual mean Square}} .$$

Under the hypothesis of no significant regression both the numerator and denominator of this quantity estimate the variance of the lifetimes. Hence a significant F means a significant fit.

The calculated F value for each of the test runs is shown in Table 2-11. The $F_{.05}$ value for 1 and 8 degrees of freedom which must be exceeded in order to signify that the test data does fit the Weibull distribution is 5.32. The $F_{.01}$ value for the same situation is 11.3. It is seen that every one of the 27 test runs fits the Weibull distribution at the level of the $F_{.01}$ level of significance.

2. Kolmogorov - Smirnov Test.

This one sample procedure provides a test of whether an empirical distribution function agrees with a specified theoretical distribution. In this case the specified theoretical distribution is the Weibull with parameters $\tilde{\alpha}$,

TABLE 2-11. F TESTS FOR GOODNESS OF FIT (SWITCHES)

Test Run	F Ratio
1	147.[illegible]
2	24.9
3	207.3
4	42.9
5	85.3
6	19.4
7	11.3
8	199.0
9	116.7
10	17.6
11	66.7
12	50.8
13	116.7
14	51.1
15	58.1
16	58.0
17	66.9
18	93.6
19	63.8
20	43.1
21	47.5
22	72.2
23	35.0
24	85.4
25	48.0
26	93.9
27	93.5

Note: $F_{.05} = 5.32$

$F_{.01} = 11.3$

$\hat{\beta}$ obtained from the regression line. If $S_n(X)$ is the empirical cumulative distribution function and F(X) the theoretical, the statistic used is:

$$D = \max \left| |F(X) - S_n(X)| \right|$$

The percentage points of D have been tabulated by F. J. Massey (JASA 46, 70). All of the switch test runs were deemed to fit the Weibull from the Kolmogorov - Smirnov tests.

3. Comparison of Means.

The expectation of $\overline{X}_i$ (the sample mean of test run i) is equal to the population mean μ. For the Weibull it is known that $\mu = \alpha^{1/\beta}\Gamma(1/\beta + 1)$. Hence if the Weibull is a good fit (for a test run) $\overline{X}_i$ and $\tilde{\mu}_i = \tilde{\alpha}^{1/\tilde{\beta}}\Gamma(1/\tilde{\beta} + 1)$ should be "reasonably" close. Although the sampling distribution (for small samples) of $\overline{X}$ from a Weibull is not known in closed form, large discrepancies between $\overline{X}_i$ and $\tilde{\mu}_i$ for some i were obvious. These discrepancies were usually due to infant mortalities.

The comparisons of $\overline{X}_i$ and $\tilde{\mu}_i$ are shown in Table 2-12. The Test Runs #7, 10, 17, 18 and 25 are the ones in which $\overline{X}_i$ and $\tilde{\mu}_i$ exhibit differences that are large. A reference to the Weibull plot of each of these substantiates the test. Test Run #7 definitely shows signs of being a mixed Weibull. Test Run #10 contains some parts that failed by welding of the contacts and some that failed by erosion and material transfer. Test Run 17, 18 and 25 each contain early failures which may have been cases of infant mortality.

4. Tests for Infant Mortality.

Two estimates of the Weibull mean μ_i (for each test run) were obtained. First Weibull graph paper was used to find (by least squares) a line giving $\tilde{\alpha}_i$ and $\tilde{\beta}_i$. Then using known relations between β_i and μ_i/y_{oi} $= \alpha_i^{1/\beta_i}$) an estimate $\tilde{\mu}_i$ of μ_i was available, i.e.:

$$\tilde{\mu}_i = \frac{\tilde{\mu}_i}{y_{oi}} \times \tilde{y}_{oi} \qquad (1)$$

Secondly, since $E(\overline{X}_i) = \frac{1}{n}\left[E(X_i) + \cdots + E(X_n)\right] = \frac{n\mu_i}{n} = \mu_i \qquad (2)$

(where $\overline{X}_i$ is the sample mean of test run i) an unbiased estimate of μ was obtainable from the failure data of test run i. Note that since the first method used the method of least squares the estimates of α and β were essentially maximum likelihood estimates and hence $\tilde{\mu}$ is what amounts to a maximum likelihood estimate. Now it is cumbersome to obtain the sampling distribution of $\overline{X}$ from a Weibull distribution especially when n is small. However, a visual inspection (by test run) of the discrepancy between $\overline{X}_i$ (i the test run) and $\tilde{\mu}_i$ as obtained from (1) certainly indicates whether or not the Weibull was a reasonable fit since if it is not $\tilde{\mu}_i$ is not a good estimator of μ_i. In most cases where a large discrepancy occurred (e.g., relays test run number 23, $\overline{X}_i$ = 428,552, $\tilde{\mu}_i$ = 25,000,000) between μ_i and $\overline{x}_i$ it was an obvious case of infant mortality. However, for this "test" of early failure

TABLE 2-12. COMPARISON OF $\bar{X}_i$ AND $\tilde{\mu}_i$ FOR SWITCHES

Test Run	$\bar{X}_i$	$\tilde{\mu}_i$
1	197,715	195,220
2	126,892	129,050
3	95,922	97,460
4	174,383	174,610
5	142,233	147,180
6	131,837	142,445
7	151,577	215,250
8	108,031	106,560
9	161,982	159,660
10	9,267	7,177
11	4,075	4,076
12	3,992	4,099
13	17,816	16,783
14	13,801	14,028
15	13,725	14,500
16	65,358	64,750
17	38,056	47,223
18	30,858	40,250
19	2,791	2,838
20	4,864	4,978
21	2,548	2,777
22	2,048	5,162
23	4,839	4,790
24	3,415	3,780
25	7,333	9,512
26	6,896	6,672
27	6,213	6,541

one is unable to assess the type I and II errors associated with it and moreover it only "tests" if the Weibull is a good fit, not if there is an early failure. The results of this test are given in Table 2-12.

The following test, which used the first order statistic, i.e., the minimum of the sample, has the property that its type I and type II errors can be assessed. If test run number i is really Weibull with parameters $\tilde{\alpha}_i$ and $\tilde{\beta}_i$ then the probability that $x_{i1} = \min \{x_{ij}\}$ (where for switches j = 1, 2, ---, 10 and for relays j = 1, 2, ---, 5) is less than some fixed value x is given by (for switches say):

$$P(x_{i1} < x) = 1 - P(x_{i1} \geq x) \tag{3}$$

If, however, $x_{i1} \geq x$ then so are the other 9 failure times because $x_{i1} \leq x_{ij}$ j = 2, 3, ---, 10. On the other hand, if all ten failure times are $\geq x$ then certainly x_{i1} is. Hence:

$$1 - P(x_{i1} \geq K) = 1 - \left[1 - F_i(x)\right]^{10}$$

and then

$$P(x_{i1} < x) = 1 - \left[1 - F_i(x)\right]^{10} \tag{4}$$

and for relays

$$P(x_{i1} < x) = 1 - \left[1 - F_i(x)\right]^{5} \tag{5}$$

where

$$F_i(x) = 1 - e^{-x^{\tilde{\beta}_i}/\tilde{\alpha}_i} \tag{6}$$

Thus if test run i is really Weibull with $\tilde{\alpha}_i$ and $\tilde{\beta}_i$ then (again for switches:

$$Q = P\text{ (the smallest failure time} < x_{i1}) = 1 - \left[1 - F_i(x_{i1})\right]^{10} \tag{7}$$

Now if this number Q is too small say Q < .01 then certainly the first failure i.e., x_{i1}, has occurred abnormally early and thus $F_i(x_{i1})$ in (7) provides a "statistic" to test the hypothesis that the first failure is too early. One can set the type I error (.01 in this case) at any level desired. The type II error (saying an early failure did not occur when it did) must be evaluated in terms of what α and β really hold. The results indicated no early failures.

2.3.3.3 CUMULATIVE FAILURE DISTRIBUTIONS

The cumulative failure distributions for each of the 27 test runs have been plotted and are shown in Appendix I.

Their importance in the theory of accelerated testing is based on the following properties:

1. The comparison between the cumulative distribution function under accelerated conditions and the cumulative distribution function (probability of failure before time x) under normal conditions indicates persistent acceleration.

2. The "relative" rapidity with which the accelerated conditions kill units off in the time (cycle) intervals of interest.

In many important cases of life testing mechanical devices, the Weibull distribution often provides a good fit to failure times. The form of the Weibull is:

$$P(\text{life} < x) = \text{Cumulative Distribution Function} = F(x)$$

$$F(x) = 1 - e^{-\frac{x^{\beta}}{\alpha}}; \quad x \geq 0; \; \alpha > 0; \; \beta > 0.$$

It is expected, from present evidence, that this particular distribution (with γ = guarantee time = 0) will be a good model for the failure time distributions.

It should be pointed out that the cumulative failure distribution plots and the Weibull plots (Appendix VI-1) present basically the same information. However, the cumulative failure distribution plots were prepared for each test run because they are easier to use in comparing the probabilities of failure of parts operated at different combinations of stresses. The Weibull plots show the same information but are presented with the use of different time scales thus making physical comparison difficult.

An analysis of the cumulative failure distribution charts indicates that all of them except Test Run #7 meet the criteria of reducing the life of switches more quickly than Test Run #1 (3 amps., .005 inches overtravel, and 70 cpm) which was designated as normal operating conditions. It can be remembered from the discussion on goodness of fit that Test Run #7 exhibited mixed Weibull properties.

In the final selection of the optimum set of accelerated test conditions, the relationship of the failure distributions as compared to normal operating conditions will be one of the factors determining the final selection of a test method.

2.3.3.4 CALCULATION OF HAZARD RATES

Another parameter of interest of the switches tested at each of the 27 combinations of environmental and operating stresses is that of hazard rate. The hazard rate is represented by the expression $h(x) = \frac{\beta x^{\beta - 1}}{\alpha}$

where

β = the Weibull shape parameter

α = the Weibull scale parameter

x = time in cycles

Since it has been determined that the failure of the switches under study is described by the Weibull distribution, the hazard rate of each test run is time dependent except in cases where the Weibull shape parameter (β) is equal to 1 (which is the constant failure rate exponential distribution).

Table 2-13 is a listing of the hazard rates of each Test Run with first miss as failure criterion. The hazard rate for each set of conditions is given for time x = 10, 100, and 1000. From these points a graphical presentation of the hazard rates can be easily plotted on log log paper.

The hazard rate, h(x), is formally defined as the conditional rate of failure at x given survival to time x i.e.,

$$P(x < \text{death} < x + \Delta x \quad | \text{survival to } x) \equiv h(x) = \frac{f(x)}{1 - F(x)}$$

h(x) is an important quantity for two reasons: 1) it measures the failure in terms of x and hence provides one of the criteria for selecting an accelerated test; 2) it can form a basis for relating accelerated and normal environments.

2.3.3.5 CONFIDENCE LIMITS FOR WEIBULL PARAMETERS

The line of best fit for each test run of switches was calculated by the method of least squares. The slope of the linear regression line is the Weibull shape parameter (β) and the intercept is log ($\frac{1}{\alpha}$) where α is the Weibull scale parameter. Tables 2-14 and 2-15 represent the 95% confidence limits about the slopes and intercepts of the calculated regression lines.

2.3.4 ANALYSIS OF SWITCH OPERATING PARAMETERS

A side experiment was performed during the accelerated life tests on snap action switches. It consisted of the initial and periodic measurement of the following operating parameters:

Contact resistance (normally open)
Contact resistance (normally closed)

TABLE 2-13. HAZARD RATES FOR SNAP ACTION SWITCHES WHERE FAILURE CRITERION IS FIRST MISS

Test Run	Hazard Rate ($\times 10^{10}$)		
	x = 10 cycles	x = 100 cycles	x = 1000 cycles
1	$.888 \times 10^{-8}$	$.104 \times 10^{-4}$	$.1226 \times 10^{-1}$
2	$.57 \times 10^{-2}$	$.37 \times 10^{0}$	$.24 \times 10^{2}$
3	$.183 \times 10^{1}$	$.325 \times 10^{2}$	$.578 \times 10^{3}$
4	$.638 \times 10^{-12}$	$.8 \times 10^{-8}$	$.111 \times 10^{-3}$
5	$.1095 \times 10^{3}$	$.549 \times 10^{3}$	$.275 \times 10^{4}$
6	$.3315 \times 10^{4}$	$.709 \times 10^{4}$	$.1515 \times 10^{5}$
7	$.11 \times 10^{6}$	$.89 \times 10^{5}$	$.716 \times 10^{5}$
8	$.539 \times 10^{2}$	$.373 \times 10^{3}$	$.258 \times 10^{4}$
9	$.17 \times 10^{2}$	$.132 \times 10^{3}$	$.1025 \times 10$[illegible]
10	$.12 \times 10^{7}$	$.123 \times 10^{7}$	$.126 \times 10^{7}$
11	$.214 \times 10^{4}$	$.39 \times 10^{5}$	$.71 \times 10^{6}$
12	$.557 \times 10^{2}$	$.453 \times 10^{4}$	$.368 \times 10^{6}$
13	$.242 \times 10^{6}$	$.3196 \times 10^{6}$	$.421 \times 10^{6}$
14	$.2 \times 10^{5}$	$.677 \times 10^{5}$	$.229 \times 10^{6}$
15	$.6925 \times 10^{6}$	$.6925 \times 10^{6}$	$.6925 \times 10^{6}$
16	$.6085 \times 10^{-12}$	$.312 \times 10^{-7}$	$.16 \times 10^{2}$
17	$.582 \times 10^{3}$	$.32 \times 10^{4}$	$.176 \times 10^{5}$
18	$.143 \times 10^{7}$	$.862 \times 10^{6}$	$.519 \times 10^{6}$
19	$.1926 \times 10^{5}$	$.1926 \times 10^{6}$	$.1926 \times 10^{7}$
20	$.1977 \times 10^{5}$	125×10^{6}	$.787 \times 10^{6}$
21	$.24 \times 10^{7}$	$.295 \times 10^{7}$	$.363 \times 10^{3}$
22	$.206 \times 10^{5}$	$.127 \times 10^{6}$	$.783 \times 10^{6}$
23	$.578 \times 10^{4}$	$.605 \times 10^{5}$	$.634 \times 10^{6}$
24	$.424 \times 10^{7}$	$.345 \times 10^{7}$	$.28 \times 10^{7}$
25	$.42 \times 10^{7}$	$.248 \times 10^{7}$	$.146 \times 10^{7}$
26	$.146 \times 10^{6}$	$.343 \times 10^{6}$	$.823 \times 10^{6}$
27	$.104 \times 10^{7}$	$.122 \times 10^{7}$	$.143 \times 10^{7}$

TABLE 2-14. CONFIDENCE LIMITS FOR β (SWITCHES)

Test Run	β	$\beta_{(.025)}$	$\beta_{(.975)}$
1	4.07	3.896	4.244
2	2.81	2.427	3.193
3	2.25	2.075	2.425
4	5.12	4.812	5.428
5	1.70	1.473	1.927
6	1.33	1.005	1.655
7	.906	.497	1.315
8	1.84	1.690	1.990
9	1.89	1.697	2.083
10	1.01	.578	1.442
11	2.26	2.003	2.517
12	2.91	2.621	3.199
13	1.12	.929	1.311
14	1.53	1.248	1.812
15	1.00	.736	1.264
16	5.718	5.439	5.979
17	1.74	1.485	1.989
18	.78	.557	.997
19	2.00	1.869	2.131
20	1.80	1.586	2.014
21	1.09	.889	1.285
22	1.79	1.557	2.027
23	2.02	1.682	2.354
24	.91	.699	1.121
25	.77	.479	1.065
26	1.38	1.165	1.603
27	1.07	.846	1.288

TABLE 2-15. CONFIDENCE LIMITS FOR α_o (SWITCHES)

Test Run	α_o	$\alpha_o(.025)$	$\alpha_o(.975)$
1	5.385×10^{21}	4.408×10^{21}	6.511×10^{21}
2	3.175×10^{14}	2.065×10^{14}	4.831×10^{14}
3	2.187×10^{11}	1.796×10^{11}	2.652×10^{11}
4	1.058×10^{27}	7.456×10^{26}	1.485×10^{27}
5	7.778×10^{8}	6.057×10^{8}	9.986×10^{8}
6	8.577×10^{6}	5.970×10^{6}	1.226×10^{7}
7	66,066	41,798	103,839
8	2.362×10^{9}	1.995×10^{9}	2.803×10^{9}
9	8.623×10^{9}	7.509×10^{9}	1.154×10^{10}
10	8576	5257	13,867
11	1.917×10^{8}	1.449×10^{8}	2.562×10^{8}
12	4.244×10^{10}	3.082×10^{10}	5.845×10^{10}
13	60,895	48,862	75,113
14	2.594×10^{6}	1.884×10^{6}	3.537×10^{6}
15	14,440	10,805	19,492
16	4.812×10^{27}	3.532×10^{27}	6.436×10^{27}
17	1.642×10^{8}	1.207×10^{8}	2.112×10^{8}
18	3286	2634	4299
19	1.038×10^{7}	9.025×10^{6}	1.206×10^{7}
20	5.745×10^{6}	4.520×10^{6}	7.305×10^{6}
21	5586	4397	6828
22	5.361×10^{6}	4.192×10^{6}	7.052×10^{6}
23	3.659×10^{7}	2.488×10^{7}	5.214×10^{7}
24	1745	1375	2200
25	1078	767.2	1484
26	231,564	185,407	302,644
27	12,100	9329	15,227

Operate force
Release force

The objective was to note how these parameters changed during the life cycle of a switch when it was operated at different combinations of stresses.

The results of this analysis were inconclusive. This was very likely due to measurement errors which were large relative to the actual changes in the parametric values over time.

2.4 SELECTION OF ACCELERATED RELIABILITY TEST METHOD (SWITCHES)

The general procedure for locating desirable test runs for use as accelerated reliability test methods is described in Section 1.4. The application of the rules outlined there to the results generated in this study on snap action switches is given in Table 2-16. Each test run except Test Run 1 (normal operating conditions) is compared to each of the factors defined as measures of a good or bad accelerated test method.

The application of the rules stated on the following page to the 26 possible combinations of accelerating stresses investigated during this study program on snap action switches results in the following logic:

From the analysis of variance and its accompanying t tests, contact load, actuation rate, and overtravel, as well as the contact load and overtravel interaction and contact load and actuation rate interaction were significant in affecting switch life. However, all of the tests performed at 5 amps resulted in mean lives that could not be recognized as being significantly shorter than Test Group 1. Hence Test Runs 2 through 9 are eliminated from contention.

The t tests indicated that the 15 amp test runs and those at 10 amps and .005 inches overtravel belonged to the group displaying the shortest mean lives. However, the failure analysis discovered that these test runs were characterized by a change in failure mode. Welding rather than the burning off of the contacts took over as the predominant failure observed in these test runs. This leaves as candidates test runs 13, 14 and 15, the 3 actuation rates at 10 amps and .010 inches overtravel and 16, 17, and 18, the 3 actuation rates at 10 amps and .015 inches overtravel.

Test Run 16 displays signs of a failure mode change. Four of the ten switches in this group failed due to failure mode 2 (blade distorted and annealed) while the other six failed in the same manner as Test Group 1 (leaf spring burned off). On this basis this test run is eliminated from consideration.

Test Runs 17 and 18 gave indications of not fitting the Weibull in the goodness of fit tests which compared $\tilde{\mu}_i$ and $\bar{x}_i$ (Table 2-12).

This leaves Test Runs 13, 14 and 15. Reference to the cumulative density functions of each of these (Figure I-5) indicates that Run 13 exhibits a lower probability of failure than the other two runs. Test Run 15 has the highest probability of failure up to about 18,000 cycles where Run 14 crosses and becomes the highest. The mean lives of these two runs was approximately 14,000 and therefore this crossing point becomes less important.

Therefore either Test Run 14 or 15 display the most promise of resulting in useful accelerated reliability test methods. Test Run 14 is performed at an actuation rate of 150 cycles/minute while Test Run 15 is at 300 cycles/minute. Therefore 15 would be most desirable from the standpoint of shortest elapsed calendar time. However both of these sets of stresses meet all of the criteria deemed as desirable factors for use as accelerated reliability test methods.

TABLE 2-16. FACTORS FOR SELECTING DESIRABLE ACCELERATED RELIABILITY TEST METHODS (SNAP ACTION SWITCHES)

Factors / Test Run	1	2	3	4	5	6	7	8	9	10	11	12	13	14	15	16	17	18	19	20	21	22	23	24	25	26	27
Short Mean Life										x	x	x	x	x	x	x	x	x	x	x	x	x	x	x	x	x	x
Significant Accelerating Stresses										x	x	x	x	x	x	x	x	x	x	x	x	x	x	x	x	x	x
Constant Failure Mode		x	x	x	x	x	x	x	x				x	x	x		x	x									
Cumulative Failure Distribution		x	x		x	x	x	x	x	x	x	x	x	x	x	x	x	x	x	x	x	x	x	x	x	x	x
Hazard Rate		x	x		x	x		x	x	x	x	x	x	x	x		x	x	x	x	x	x	x	x	x	x	x
Fits Weibull Distribution			x	x	x	x		x	x		x		x	x	x	x			x	x	x	x	x	x		x	x
Short Calendar Test Time										x	x	x	x	x	x	x	x	x	x	x	x	x	x	x	x	x	x
Economical		x	x	x	x	x	x	x	x	x	x	x	x	x	x	x	x	x	x	x	x	x	x	x	x	x	x

SECTION 3.0 CRYSTAL CAN RELAYS

3.1 SUMMARY

This section is devoted to the presentation of all of the data generated on crystal can relays during the course of this study program. It begins by giving the details of the mathematical studies conducted to establish stresses and stress levels which contributed most heavily in the reduction of both the number of cycles to first miss and number of cycles to total failure. The failure times are studied in an attempt to establish th failure distribution associated with each set of combined stresses. The results of each of these series of analyses are combined with the findings of the analysis of failed parts. These then are used as ground rules for selecting the most promising test runs for further study as possible accelerated reliability test methods.

A total of 135 relays were tested during the study program. Five parts were operated at normal operating and environmental stress levels. These conditions were defined as follows:

Contact load	3 amps
Ambient temperature	25°C
Actuation rate	1 cycle/second

Five relays were also tested at each of 26 other combinations of these three stresses in the form of a full factorial experiment. The contact loads used were 3, 6, and 8 amps. The ambient temperatures were 25°C, 100°C, and 150°C. The actuation rates were 1, 10, and 30 cycles per second.

The cycles to first miss of each relay were recorded as well as the number of cycles at third miss which was defined as total failure. An analysis of variance was performed on both the first miss and on the total failure data. Its purpose was to identify those stresses and interactions of stresses which significantly affected the life of this relay.

The following stresses were found to affect relay life under their respective failure definitions:

	1st Miss	Total Failure
Contact Load	X	X
Ambient Temperature	X	X
Interactions (Contact Load and Temperature)	X	X

As a measure of the magnitude of the contribution of each of the applied stresses to the total variance, the components of variance were calculated. Contact load was by far the most important factor affecting relay life since it contributed 48% of the total variance in the first miss analysis and 49%

when total failure was the failure definition. Ambient temperatures at first miss and total failure accounted for 2.5 and 3.0% of total variance, respectively, and their interactions were responsible for from 5.9% to 5.4% respectively. Residual was 43.6% for the first miss and 42.6% for total failure.

Student's t test was used to group the test runs into ones that could have come from populations with like means. This was done to compare the mean life of the relays operated at rated conditions (Test Run 1) with that of the parts operated at accelerated conditions. All test runs which operated at the same contact load (3 amps) as Test Run 1 exhibited no significant differences and hence were discounted as feasible accelerated test methods on this account. The relays operated at 8 amps exhibited the shortest mean life but a failure mode change in the form of contact welding showed up thus negating the usefulness of this stress level as an accelerating stress. The relays tested at 6 amps contact load failed due to contact erosion and material transfer which was also the most prevalent failure mode observed in Test Run 1 (normal conditions).

Up to this point, the results of the first miss failure definition concurred very closely with those in which failure was defined as third miss (total failure). This then constitutes a form of accelerated test in itself.

To study the distribution of failure times for relays, each test run was plotted on Weibull probability paper. The Weibull shape parameter (β) and scale parameter (α) were calculated for normal conditions (Test Run 1) and the 26 other combinations of stresses. The Weibull location parameter (λ) was assumed to be zero. The cumulative failure distribution and hazard rates for each test run were also calculated and evaluated for determining the most promising set of combined stresses for use as an accelerated reliability test method.

Each relay tested was opened and visually examined under a microscope to determine the reason for failure. The results of these analyses were used in selecting accelerated test methods with the same failure modes as that of Test Run 1 (normal conditions).

The final selection of an accelerated reliability test method was made by weighing the findings of the analysis of variance, the Weibull plots, the cumulative failure distributions, the hazard rates, and the failed parts analyses. Both Test Run 15 (6 amps, 10 cycles/second, and 150°C) and Test Run 22 (6 amps, 30 cycles/second, and 25°C) were selected as satisfactory accelerated reliability test methods.

3.2 DETAILS OF THE INVESTIGATION

3.2.1 SELECTION OF STRESSES

The relay selected for study was of the crystal can variety with the following characteristics:

Double Pole, Double Throw

Contact Load Rating --------------------3 amps

Contact Voltage ------------------------- 28 Volts DC

Actuation Rate ------------------------- To 30 Cycles/Second

Coil Resistance ------------------------ 675 OHMS

Coil Voltage --------------------------- 26.5 Volts

Temperature Range --------------------- -65°C to +125°C

The following stresses were considered for inclusion in the study program to evaluate environments or operating conditions that would reduce relay life at some predictable rate:

Actuation Rate

Coil Voltage

Vibration

Contact Voltage

Ambient Temperature

Contact Load

Contamination

The criteria for selecting the stresses to be applied were:

1. probable effect on life and/or test time
2. probable effect on failure modes
3. uniformity of application at several levels or throughout a given range
4. complexity of test set up
5. ease of control of stresses
6. accuracy of measurement of stresses

An evaluation of the suggested stresses in the light of the above objectives resulted in the selection of:

Contact load

Actuation rate

Ambient temperature

The selection of operating levels of these stresses began with a definition of normal operating conditions. This was necessary since a benchmark was required with which to compare accelerated test results. Therefore, normal conditions were defined as 3 amps contact load, ambient temperature of 25°C, and an actuation rate of one cycle/second. Slower actuation rates were considered but had to be discarded because of time limitations.

Preliminary screening tests were run to establish the feasible limits of each stress. For example some relays were tried at 10 amps and at 12 amps contact load. In a similar manner, there was a probing type study of the other parameters to establish feasible levels.

The final selection of stresses for inclusion in the study was:

Contact Load:	3, 6 and 8 amps
Ambient Temperature:	25°C, 100°C, and 150°C
Actuation Rate:	1, 10 and 30 cycles/second

A description of the physical test methods and equipment developed for relay testing is given in Appendix V-2.

3.2.2 STATISTICAL EXPERIMENTAL DESIGN

In order to evaluate not only the main effects of the applied stresses on the life of relays, but also their interactions, a full 3^3 factorial experiment was specified. Five relays were tested at each of 27 combinations of the selected stresses. Each of the test runs was numbered as shown in Table 3-1 for simplicity. These Test Run Number designations will be used throughout the discussion. Test Run 1 (3 amps, 25°C, and 1 cycle/second) is designated as normal operating conditions.

TABLE 3-1. FACTORIAL EXPERIMENT ON CRYSTAL CAN RELAYS

		Actuation Rate (cycles/second)								
		1			10			30		
Contact Load (amps)		3	6	8	3	6	8	3	6	8
Ambient Temperature (°C)	25	(1)	(4)	(7)	(10)	(13)	(16)	(19)	(22)	(25)
	100	(2)	(5)	(8)	(11)	(14)	(17)	(20)	(23)	(26)
	150	(3)	(6)	(9)	(12)	(15)	(18)	(21)	(24)	(27)

Note: The numbers in parentheses are designations used throughout the study to identify each of the 27 test runs. For example Test Run 22 consists of 5 relays operated at 6 amps, 25°C and 30 cycles per second. Each test run contains 5 relays.

3.2.3 DEFINITION OF FAILURE

The major objective of the test program on relays was to search for an accelerated reliability test method. This made it important to analyze all test data by two different failure definitions. The first one defined failure as the first miss (failure of the contacts to make or break). A second failure definition was selected as cycles to total failure (total inoperation of the part). Contractual schedules made it mandatory to revise the definition of total failure to the number of cycles to 3rd miss. Therefore records were made of the number of cycles at which the first miss occurred and then the test was continued until third miss. Two separate analyses were made to see if the results of the two failure definitions resulted in similar conclusions. If the results from both were the same, then test time could be immediately reduced by testing only to first miss.

3.3 PRESENTATION OF TEST RESULTS

Five relays were tested in each of 27 test runs. Each test run was defined in terms of 3 controlled stresses (environmental or operating). Contact load was applied at 3, 6, and 8 amps; actuation rates were 1, 10 and 30 cycles per second; ambient temperature was controlled at 25°, 100°, and 150° centigrade. The cycles to first miss of all 135 relays included in the study are summarized in Table 3-2. The test runs are numbered 1-27 beginning in the upper left hand corner of the matrix and continuing down in the columns and is so shown by the number at the bottom of each cell of the matrix. For example Test Run 1 (normal conditions) is the five relays operated at 3 amps contact load, 25°C, and 1 cycle per second. Test Run 9 is the five relays operated at 8 amps contact load, 150°C, and 1 cycle per second. The mean value of each test run is designated $\overline{X}$ and is shown in each cell of the matrix. Test Run 1 was designated as "normal operating conditions" and the other 26 runs were construed to be combinations of stresses that would induce either a different mean number of cycles to first miss, or different failure distribution parameters. It was the objective of this study to find some set of combined stresses which would result in a test run time which was shorter than Test Run 1, and that could be related to it by some transformation function.

The cycles to total failure for the same 135 relays described above are presented in Table 3-3.

3.3.1 ANALYSIS OF VARIANCE

The statistical method used for discovering the stresses or combinations of stresses which reduce relay life was the analysis of variance. It is based on the assumption that there is equal variance in each cell of the factorial experiment. An inspection of the number of cycles to first miss of the relays tested indicated that this was not the case. A method of dealing with this problem is suggested by Davies (Reference 14). It involves the use of a logarithmic transformation in cases where the variance is proportional to the magnitude of the mean. It also tends to normalize the data. Therefore this procedure was used before the analysis of variance was performed.

TABLE 3-2. RELAY CYCLES TO FIRST MISS

Actuation Rate	1 cycle/second			10 cycle/second			30 cycles/second		
Contact Load	3 amps	6 amps	8 amps	3 amps	6 amps	8 amps	3 amps	6 amps	8 amps
Ambient Temperature 25°C	35) 473,323 36) 1,088,447 87) 474,388 88) 284,883 89) 1,058,123 $\tilde{x}$ = 675,842 1	3) 63,916 4) 8,996 90) 162,434 91) 137,616 92) 145,385 $\tilde{x}$ = 103,066 4	22) 87 23) 208 81) 102,920 82) 163,320 83) 100,270 $\tilde{x}$ = 72,681 7	46) 182,730 47) 517,322 115) 595,820 116) 70,368 117) 408,373 $\tilde{x}$ = 353,273 10	110) 381,819 111) 326,116 112) 285,298 113) 80,437 114) 218,939 $\tilde{x}$ = 258,522 13	43) 98,961 44) 169 104) 264,628 105) 76,063 106) [illegible] $\tilde{x}$ = 79,962 16	37) 1,676,309 38) 1,717,118 93) 935,856 94) 405,746 95) 858,427 $\tilde{x}$ = 1,118,691 19	99) 230,218 100) 51,208 101) 482,887 102) 424,906 103) 224,403 $\tilde{x}$ = 282,724 22	16) 450 17) 314,700 70) 218 71) 6,540 72) 26,118 $\tilde{x}$ = 69,604 25
Ambient Temperature 100°C	50) 683,946 51) 1,170,538 141) 1,184,727 142) 33,897 143) 320,641 $\tilde{x}$ = 679,790 2	5) 650,000 6) 130,700 146) 46,515 145) 30,756 157) 221,813 $\tilde{x}$ = 214,757 5	54) 10 55) 145 148) 63,350 149) 3,243 150) 21,441 $\tilde{x}$ = 17,638 8	52) 2,010,969 53) 1,384,983 126) 928,072 127) 1,866,468 128) 1,823,142 $\tilde{x}$ = 1,762,647 11	150) 117,805 151) 170,413 152) 213,690 153) 211,650 154) 17,739 $\tilde{x}$ = 146,275 14	56) 34,370 57) 1,107 129) 56,865 130) 8,409 131) 127,316 $\tilde{x}$ = 45,613 17	48) 1,818,618 49) 2,084,808 123) 2,984,410 124) 3,269,724 125) 1,345,591 $\tilde{x}$ = 2,299,030 20	20) 532,910 21) 451,140 76) 592,960 77) 5,013 78) 960,740 $\tilde{x}$ = 428,552 23	12) 250,100 13) 105,940 64) 159,340 65) 30,160 66) 46,270 $\tilde{x}$ = 118,362 26
Ambient Temperature 150°C	39) 759,921 40) 434,909 96) 212,926 97) 1,575,348 98) 1,455,644 $\tilde{x}$ = 885,750 3	118) 204,182 119) 237,779 120) 246,681 121) 354,347 122) 83,776 $\tilde{x}$ = 225,353 6	41) 49,053 45) 19,314 107) 93,662 108) 28,835 109) 15,200 $\tilde{x}$ = 41,321 9	58) 1,224,461 59) 1,670,580 132) 647,306 133) 2,016,758 134) 255,652 $\tilde{x}$ = 1,162,951 12	135) 80,781 136) 248,228 137) 123,295 155) 199,766 154) 545,303 $\tilde{x}$ = 239,474 15	7) 398,606 8) 475,000 138) 171,871 139) 59,214 140) 50,490 $\tilde{x}$ = 231,035 18	26) 1,985,475 27) 2,530,050 84) 1,257,468 85) 2,399,326 86) 800,879 $\tilde{x}$ = 1,774,647 21	18) 697,820 19) 480 73) 44,740 74) 524,840 75) 13,030 $\tilde{x}$ = 256,182 24	10) 184,590 11) 75,620 61) 126,280 62) 235,550 63) 73,880 $\tilde{x}$ = 139,184 27

TABLE 3-3 RELAYS. CYCLES TO TOTAL FAILURE

Actuation Rate	1 Cycle/Second			10 Cycles/Second			30 Cycles/Second		
Contact Load	3 amps	6 amps	8 amps	3 amps	6 amps	8 amps	3 amps	6 amps	8 amps
Ambient Temperature 25°C	566,422(15) 1,088,499(16) 1,525,717(87) 668,996(88) 1,483,682(89) $\hat{x}$ = 1,066,267 Ø1	63,912(1) 9,261(4) 378,790(90) 138,093(91) 145,43[illegible](92) $\hat{x}$ = 132,699 Ø4	545(22) 210(32) 145,409(81) 175,743(82) 157,015(83) $\hat{x}$ = 95,960 Ø7	182,782(46) 911,027(47) 600,662(115) 412,085(116) 527,124(117) $\hat{x}$ = 446,736 Ø10	381,821(110) 326,137(111) 285,459(112) 80,439(113) 218,941(114) $\hat{x}$ = 250,559 Ø13	68,715(43) 171(44) 267,753(104) 76,07[illegible](105) 37(106) $\hat{x}$ = 82,950 Ø16	1,676,366(37) 1,717,120(38) 1,143,382(93) 596,036(94) 861,558(95) $\hat{x}$ = 1,198,091 Ø19	369,138(99) 52,063(100) 516,961(101) 496,483(102) 433,488(103) $\hat{x}$ = 373,623 Ø22	788(16) 315,098(17) 212(70) 6,562(71) 27,108(72) $\hat{x}$ = 69,957 Ø25
100°C	684,576(50) 1,170,561(51) 1,659,108(141) 730,691(142) 323,049(143) $\hat{x}$ = 913,637 Ø2	650,002(5) 136,703(6) 428,608(144) 32,362(145) 222,259(157) $\hat{x}$ = 297,803 Ø5	71(54) 147(55) 104,374(148) 41,540(149) 28,938(150) $\hat{x}$ = 35,80[illegible] Ø8	2,810,592(52) 1,38[illegible],532(53) 1,010,673(126) 1,869,359(127) 1,830,506(128) $\hat{x}$ = 1,781,9[illegible]2 Ø11	397,565(150) 347,673(151) 213,694(152) 211,652(153) 17,793(154) $\hat{x}$ = 237,675 Ø14	34,372(56) 1,109(57) 90,640(129) 65,697(130) 127,318(131) $\hat{x}$ = 57,427 Ø17	2,149,543(48) 2,089,549(49) 3,022,469(133) 4,519,260(124) 1,345,717(125) $\hat{x}$ = 2,624,587 Ø20	547,288(20) 452,130(21) 592,962(76) 5,828(77) 960,744(78) $\hat{x}$ = 431,707 Ø23	251,431(12) 263,178(13) 164,223(64) 41,008(65) 279,618(66) $\hat{x}$ = 199,886 Ø26
150°C	760,021(39) 436,134(40) 222,844(96) 1,595,381(97) 1,465,653(98) $\hat{x}$ = 888,099 Ø3	204,184(118) 238,017(119) 246,685(120) 354,733(121) 185,214(122) $\hat{x}$ = 245,766 Ø6	85,447(61) 68,967(45) 119,520(107) 28,545(108) 23,553(109) $\hat{x}$ = 65,206 Ø9	1,225,248(58) 1,701,864(59) 648,114(132) 2,016,832(133) 575,608(134) $\hat{x}$ = 1,233,533 Ø12	80,793(135) 320,686(136) 123,297(137) 199,768(155) 545,305(156) $\hat{x}$ = 253,968 Ø15	398,602(7) 475,002(8) 171,961(138) 59,216(139) 50,492(140) $\hat{x}$ = 231,954 Ø18	2,019,487(26) 2,530,349(27) 1,292,929(84) 2,322,495(85) 2,674,541(86) $\hat{x}$ = 2,167,088 Ø21	707,538(18) 483(19) 1[illegible]0,830(73) 521,843(74) 233,428(75) $\hat{x}$ = 321,421 Ø24	190,838(10) 174,758(11) 133,098(61) 266,268(62) 104,958(63) $\hat{x}$ = 173,976 Ø27

The results of the analysis of variance on first miss data are presented in Table 3-4. The indications are that contact loads, temperatures, and the first order interaction between contact loads and temperatures are the stresses that significantly affect the life of the relays under study. The comparison of the "F Ratio" column with the "$F_{.05}$" column in Table 3-4 presents the results of the significance tests. The F ratio of actuation rates was 3.04 while a value greater than 3.07 was required for significance. This is probably an indication that actuation rate does in fact affect the life of this type of relay but the differences are noticeable over a wider range of values than were included in this experiment.

TABLE 3-4. ANALYSIS OF VARIANCE - RELAYS (FIRST MISS)

Source of Variance	Sum of Squares	Degrees of Freedom	Mean Squares	F Ratio	$F_{.05}$	% of Contribution To Variance
Between Actuation Rates	3.695	2	1.848	3.04	3.07	0
Between Contact Loads	61.656	2	30.828	50.65*	3.07	48.0
Interactions Between Actuation Rate, Contact Load	2.370	4	1.185	1.95	2.45	0
Between Temperatures	4.387	2	2.193	3.60*	3.07	2.5
Interactions Between Actuation Rate, Temperature	3.762	4	.941	1.55	2.45	0
Interactions Between Contact Load and Temperature	7.438	4	1.860	3.06*	2.45	5.9
Interactions Between Actuation Rates, Loads Temperatures	5.236	8	.654	1.08	2.02	0
Residual	65.738	108	.609			43.6
Total	154.282	134				

As in the case of the data on cycles to first miss, the total failure data was converted to a more statistically useful form by means of a logarithmic transformation. The results of the analysis of variance for total failure are shown in Table 3-5. Again contact load, temperature, and the contact load-temperature interaction are the significant affectors of cycles to failure.

To obtain a clearer meaning of the magnitude of the contribution to variance of the significant factors, calculations were made of the components of variance. These results for first miss shown in the right hand column of Table 3-4 indicate that contact load is responsible for 48% of the variance observed in this experiment. The interaction between temperature and contact load produced 5.9% of the total variation. It was further indicated that 2.5% of the variation was a direct result of the different temperature levels used, while 43.6% of the variation is residual variance.

TABLE 3-5. ANALYSIS OF VARIANCE FOR RELAYS TO TOTAL FAILURE

Source of Variance	Sums of Squares	Degrees of Freedom	Mean Squares	F Ratio	$F_{.05}$	% of Contribution To Variance
Between Actuation Rates	2.39033	2	1.19517	2.25	3.07	0
Between Contact Loads	56.00185	2	28.00093	52.72*	3.07	49 0
Interactions Between Actuation Rates, Contact Load	1.21974	4	.30494	.57	2.45	0
Between Temperatures	4.32667	2	2.16334	4.07*	3.07	3.0
Interactions Between Actuation Rates, Temperatures	1.98908	4	.49727	.94	2.45	0
Interactions Between Contact Loads, Temperatures	6.17958	4	1.54490	2.91*	2.45	5.4
Interactions Between Actuation, Contact Loads, Temperature	5.05228	8	.63154	1.19	2.02	0
Residual	57.35920	108	.53110			42.6
Total	134.51873	134				

*Denotes significance at the $F_{.05}$ level.

Residual variance is a conglomeration of the differences from part to part, testing error, and variations due to other stresses that may not have been controlled during the experiment. Another possible source of error included may have been the infant mortality failure of several of the parts at the higher stress levels.

The components of variance for total failure in the right hand column of Table 3-5 lists 49% of the variance as explainable by the differences in contact load. The interaction accounted for 5.4% and temperatures for 3%. The residual was 42.6%. Therefore, the results of the analyses performed to date on both first miss and total failure criteria are very similar.

3.3.1.1 t TESTS

The analysis of variance indicated that the main effects of contact load and temperature and the interaction between these two stresses affected the life of relays. To gain knowledge of the manner in which they affected mean life it is necessary to perform a series of t tests to recognize the test runs which result in mean cycles to failure that are significantly different.

Since actuation rate was not significant it is reasonable to lump the data across all levels of it before performing the t tests to evaluate the differences between the means of the significant stress levels. This combination resulted in the logarithmic mean values shown in Table 3-6 for the data on first miss.

TABLE 3-6. CONTACT LOAD AND TEMPERATURE INTERACTIONS - RELAYS (FIRST MISS)

	Contact Load		
Temperature	3 amps	6 amps	8 amps
25°C	5.739	5.189	3.766
100°C	6.056	5.148	4.132
150°C	6.010	5.069	4.940

The t test calculations are as follows:

$$t_{.05} = \frac{\bar{x}_1 - \bar{x}_2}{\sqrt{\frac{\hat{\sigma}_x^2}{n_1} + \frac{\hat{\sigma}_x^2}{n_2}}}$$

where $\bar{x}_1 - \bar{x}_2$ = the difference between any two cells above cell values

$$1.66 = \frac{\bar{x}_1 - \bar{x}_2}{\sqrt{\frac{.609}{15} + \frac{.609}{15}}} \qquad \bar{x}_1 - \bar{x}_2 = .47$$

$\hat{\sigma}_r^2$ = the residual error term from the analysis of variance

n = the sample size of each cell

$t_{.05}$ = Students t value for a significance level of .05

Therefore a difference of greater than .47 between any two values in the above matrix suggests a high probability that they came from populations with different means. Inspection of the matrix shows that the combined stress treatments fall into the following groups:

3 amps, 100°C = 6.056 3 amps, 150°C = 6.010 3 amps, 25°C = 5.739	Group 1
6 amps, 25°C = 5.189 6 amps, 100°C = 5.148 6 amps, 150°C = 5.069 8 amps, 150°C = 4.940	Group 2
8 amps, 100°C = 4.132 8 amps, 25°C = 3.766	Group 3

The implication here is that the variation within each group could have occurred by chance. The variation between groups is large enough to say with confidence that the observed differences were due to the significant stresses applied or to their interactions.

A closer analysis therefore says that at 3 amps of contact load the differences observed between all 3 levels of temperature and all 3 levels of actuation rate were not large enough to say that they did not occur by chance. This same condition held for the parts operated at 6 amps. However an interaction between temperature and contact load at 150°C and 8 amps respectively also made the relays tested at these conditions a member of group 2 with respect to mean cycles to first miss. Group 3 is made up of the test conditions which resulted in an even greater reduction in mean cycles to first miss.

An explanation of the physical meaning of Groups 1, 2, and 3 is in order. Group 1 includes Test Run No. 1 (3 amps, 25°C, 1 cycle/second) which was designated as normal operating conditions. All the other test runs were selected in the hope of inducing a shorter number of cycles to failure in an orderly manner in order to be able to specify a useful accelerated test method.

The analysis of variance suggested that contact load was the greatest contributor to reducing the mean number of cycles to failure. The other stresses applied to the relays operated at 3 amps changed the life characteristics in a random manner. Six amps contact load accounted for a large reduction in average cycles to first miss. Eight amps and 150°C produced similar results. The interaction can probably be explained in the following terms. At 150°C there is outgassing of organic material from either the coil or insulation material. It is hypothesized that this material forms on the contacts and reduces the probability of the contacts sticking and welding.

The t tests on the total failure data resulted in almost identical results. The matrix of logarithmic means lumped across actuation rates is shown in Table 3-7.

TABLE 3-7. CONTACT LOAD AND TEMPERATURE INTERACTIONS

Temperature	Contact Load		
	3 amps	6 amps	8 amps
25°C	5.885	5.246	3.905
100°C	6.167	5.276	4.432
150°C	6.069	5.214	5.051

The interval required for significance at the $t_{.05}$ level between any two of the above means was calculated to be .44.

Therefore the cells in the above matrix fall into the following groups:

3 amps, 100°C = 6.167 3 amps, 150°C = 6.069 3 amps, 25°C = 5.885	Group 1
6 amps, 100°C = 5.276 6 amps, 25°C = 5.246 6 amps, 150°C = 5.214 8 amps, 150°C = 5.051	Group 2
8 amps, 100°C = 4.432	Group 3
8 amps, 25°C = 3.905	Group 4

Group 1 is representative of normal operating conditions, while Groups 2, 3, and 4 are cases where the combined stresses reduced the mean life. This grouping incidentally is exactly the same as was found in the first miss data, except that the first miss data analysis showed that 8 amps, 100°C, and 8 amps, 25°C were not significantly different from each other. Groups 3 and 4 above are thought to be unsuitable for use as accelerated reliability test methods because the stresses induced were so severe that they caused many initial failures. Also the analysis of the failed parts from these cells reflected this severity in the form of a greater incidence of early failures due to contact welding. Therefore based on the analysis concluded to this point, it would appear that the most logical set of stresses to be investigated for use as an accelerated reliability test method is one of the test runs from Group 2.

3.3.1.2 COMPARISON OF FIRST MISS AND TOTAL FAILURE RESULTS

The analysis of variance performed on the data where failure was defined as first miss, indicated that the stresses affecting relay life were contact load, temperature, and the interactions between contact load and temperature. These same factors were significant after an analysis of the results where total failure (3rd miss) was the definition of failure. Furthermore the components of variance study produced results that were extremely similar in both cases. The residual variance of first miss data was .609 while for total failure it was .531.

The t tests found the same combinations of effects belonged to groups which could have come from populations with the same mean.

Based on these similarities of results, it was assumed that the same results could be obtained by analyzing data from either first miss or from third miss (so called, total failure). Since reduced test time is one of the objectives of accelerated testing it would seem that all future analyses of this type could be limited to first miss.

As an additional measure of how well the first miss and total failure test results agreed, a linear regression was performed. The objective was to calculate the correlation coefficient using the mean values of each of the 27 test runs. The total failure means were considered the independent variable while the first miss means were the dependent variable. The correlation coefficient was .991. This is considered another strong justification for basing future results on first miss information.

3.3.2 FAILURE ANALYSIS OF CRYSTAL CAN RELAYS

At the conclusion of the test to total failure, each relay was removed from its can and inspected under a microscope to establish the reason for failure. A detailed description of the inspection report for each relay is given in Appendix III.

The failure modes detected and the definition of each is as follows:

1. Material transfer between the normally open contact and the blade, increased the contact gap beyond the limits of blade travel.

2. Material erosion from the normally open contacts or from the blades, increased the contact gap beyond the limits of blade travel.

3. Normally open contacts welded to the blade.

4. Normally open contact melted, forming into a droplet or ball, reducing the contact gap.

5. Blade became distorted so that the normally open contact makes before the normally closed contact breaks.

The numbers designating each of the failure modes defined above are shown in Table 3-8. The failure mode of each relay tested is shown beside the number identifying each part.

A general conclusion is immediately evident from this table. The relays operated at 8 amps in most cases reflected a high incidence of welding (Failure Mode No. 3) and melting of contacts (Failure Mode No. 4). The contacts of the relay were bifurcated and unless they were perfectly aligned the 8 amp load literally destroyed the part quite quickly. It can probably be safely assumed that 8 amps is beyond the upper limit of usefulness as an accelerating factor since it definitely introduces a change in failure mode. It can be noted from Table 3-8 that even the 8 amp test runs at 150°C (the ones which were reflections of the interaction between contact load and temperature in the analysis of variance) experienced some initial failures in the form of welded contacts after only one to ten actuations (see the asterisks in Test Runs 7, 9, and 27).

Other observations from the standpoint of failure mode analysis seem to indicate that 6 amps and 1 cycle per second tends to result in some welding (No. 3) and melting (No. 4). This condition is not evident at 10 and 30 cycles per second. A satisfactory explanation of this is given by Yanikoski (Reference 55). He points out that higher actuation rates result in lower mean temperature rises. This explains the much longer mean life found in the present study at higher actuation rates and the change in failure modes experienced at 6 amps and 1 cycle per second.

Failure modes 1 (material transfer) and 2 (material erosion) are closely allied. It is questionable as to whether they should have been described separately. The appearance is that they represent a matter of degree of severity of the effect of the same failure mechanism.

In summary the failure analysis suggests that the most desirable ranges of stresses for use as accelerated reliability test methods is in the area of 6 amps contact load and the higher actuation rates. The test runs at 3 amp loads nearly all result in mean cycles to failure not significantly different from Test Run 1 (normal conditions) and 8 amps is too severe since it causes initial failures and erratic performance unless the parts are perfect specimens. Six amps and either of the two highest actuation rates seem desirable since they display the same failure mode as Test Run 1. The higher temperature levels result in random life patterns with the suspicion that Test Runs 23 and 24 do not fit the Weibull distribution. Also a test at different than room temperature must clearly demonstrate superiority in order to merit the use of the additional equipment.

3.3.3 ANALYSIS RELATED TO RELAY LIFE DISTRIBUTION FUNCTIONS

The data analysis methods utilized in the study of accelerated reliability test methods for relays follows the procedure used in the study of switches. The same procedure of studying the life distribution functions of relays on first miss data only will be followed.

TABLE 3-8. RELAYS: FAILURE MODES

Actuation Rate		1 Cycle/Second			10 Cycles/Second			30 Cycles/Second		
Contact Load		3 amps	6 amps	8 amps	3 amps	6 amps	8 amps	3 amps	6 amps	8 amps
Ambient Temperature	25°C	35-1 36-1 87-1 88-1 89-1, 4 #1	1-1, 3 4-1, 4 90-1 91-1, 4 92-1 #4	22-3, 4 32-1 81-1 82-1, 4 83-1 #7 *9-Initial Failures	66-1 47-1 115-1 116-1 117-1 #10	110-1 111-1 112-2 113-1 114-1 #13	43-1 44-3, 5 104-1 105-3 106-3, 5 #16	37-1 38-1 93-1 94-1 95-1 #19	99-2 100-2 101-2 102-2 103-2 #22	16-3 17-1 70-3 71-3 72-1 #25
	100°C	50-2 51-2 141-2 142-2 143-2 #2	5-1, 3 6-1 144-1 145-1 157-1 #5	54-4 55-4 148-1 149-1 158-1 #8	52-1 53-2 126-1 127-1 128-1 #11	150-1 151-1 152-1 153-1 154-1 #14	56-3, 4 57-3, 4 129-1 130-1 133-1, 3 #17	48-2 49-2 123-2 124-2 125-2 #20	20-1 21-1 76-1 77-1 78-1 #23	12-1 13-1 64-1 65-1 66-1 #26
		39-1 40-1 96-1 97-1 98-1 #3	118-1 119-1 120-1, 4 121-1 122-1 #6	41-1, 3 45-1, 4 107-2 108-2 109-2 #9 *1-Initial Failure	58-2 59-2 132-2 133-1 134-2 #12	135-2 136-2 137-2 155-1 156-1 #15	7-1 8-1 138-1 139-1, 3, 4 140-1 #18	26-2 27-2 84-2 85-2 86-2 #21	18-2, 3 19-5 73-1 74-1 75-1 #24	10-1 11-1 61-1 62-1, 3 63-1, 3 #27 *1-Initial Failure

3.3.3.1 WEIBULL PLOTS

A plot on Weibull probability paper of cycles to first miss for each of the 27 relay test runs was prepared. The line of best fit was calculated on the computer by the method of least squares and drawn on each chart. The Weibull charts are presented in Appendix VI-2. The ordinate on the charts, which is percent defective, was taken as the median rank value. The scale used on the cycles to failure axis was selected for ease of plotting the data and for clarity in using the graph for verifying the calculations of α_K and β. The α (Weibull scale parameter) as it appears on each chart is in coded form. The decoding theory and method are discussed in detail in Appendix VI-1 of this report. The estimates of the Weibull parameters suffer since only five relays were included in each test run. However, most of the plots exhibit reasonably good Weibull fits. In some cases however the range of cycles to first miss was so great that three cycle paper was not sufficient to allow plotting of all the points. This situation prevailed on Test Runs 7, 8, 16, 24, 25. It is interesting to note that four out of five of these test runs were at contact loads of 8 amps. These were test conditions where many early failures were experienced due to the deterioration or welding of one arm of the bifurcated normally open contact.

Several test runs such as numbers 4, 10, 13, 14 and 23 give the appearance that perhaps they would display much different Weibull parameters if a few more observations were available and if some of the early failures were discarded from inclusion in the selection of the line of best fit. The Weibull parameters calculated for them should be used with reservation. A summary of the α_K (coded Weibull scale parameter), α_o (uncoded Weibull scale parameter) and β (Weibull shape parameter) is shown in Table 3-9.

3.3.3.2 TESTS FOR GOODNESS OF FIT

The tests for goodness of fit of each of the 27 test runs to its respective Weibull distribution were performed on relays in the same manner as on switches. The reader is referred to Section 2.3.3.2 for the explanations of the principles underlying the use of each of the three tests. The results were:

1. **F Tests**

   The F tests performed on the 27 relay test runs indicated that all fit the Weibull at the $F_{.05}$ level of significance except Test Runs 14 and 23. It will be recalled that these runs were also mentioned as suspect from the visual inspection of the Weibull plots. The pattern at the $F_{.01}$ level of significance is much more clouded as might be suspected with only 5 observations per test run. The F test results are shown in Table 3-10. The check marks in the table are indications of lack of proof of the Weibull fit at the indicated level of significance.

2. **Kolmogorov - Smirnov Tests**

   The Kolmogorov - Smirnov Test for goodness of fit was applied to each of the 27 relay test runs and it indicated that in all cases the Weibull distribution could have been applicable.

TABLE 3-9. WEIBULL PARAMETERS FOR RELAYS (FIRST MISS)

Actuation Rate		1 Cycle/Second			10 Cycles/Second			30 Cycles/Second		
Contact Load		3 amps	6 amps	8 amps	3 amps	6 amps	8 amps	3 amps	6 amps	8 amps
Ambient Temperature	25°C	Run #1 β = 1.60 $\hat{\lambda}_s$ = 32.66 $\hat{\lambda}_o$ = 8156 x 10^6	Run #4 β = 0.78 $\hat{\lambda}_s$ = 7.56 $\hat{\lambda}_o$ = 9930	Run #7 β = 0.25 $\hat{\lambda}_s$ = 1.56 $\hat{\lambda}_o$ = 15.6	Run #10 β = 1.16 $\hat{\lambda}_s$ = 5.21 $\hat{\lambda}_o$ = 2611 x 10^3	Run #13 β = 1.99 $\hat{\lambda}_s$ = 6.11 $\hat{\lambda}_o$ = 5665 x 10^5	Run #16 β = 0.22 $\hat{\lambda}_s$ = 2.27 $\hat{\lambda}_o$ = 10.38	Run #19 β = 1.70 $\hat{\lambda}_s$ = 79.06 $\hat{\lambda}_o$ = 2525 x 10^7	Run #22 β = 1.[illegible]1 $\hat{\lambda}_s$ = 3.97 $\hat{\lambda}_o$ = 1669 x 10^3	Run #25 β = 0.33 $\hat{\lambda}_s$ = 2.09 $\hat{\lambda}_o$ = 28.24
	100°C	Run #2 β = 0.66 $\hat{\lambda}_s$ = 6.10 $\hat{\lambda}_o$ = 8190	Run #5 β = 0.79 $\hat{\lambda}_s$ = 1.08 $\hat{\lambda}_o$ = 16,756	Run #8 β = 0.28 $\hat{\lambda}_s$ = 1.8 $\hat{\lambda}_o$ = 12.5	Run #11 β = 2.69 $\hat{\lambda}_s$ = 1719.9 $\hat{\lambda}_o$ = 6067 x 10^{12}	Run #14 β = 0.79 $\hat{\lambda}_s$ = 1.06 $\hat{\lambda}_o$ = 16,390	Run #17 β = 3.55 $\hat{\lambda}_s$ = 2.32 $\hat{\lambda}_o$ = 367.7	Run #20 β = 2.00 $\hat{\lambda}_s$ = 8955.3 $\hat{\lambda}_o$ = 8955 x 10^{14}	Run #23 β = 0.25 $\hat{\lambda}_s$ = 3.69 $\hat{\lambda}_o$ = 34.9	Run #26 β = 1.17 $\hat{\lambda}_s$ = 21.33 $\hat{\lambda}_o$ = 1921 x 10^3
	150°C	Run #3 β = 1.21 $\hat{\lambda}_s$ = 17.12 $\hat{\lambda}_o$ = 1921 x 10^6	Run #6 β = 1.06 $\hat{\lambda}_s$ = 6.05 $\hat{\lambda}_o$ = 9569 x 10^6	Run #9 β = 1.35 $\hat{\lambda}_s$ = 8.17 $\hat{\lambda}_o$ = 2052 x 10^3	Run #12 β = 1.22 $\hat{\lambda}_s$ = 24.78 $\hat{\lambda}_o$ = 3180 x 10^6	Run #15 β = 1.39 $\hat{\lambda}_s$ = 4.06 $\hat{\lambda}_o$ = 3618 x 10^6	Run #18 β = 0.96 $\hat{\lambda}_s$ = 2.51 $\hat{\lambda}_o$ = 1258 x 10^2	Run #21 β = 2.11 $\hat{\lambda}_s$ = 601.06 $\hat{\lambda}_o$ = 2135 x 10^{10}	Run #24 β = 0.34 $\hat{\lambda}_s$ = 1.20 $\hat{\lambda}_o$ = 60.1	Run #27 β = 1.80 $\hat{\lambda}_s$ = 2.68 $\hat{\lambda}_o$ = 6230 x 10^6

TABLE 3-10. F TEST FOR GOODNESS OF WEIBULL FITS (RELAY)

Test Run	F Ratio	F.05	F.01
1	23.8		x
2	23.8		x
3	83.0		
4	15.0		x
5	32.8		x
6	27.8		x
7	12.3		x
8	58.4		
9	27.8		x
10	58.6		
11	83.0		
12	105.0		
13	27.6		x
14	5.3	x	x
15	50.8		
16	30.0		x
17	140.0		
18	23.9		x
19	50.1		
20	82.8		
21	58.6		
22	30.9		x
23	1.0	x	x
24	58.3		
25	27.7		x
26	82.8		
27	23.8		x

Note: $F_{.05}$ = 10.1

$F_{.01}$ = 34.1

3. Comparison of $\bar{x}_i$ and $\tilde{\mu}_i$

The third and perhaps the most sensitive method used for measuring goodness of fit of the relay test data to the Weibull distribution was by a comparison of the expected value of the Weibull distribution being fit to the test data and the mean of the test data. The explanation of the justification for its use is covered in Section 2.3.3.2 of this report. The values of $\tilde{\mu}_i$ and $\bar{x}_i$ are compared in Table 3-11. By examining the difference between the two values one can easily pick out certain cells that do not fit the Weibull distribution plotted for them. For instance, Test Runs 7, 8, 16, 17, 23, 24, 25 display great differences. Five of these are relays that had been run at 8 amps and a considerable number of early failures were noted. Test Runs 23 and 24 were conducted during a period when trouble was experienced on the miss detection equipment and hence the data in both of those cells is suspect. Test Runs 2, and 14 exhibit a fairly large difference between $\bar{x}_i$ and $\tilde{\mu}_i$ which is probably due to early failure in each of these runs.

3.3.3.3 CUMULATIVE FAILURE DISTRIBUTIONS

The cumulative failure distributions of each of the 27 relay test runs are shown in Appendix II. One of the ground rules established for the selection of an accelerated test is that the probability of failure of the accelerated test method must be higher at all points over the range of interest than that of the parts tested under normal conditions. Only Test Runs 2, 3, 11, 12, 19, 20 and 21 fail to meet this rule of thumb. They happen to be test runs where the contact loads was also 3 amps and most of them lasted longer than Test Run 1 in terms of mean cycles to failure. From the remaining possible test runs it remains to select a test run in which the probability of failure rises quite quickly and yet where no failure mode change occurs. Failure mode changes occurred at 8 amps in most cases. Hence, the selection appears to be narrowed to the 6 amps contact load. It appears from comparing the charts of the failure density functions of these runs the most favorable ones are 4, 24, 5, and 14.

3.3.4 CALCULATION OF HAZARD RATES

One of the properties of the relays operated at the various combined environmental and operating stresses that is of interest is the hazard rate. Under the assumption that the life of relays is according to the Weibull distribution, then the hazard rate is represented by the expression $\frac{\beta}{\alpha} t^{\beta-1}$ where

β = Weibull shape parameter

α = the Weibull scale parameter

t = time in cycles

A plot of the hazard rate of each test run can be easily made from the information in Table 3-12. Three values of t are given and utilizing these, the time variant hazard rates can be plotted on log log paper.

TABLE 3-11. COMPARISON OF $\tilde{\mu}_i$ AND $\bar{x}_i$ OF RELAY TEST RUNS

Test Run	$\tilde{\mu}_i$	$\bar{x}_i$
1	679, 440	675, 842
2	1, 072, 000	678, 790
3	938, 000	885, 750
4	118, 450	103, 668
5	233, 700	214, 757
6	239, 760	225, 353
7	1, 012, 500	72, 681
8	104, 000	17, 638
9	42, 182	41, 321
10	399, 840	353, 273
11	1, 766, 000	1, 762, 647
12	1, 291, 680	1, 162, 951
13	278, 380	258, 522
14	222, 300	146, 275
15	246, 240	239, 474
16	2, 088, 000	79, 962
17	78, 200	45, 613
18	278, 100	231, 035
19	1, 160, 900	1, 118, 691
20	2, 405, 700	2, 299, 030
21	1, 772, 000	1, 774, 647
22	327, 760	282, 724
23	25, 000, 000	428, 552
24	957, 000	256, 182
25	182, 000	69, 604
26	127, 845	118, 362
27	140, 304	139, 184

TABLE 3-12. HAZARD RATES FOR RELAYS WHERE FIRST MISS DENOTES FAILURE

Test Run	t = 10	t = 100	t = 1000
1	$.986 \times 10^{-3}$	$.472 \times 10^{-2}$	$.226 \times 10^{-1}$
2	$.369 \times 10^{2}$	$.169 \times 10^{2}$	$.771 \times 10^{1}$
3	$.102 \times 10^{0}$	$.166 \times 10^{0}$	$.269 \times 10^{0}$
4	$.473 \times 10^{2}$	$.265 \times 10^{2}$	$.172 \times 10^{2}$
5	$.291 \times 10^{2}$	$.179 \times 10^{2}$	$.111 \times 10^{2}$
6	$.133 \times 10^{-2}$	$.918 \times 10^{-2}$	$.635 \times 10^{-}$[illegible]
7	$.289 \times 10^{4}$	$.513 \times 10^{3}$	$.913 \times 10^{2}$
8	$.427 \times 10^{4}$	$.813 \times 10^{3}$	$.155 \times 10^{3}$
9	$.147 \times 10^{1}$	$.330 \times 10^{1}$	$.738 \times 10^{1}$
10	$.603 \times 10^{0}$	$.832 \times 10^{0}$	$.115 \times 10^{1}$
11	$.159 \times 10^{-7}$	$.491 \times 10^{-6}$	$.152 \times 10^{-4}$
12	$.649 \times 10^{-1}$	$.108 \times 10^{0}$	$.179 \times 10^{0}$
13	$.114 \times 10^{-1}$	$.442 \times 10^{-1}$	$.172 \times 10^{0}$
14	$.288 \times 10^{2}$	$.177 \times 10^{2}$	$.109 \times 10^{2}$
15	$.943 \times 10^{-1}$	$.231 \times 10^{0}$	$.568 \times 10^{0}$
16	$.352 \times 10^{4}$	$.584 \times 10^{3}$	$.969 \times 10^{2}$
17	$.531 \times 10^{3}$	$.188 \times 10^{3}$	$.668 \times 10^{2}$
18	$.651 \times 10^{1}$	$.567 \times 10^{1}$	$.494 \times 10^{1}$
19	$.337 \times 10^{-3}$	$.169 \times 10^{-2}$	$.848 \times 10^{-2}$
20	$.197 \times 10^{-9}$	$.124 \times 10^{-7}$	$.785 \times 10^{-6}$
21	$.127 \times 10^{-5}$	$.164 \times 10^{-4}$	$.211 \times 10^{-3}$
22	$.102 \times 10^{1}$	$.131 \times 10^{1}$	$.169 \times 10^{1}$
23	$.127 \times 10^{4}$	$.227 \times 10^{3}$	$.403 \times 10^{2}$
24	$.124 \times 10^{4}$	$.271 \times 10^{3}$	$.592 \times 10^{2}$
25	$.250 \times 10^{4}$	$.534 \times 10^{3}$	$.114 \times 10^{3}$
26	$.170 \times 10^{-1}$	$.251 \times 10^{-1}$	$.371 \times 10^{-1}$
27	$.229 \times 10^{-2}$	$.174 \times 10^{-1}$	$.132 \times 10^{0}$

3.3.3.5 CONFIDENCE LIMITS FOR WEIBULL PARAMETERS

The confidence limits for β (The Weibull shape parameter) and α, (the Weibull scale parameter) have been calculated for relays and are presented in Tables 3-13 and 3-14. Since the Weibull line of best fit was the regression line calculated by the method of least squares, the confidence limits are set on the slope and intercept of this line. The details of the procedure used are described in Appendix VII.

3.3.4 ANALYSIS OF RELAY OPERATING PARAMETERS

Throughout the study program on relays, periodic measurements were taken on the following operating parameters:

- Coil resistance
- Contact resistance
- Pickup voltage
- Dropout voltage
- Operate time
- Release time
- Contact bounce

As in the case of this part of the analysis performed on switches (Section 2.3.4) it should be pointed out that this evaluation of changing parameters was not one of the prime objectives of the study. However approximately 100 linear regression analyses were performed on various combinations of cycles to first miss, cycles to total failure and to the changes over time in each of the operating parameters named above.

Time did not permit the complete evaluation of all of the regression and correlation relationships studied but in general the results were inconclusive. This was probably due to measurement errors that were large in relation to the magnitude of the changes occurring in the parameters during the life cycle of the parts.

3.4 SELECTION OF ACCELERATED RELIABILITY TEST METHOD (RELAYS)

The general procedure for selecting desirable test runs for use as accelerated reliability test methods is described in detail in Section 1.4. This section is an example of the application of those rules.

Test Run 1 in the relay study program was defined as normal operating conditions (3 amps, 1 cycle/second, 25°C). Therefore the other 26 test runs were studied as potential accelerated test methods. Table 3-15 shows the comparison of each test run to the factors which define a desirable method. An "X" in the table means that a particular test run possesses the desirable trait.

The logic associated with the specification of the most desirable accelerated test method is as follows:

The analysis of variance and its associated computations indicated that all test runs at 3 amps contact load resulted in mean cycles to first miss

TABLE 3-13. CONFIDENCE LIMITS FOR β (RELAYS)

Test Run	β	$\beta(.025)$	$\beta(.975)$
1	1.68	1.127	2.233
2	.66	.181	1.139
3	1.21	.916	1.504
4	.78	.125	1.436
5	.79	.316	1.264
6	1.84	1.344	2.336
7	.25	0	.966
8	.28	0	.530
9	1.35	.866	1.834
10	1.14	.771	1.509
11	2.49	2.204	2.776
12	1.22	.948	1.492
13	1.59	1.076	2.104
14	.79	0	1.612
15	1.39	.990	1.790
16	.22	0	.709
17	.55	.318	.782
18	.94	.404	1.476
19	1.70	1.305	2.095
20	2.80	2.488	3.112
21	2.11	1.763	2.457
22	1.11	.615	1.605
23	.25	0	1.508
24	.34	.007	.673
25	.334	0	.779
26	1.17	.865	1.475
27	1.88	1.338	2.422

TABLE 3-14. CONFIDENCE LIMITS FOR a_o (RELAYS)

Test Run	a_o	$a_o(.025)$	$a_o(.975)$
1	8.154×10^9	4.611×10^9	1.442×10^{10}
2	8180	4956	13,338
3	1.921×10^7	1.409×10^7	2.592×10^7
4	9938	5084	19,612
5	16,755	10,253	27,315
6	9.589×10^9	5.758×10^9	1.613×10^{10}
7	15.4	7.334	32.22
8	12.5	9.153	17.02
9	2.052×10^6	1.244×10^6	3.091×10^6
10	2.611×10^6	1.785×10^6	3.816×10^6
11	4.847×10^{15}	3.774×10^{15}	6.878×10^{15}
12	3.200×10^7	2.334×10^7	4.128×10^7
13	5.445×10^8	3.174×10^8	7.885×10^8
14	16,398	7011	38,379
15	3.613×10^7	2.375×10^7	5.446×10^7
16	10.38	6.232	17.28
17	367.7	288.8	466.7
18	125,801	71,837	217,982
19	2.525×10^{10}	1.675×10^{10}	3.804×10^{10}
20	8.955×10^{17}	6.6342×10^{17}	1.2088×10^{18}
21	2.135×10^{13}	1.431×10^{13}	2.882×10^{13}
22	1.409×10^6	838,463	2.349×10^6
23	34.9	9.512	128.07
24	60.1	42.71	85.15
25	28.24	18.31	45.95
26	1.021×10^6	741,208	1.406×10^6
27	6.230×10^9	3.565×10^9	1.093×10^{10}

TABLE 3-15. FACTORS FOR SELECTING DESIRABLE ACCELERATED RELIABILITY TEST METHOD (RELAYS)

Factors	Test Run 1	2	3	4	5	6	7	8	9	10	11	12	13	14	15	16	17	18	19	20	21	22	23	24	25	26	27
Short Mean Life				x	x	x	x	x	x				x	x	x	x	x	x				x	x	x	x	x	x
Significant Accelerating Stresses				x	x	x	x	x	x				x	x	x	x	x	x				x	x	x	x	x	x
Constan Failure Mode		x	x	x	x	x				x	x	x	x	x	x				x	x	x	x	x	x			
Cumulative Failure Distribution							x	x	x	x			x	x	x	x	x	x				x	x	x	x	x	x
Hazard Rate				x	x	x	x	x	x	x			x	x	x	x	x	x				x		x	x		x
Fits Weibull Distribution		x	x		x	x			x		x	x			x			x	x	x	x	x				x	x
Short Calendar Test Time										x	x	x	x	x	x	x	x	x	x	x	x	x	x	x	x	x	x
Economical		x	x	x	x	x	x	x	x	x	x	x	x	x	x	x	x	x	x	x	x	x	x	x	x	x	x

that could have come from populations with the same mean. Hence they would not qualify as good accelerated test methods. The test runs at 8 amps and 25°C and 8 amps and 100°C resulted in the shortest mean lives but these conditions resulted in many initial failures and changes in failure mode. The relays in Test Run 1 (normal operating conditions) failed due to material transfer between the blade and contacts increasing the contact gap beyond the range of blade travel. The 8 amp condition resulted in many welded contacts. If the two arms of the bifurcated contacts were not perfectly aligned, one of them was melted back into a molten ball which reduced the gap and sometimes welded to the blade.

Eight amps and 150°C, although its mean life was higher, still suffered from the welding and initial failures problem when the arms of the bifurcated contacts were not perfectly aligned. This contact load is simply too severe to hope to use on this type of relay as an accelerated test method. (Note that the 8 amps contact load stress would appear to be an excellent burn-in test. Any relays that were out of adjustment would very likely fail quite quickly. Ones that were perfectly aligned were operated during this study for over 200,000 cycles at this load.)

The selection of the accelerated test method is reduced to the nine test runs at 6 amps contact load.

The tests for goodness of fit by the comparison of $\tilde{\mu}_i$ and $\overline{x}_i$ indicate that of the test runs at 6 amps contact load runs 23 and 24 exhibit a large deviation and hence probably do not fit the Weibull. These were test runs where trouble was experienced with the miss detection device hence the cycles to first miss are probably inaccurate.

Visual inspection of the Weibull plots of Test Runs 4, 13 and 14 indicates that perhaps the line fit to the data would not hold if more observations were available. Early failures tend to deflect the line when it is fit by the method of least squares.

This leaves Test Runs 5, 6, 15 and 22 for consideration as accelerated reliability test methods. Test Run 5 displays a decreasing hazard rate and therefore an indication of a severe early stress type of phenomenon that does not seem to lend itself to a study of wearout type of failure.

Test Runs 6 and 15 are very close when their respective cumulative failure density functions are compared. However 15 results in the highest probability of failure until approximately 240,000 cycles. If Test Runs 6 and 15 are compared with regard to elapsed calendar time for performance of the test it is clear that Test Run 15 at 6 amps, 150°C, and 10 cycles per second is preferred. Test Run 22 at 6 amps, 25°C and 30 cycles per second is even more satisfactory in terms of required calendar time. However Test Run 15 displays a higher cumulative failure distribution over the range of interest. Therefore either of these test runs has merit as an accelerated reliability test method.

3.5 VALIDATION OF NORMAL TEST CONDITIONS

The failure distribution describing life times under the normal conditions of this report has been shown to be Weibull. In obtaining valid comparisons of the experience of this report with respect to relays with those of the literature, three problems arose:

1. Test conditions (environmental and operating) could not be found which exactly duplicated the normal test conditions of this report.

2. The failure data in the literature usually appeared in summary form i.e., failure rate in percent per 1000 cycles or failure rate in percent per 10,000 cycles etc. The actual test time, number of failures, number of items on test were not given.

3. Failure definitions were generally not given in the literature.

Actually problem 1 is not as serious as it appears since "similar" conditions can certainly give indications of agreement. However 2 and 3 could seriously affect the comparisons. The reason 2 is a problem is because when a Weibull distribution prevails the interchange of time and units on test is not permissible and moreover the failure rate depends on t (is not constant) hence to compare test experience requires test time to be known, number of failures and number of items on test. The problem caused by 3 is obvious.

Fortunately FARADA and manufacturer data was available which provided the necessary information even though the conditions of the test were somewhat different. Failures caused by definitions not used in this report were eliminated from the FARADA failure data.

Table 3-16 presents for the FARADA data and the manufacturer the number of failures experienced in the tests of 100,000 cycles in length and the number of relays put on test. The number of failures quoted is the actual number in the case of the manufacturer's data. For the FARADA data one failure was deducted because it was due to a definition which would not have been a failure in this study. The operating temperature of the FARADA and manufacturer data was 125°C. The expected failures in 100,000 cycles is shown for test run #1 and test run #3. Test run #1 shows a discrepancy between the expected and observed results. However when test run #3 is used (operating temperature 150°C) a statistical test shows no difference in the observed and expected results. The numbers in the last two columns were computed by:

Expected number of failures Test Run #1 = $230F_1$ (100,000)
Expected number of failures Test Run #1 = $9F_1$ (100,000)

Expected number of failures Test Run #3 = $230F_3$ (100,000)
Expected number of failures Test Run #3 = $9F_3$ (100,000)

TABLE 3-16. COMPARISON OF TEST RESULTS WITH FIELD DATA

Source	Number of Items on Test	Length of Test	Number of Failures	Expected Number of Failures Based on this Report, Test Run 1	Expected Number of Failures Based on this Report, Test Run 3
Relay Manu-facturer	230	100,000 opera-tions	14	6.9	13.8
FARADA Reports	9	100,000 opera-tions	1	0.27	0.54

SECTION 4.0 MATHEMATICAL MODELS

4.1 SUMMARY

The goal of this section is to present possible mathematical representations of the physical process which occurs when moving from accelerated test conditions to normal test conditions. This is necessary so that when other accelerated tests (denoted by * throughout) are conducted (at conditions similar to those of this report) the normal condition parameters α, and β can be estimated. Five separate models are derived, presented, and discussed.

Model 1

This model makes the (restrictive) assumption that β_A and β_N are equal and thus only the α_A and α_N differ. In this case there exists a transformation

$$y = cx \qquad c > 0$$

and if $c < 1$ the acceleration is a true time acceleration, i.e., the physical laws being left unchanged.

Model 2

The model considers a time transformation of the form $y = cx^d + a$. It is shown that it appears $a \equiv 0$. This transformation allows for $\beta_A \neq \beta_N$ and $\alpha_A \neq \alpha_N$. Model 1 is a special use of this model with $d \equiv 1$ and $a \equiv 0$.

Model 3

This model is based on the assumption that the time transformation function on the cumulative distribution function TFC, say $g(x)$.

where

$$F_N(x) = F_A\,[g(x)] \text{ all } x$$

is constant for all accelerated tests, i.e.,

$$g(x) = g^*(x)$$

where $g(x)$ is the TFC of this report and $g^*(x)$ is the TFC of a future accelerated test. It was shown that Models 2 and 3 are identical.

Model 4

This model assumes that the time transformation function on the hazard rates (TFH) say $j(x)$ where

$$h_N(x) = h_A\,[j(x)]$$

is constant for all accelerated tests, i.e.,

$$j(x) = j^*(x) \quad \text{all } x.$$

Model 5

This model is based on the assumption that the ratio of the hazard rates

$$K(x) = \frac{h_N(x)}{h_A(x)}$$

is the same for all accelerated tests, i.e.,

$$K(x) = K^*(x)$$

The algorithms for these models appear in table 4-1. Table 4-2 presents $\tilde{\alpha}_A$, $\tilde{\beta}_A$, $\tilde{\alpha}_N$, $\tilde{\beta}_N$ as discovered for switches and relays in this report. Note that the "~" always denotes an estimate of the quantity under the "~" and that * denotes a test other than the tests of this report.

There are certainly models other than the ones presented which could be considered but the five presented have the advantages that

1. They are simple to express mathematically
2. They are intuitively appealing as representatives of the physical process.

Numerical examples of each model are given in Appendix VIII-6

Which of the five models presented most faithfully represents the physical phenomena occurring in switches and relays when operating and environmental stresses are increased will be further studied. However Models 2 and 3 would appear to be the most logical choices since they relate the cumulative failure distributions of parts failing at both normal and accelerated stress levels and since they describe a compression of the time axis.

4.2 RELATIONSHIP OF THE FAILURE DISTRIBUTION UNDER ACCELERATED AND NORMAL CONDITIONS

In the previous sections accelerated test(s) were recommended which appear feasible from a physical and time standpoint. That is they preserve modes of failure and obtain failure data in short periods of time. However the task still remains to describe (hopefully in mathematical terms) what went on physically when the test conditions were accelerated. More specifically this section addresses itself to this problem:

Suppose, at a future time, an accelerated test similar to the one recommended is run. The problem is: what algorithm or instructions should be

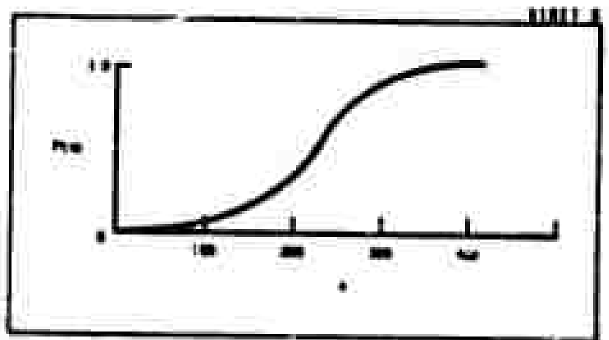

Figure 4-1. Failure Distribution Function (Weibull) Under Normal Conditions

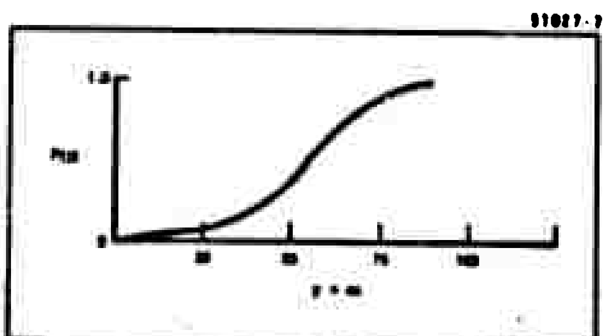

Figure 4-2. Failure Distribution Function (Weibull) Under (Accelerated) Change $y = 1/4\,x$

followed using $\tilde{\alpha}_A^*$ and $\tilde{\beta}_A^*$ to obtain estimates of the normal condition α_N^* and β_N^* say $\tilde{\alpha}_N^*$ and $\tilde{\beta}_N^*$?

For example it is not at all clear that differences are appropriate, i.e.:

$$\tilde{\alpha}_N^* = \tilde{\alpha}_A^* + (\tilde{\alpha}_N - \tilde{\alpha}_A)$$
$$\tilde{\beta}_N^* = \tilde{\beta}_A^* + (\tilde{\beta}_N - \tilde{\beta}_A) \qquad (1)$$

or that ratios are apropos, i.e.:

$$\tilde{\alpha}_N^* = \tilde{\alpha}_A^* \frac{\tilde{\alpha}_N}{\tilde{\alpha}_A}$$
$$\tilde{\beta}_N^* = \tilde{\beta}_A^* \frac{\tilde{\beta}_N}{\tilde{\beta}_A} \qquad (2)$$

If these algorithms are used it is not obvious what physical laws are governing. The best method then is to propose mathematical models, see what algorithm results and then validate these models. The various models are considered in the following subsections.

4.3 MATHEMATICAL MODEL #1: FOR A TRUE ACCELERATED TEST WHEN THE FAILURE DISTRIBUTION IS KNOWN TO BE WEIBULL BOTH AT ACCELERATED AND NORMAL CONDITIONS

It has been demonstrated in this report that the failure distributions are Weibull at both accelerated and normal conditions. Now a certainly appealing definition of a "true" accelerated test is one that: leaves the physical laws of failure unmolested but merely accelerates their action. That is, the time axis is "compressed" but the shape of the distribution is left untouched. For the Weibull distribution this can be accomplished as follows. Suppose the lifetime x at <u>normal conditions</u> is Weibull, i.e.:

$$F(x) = 1 - e^{-\left(\frac{x}{\alpha_N}\right)^{\beta_N}} \qquad x,\ \beta_N,\ \alpha_N > 0 \qquad (3)$$

where the N subscript denotes normal conditions. Now suppose the change of variable:

$$y = cx \text{ is made.} \qquad (4)$$

Then

$$F(y) = 1 - e^{-\frac{(\frac{y}{c})^{\beta_N}}{\alpha_N}}$$

$$= 1 - e^{-y^{\beta_N}/c^{\beta_N}\alpha_N} \qquad y, \beta_N, \alpha_N, c > 0 \tag{5}$$

and hence y is again Weibull with

shape parameter beta = $\beta_N = \beta_A$

and scale parameter alpha = $c^{\beta_N}\alpha_N = \alpha_A$ (6)

Moreover if the distribution of failures at accelerated conditions is Weibull with:

$\beta_A = \beta_N$

and

$\alpha_A \neq \alpha_N$, i.e., $\alpha_A = K\alpha_N$

then there always exists a nontrivial solution to the equation

$$c^{\beta_N} = K \qquad K > 0 \tag{7}$$

and hence if the failure distributions are Weibull at both accelerated and normal conditions with $\beta_A = \beta_N$ there always exists a transformation, $y = cx$ such that there is a compressing or stretching of the time axis by a factor of c. Now if:

$\alpha_A < \alpha_N$

then $\alpha_A = K\alpha_N \rightarrow K < 1 \rightarrow c < 1$ and the transformation $y = cx$ is a compression of the time axis. Since $y = cx = 0$ when $x = 0$ this compressing can be thought of as <u>fastening</u> an elastic line at $x = 0$ and pushing on the line (at $x = \infty$) by a force of "magnitude" c. Since the change $y = cx$ left β unchanged this transformation amounts to lifting the failure distribution off the time axis, compressing the time axis and then setting down the distribution again with its shape unchanged. These ideas are presented in Figures 4-1 and 4-2.

The algorithm for this model 1 is presented in Table 4-1. The derivation of the algorithm is contained in Appendix VIII-1

4.4 MATHEMATICAL MODEL #2: THE GENERAL FORM

When (as it is always assumed) the failure distributions are Weibull at both accelerated and normal conditions the most "general" mathematical expression for the change relationship is: (where x is time under normal conditions)

$$y = cx^d + a$$

$$\Rightarrow x = \frac{(y - a)^{1/d}}{c^{1/d}} \qquad (9)$$

hence

$$F(y) = 1 - e^{-\frac{\left[\frac{(y-a)^{1/d}}{c^{1/d}}\right]^{\beta_N}}{\alpha_N}}$$

$$= 1 - e^{-\frac{(y-a)^{\frac{\beta_N}{d}}}{\left(c^{\frac{\beta_N}{d}}\right)\alpha_N}} \qquad a, y, \alpha_N, \beta_N, d, c > 0 \qquad (10)$$

thus y is again Weibull with

location parameter $\gamma = a$

scale parameter $\alpha_A = \left(c^{\frac{\beta_N}{d}}\right)\alpha_N$ (11)

shape parameter $\beta_A \quad \beta_N/d$

Now in this study γ was always zero so the general form appears to be

$$y = cx^d \qquad (12)$$

It will be noted from (11) that this transformation allows for changes in α and β going from normal to accelerated conditions. The parameter d can be estimated from this report as follows. Since from (11)

$$\beta_A = \frac{\beta_N}{d}$$

$$d = \frac{\beta_N}{\beta_A}$$

and hence

$$\tilde{d} = \frac{\tilde{\beta}_N}{\tilde{\beta}_A} \qquad (13)$$

similarly from (11)

$$\alpha_A = c^{\frac{\beta_N}{d}} \alpha_N$$

$$c = \left(\frac{\alpha_A}{\alpha_N}\right)^{d/\beta_N}$$

and hence

$$\tilde{c} = \left(\frac{\tilde{\alpha}_A}{\tilde{\alpha}_N}\right)^{\tilde{d}/\tilde{\beta}_N} \qquad (14)$$

If it is required that

$F_A(x) \geq F_N(x)$ for all x

restrictions on c and d are easily derived. However it is unnecessary to set this requirement as long as $F_A(x) \geq F_N(s)$ for "small" x so restrictions on c and d are not necessary. The algorithm for this model 2 is given in Table 4-1. The derivation is contained in Appendix VIII-2.

In the next section a model called the: Time transfer function on the cumulative distribution functions (TFC) will be used. It will be shown in that section that that model (TFC) is equivalent to the model of this section, i.e., equivalent to

$$y = cx^d$$

Note that the model of Section 4.3 is this model with d = 1.

4.5 MODEL #3. A TIME TRANSFER FUNCTION ON THE CUMULATIVE DISTRIBUTION FUNCTION (TFC)

Definition: The time transfer function on the cumulative distribution function (TFC) is a function g(x) such that

$$F_N(x) = F_A\,[g(x)] \tag{15}$$

g(x) is easily found for

$$F_N(x) = F_A\,[g(x)] \Rightarrow 1 - e^{-\frac{x^{\beta_N}}{\alpha_N}} = 1 - e^{-\frac{[g(x)]^{\beta_A}}{\alpha_A}}$$

$$\Rightarrow \frac{x^{\beta_N}}{\alpha_N} \quad \frac{g(x)^{\beta_A}}{\alpha_A}$$

$$g(x) = \left(\frac{\alpha_A}{\alpha_N}\right)^{1/\beta_A} x^{\beta_N/\beta_A} \tag{16}$$

Note that from section 4.4 equation (13)

$$d = \frac{\beta_N}{\beta_A}$$

and from equation (14)

$$c = \left(\frac{\alpha_A}{\alpha_N}\right)^{d/\beta_N}$$

hence

$$y = cx^d = \left(\frac{\alpha_A}{\alpha_N}\right)^{1/\beta_A} x^{\beta_N/\beta_A} \tag{17}$$

Thus the TFC is identical with the transformation of section 4.4.

It must be then that the two represent the same physical model. Nonetheless, for completeness the algorithm is derived in Appendix VIII-3, for proceeding from a (future) accelerated test to normal conditions. It will be assumed that the physical law is such that: $g(x)$ IS ALWAYS THE SAME, I. E. $g(x) = g^*(x)$ where $g(x)$ is the TFC for this report and $g^*(x)$ is the TFC for a future accelerated test (at the <u>same</u> accelerated conditions as this report of course). The algorithm for this model 3 is given in Table 4-1.

4.6 MODEL #4: A TIME TRANSFER FUNCTION OF HAZARD RATES (TFH)

Definition: The time transfer function on hazard rates (TFH) is a function $j(x)$ such that

$$h_N(x) = h_A[j(x)]$$

where $h_A(x)$ and $h_N(x)$ are the hazard rates for the Weibull distribution under accelerated and normal conditions respectively, i. e.,

$$h(x) = \frac{\beta}{\alpha} x^{\beta - 1}$$

$j(x)$ is easily found for

$$h_N(x) = \frac{\beta_N x^{\beta_N - 1}}{\alpha_N} = \frac{\beta_A [j(x)]^{\beta_A - 1}}{\alpha_A} = h_A[j(x)]$$

$$\Rightarrow j(x) \left(\frac{\alpha_A \beta_N}{\alpha_N \beta_A}\right)^{1/\beta_A - 1} x^{\left(\frac{\beta_N - 1}{\beta_A - 1}\right)}$$

It is interesting to note that the TFH and the TFC (defined in section 4.5) are never identically equal; not even for the exponential distribution. The proof of this is contained in Appendix VIII-4.

The above considerations indicate that (excepting the trivial situation when $\beta_A = \beta_N$; $\alpha_A = \alpha_N$) the model of section 4.5 and the model of this section describe <u>different physical processes</u>.

Suppose now that it is decided that the physical process is such that the hazard rate transfer function, TFH, ALWAYS REMAINS THE SAME from test to test (provided the same stress environment as in this report is maintained) i.e., in a future accelerated test the physics of the process are such that

$$j(x) = j^*(x) \qquad (18)$$

where $j^*(x)$ is the transfer function from normal to accelerated hazard rate in a future test. The resulting algorithm is given in Table 4-1 under model 4. The proof is contained in Appendix VIII-4.

4.7 MODEL #5: CONSTANT RATIO OF HAZARD RATES (CRH)

This model is suggested by the well known "K factor." This K factor is known in reliability circles as the stress factor which converts the failure in one set of environments, say normal, to the failure rate under stress conditions. In this report it is given by equation A-19 in Appendix VIII-4:

$$j^1(x) = K\left(\frac{\alpha_A}{\alpha_N}\right) \text{(for the exponential distribution)}$$

From equation A-18 in Appendix VIII-4 it can be seen K is indeed the ratio of the hazard rates. Unfortunately in the case of the Weibull distribution the K factor relating two environments (normal and accelerated say) is not a constant but depends on x and is more properly written K(x). In any case it certainly seems to make sense to try a model such that the physical laws operating ALWAYS KEEP K(x) THE SAME, i.e.

$$K(x) = K^*(x) \text{ for all } x \tag{19}$$

where

$$K(x) = \frac{h_N(x)}{h_A(x)}$$

$$K^*(x) = \frac{h_N^*(x)}{h_A^*(x)}$$

The algorithm for this model 5 (CRH) is given in Table 4-1. Its derivation is contained in Appendix VIII-5.

TABLE 4-1. ALGORITHMS

	$\tilde{\alpha}^*_N$	$\tilde{\beta}^*_N$
Model 1	$\tilde{\alpha}^*_N = \tilde{\alpha}^*_A \Big/ \left(\dfrac{\tilde{\alpha}_A}{\tilde{\alpha}_N}\right)^{\tilde{\beta}^*_A/\tilde{\beta}_A}$	$\tilde{\beta}^*_N = \tilde{\beta}_A$
Model 2 and 3	$\tilde{\alpha}^*_N = \tilde{\alpha}^*_A \Big/ \left(\dfrac{\tilde{\alpha}_A}{\tilde{\alpha}_N}\right)^{\tilde{\beta}^*_A/\tilde{\beta}_A}$	$\tilde{\beta}^*_N = \dfrac{\tilde{\beta}_N}{\tilde{\beta}_A}\tilde{\beta}^*_A$
Model 4	$\tilde{\alpha}^*_N = \dfrac{\tilde{\alpha}^*_A\tilde{\beta}^*_N}{\tilde{\beta}^*_A} \Big/ \left(\dfrac{\tilde{\alpha}_A\tilde{\beta}_N}{\tilde{\alpha}_N\tilde{\beta}_A}\right)^{\frac{\tilde{\beta}^*_A - 1}{\tilde{\beta}_A - 1}}$	$\tilde{\beta}^*_N = \left(\dfrac{\tilde{\beta}_N - 1}{\tilde{\beta}_A - 1}\right)(\tilde{\beta}_A - 1) + 1$
Model 5	$\tilde{\alpha}^*_N = \left(\dfrac{\tilde{\alpha}_N\tilde{\beta}_A}{\tilde{\alpha}_A\tilde{\beta}_N}\right)\dfrac{\tilde{\alpha}^*_A\tilde{\beta}^*_N}{\tilde{\beta}^*_A}$	$\tilde{\beta}^*_N = \tilde{\beta}^*_A + (\tilde{\beta}_N - \tilde{\beta}_A)$

TABLE 4-2. OBSERVED WEIBULL PARAMETERS

Switches		Relays	
Test Run 1	$\tilde{\beta}_N = 4.07$ $\tilde{\alpha}_N = 53,848 \times 10^{17}$	Test Run 1	$\tilde{\beta}_N = 1.68$ $\tilde{\alpha}_N = 8154 \times 10^{6}$
Test Run 14	$\tilde{\beta}_A = 1.53$ $\tilde{\alpha}_A = 2,594,241$	Test Run 15	$\tilde{\beta}_A = 1.39$ $\tilde{\alpha}_A = 3618 \times 10^{4}$
Test Run 15	$\tilde{\beta}_A = 1.00$ $\tilde{\alpha}_A = 14,440$	Test Run 22	$\tilde{\beta}_A = 1.11$ $\tilde{\alpha}_A = 1409 \times 10^{3}$

4.8 CONCLUSIONS ON MATHEMATICAL MODELS

Further investigation can provide data for validating one of the models suggested. However it is well to perhaps look ahead as to the probable outcome. As pointed out previously models 2 (the transformation $y = cx^d$) and 3 (the time transformation on the cumulative distribution function) are identical and model 1 (the transformation $y = cx$) is a special case of model 2. Model 1 will not be applicable because the β's change from accelerated to normal and hence $d \neq 1$.

The fact that models 2 and 3 are identical provides a possible clue as to which of the models (2 and 3 or 4 or 5) will best describe the relationship between accelerated and normal conditions. The cumulative failure distribution F provides a complete statistical description of part life behavior at both normal and accelerated conditions. Now model 3 uses the accelerated and normal F's and relates them by a constant function. On the other hand model 2 assumes that the physical laws are such that the time axis x is being compressed to y by $y = cx^d$ and this expression provides a link between "time units" at accelerated conditions (y) and time units at normal conditions (x). Thus models 2 and 3 answer two of the most important questions of accelerated testing, namely:

1) what is happening to the failure distributions?

2) what is happening to the time units?

In addition it turns out that models 2 and 3 are identical. Hence it is suspected that these models will adequately describe the algorithm for proceeding from accelerated to normal conditions.

Models 4 and 5, although distinct possibilities, suffer from the same shortcomings. That is it is difficult to heuristically justify why the hazard functions should be related by an unchanging function (model 4) and (model 5) why the ratio of the accelerated and normal hazard rates should remain constant. Model 5 is a general case of the well known K factor. However when the single parameter exponential does not hold it is difficult to interpret just what the K factor means. In addition, since models 4 and 5 are different from each other and different from 2 and 3, the validity of model 4 or 5 would indicate that the physical process cannot be interpreted in terms of time compression (model 2) or relating the failure distribution (model 3). This would be a somewhat surprising result.

5.0 MECHANICAL SEALS (O-RINGS)

5.1 SUMMARY

The life tests performed on O-rings in the search for accelerated reliability test methods involved the use of part type AN 6227B-11. The stresses studied were: 1) ambient temperature at 200, 250, 275°F and 2) ultraviolet exposure at none, .1 watt/ft^2, and .2 watt/ft^2. Ten parts were life tested at each of the 9 combinations of temperature and ultraviolet.

An analysis of variance indicated that both the temperature, and ultraviolet and the interactions between them affected part life. The parts tested at 200°F and no ultraviolet lasted an average of approximately 1750 hours. Those tested at 200°F and .2 watts/ft^2 lasted approximately 1300 hours. Those tested at 275°F and .2 watts/ft^2 averaged 135 hours. From these typical numbers it can be seen that increasing the temperature under which this type of O-ring operates will reduce its life very significantly. However the inclusion of a second stress in the form of ultraviolet in combination with the ambient temperature results in a substantial additional reduction in test time. This is an illustration of the value of testing using combined environments in preference to the application of single accelerating stresses or of testing using stresses applied sequentially.

The failed parts were subjected to microscopic inspection after failure. Radial cracks were the predominant failure mode found although many parts also contained networks of circumferential cracks.

The failure times of O-rings were studied to determine their characteristic life distribution. The nine combinations of accelerating stresses included in this study program indicated that this type of part fails according to the Weibull distribution.

The essence of any accelerated reliability test method is the requirement that there must be some way to relate part life at stressed conditions to part life at normal or manufacturer's rated operating and environmental conditions. In the case of the O-rings studied here, time did not permit the testing of parts at room temperature and therefore no true benchmark to normal conditions exists. However a study of the test results clearly shows how part life varies over the applied range of accelerated stresses.

5.2 DETAILS OF THE INVESTIGATION

5.2.1 STRESS SELECTION

The mechanical seal selected for study was an O-ring of the type AN 6227B-11. It was of Buna N rubber, had an OD of 3/4", ID of 9/16" and cross sectional width of 3/32".

Unlike switches very little information relating mechanical life to environmental stresses was available. An investigation of potentially usable accelerating stresses indicated the following general properties.

Tear resistance	fair
Abrasion resistance	good
Aging (Ultraviolet)	fair
Oxidation (Ozone)	fair
Resistance to compression set	good
Oil and gasoline resistance	excellent
Acid resistance	good
Cold resistance (freezing)	good
Heat resistance	good
Permeability to gases	medium
Electrical resistivity	low
Resistance to cutting	good
Resistance to water swelling	excellent

An examination of the above properties resulted in the elimination of those that would be difficult to repeat with confidence. Also eliminated were stresses that would require removal of the rings from their test block since handling would be a difficult to control condition. Since a combined environment test was an objective of the project known non-compatible tests were ruled out.

This resulted in an initial accelerating stress selection of:

Aging (Ultraviolet)

Oxidation (Ozone)

Heat Resistance

The test method and test equipment used are described in detail in Appendix V-3.

While conducting tests to determine stress levels to be utilized it was found that total breakdown of the ozone occurred at temperatures above 200°F. This resulted in elimination of ozone as an accelerating stress. References indicated that Buna N rubber compounds are relatively insensitive to damage at temperatures below 250°F, therefore samples were tested at 300°F and found that failure occurred in less than 88 hours.

It was felt that measurement error resulting from the combinations of heating and cooling cycles involved in the testing procedure would be too great with this short of life span. Subsequent tests and information led to the specification of 275°F as the upper limit, 200°F as the lower limit and an intermediate condition of 250°F. All available information indicated that a lower temperature would not produce failures within the contractual period. The level of the ultraviolet exposure was determined from a study of manufacturers data on the light sources.

A summary of the overall stress selection is:

Applied Stress	Normal	Intermediate	Maximum
Temperature	200°F	250°F	275°F
Ultraviolet Exposure	None	0.1 watt/ft^2	0.2 watt/ft^2

5.2.2 STATISTICAL EXPERIMENTAL DESIGN (O-RINGS)

A 2^3 factorial experiment with 10 replications was selected for the study program on O-rings. This was to allow for the evaluation of the main effects of temperature and ultraviolet as well as their interactions when applied as combined stresses. Table 5-1 describes the different combinations of test conditions included in the test program.

It was impossible to operate these parts at temperatures lower than 200°F and still be able to observe a sufficient number of failures during the contractual period to perform an analysis. However, ranges of temperature and ultraviolet exposure were included as test conditions which would yield a general idea as to the manner in which life varied as stress levels were varied.

TABLE 5-1. FACTORIAL EXPERIMENT FOR O-RINGS

Temperature (°F)	Ultraviolet Exposure: None	Ultraviolet Exposure: .1 Watt/Ft.^{2}	Ultraviolet Exposure: .2 Watt/Ft.^{2}
200	(1)	(2)	(3)
250	(4)	(5)	(6)
275	(7)	(8)	(9)

Note: The numbers in parentheses are designations used throughout the study to identify each of the nine test runs. For example Test Run #5 consists of 10 O-rings which were tested at 250°F and .1 Watt/Ft.^{2}. Each test run contained 10 O-rings.

5.2.3 DEFINITION OF FAILURE

O-rings are parts that can be used for many different applications involving many different operational stresses and ranges of use conditions. The test results obtained in this study to measure O-ring life might differ greatly from those encountered in other applications. For this application the definition of failure is that there will be no leakage during three cycles during which the pressure on the test fixture is raised to 1500 psi and held for one minute. The details of the test method are described in Appendix V.

5.3 PRESENTATION OF TEST RESULTS

The study to find an accelerated reliability test method for O-rings was performed by testing 10 parts at each of 9 different combinations of two stresses. The stresses induced in the study were temperature, and ultraviolet exposure. Each stress was applied at 3 levels of severity. The results of the tests on individual parts at each of the test conditions are shown in Table 5-2. Each cell in the matrix representing a given level of temperature in combination with a fixed level of ultraviolet radiation is numbered in the lower left hand corner in the table. These numbers designate the terminology to be used in explaining the test results. For example Test Run 1 represents the hours to failure of 10 O-rings tested at 200°F and no ultraviolet exposure. The mean value ($\overline{X}$) of each test run is shown in the table. The numbers in parentheses are the failure modes (see Part 5.3.2 of this Section for definitions).

5.3.1 ANALYSIS OF VARIANCE

Before an analysis of variance could be performed on the O-ring life test data, a logarithmic transformation had to be made on the data. The reason for this was, as in the case of switches and relays, that the variance of the longer life test runs was much higher than those tested at accelerated conditions. The analysis of variance indicated that both temperature and ultraviolet and their interactions affected the life of O-rings. The details of these effects are shown in Table 5-3.

The F Ratio indicates that both temperature, ultraviolet exposure, and their interactions are highly significant. This is evaluated by comparing the values in the column in Table 5-3 marked $F_{.05}$ to the values in the F Ratio column. A larger number in the F Ratio column denotes significance. The Components of Variance analysis substantiates the values of the F Ratio but points out that temperature exerts an extremely powerful effect on the life of these parts (about 98.4% of the observed variance). In spite of this overwhelming amount, the effects of ultraviolet and their interactions are large enough to be felt. The right hand column in Table 5-3 gives a complete list of the % contribution to total variance of all of the effects.

5.3.1.1 t TESTS

As in the previous analyses on switches and relays, the t tests are performed to observe how the interactions are grouped in order to select those

TABLE 5-2. O-RINGS: HOURS TO FAILURE

	No Ultraviolet	0.1 Watts Per Ft.^{2}	0.2 Watts Per Ft.^{2}
200°F	1683 (1) 1784 (1) 1683 (1,2) 1784 (1) 1862 (1,2) 1784 (1) 1683 (1) 1784 (1,2) 1683 (1,2) 1784 (1) $\bar{X}$ = 1751.4 #1	1143 (1) 1628 (1) 1373 (1) 1445 (1) 1373 (1) 1628 (1,2) 1309 (1) 1373 (1) 1373 (1,2) 1309 (1) $\bar{X}$ = 1395.4 #2	1373 (1,2) 1445 (1) 1445 (1) 1309 (1) 1143 (1) 1309 (1) 1215 (1) 1373 (1) 1215 (1) 1143 (1) $\bar{X}$ = 1297.0 #3
250°F	399 (1) 422 (1) 338 (1) 444 (1) 367 (1) 367 (1) 393 (1) 393 (1) 314 (1) 292 (1) $\bar{X}$ = 372.9 #4	314 (3) 343 (1) 393 (1,2) 393 (1,2) 314 (1) 343 (3) 314 (1) 343 (1,2) 314 (1) 338 (1) $\bar{X}$ = 340.9 #5	393 (1) 366 (1) 338 (3) 338 (1) 338 (1) 343 (1) 338 (1,2) 314 (1) 338 (1,2) 367 (1) $\bar{X}$ = 347.3 #6
275°F	147 (1) 147 (1,2) 128 (2) 147 (1,2) 165 (1,2) 147 (1,2) 147 (1,2) 165 (2) 147 (1,2) 147 (1,2) $\bar{X}$ = 148.7 #7	121 (1) 129 (1,2) 147 (1,2) 147 (1,2) 147 (1,2) 129 (1) 129 (1) 129 (1,2) 165 (1,2) 121 (1,2) $\bar{X}$ = 136.4 #8	129 (2) 121 (1,2) 121 (1,2) 129 (2) 129 (2) 165 (1,2) 121 (2) 165 (1,2) 121 (1) 147 (1,2) $\bar{X}$ = 134.8 #9

TABLE 5-3. ANALYSIS OF VARIANCE - O-RINGS

Source of Variance	Sum of Squares	Degrees of Freedom	Mean Squares	F Ratio	$F_{.05}$	% Contribution To Variance
Between temperatures	15.90668	2	7.95334	4791.2*	4.00	98.4
Between Ultra-violet Levels	.08211	2	.04106	24.7*	4.00	.5
Interaction Between Temperature and Ultraviolet	.03199	4	.01600	9.6*	2.53	.5
Residual	.13473	81	.00166			.6
Total	16.15551	89				100.0 %

*Denotes significance at the $F_{.05}$ level.

combinations of stresses causing differences to occur in the mean lives of the parts under test.

The logarithmic means of each of the 9 O-ring test runs are shown in Table 5-4. The interval between means required before significant differences can be said to exist is calculated as .03. This is based on $t_{.05}$ with 81 degrees of freedom and the residual mean square of .00166 from the analysis of variance. The interactions form into six distinctive groups as described by their means.

TABLE 5-4. TEMPERATURE AND ULTRAVIOLET INTERACTIONS ON O-RINGS

Temperature (°F)		Ultraviolet		
		No UV	.1 Watt/Ft.^{2}	.2 Watt/Ft.^{2}
	200	3.24	3.14	3.11
	250	2.57	2.53	2.54
	275	2.17	2.13	2.12

$$t_{.05} \; \frac{\bar{X}_1 - \bar{X}_2}{\sqrt{\frac{\sigma_R^2}{n} + \frac{\sigma_R^2}{n}}}$$

$$1.66 \; \sqrt{\frac{.00166(2)}{10}} \quad \bar{X}_1 - \bar{X}_2$$

$$1.66 \; \sqrt{.000332} = 1.66\,(.0182) = \bar{X}_1 - \bar{X}_2$$

$$.030 = \bar{X}_1 - \bar{X}_2$$

The groups form as follows in order of largest mean life and descend to the shortest

Temperature	Ultraviolet	
200°F,	no U. V. = 3.24	Group 1
200°F, 200°F,	.1 watts/ft.^{2} UV = 3.14 .2 watts/ft.^{2} UV = 3.11	Group 2
250°F,	no U. V. = 2.57	Group 3
250°F, 250°F,	.1 watt/ft.^{2} = 2.54 .2 watt/ft.^{2} = 2.53	Group 4
275°F,	no U. V. = 2.17	Group 5
275°F, 275°F,	.1 watt/ft.^{2} = 2.13 .2 watt/ft.^{2} = 2.12	Group 6

From the above analysis it can be seen that the major change in life reduction occurs as higher temperatures are used. However, where ultraviolet is used a significantly shorter life is noticed. In no case is the effect of the 2 levels of ultraviolet of sufficient difference to be noticeable.

5.3.2 FAILURE ANALYSIS OF O-RINGS

Each O-ring, after failing the pressure test, was inspected under a microscope to determine the nature of the failure mode. There are only two failure modes that appeared predominantly. They were:

1. Radial fracture or deep radial cracking.
2. Circumferential cracks usually on the outside diameter of the ring.
3. No defect visible.

To give a better view of the frequency of occurrence of each of the above failure modes, reference is made to Table 5-2. The numbers in parentheses correspond to the failure mode definitions above. The circumferential cracks that appear occasionally throughout all but Test Run 4 were located randomly along the outer surfaces. They usually, but not always, were connected to deeper radial cracks. The circumferential cracks periodically crossed the mold line on the outer diameter of the O-ring. The severity and frequency of both the radial and the circumferential cracks did not seem to form a pattern that increased in severity with stress. The lone exception to this was at 275°F where a larger proportional amount of circumferential cracks occurred. The detailed description of the failure analysis of each O-ring appears in Appendix IV.

5.3.3 ANALYSIS RELATED TO LIFE DISTRIBUTION FUNCTIONS

The failure data for O-rings was plotted on the Weibull probability paper. The results of this are shown in Appendix VI-3. The lines of best fit were calculated on the computer by the method of least squares. The Weibull shape (β) and scale (α) parameters were calculated and are summarized in Table 5-5. Alpha (α_k) is the coded value corresponding to the scale parameter that can be obtained from the Weibull plot of each test run. Alpha (α_o) is the uncoded value of the scale parameter.

TABLE 5-5. SUMMARY OF WEIBULL PARAMETERS FROM O-RING TESTS

Temperature (°F)	Ultraviolet Exposure: No UV	.1 Watt/Ft²	.2 Watt/Ft²
200	β = 17.75 α_3 = 19,930 α_o = 35,436 x 10^{53}	β = 10.71 α_3 = 48,424 α_o = 65,324 x 10^{29}	β = 11.01 α_3 = 22,646 α_o = 24,277 x 10^{30}
250	β = 8.46 α_2 = 102,740 α_o = 85,069 x 10^{17}	β = 8.12 α_2 = 25,330 α_o = 43,618 x 10^{16}	β = 22.46 α_2 = 2314 x 10^{9} α_o = 19,248 x 10^{41}
275	β = 14.68 α_2 = 403.43 α_o = 92,426 x 10^{27}	β = 7.94 α_2 = 15.487 α_o = 119,111 x 10^{12}	β = 5.17 α_2 = 4.95 α_o = 106,326 x 10^{6}

5.4 SELECTION OF ACCELERATED TEST METHOD (O-RINGS)

It would appear that any of the stresses induced during the O-ring tests would result in an acceleration of the failure of the parts. Temperature exerts by far the most significant effect on the life of O-rings, but ultraviolet has demonstrated its usefulness also as an accelerating stress. The true validation of whether or not the results found in this study are translatable to the life of O-rings at some other range of temperatures cannot be answered. The basic relationships shown here doubtless vary for parts produced from different materials. However the main objective of the test has been accomplished -- namely demonstrating how the life of a given type of O-ring varies when subjected to a given application, under various combinations of ultraviolet and temperature stresses. It has also been demonstrated that a combined environments test involving both temperature and ultraviolet results in an added reduction in life that would not be in effect if the temperature and ultraviolet were applied separately or sequentially.

SECTION 6.0 TIMING BELTS

6.1 SUMMARY

The timing belts selected for study were operated at normal stress levels (1/15 H.P. load with a pulley containing 18 teeth) and at 8 other combinations of load and pulley diameter calculated to result in accelerated stress levels. A full factorial experiment was planned with 5 replications in each cell. Not enough failures were observed during the contract period to allow performance of either an analysis of variance or to study the characteristic failure distributions of these parts operated at the various combined stresses. Several of the failures that were observed appeared to be infant mortalities however and this point bears further study.

6.2 DETAILS OF THE INVESTIGATION

6.2.1 SELECTION OF STRESSES

The timing belt selected for study had the following properties:

1/5 pitch
12 inch pitch length
60 teeth
.037 inches wide

The teeth were of neoprene with nylon facing. The tension member was steel cable with neoprene backing.

Manufacturer's information was primarily aimed at selection for specific application. A maximum operating temperature range of -30° to +185°F was indicated. Field experience has shown a life expectancy of 8000 hours if operated at room temperature and if all recommended design practices were followed for the application.

An investigation of usable accelerating stresses included those that would be introduced by the following conditions:

Fluctuating load
Reverse bending
Belt speed
Belt load
Pulley size (Flexing Radius)
Temperature
Sunlight
Ozone
Humidity
Corrosive Atmosphere
Misalignment
Initial Tension

Since forecasts and initial tests indicated that a long duration of test time would be involved, those factors that would cause relatively rapid failures of the test setup were eliminated. Stresses that would present difficult control or duplication problems were eliminated. This resulted in the selection of the following accelerating stress factors:

Load
Pulley size
Ozone

Preliminary tests indicated that a load in excess of 1/4 horsepower resulted in consistent "tooth jumping" on the minimum pulley size which provided the upper load limit. The lower limit was established by calculating the recommended load condition and adding 15% resulting in a load of 1/15 horsepower. An intermediate load of 1/8 horsepower was then selected.

Maximum pulley size was established by using the 18 tooth pulley which is the smallest size indicated by design charts for the recommended load. The minimum pulley size was established by selecting the smallest standard size available that would fit on the shaft diameter required. The 12 tooth pulley size fitted these requirements.

While ozone was selected as an accelerating stress to be applied, exploratory tests resulted in great difficulty in its generation and measurement. Hence its use as an accelerating stress was discontinued.

The stress levels selected and used in the tests were:

Applied Stress	Normal	Intermediate	Maximum
Load	1/15 H.P.	1/8 H.P.	1/4 H.P.
Pulley Size	18 tooth	15 tooth	12 tooth

The test method used is described in detail in Appendix V-4.

6.2.2 STATISTICAL EXPERIMENTAL DESIGN

As in the studies relating to switches, relays, and O-rings, a factorial experiment was devised for use in studying the reliability characteristics of timing belts under various combinations of stresses. The stresses and stress levels specified are shown in Table 6-1.

TABLE 6-1. FACTORIAL EXPERIMENT FOR TIMING BELTS

Load (Horsepower)	Pulley Size (No. of Teeth) 18	15	12
1/15	(1)	(4)	(7)
1/7	(2)	(5)	(8)
1/4	(3)	(6)	(9)

The numbers in parentheses are designations used to identify each group of five belts tested at a given combination of stress levels. For example Test Run 9 consisted of 5 belts tested at a load of 1/4 horsepower using 12 tooth pulley.

6.2.3 FAILURE ANALYSIS OF TIMING BELTS

At failure each belt was subjected to a visual failure analysis. The results of this inspection were entered on the data record sheet and the belt was placed into an envelope bearing its identification number.

6.2.4 DEFINITION OF FAILURE

Failure of a timing belt was defined as the loss of ability to transmit the required load. Cracking or other deterioration were not considered failures as long as the belt still could transmit power. In general failure occurred by either breaking of the belt or by shearing off of the teeth.

6.3 RESULTS OF TEST PROGRAM

The original test plan called for the operation of 5 belts to failure in each of the 9 test runs. However only a total of 9 failures were observed during the entire test. Table 6-2 shows the test hours accumulated at each of the combined stress conditions. A total of 66,460 part hours were recorded.

It will be noted that different production lots are included in the test program. This occurred because a pilot purchase lot was obtained to do exploratory testing in the selection of stress levels. After the stress levels were fixed a large lot of parts was obtained from a single manufacturing lot with the purpose of testing 5 belts in each test run from this lot. However it was observed that all failures were of parts from the first lot. Furthermore the results which have been obtained are quite erratic. An insufficient number of failures was observed and therefore no analysis was attempted with the available data. The only possible conclusion that might be reached is that some infant mortality failures were observed and perhaps burn in tests of one type or another might be considered as a reliability screening device for this type of part. A failure mode change did seem to be operating at the higher stress levels where failure occurred by stripped teeth rather than by belt breakage.

TABLE 6-2. TIMING BELT TEST RESULTS

Pulley Size (No. of Teeth)

Load (Horsepower)	18	15	12
1/15	Belt # 3-5-2 863.7 hrs ● ① 3-5-3 3912 hrs ②	Belt # 3-1-2 3074 1 hrs ② 3-2-1 3074.1 hrs ②	Belt # 3-5-0 553.0 hrs ● ① 3-3-0 5574.2 hrs ① 3-4-0 5574.2 hrs ①
1/7	Belt # 2-4-1 2292.5 hrs ● ① 2-3-1 4287.4 hrs ① 2-4-2 1994.9 hrs ②	Belt # 2-5-1 2602.5 hrs ● ① 2-5-0 1136.5 hrs ● ① 2-5-2 2732.4 hrs ② 2-2-0 5080.9 hrs ①	Belt # 2-1-2 3934.4 hrs ①
1/4	Belt # 1-1-2 5206.9 hrs ① 1-2-1 5210.2 hrs ① 1-3-6 2926.5 hrs ② 1-4-6 2926.5 hrs ②	Belt # 1-3-4 64.5 hrs * ① 1-4-4 494.0 hrs * ① 1-3-5 1552.6 hrs ② 1-4-5 1123.1 hrs ②	Belt # 1-3-2 157.4 hrs * ① 1-4-2 111 hrs * ①

● Belt had total break

* Belt teeth stripped or "jumping"

① [illegible]

7.0 CONCLUSIONS

This section is a summary of the conclusions of the entire study. The first part of the discussion will be devoted to general comments and then the specific conclusions related to each part studied will be presented.

7.1 GENERAL

As stated in the discussion on validation, the true measure of whether or not the accelerated test models developed in this study can relate the reliability of a part tested under severe stresses to that of the same part had it been operated at normal stresses will have to await additional verification. One or perhaps more than one of the models must mathematically represent the physical failure process occurring over the life span of the parts being operated. Additional test results performed at both accelerated and normal conditions must be compared with those obtained in the present study.

A second general conclusion relating to accelerated reliability testing is that tests of this nature should be performed in the presence of combined stresses. The analyses performed on snap action switches, crystal can relays, and on O-rings all yielded interactions that resulted in test time reductions greater than if only a single stress had been used.

The cumulative failure distribution is a measure of the desirability of a given combination of stresses for use as an accelerated reliability test method. If the stresses result in a Weibull life distribution having parameters that result in a high probability of failure at a mean life that is shorter than that of parts tested at normal operating conditions, then a plot of the cumulative failure distribution will demonstrate this attribute.

Five mathematical models have been presented which could be representations of the physical deterioration occurring during an accelerated test. These are: (1) the special case where the Weibull shape parameter (β) for the accelerated test is the same as for the test at normal conditions, and the Weibull scale parameter (α) changes by some constant factor; (2) and (3) where the Weibull shape parameters (β) of the accelerated and normal tests are in constant ratio to each other (4) where the change from accelerated to normal conditions is reflected as a time transformation of hazard rates, and (5) the change from accelerated to normal conditions is reflected as the arithmetic difference between the Weibull shape parameters (β).

7.2 SNAP ACTION SWITCHES

The specific conclusions found regarding the reliability characteristics of snap action switches are as follows.

1. Some stresses that affect the mean life of these parts are activation rate, contact load and contact overtravel. The interactions of contact loads and actuation rates and contact loads and overtravel also are significant affectors of life over the ranges included in this study. Of the stresses mentioned, contact load exerts the greatest amount to

the reduction in the expected number of cycles to failure and hence should very likely always be included as one of the accelerating stresses in any accelerated reliability test method for snap action switches.

2. Approximately the same results are obtained for factors affecting the mean life of snap action switches whether the criterion for failure is either cycles to first miss or cycles to total failure.

3. The cycles to failure of snap action switches appears to fit the Weibull distribution. The estimates of the Weibull shape parameter (β) and the Weibull scale parameter (α) vary when the parts are tested under varying combinations of operating and/or environmental stresses. The Weibull location parameter (γ) appears to be zero over all ranges of test conditions studied.

4. The operating parameters (operate force, release force, and contact resistance) of snap action switches vary over time, but it was not possible to say that a pattern was observed that could be utilized in some form as an indication of part life.

5. Test Run 15 (10 amps contact load, .010 inches contact overtravel, and 300 cycles/minute actuation rate) and Test Run 14 (10 amps contact load, .010 inches contact overtravel, and 150 cycles per minute) represent the combinations of operating and environmental stresses that appear to be the most favorable sets of conditions for use as accelerated reliability test methods for snap action switches.

6. The major failure mode observed was a burning and erosion of the leaf spring and contacts. At 15 amps regardless of actuation rate and overtravel the predominant failure mode changed to welded contacts. This was also true at 10 amps and .005" overtravel.

7.3 CRYSTAL CAN RELAYS

1. The mean life of relays is affected by contact load, ambient temperature and the contact load X temperature interaction. Contact load is the stress that most seriously reduces life over the ranges of stresses studied.

2. Approximately the same effects are noticed as determinants of relay mean life whether the failure criterion is first miss or total failure (3rd miss.)

3. Cycles to first miss of crystal can relays fail according to the Weibull distribution. The Weibull shape parameter (β) and the Weibull scale parameter (α) are different at varying combinations of stresses. The Weibull location parameter (γ) appears to be zero over the ranges of stresses studied.

4. The operating parameters of relays which were measured (coil resistance, contact resistance, pickup voltage, dropout voltage, operate time, release time, and contact bounce) vary over time as

expected but further study will be required to determine whether or not they can be used as predictors of the expected life of relays operated under a given set of stresses.

5. Test Run 22 (6 amps, 25°C, and 30 cycles/second) and Test Run 15 (6 amps, 150°C and 10 cycles per second) are the sets of combined environmental and operating stresses that appeared to offer the promise of favorable results when used as an accelerated reliability test methods for this type of relay.

6. The predominant failure mode was material transfer of the contacts or blade with failure eventually occurring when the contact gap was beyond the range of blade travel. At 8 amps contact load the failure mode changed to a predominance of welding of the contacts and blade. There was also a good deal of failure due to melting of one of the two arms of the bifurcated contacts if they were not perfectly aligned.

7.4 O-RINGS

The tests conducted on O-rings for the purpose of developing an accelerated reliability test method have resulted in the following conclusions:

1. The mean life of O-rings is significantly reduced by the application of temperatures from 200 to 275°F and by exposure to ultraviolet radiation. The net effect in reducing test time is enhanced by the use of both temperature and ultraviolet in a combined environments test. Temperature contributes the major share of the damage but ultraviolet does add a significant amount also.

2. The O-rings tested appear to fit either the Weibull or the normal distribution. The Weibull shape (β) and scale (α) parameters vary with the severity of the test conditions. The location parameter (γ) appears to be zero.

3. The major failure mode observed was radial cracking. There was some circumferential cracking usually in combination with radial cracking but it did not form a pattern that could be construed to be a change in failure mode as the severity of stresses increased.

7.5 TIMING BELTS

Not enough failures were observed to result in the specification of an accelerated test method. It is possible that the major fact gained from the study of timing belts is that there did seem to be a few infant mortality failures which might suggest that burn in tests might screen these out.

SECTION 8.0 RECOMMENDATIONS

8.1 GENERAL

1. This report has proposed a certain accelerated test method for the parts under test and certain mathematical models which can be used to relate normal and accelerated test conditions.

   The selection of accelerated test conditions has amounted to specifying a unique point in three dimensional euclidean space after having studied a total of 27 points in three space. These 27 points were relatively widely spaced in this study and the optimum point (with regard to the 27) was reasonably easily located. It is recommended that in further study the region around the optimum point be evaluated for a "local optimum." Slight changes in the levels of the environmental factors may lead to better results than those obtained at the present optimum. This will be accomplished by an experimental design similar to the one used in this study with the difference that a fractional factorial may be used.

   Another area requiring rather intensive study is the selection of one model which reasonably represents the manner of proceeding from accelerated test parameter, say α_A and β_A to normal test parameters say α_N and β_N. It is suggested that in future investigations, data be obtained which will check the validity of the algorithms of the models (1, 2, 3, 4, 5) given and select the model which best represents the failure laws operating.

   Finally the actual results obtained from this study in the analysis of variance will be compared to the results obtained in future investigations to make sure that the observed results of this study are reproducible to some extent.

2. There were definite indications in the present study on both switches and relays that approximately the same conclusions can be made whether these parts are tested to first miss or to some form of total failure. One drawback to this might be that the analysis of failed parts would not show the degree of damage that longer tests provide. It is felt from having inspected all of the failed parts that a satisfactory trend could be observed. It is therefore recommended that future tests of this nature not be continued until total inoperability of the part occurs.

3. Future studies on switches and relays should be conducted on the same part used in this study, using the same test method and the same stress levels which were defined as normal operating conditions in this study program. This will result in an estimate of the variation between manufacturing lots of parts.

4. Future studies should be directed to an examination of possibility of using a given accelerated reliability test method for parts produced by different manufacturers.

5. There should be continued periodic surveillance of the operating parameters at certain key stress levels to obtain more conclusive evidence of their movement during switch life.

8.2 SNAP ACTION SWITCHES

Further study in the refining of the specification of an optimum accelerated reliability test method for snap action switches should be centered around either Test Run 14 (10 amps contact load, .010 inches contact overtravel, and 150 cycles/minute) or Test Run 15 (10 amps contact load, .010 inches contact overtravel, and 300 cycles/minute.) These two combinations of operating and environmental stresses met all of the criteria suggested in Section 1.4 and thus qualified as methods worthy of further study and validation as accelerated reliability test methods.

8.3 RELAYS

The search for an accelerated reliability test method for relays should be centered around Test Run 22 (6 amps, 25°C, and 30 cycles/second) and Test Run 15 (6 amps contact load, 150°C, and 10 cycles/second) from the present study. Additional study in these general areas of stress levels may lead to a set of conditions that will yield an optimum accelerated test method.

8.4 O-RINGS

1. More information is required on the life characteristics of O-rings at less severe operating stresses. The results in this study are valid for only the range 200°F to 275°F. Estimates of life at room temperature are required.

2. A stronger ultraviolet exposure is suggested. The two exposure rates used in the present study did not result in mean part lives different from one another. They did reduce life significantly over the test runs where no ultraviolet was used. Therefore a more severe ultraviolet environment would likely result in a larger reduction in mean part life.

8.5 TIMING BELTS

1. The major recommendation regarding timing belts is that a greater number of observations of failure is required before any determination can be made as to the desirability of these combinations of stresses as accelerated test methods.

APPENDIX I. CUMULATIVE FAILURE DISTRIBUTIONS (SWITCHES)

The following charts (Figures I-1 through I-9) are the cumulative failure distributions for Test Runs 1 through 27 for snap action switches.

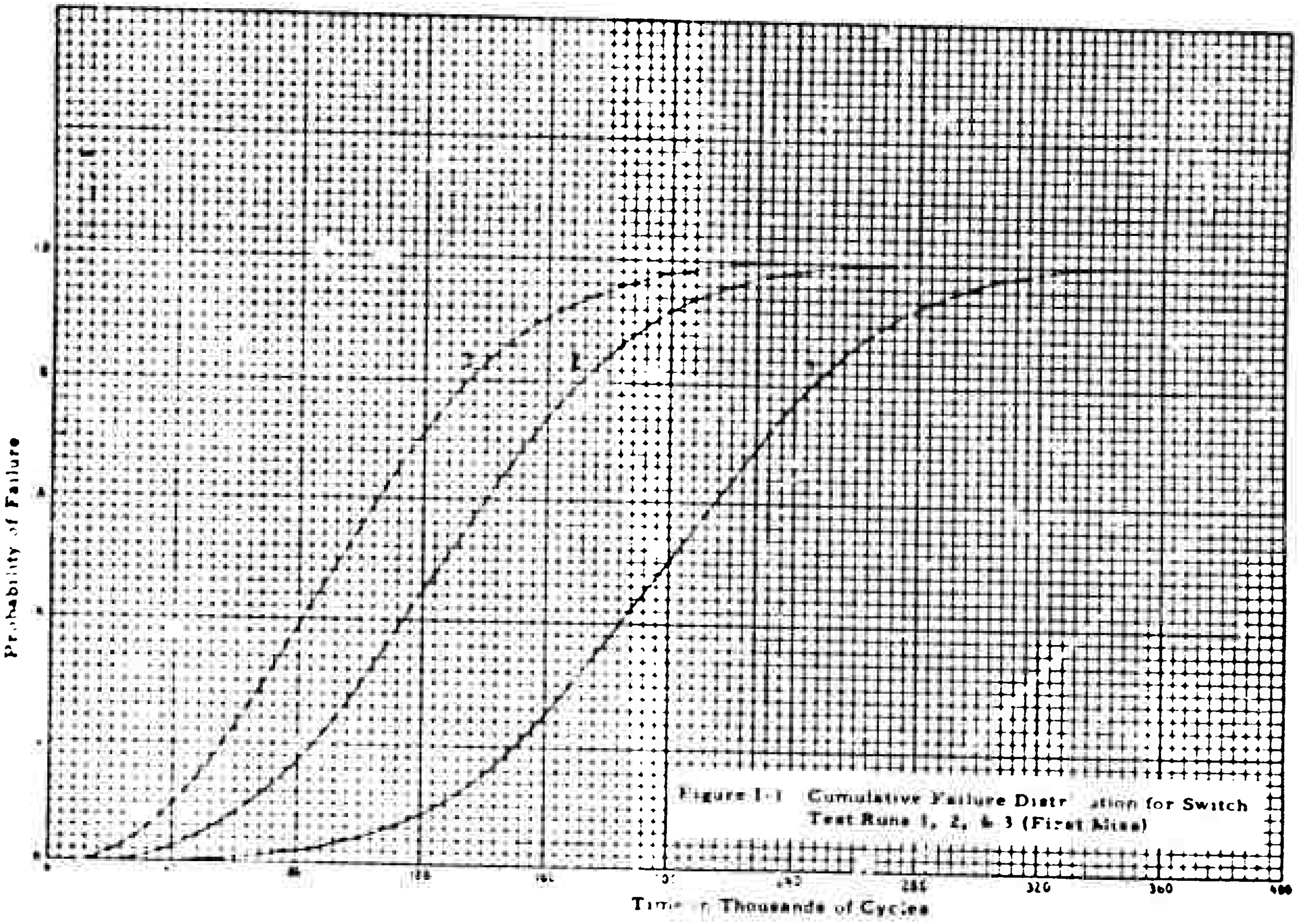

Figure I-1 Cumulative Failure Distr[illegible]ation for Switch Test Runs 1, 2, & 3 (First Miss)

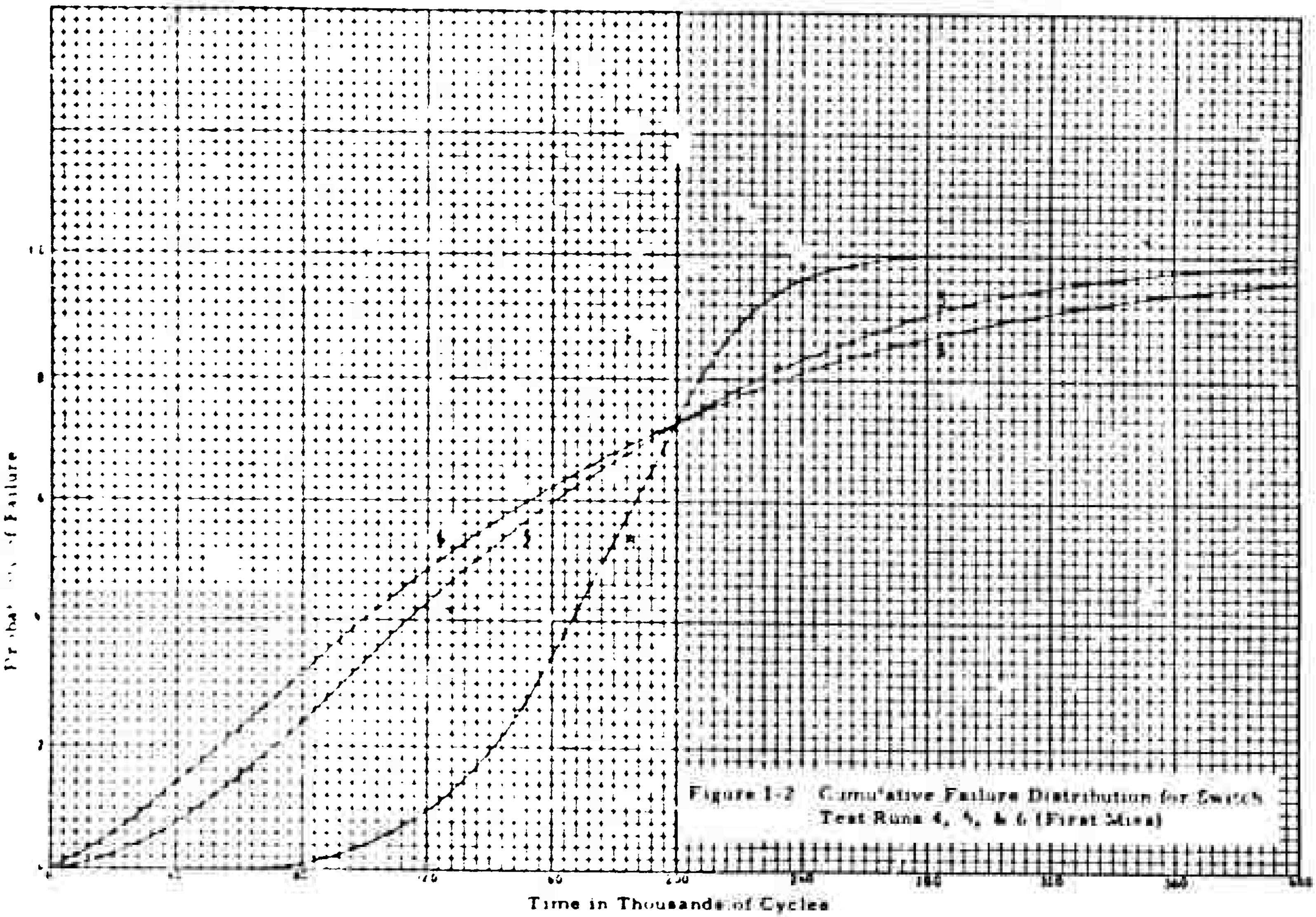

Figure I-2 Cumulative Failure Distribution for Switch Test Runs 4, 5, & 6 (First Mica)

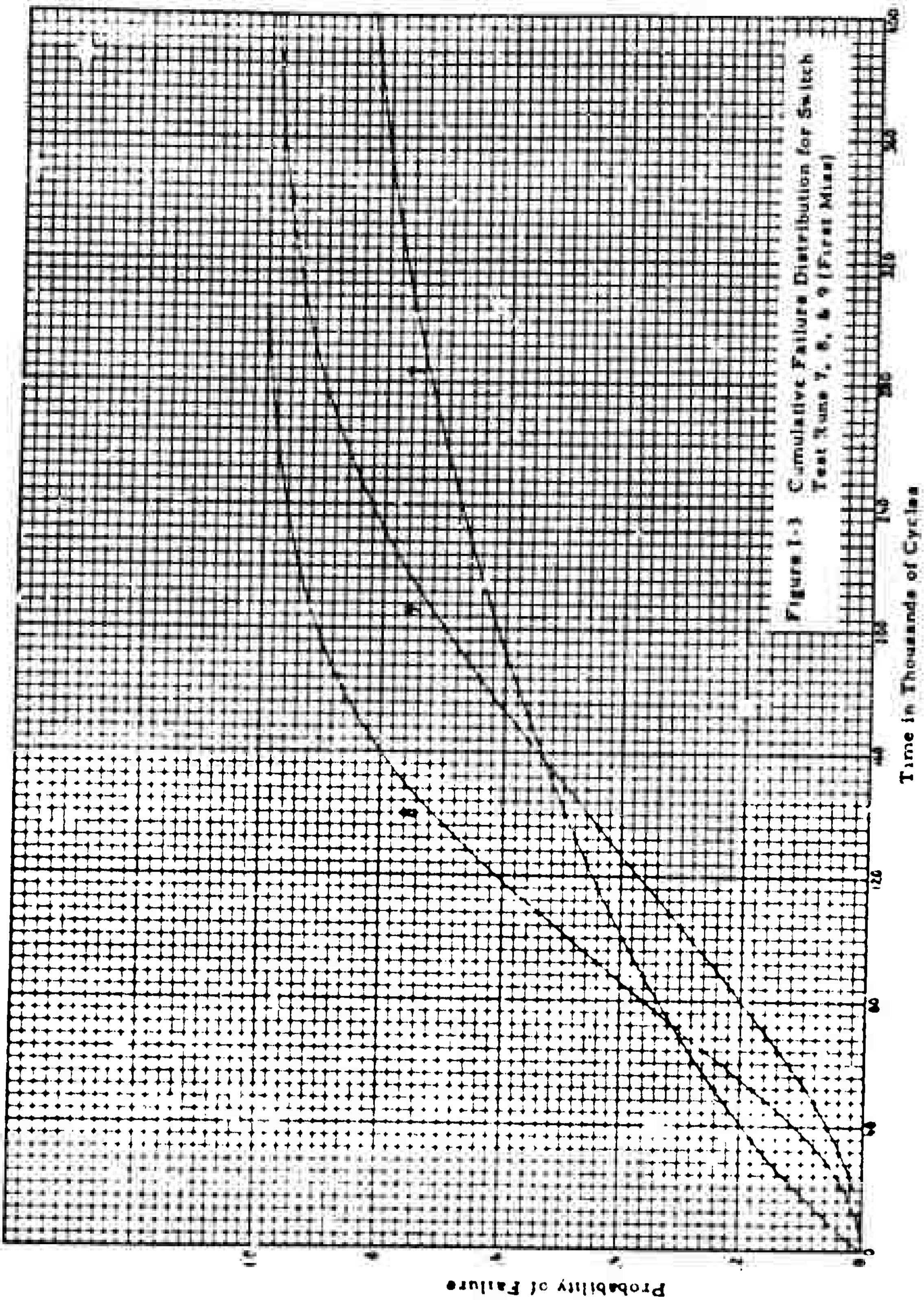

Figure I-3 Cumulative Failure Distribution for Switch Test Runs 7, 8, & 9 (First Miss)

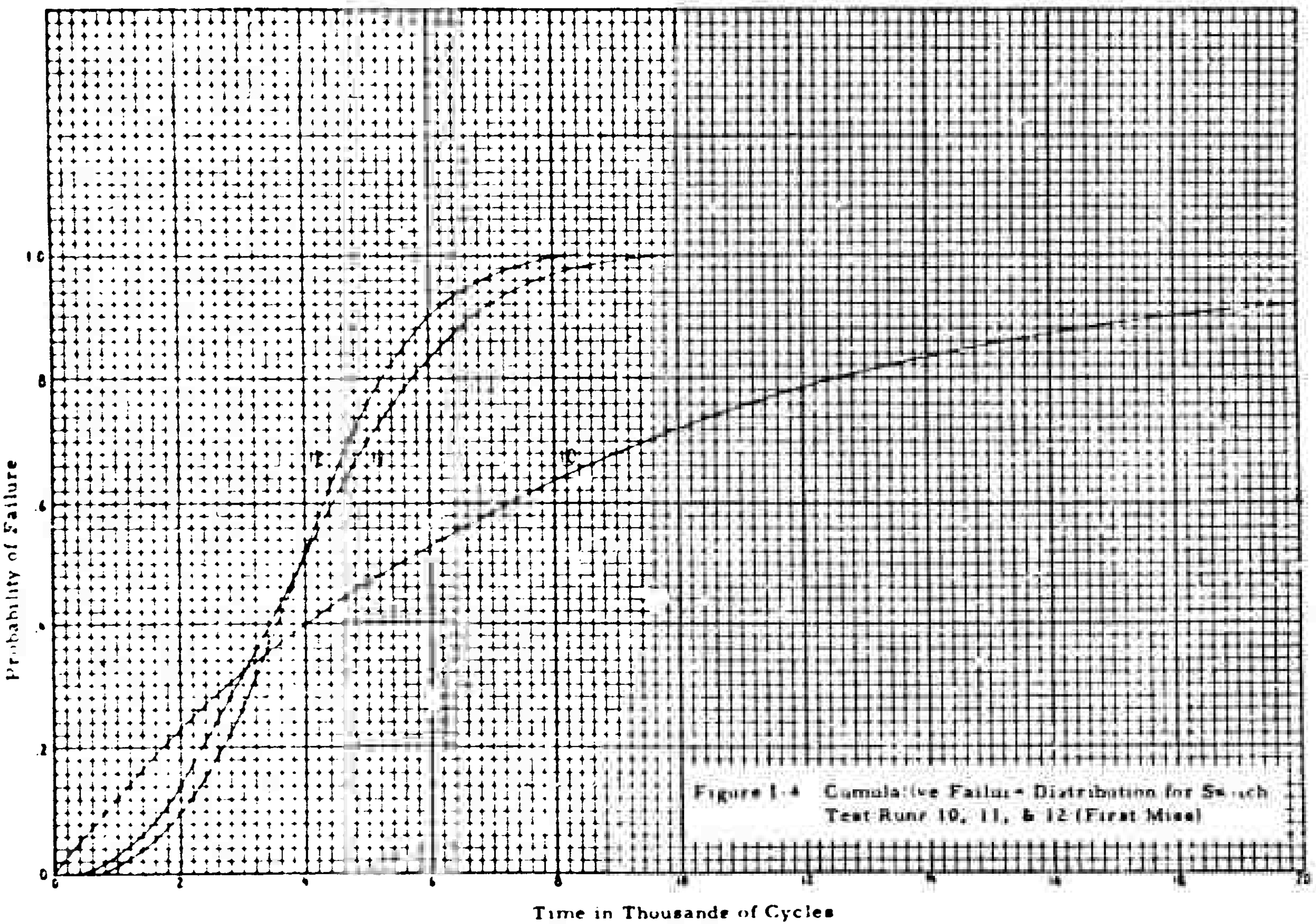

Figure I-4 Cumulative Failure Distribution for Switch Test Runs 10, 11, & 12 (First Miss)

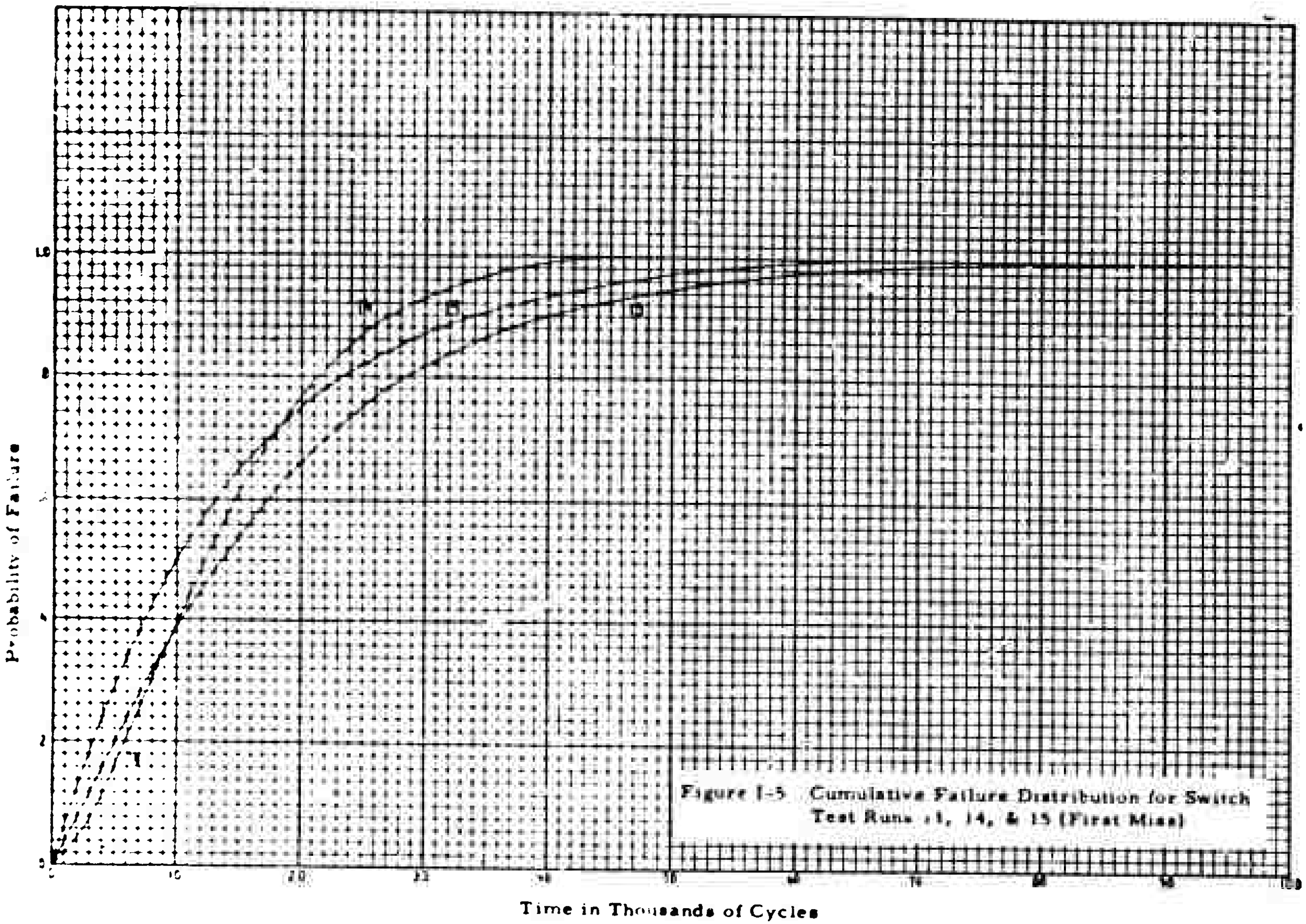

Figure I-5 Cumulative Failure Distribution for Switch Test Runs 11, 14, & 15 (First Miss)

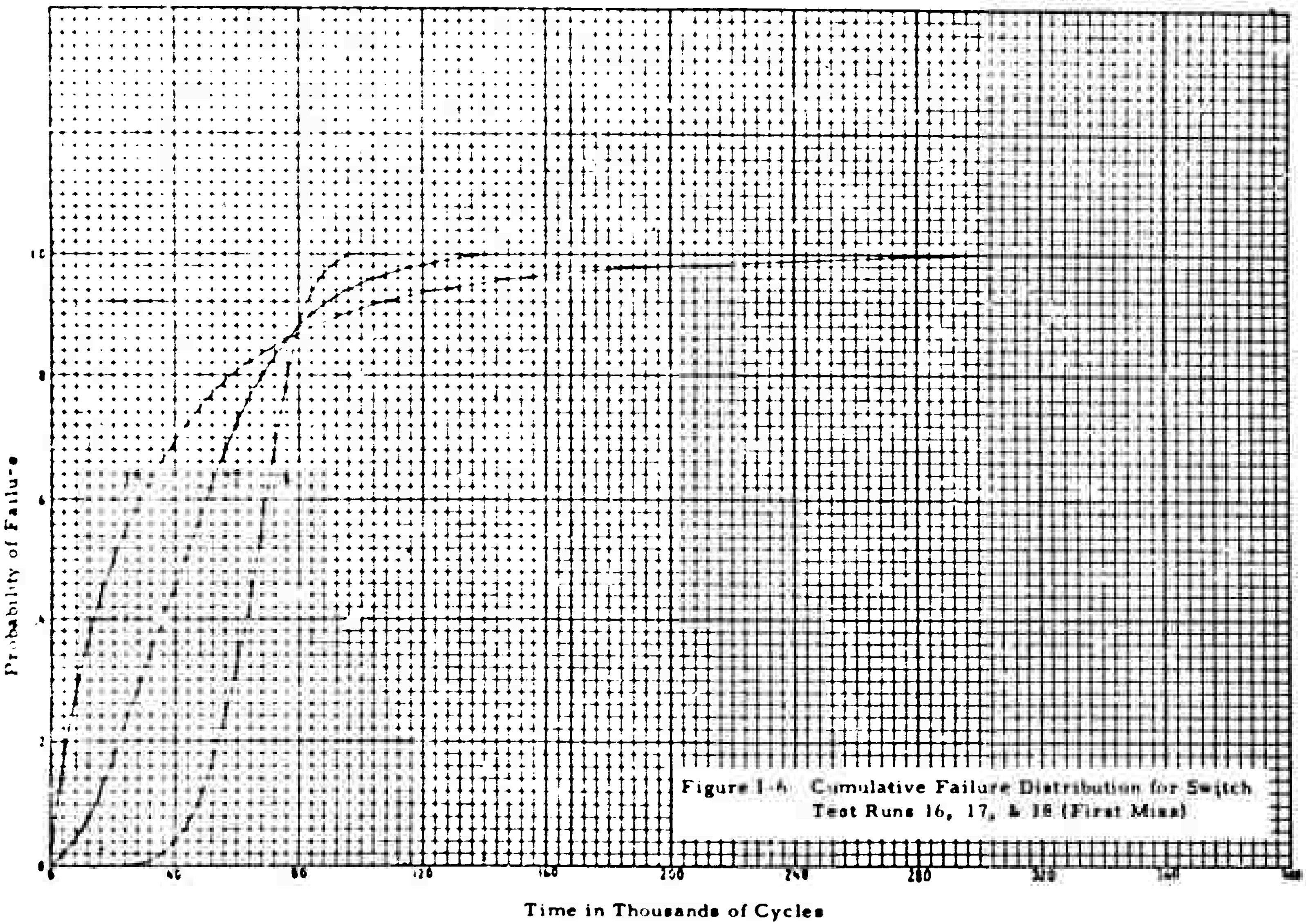

Figure I-6 Cumulative Failure Distribution for Switch Test Runs 16, 17, & 18 (First Miss)

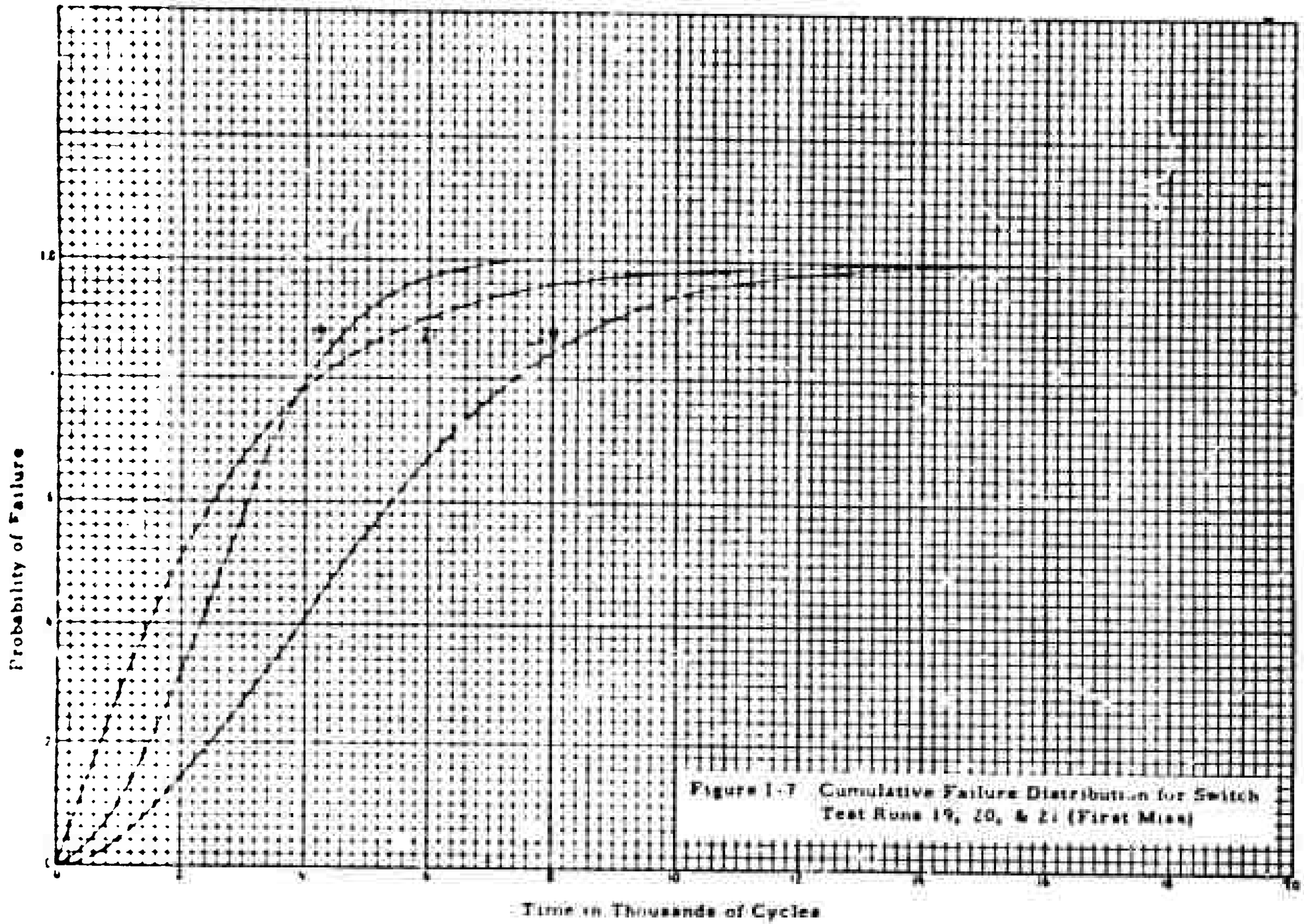

Figure 1-7 Cumulative Failure Distribution for Switch Test Runs 19, 20, & 21 (First Miss)

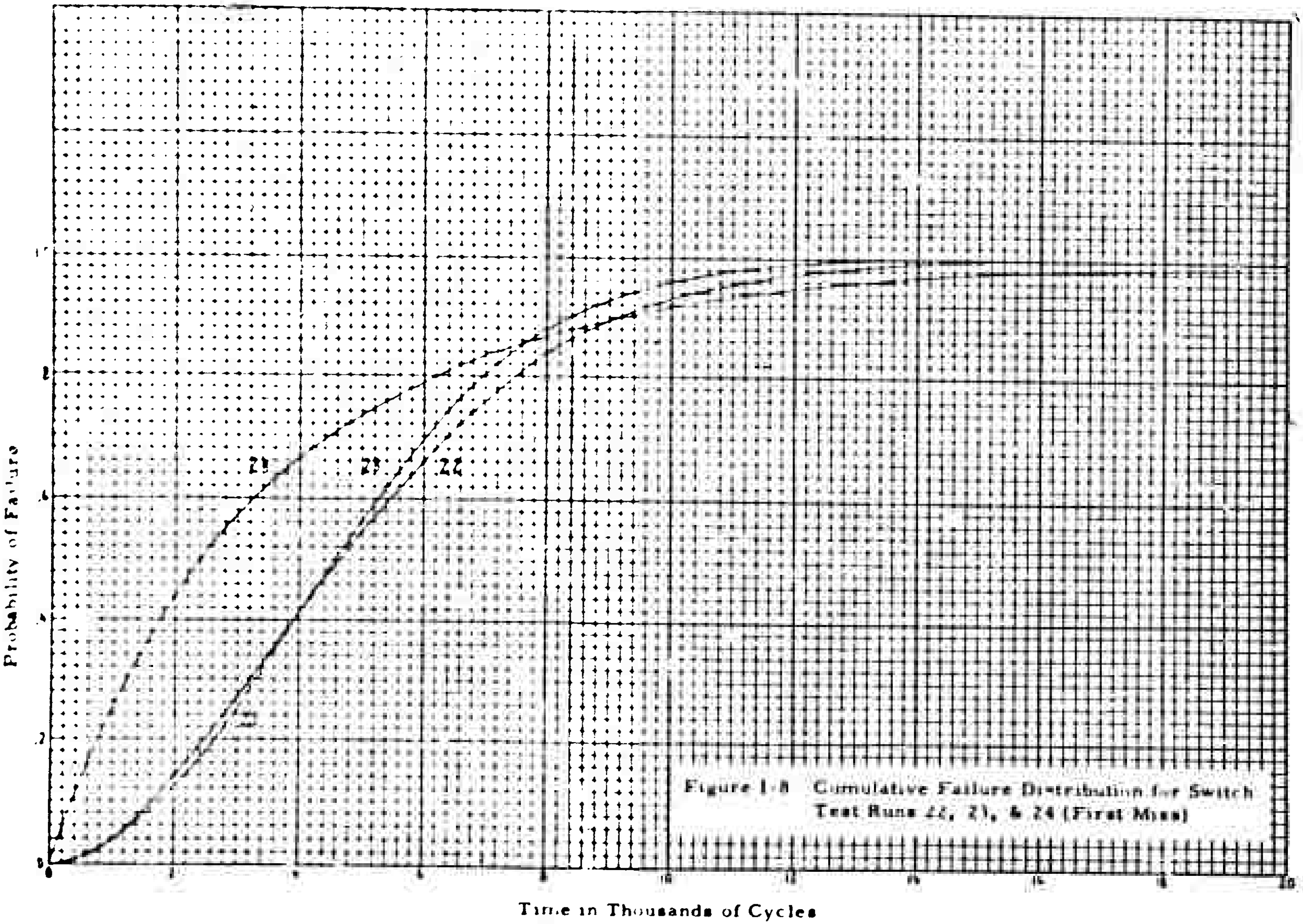

Figure I-8 Cumulative Failure Distribution for Switch Test Runs 22, 23, & 24 (First Miss)

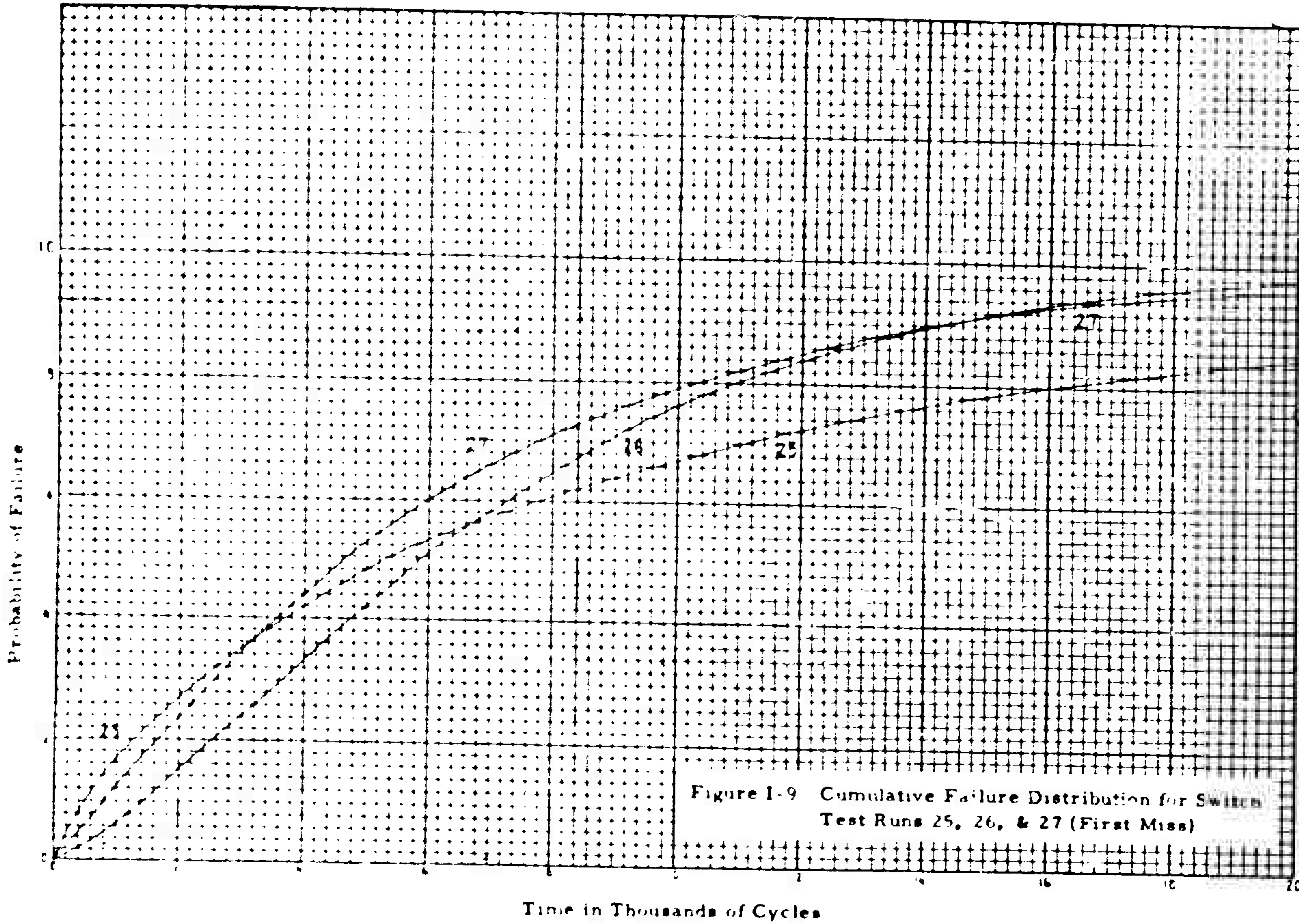

Figure I-9 Cumulative Failure Distribution for Switch Test Runs 25, 26, & 27 (First Miss)

APPENDIX II. CUMULATIVE FAILURE DISTRIBUTIONS (RELAYS)

The following charts (Figures II-1 through II-9) are the cumulative failure distributions for Test Runs 1 through 27 for crystal can relays.

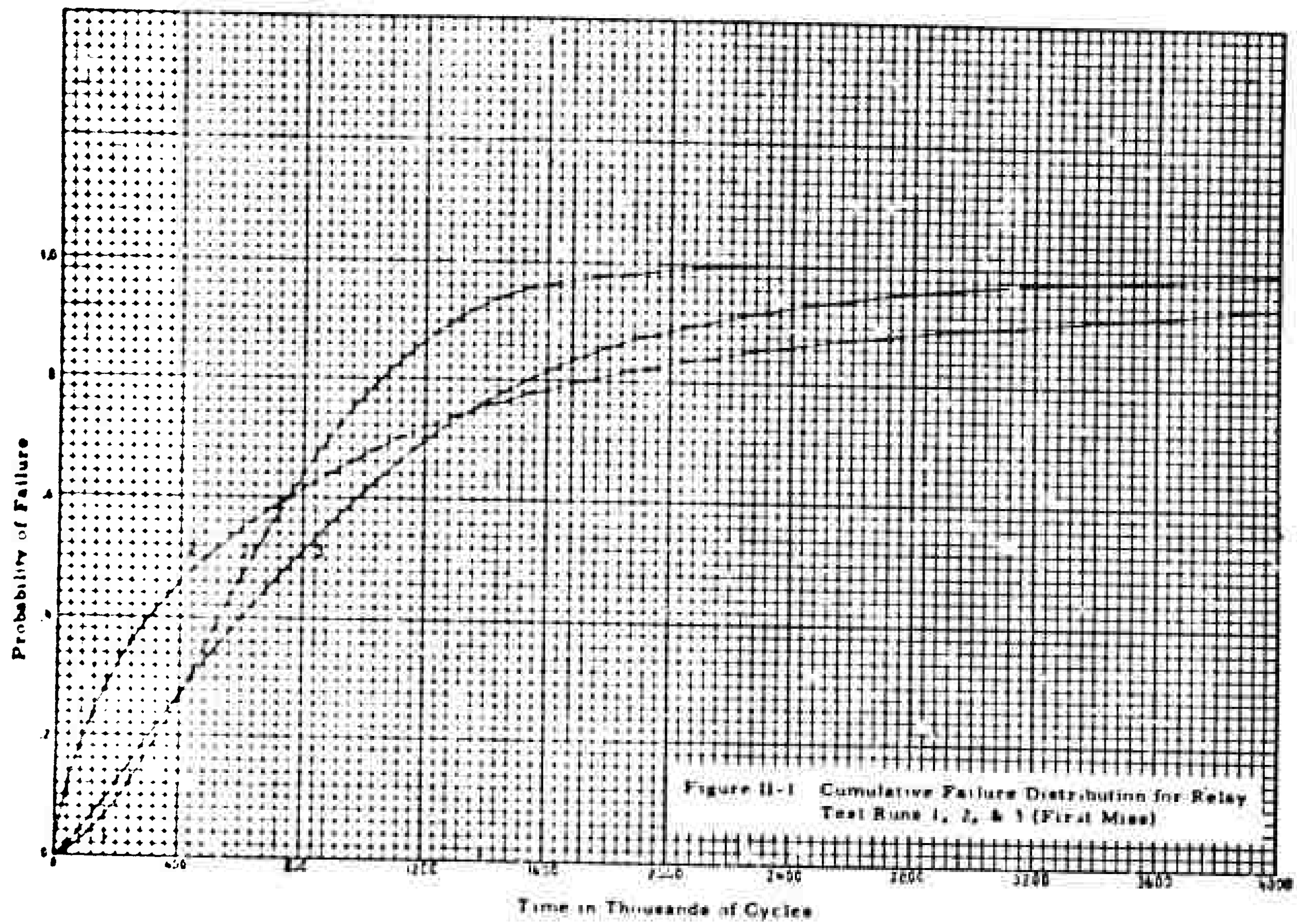

Figure II-1 Cumulative Failure Distribution for Relay Test Runs 1, 2, & 3 (First Miss)

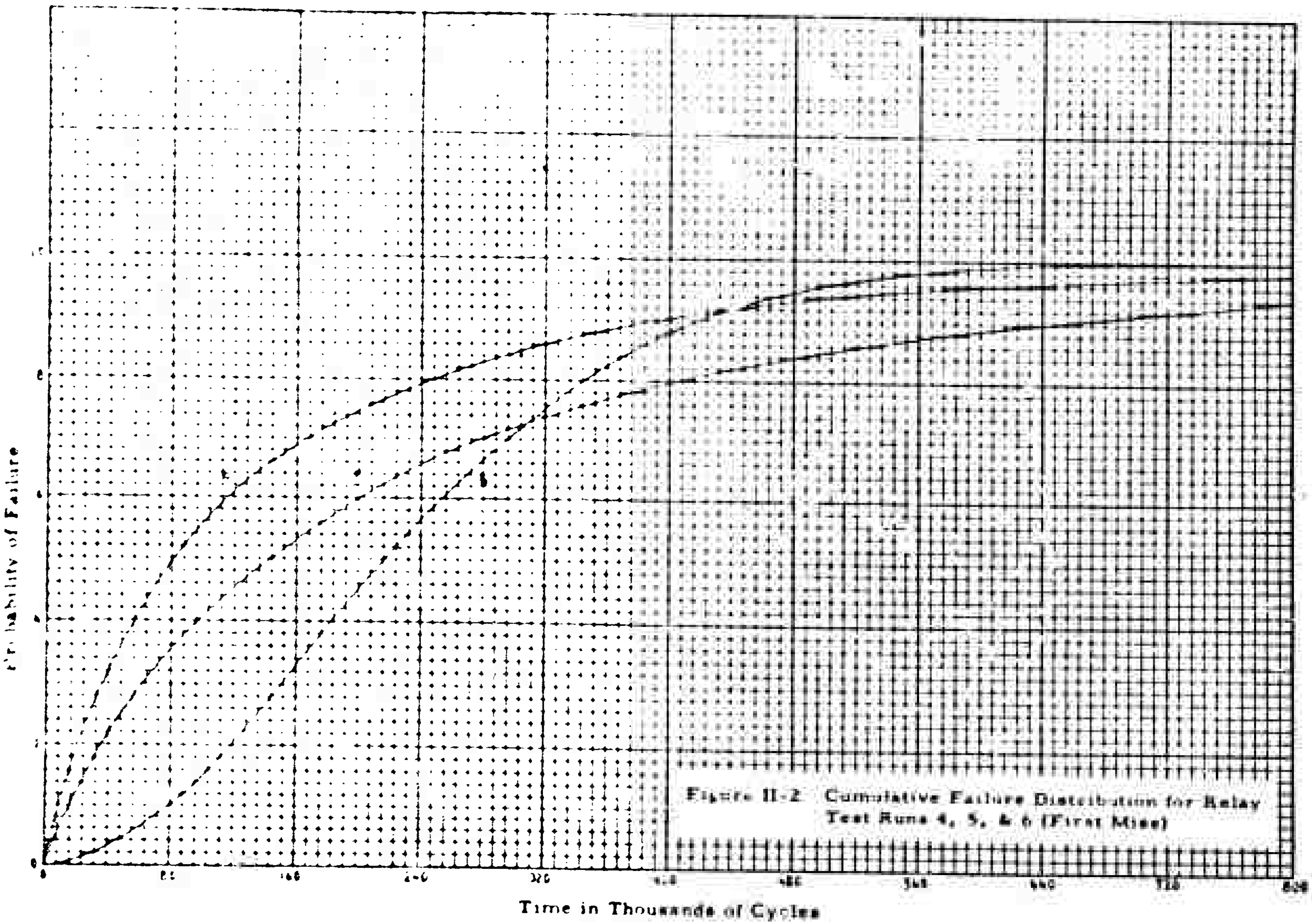

Figure II-2 Cumulative Failure Distribution for Relay Test Runs 4, 5, & 6 (First Miss)

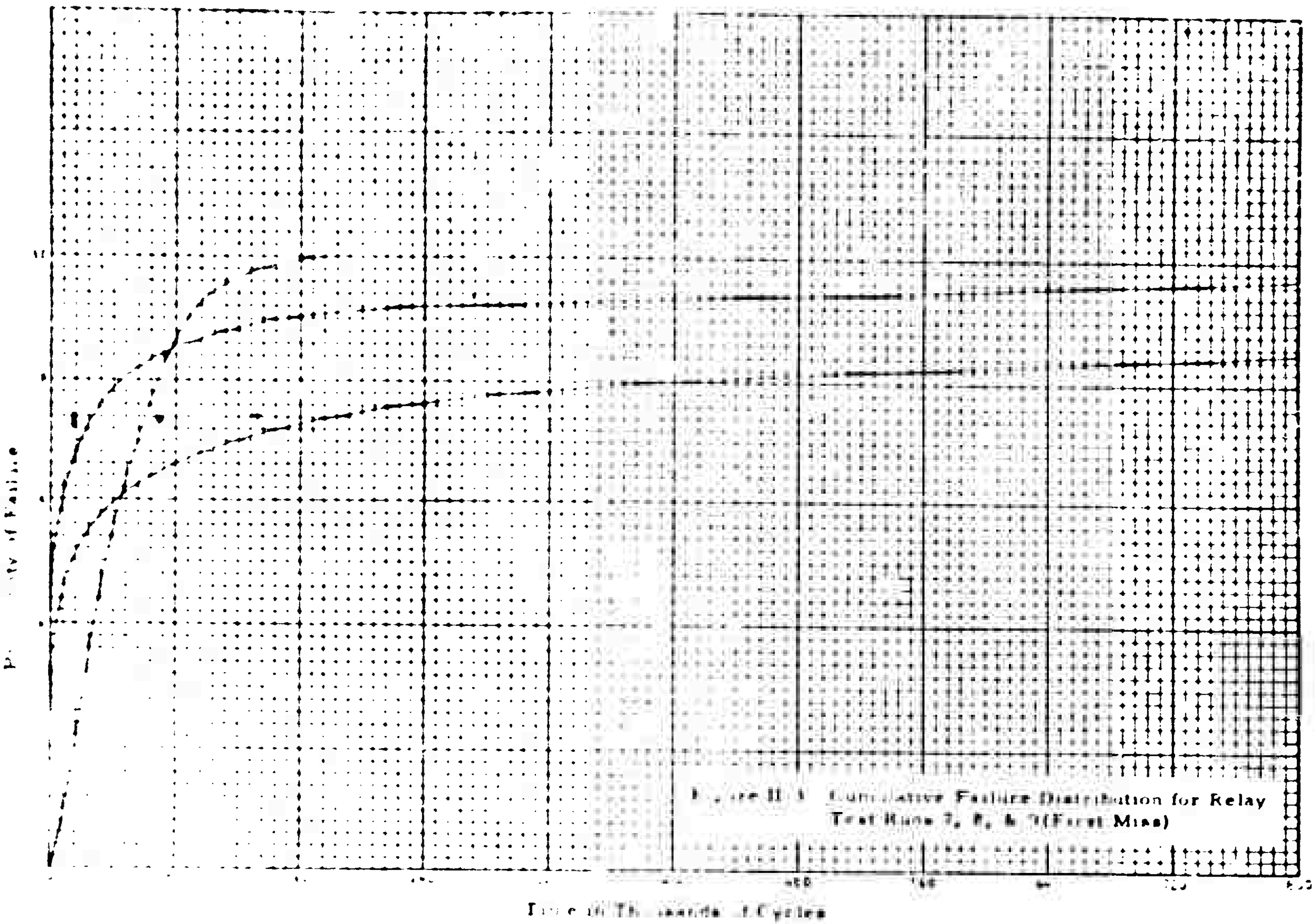

Figure II.3 Cumulative Failure Distribution for Relay Test Runs 7, 8, & 9 (First Miss)

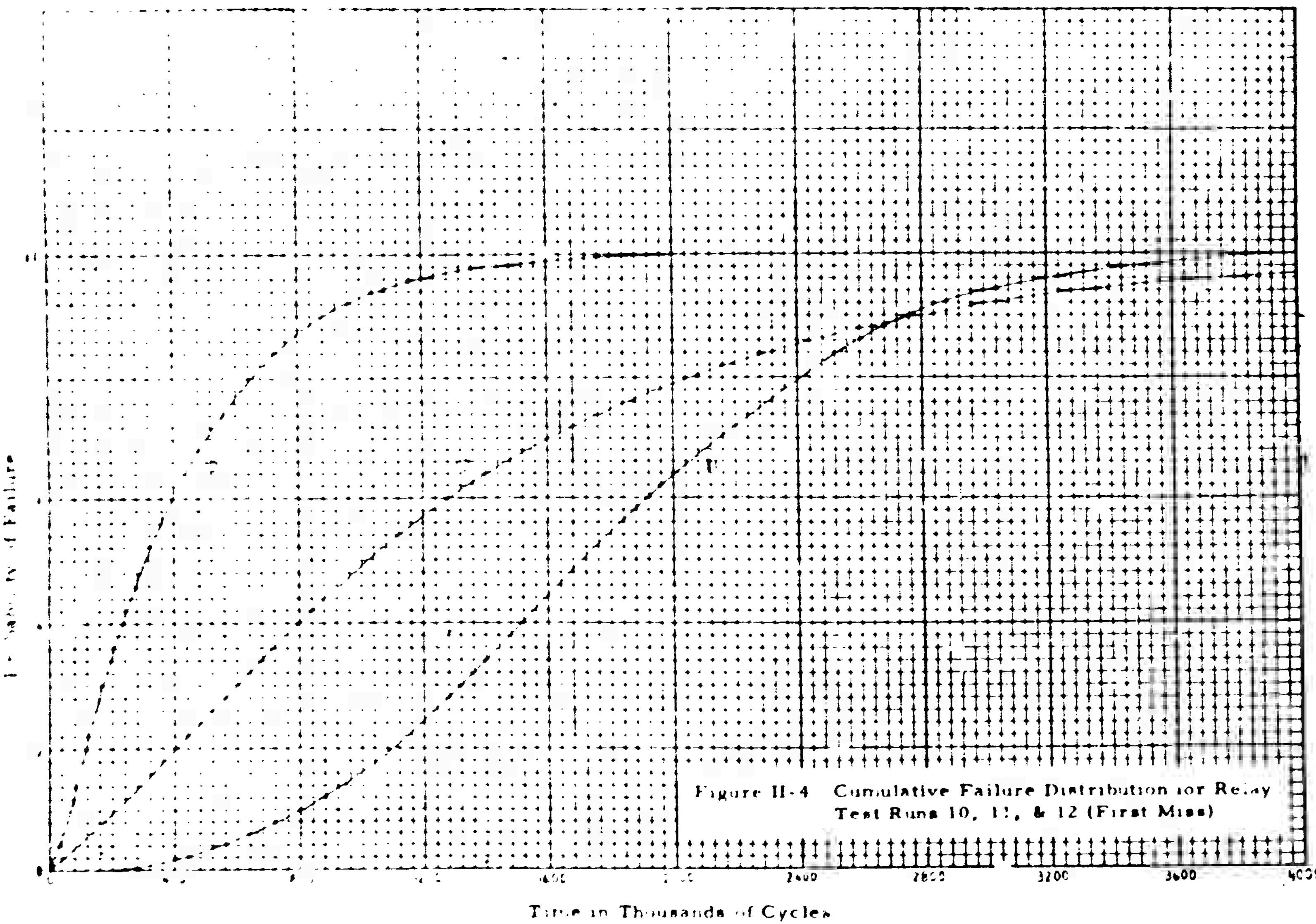

Figure II-4 Cumulative Failure Distribution for Relay Test Runs 10, 11, & 12 (First Miss)

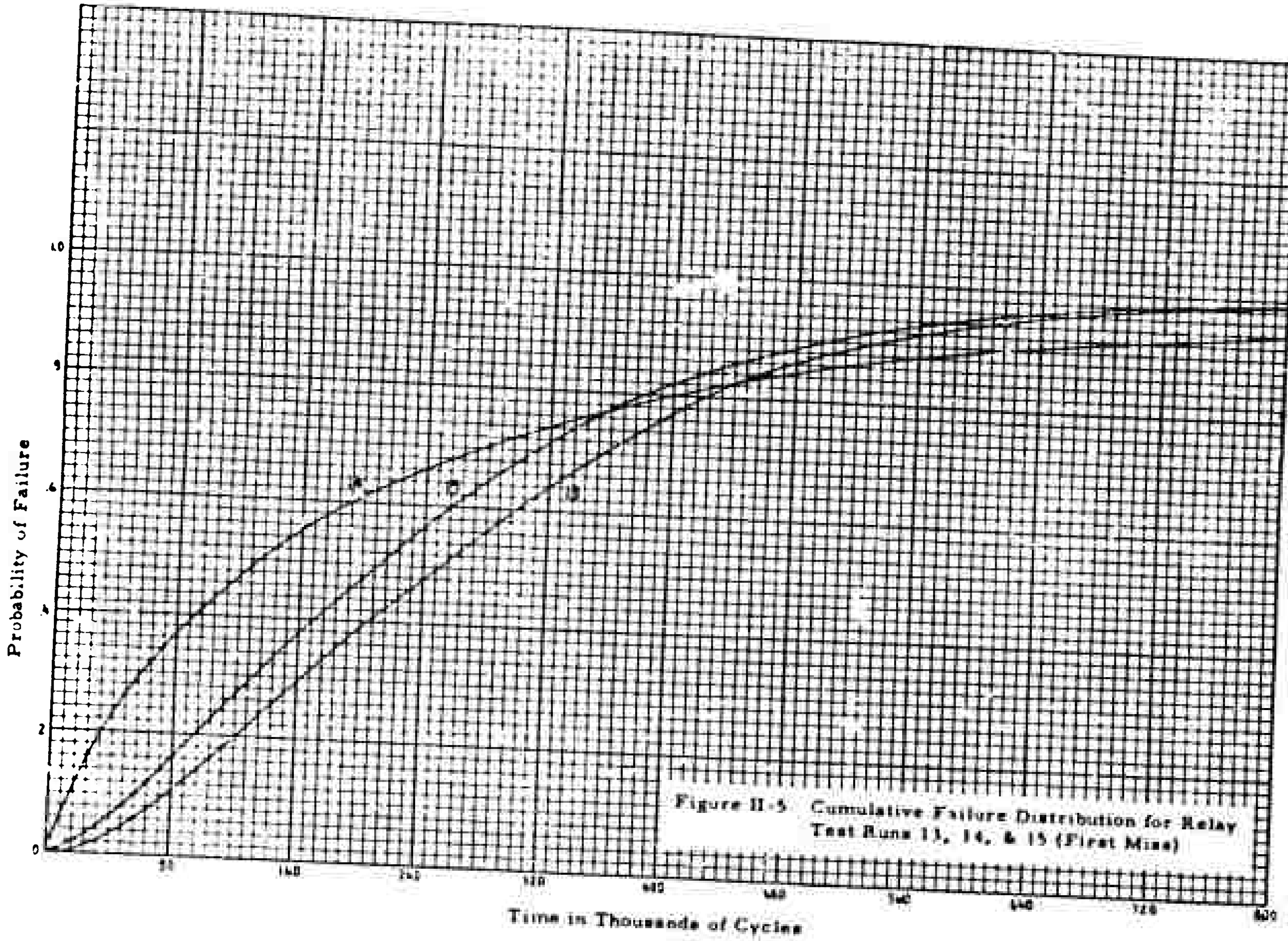

Figure II-5 Cumulative Failure Distribution for Relay Test Runs 13, 14, & 15 (First Miss)

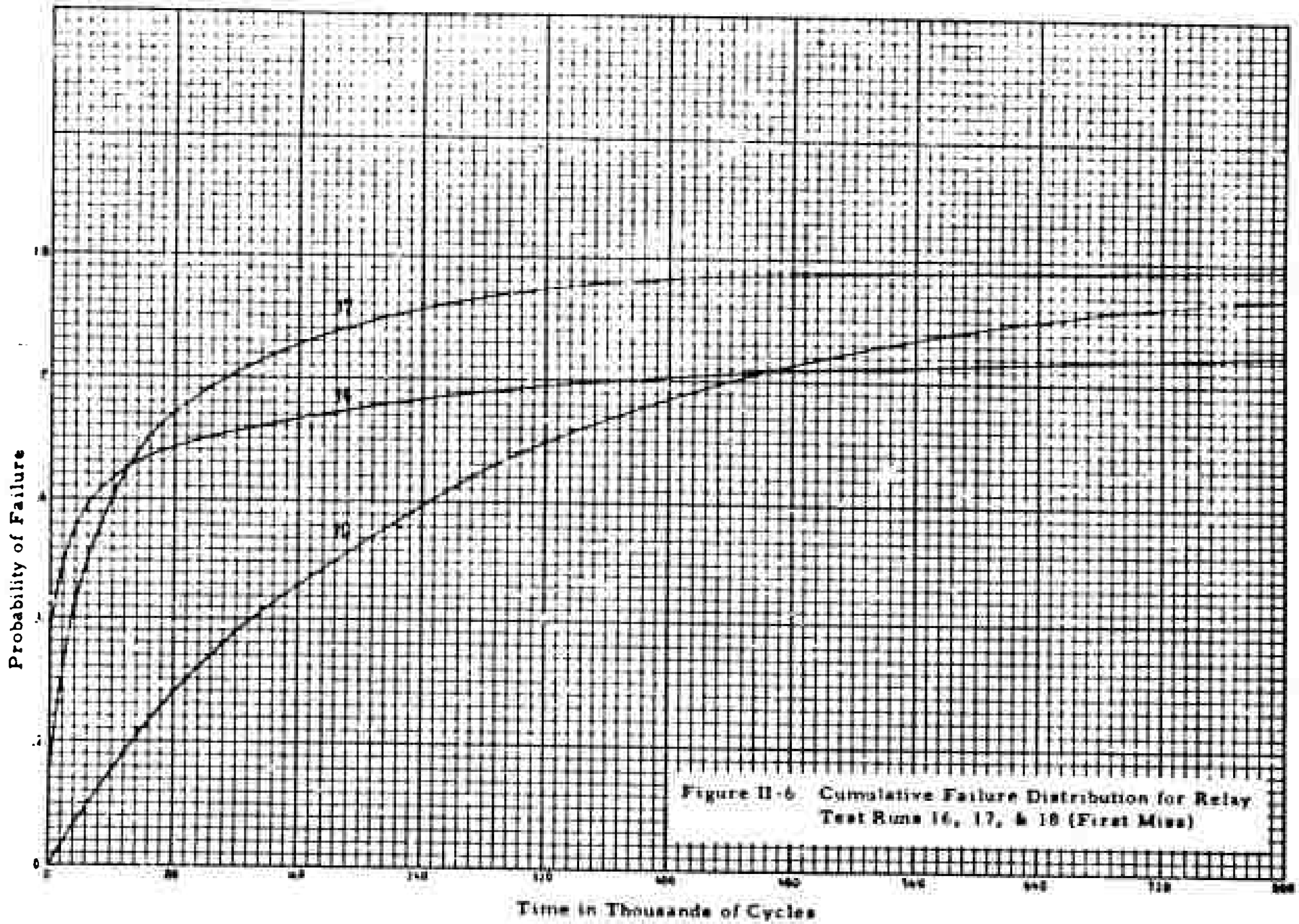

Figure II-6 Cumulative Failure Distribution for Relay Test Runs 16, 17, & 18 (First Miss)

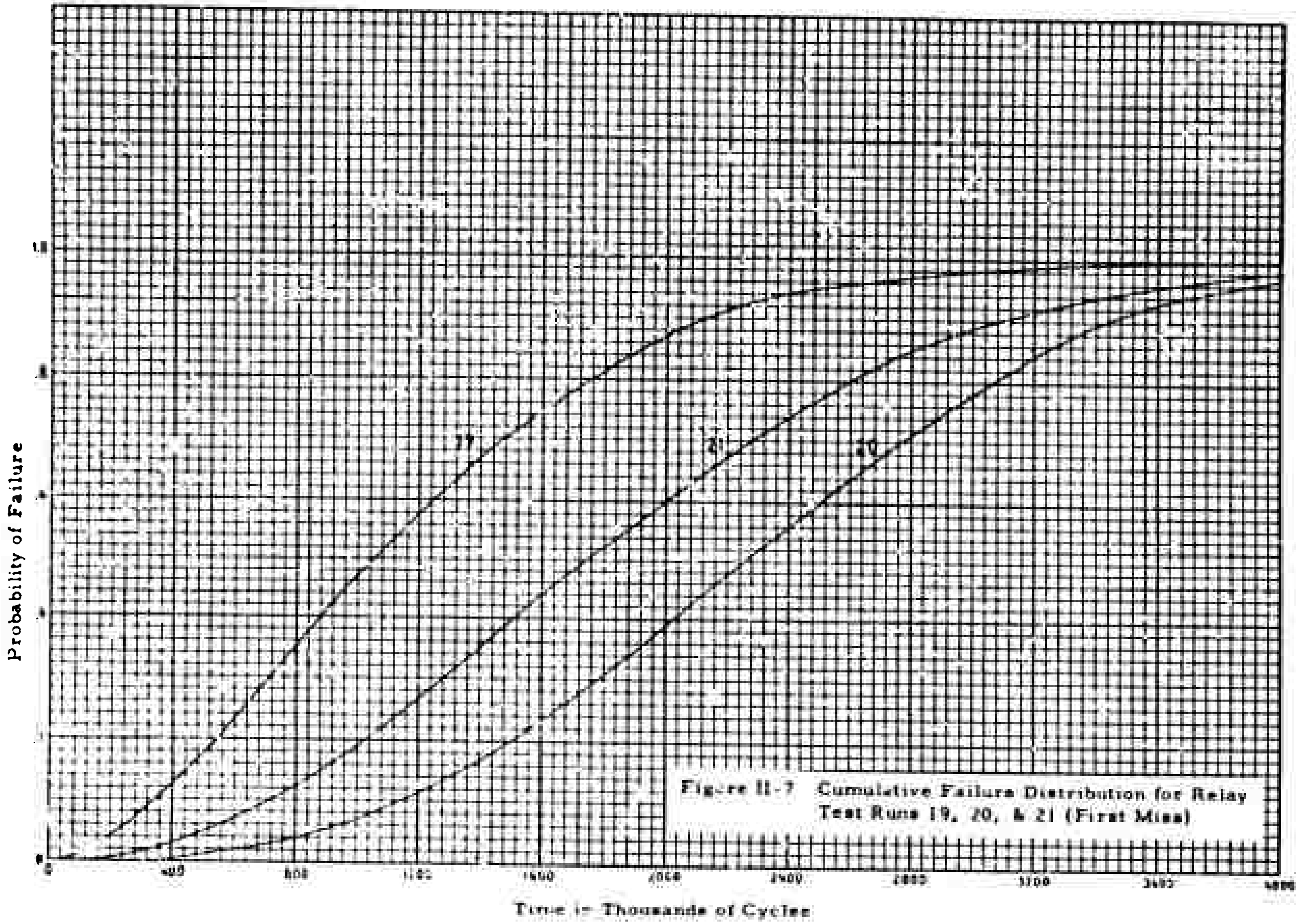

Figure II-7 Cumulative Failure Distribution for Relay Test Runs 19, 20, & 21 (First Miss)

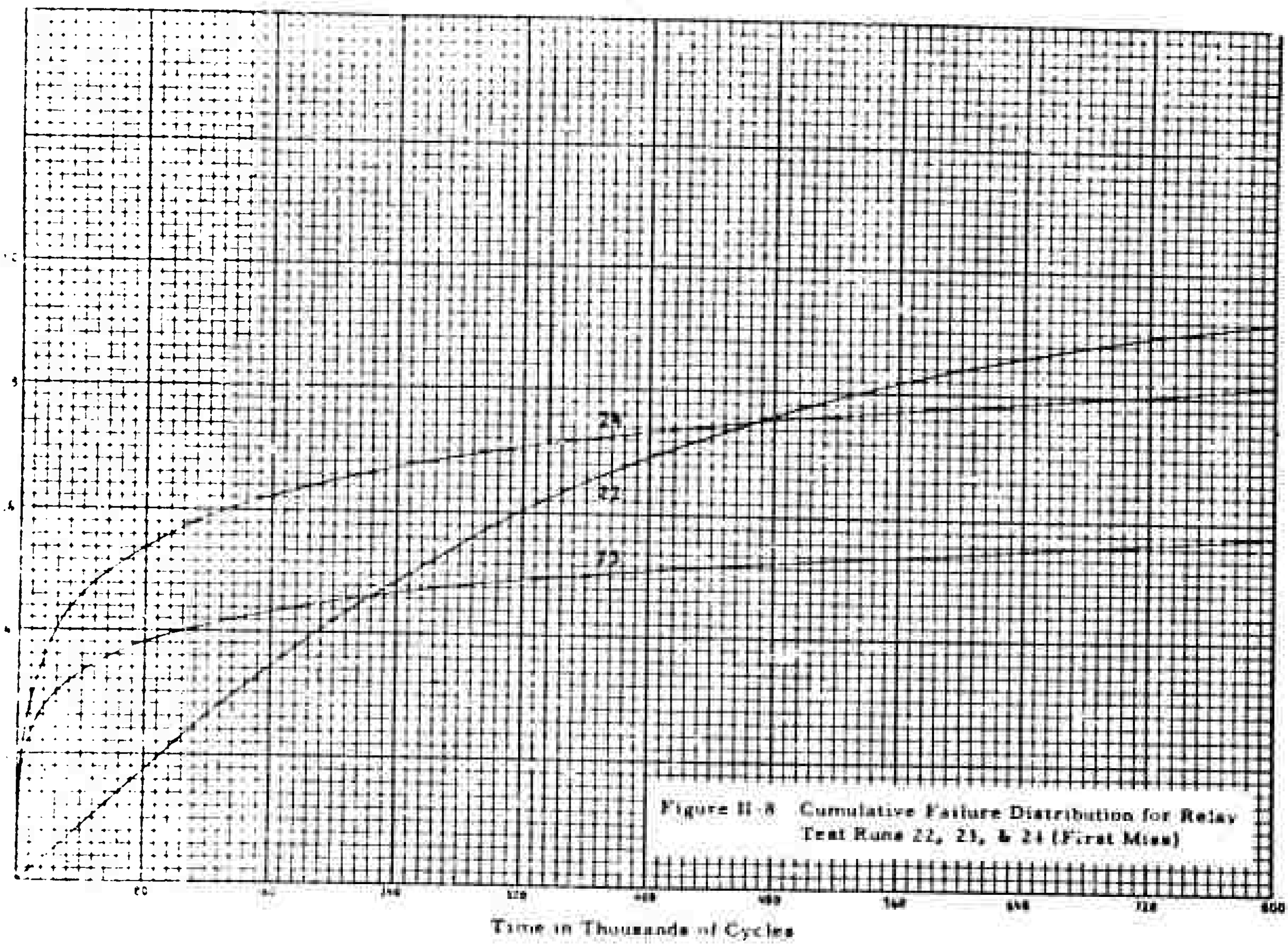

Figure II-8 Cumulative Failure Distribution for Relay Test Runs 22, 23, & 24 (First Miss)

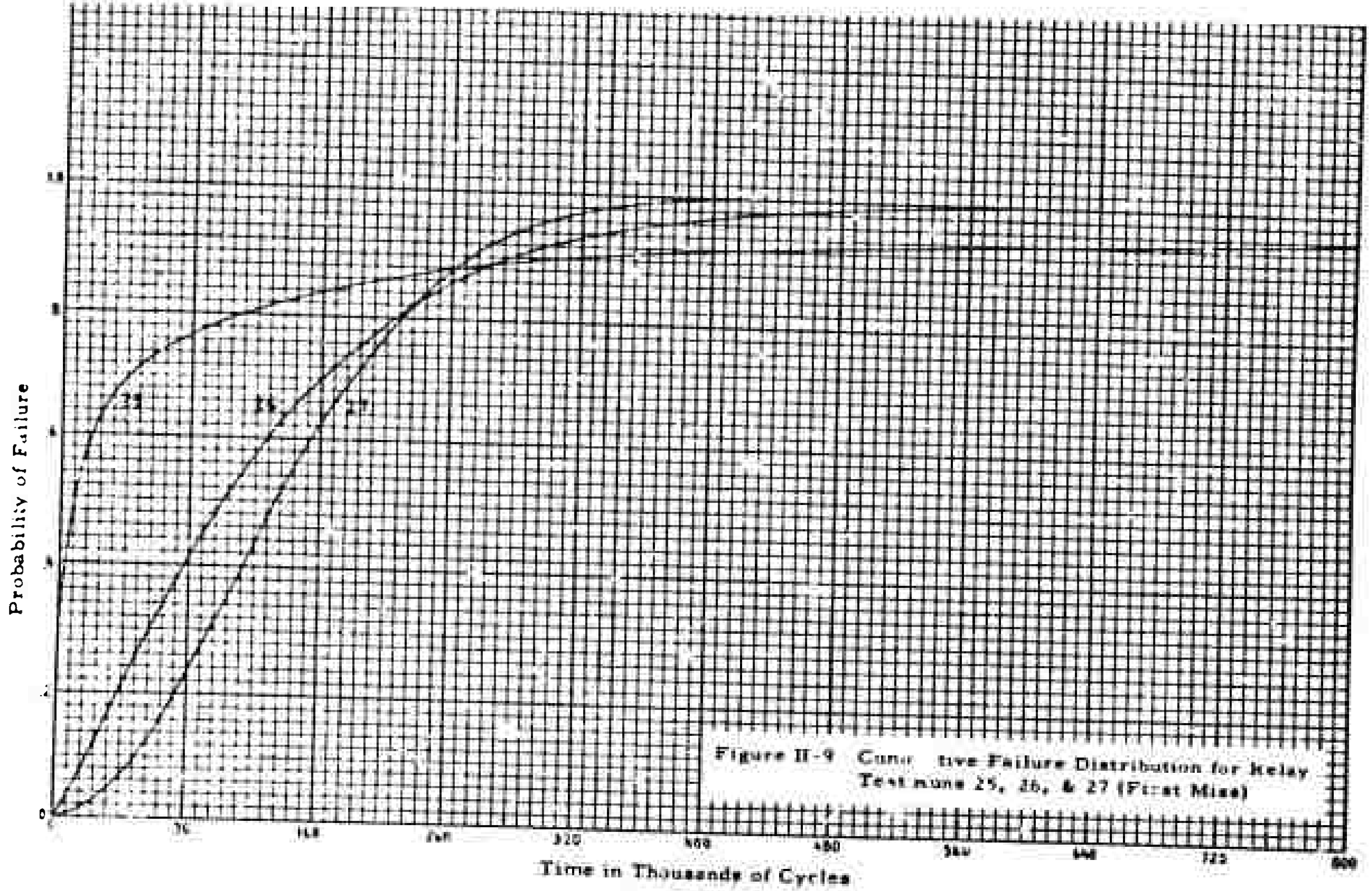

Figure II-9 Cumulative Failure Distribution for Relay Test Runs 25, 26, & 27 (First Miss)

APPENDIX III

FAILURE ANALYSIS OF RELAYS

This appendix is a detailed description of the failure analysis performed on the relays tested during this study program.

A. Failure Modes

1. Material transfer between the normally open contact and the blade, increased the contact gap beyond the limits of blade travel.
2. Material erosion from the normally open contacts or from the blade, increased the contact gap beyond the limits of blade travel.
3. Normally open contacts welded to the blade.
4. Normally open contact melted forming into a droplet or ball, reducing the contact gap.
5. Blade became distorted so that the normally open contact makes before the normally closed contact breaks.

B. Detailed Description of Failures of Each Relay

Test Run #1: 3 amps, 25°C, 1 cycle/second

Relay #35; Failure Mode: 1
Bottom arm of bifurcated contact has burned through blade. Material transferred to NO contact.

Relay #36; Failure Mode: 1
Top arm of bifurcated contact burned through blade; heavy material transfer to NO contact.

Relay #87, 88; Failure Mode: 1
Heavy material transfer to NO contacts increasing gap beyond range of blade travel.

Relay #89; Failure Mode: 1, 4
Lower arm of bifurcated contact burned through blade, then melted back to nub; upper arm burned through blade with heavy material transfer to NO contact.

Test Run #2: 3 amps, 100°C, 1 cycle/second

Relay #50; Failure Mode: 2
Moderate blade erosion, slight contamination on header, posts and NO contacts.

Relay #51; Failure Mode: 2
Moderate blade erosion; one arm of contact finally wore through the blade; very little contamination.

Relay #141, 142, 143; Failure Mode: 2
Moderate blade erosion; some material transfer to NO contact; slight contamination on header.

Test Run #3; 3 amps, 150°C, 1 cycle/second

Relay #39, 40, 96, 97, 98; Failure Mode: 1
Slight material transfer to blade; holes worn in NO contacts; powdery white deposit on entire header surface; brownish powder deposited on header, post.

Test Run #4: 6 amps, 25°C, 1 cycle/second

Relay #1; Failure Mode: 1, 3
Heavy material transfer to NO contact; finally welded and then broke off; black deposit on header, posts.

Relay #4; Failure Mode: 1, 4
Moderate material transfer to NO contact (upper arm of bifurcated contact); lower arm of contact melted back into a ball, reducing contact gap.

Relay #90; Failure Mode: 1
Heavy material transfer to NO contact.

Relay #91; Failure Mode: 1, 4
Ends of NO contact melted back into ball, decreasing gap; small amount of material transfer.

Relay #92; Failure Mode: 1
Moderate material transfer to NO contact; heavy contamination on header and frame.

Test Run #5: 6 amps, 100°C, 1 cycle/second

Relay #5; Failure Mode: 1, 3
Heavy material transfer to NO contact and finally welded; contamination resembles vaporized metal (brownish color).

Relay #6; Failure Mode: 1
End of NO contact melted; slight transfer of material to blade; slight contamination.

Relay #144, 157; Failure Mode: 1
Heavy material transfer to NO contact; holes in blades.

Relay #145; Failure Mode: 1
Slight material transfer to NO contact; slight contamination (black).

Relay #146; Failure Mode: 1
Moderate material transfer to NO contact; heavy metallic contamination on header; holes in blade.

Test Run 6: 6 amps, 150°C, 1 cycle/second

Relay #118, 119, 121; Failure Mode: 1
Heavy material transfer to blade; metallic deposit on header; heavy contamination on header, posts (brown powder).

Relay #120; Failure Mode: 1, 4
Heavy material transfer to NO contact; one arm of contact melted back to form ball; holes worn in blade; heavy contamination (metallic) on all header surfaces.

Relay #122; Failure Mode: 1
Heavy metal transfer between blade and NO contact; heavy contamination on header.

Test Run #7: 8 amps, 25°C, 1 cycle/second

Relay #22, Failure Mode: 3, 4
NO contact melted into large droplet which welded to blade; could have been caused by bad solder joint on contact post.

Relay #32, 81, 83; Failure Mode: 1
Holes in blade: heavy material transfer to NO contact; heavy contamination on header, posts.

Relay #82; Failure Mode: 1, 4
Holes in blade; heavy material transfer to one arm of contact; other arm melted into ball.

Relay #23, 25; Failure Mode: 4
Contacts melted forming droplet or ball, reducing gap.

Relay #24, 29, 30, 31, 33; Failure Mode: 3, 4
One contact arm melted and formed ball, other welded to blade.

Relay #28; Failure Mode: 4
One arm melted forming ball, reducing gap.

Relay #34; Failure Mode: 1, 4
One contact arm melted into ball, other burned hole in blade.

Test Run 8: 8 amps, 100°C, 1 cycle/second

Relay #54, 55; Failure Mode: 4
One arm of bifurcated NO contact melted into ball, reducing gap.

Rela, #147, 148; Failure Mode: 1
Heavy material transfer to NO contact; holes in blade.

Relay #149; Failure Mode: 1
Heavy material transfer to NO contact; holes in blade; same as #147 and 148 but more severe.

Relay #158; Failure Mode: 1
Moderate transfer to NO contact; contamination moderate.

Test Run 9: 8 amps, 150°C, 1 cycle/second

Relay #41; Failure Mode: 1, 3
Hole eroded in blade; moderate material transfer to NO contact; blade and contacts welded.

Relay #42; Failure Mode: 3, 4
Initial failure; one arm of bifurcated contacts melted into a ball and welded to blade.

Relay #45; Failure Mode: 1, 4
One arm of bifurcated contact melted into ball; other arm received moderate material transfer from blade (hole in blade); light contamination on header.

Relays 107, 108, 109; Failure Mode: 2
Erosion from NO contact to blade, slight contamination on header.

Test Run 10: 3 amps, 25°C, 10 cycles/second

Relay #46; Failure Mode: 1
Moderate erosion and slight material buildup on blade; heavy contamination on header (black).

Relay #47, 115, 117; Failure Mode: 1
Heavy material transfer to blade; ends of NO contacts melted and transferred; moderate contamination (black).

Relay #116; Failure Mode: 2
Erosion from NO contact to blade; slight contamination on header.

Test Run #11: 3 amps, 100°C, 10 cycles/second

Relay #52, 126, 127; Failure Mode: 1
Ends of contacts melting and transferring to blade; heavy contamination.

Relay #53; Failure Mode: 2
Contacts eroded very thin, but only slight buildup on blade; slight contamination on header.

Relay #128; Failure Mode: 1, 3
Ends of contacts melting and moderate material transfer to blade; lightly welded; weld broke during inspection.

Test Run #12: 3 amps, 150°C, 10 cycles/second

Relays #58, 59, 132, 134; Failure Mode: 2
Slight erosion of blade toward contact; very slight damage however.

Relay #133; Failure Mode: 1
Moderate material transfer to blades; ends of contacts not melting off though--buildup is in center of blade and is smooth in contour with corresponding depressions in contacts.

Test Run #13: 6 amps, 25°C, 10 cycle/second

Relays #110, 111; Failure Mode: 1
Heavy material transfer to blade; heavy black contamination on header, posts.

Relay 112; Failure Mode. 2
Erosion in direction of blade.

Relay 113, 114: Failure Mode: 1
Material transferring to blade but from only one arm of bifurcated contact; contamination black and sooty.

Test Run #14: 6 amps, 100°C, 10 cycles/second

Relays #150, 151, 152, 153; Failure Mode: 1
Contacts worn through; heavy material transfer to blade; dark grey contamination.

Relay #154; Failure Mode: 1
Something violent appears to be going on. Both edges of the blade have burned off with lots of metal splashing around. Metal transferring in direction of contacts

Test Run #15: 6 amps, [illegible]°C, 10 cycles/second

Relays #135, 136, [illegible]; Failure Mode: 2
Slight erosion; appears to be toward blade, but hard to be sure.

Relay 155, 156; Failure Mode: 1
Considerable erosion to blade; some material transfer; holes worn into contacts.

Test Run #16: 8 amps, 25°C, 10 cycles/second

Relays #43, 104; Failure Mode: 1
Heavy material transfer to blade; heavy contamination (black and sooty).

Relays #44, 106; Failure Mode: 3, 5
Contacts welded to blade (both arms of contact); contacts way out of alignment; metal discolored and annealed; distortion possibly due to heating, stress relief.

Relay #105; Failure Mode: 3
Both arms of contact welded tightly to blade.

Test Run #17: 8 amps, 100°C, 10 cycles/second

Relay #56, 57; Failure Mode: 3, 4
One arm of contact welded tight; other arm melted into ball.

Relay #129, 130; Failure Mode: 1
Heavy material transfer to blade; lots of splatter.

Relay #131; Failure Mode: 1, 3
Ends of contacts metled and built up heavily on blade; welded.

Test Run #18: 8 amps, 150°C, 10 cycles per second

Relay #7; Failure Mode: 1
Heavy material transfer to blade; contamination golden brown metallic color; header base completely coated with white powder.

Relay #8, 138; Failure Mode: 1
Ends of contacts melting back with moderate material transfer to blade; header posts coated golden brown metallic color.

Relay #139; Failure Mode: 1, 3, 4
One arm of bifurcated contact welded tight; appears to have begun melting into a ball prior to welding; other arm has slight wear and metal transfer to blade.

Relay #140; Failure Mode: 1
Both arms of contact show some erosion; one arm of contact however shows heavy material transfer to blade.

Test Run #19: 3 amps, 25°C, 30 cycles/second

Relays #37, 38, 93, 95; Failure Mode: 1
Heavy material transfer to blade as tips of NO contacts melted back; light contamination on header.

Relay #94; Failure Mode: 1
Heavy material transfer to blade however buildup was on only one arm of bifurcated contact.

Test Run #20: 3 amps, 100°C, 30 cycles/second

Relays #48, 49, 123, 124, 125; Failure Mode: 2
Material erosion in direction of blade; very little splatter or contamination.

Test Run #21: 3 amps, 150°C, 30 cycles/second

Relays #26, 27, 84, 85, 86; Failure Mode: 2
Material erosion in direction of blade; almost no contamination on header.

Test Run #22: 6 amps, 25°C, 30 cycles/second

Relays #99, 100, 101, 102, 103; Failure Mode: 2
Material erosion in direction of blade; no appreciable material transfer; slight contamination on header.

Test Run #23: 6 amps, 100°C, 30 cycles/second

Relays 20, 21, 76, 77, 78, Failure Mode: 1
Heavy material transfer to blade, contact burned off; slight contamination on header.

Test Run #24: 6 amps, 150°C, 30 cycles/second

Relay #18; Failure Mode: 2, 3
Erosion from blade to contact; NO contacts welded to blade; heavy contamination on header.

Relay #19; Failure Mode: 5
Blade distorted and annealed; NO contact appears to make before NO contact breaks.

Relays #73, 74, 75; Failure Mode: 1
Heavy material transfer to blade; moderate to heavy contamination on header.

Test Run #25: 8 amps, 25°C, 30 cycles/second

Relay #16, 70; Failure Mode: 3
One arm of bifurcated contacts welded to blade.

Relay #17, 72; Failure Mode: 1
Heavy material transfer to blade; moderate to heavy contamination.

Relay #71; Failure Mode: 3
Both arms of NO contacts welded tightly to blade.

Test Run 25a: 8 amps, 25°C, 30 cycles/second

Note: The relays in Test Run 25a were tested using a different power supply. Since the results were vastly different, the test method was returned to its original form.

Relays 15, 16, 67, 68, 69; Failure Mode: 3
NO contacts and blades welded.

Test Run #26: 8 amps, 100°C, 30 cycles/second

Relays #12, 13, 64, 65, 66; Failure Mode: 1
Ends of NO contacts melted back slightly with heavy material transfer to blade; heavy contamination on header.

Test Run #27: 8 amps, 150°C, 30 cycles/second

Relay #9; Failure Mode: 5
Initial failure; blade distorted and annealed; NO contact makes before NO contacts make.

Relays 10, 61; Failure Mode: 1
Heavy material transfer to blade; ends of NO contacts burned off; heavy contamination on header.

Relay 11; Failure Mode: 1
Erosion in direction of blade.

Relays 62, 63; Failure Mode: 1, 3
NO contact welded to blade; one arm of bifurcated NO contact burned on end with heavy material transfer to blade.

APPENDIX IV

FAILURE ANALYSIS OF O-RINGS

This appendix is a detailed description of the failure analysis performed on the O-rings tested during this study program.

A. FAILURE MODES

1. Radial crack or fracture

2. Circumferential crack

3. No visible defect

B. DETAILED DESCRIPTION OF FAILURES OF EACH O-RING

Test Run No. 1: 200°F, No Ultraviolet

O-Ring No. 2-1; Failure Mode: 1

Fractured.

O-Ring No. 2-2; Failure Mode: 1

Several hairline cracks running radially across outer surface.

O-Ring No. 2-3; Failure Mode: 1, 2

One large radial crack, 2 circumferential cracks

O-Ring No. 2-4; Failure Mode: 1

One large radial crack, numerous smaller hairline radial cracks across outer edges of ring.

O-Ring No. 2-5; Failure Mode: 1, 2

Ring fractured probably at splice. The entire surface is made up of circumferential cracks which periodically cross the mold juncture radially.

O-Ring No. 2-6; Failure Mode: 1

Numerous deep radial cracks across mold juncture.

O-Ring No. 2-7; Failure Mode: 1

Fractured twice. Surface hard and smooth; no cracking.

O-Ring No. 2-8; Failure Mode 1, 2

Deep radial crack across mold juncture; connects to small series of lesser cracks.

O-Ring No. 2-9; Failure Mode: 1, 2

Broke in 2 places; very small hairline crack on circumference.

O-Ring No. 2-10; Failure Mode: 1

Radial fracture; 2 other deep radial cracks across mold juncture.

Test Run No. 2: 200°F, 0.1 Watts/Ft^2 Ultraviolet

O-Ring No. 1-51; Failure Mode: 1

Radial fracture; several other deep radial cracks.

O-Ring No. 1-52; Failure Mode: 1

Six very deep radial cracks; nearly through ring cross-section. One crack from inside diameter, rest from OD.

O-Ring No. 1-53; Failure Mode: 1

Five or six very deep radial cracks across OD.

O-Ring No. 1-54; Failure Mode: 1

Three very deep radial cracks across OD.

O-Ring No. 1-55; Failure Mode: 1

Fractured radially; 2 other very deep radial cracks in OD.

O-Ring No. 1-56; Failure Mode: 1, 2

One deep radial crack across OD. Also a series of circumferential cracks at mold juncture which periodically cross it radially.

O-Ring No. 1-57, 1-58; Failure Mode: 1

Radial fracture.

O-Ring No. 1-59; Failure Mode: 1, 2

Whole series of closely spaced radial cracks in OD. One large one in ID. A few circumferential cracks connecting the radials.

O-Ring No. 1-60; Failure Mode: 1

Radial fracture. One other deep radial crack.

Test Run No. 3: 200°F, 0.2 Watts/Ft^2 Ultraviolet

O-Ring No. 1-41; Failure Mode: 1, 2

Radial fracture. Also small circumferential crack.

O-Ring No. 1-42; Failure Mode: 1

Seven or eight deep radial cracks on OD. Two or three deep radial cracks in ID.

O-Ring No. 1-43, 1-46; Failure Mode: 1

Fractured radially; one other deep radial crack on OD.

O-Ring No. 1-44, 1-45, 1-49, 1-50; Failure Mode: 1

Radial fracture.

O-Ring No. 1-47; Failure Mode: 1

Very deep radial cracks (many) on both ID and OD. Specimen fractured during inspection.

O-Ring No. 1-48; Failure Mode: 1

Three deep radial cracks on OD, one on ID.

Test Run No. 4: 250°F, No Ultraviolet

O-Ring No. 2-61; Failure Mode: 1

Very deep radial cracks on OD.

O-Ring No. 2-62, 2-66; Failure Mode: 1

One deep radial crack on OD.

O-Ring No. 2-63, 2-65, 2-70; Failure Mode: 1

Radial fracture.

O-Ring No. 2-64; Failure Mode: 1

One very deep radial crack on OD; several less severe.

O-Ring No. 2-67, 2-68; Failure Mode: 1

Two deep radial cracks in OD.

O-Ring No. 2-69; Failure Mode: 1

Radial fracture - at foreign matter inclusion.

Test Run No. 5: 250°F, 0.1 Watts/Ft^2 Ultraviolet

O-Ring No. 2-71, 2-76; Failure Mode: 3

No defects visible.

O-Ring No. 2-72; Failure Mode: 1

Fractured radially; also deep radial crack on ID.

O-Ring No. 2-73; Failure Mode: 1, 2

Radial fracture; several deep radial cracks on OD and a few minor circumferential cracks at OD.

O-Ring No. 2-74; Failure Mode: 1, 2

Radial fracture - a few deep circumferential cracks.

O-Ring No. 2-75, 2-77, 2-80; Failure Mode: 1

Radial fracture.

O-Ring No. 2-78; Failure Mode: 1, 2

Deep radial crack on OD, connecting with network of circumferential cracks.

O-Ring No. 2-79; Failure Mode: 1

Deep radial crack on OD.

Test Run No. 6: 250°F, 0.2 Watts/Ft^2 Ultraviolet

O-Ring No. 2-81, 1-82, 2-88; Failure Mode: 1

Radial fracture; deep radial crack on OD.

O-Ring No. 2-83; Failure Mode: 3

No defect visible.

O-Ring No. 2-84, 2-86; Failure Mode: 1

Deep radial crack.

O-Ring No. 2-85, 2-90; Failure Mode: 1

Radial fracture.

O-Ring No. 2-87; Failure Mode: 1, 2

Deep radial crack connected to a network of lesser circumferential cracks.

O-Ring No. 2-89; Failure Mode: 1, 2

Radial fracture; deep radial crack, connected to network of circumferential cracks.

Test Run No. 7: 275°F, No Ultraviolet

O-Ring No. 1-61; Failure Mode: 1

Radial fracture.

O-Ring No. 1-62; Failure Mode: 1, 2

Deep radial crack on OD; several hairline cracks both radial and circumferential; deep circumferential crack on internal mold line.

O-Ring No. 1-63; Failure Mode: 2

Deep circumferential cracks near inner mold line. A few hairline circumferential cracks on OD.

O-Ring No. 1-64; Failure Mode: 1, 2

Deep radial crack on OD. Several lesser circumferential cracks on both ID and OD.

O-Ring No. 1-65; Failure Mode: 1, 2

Network of circumferential cracks on entire surface which cross mold line periodically. One moderately severe radial crack.

O-Ring No. 1-66; Failure Mode: 1, 2

Several severe radial cracks on side connecting to a network of circumferential cracks on OD mold line.

O-Ring No. 1-67; Failure Mode: 1, 2

Deep radial crack connecting to network of circumferential cracks on OD. Several deep circumferential cracks on ID.

O-Ring No. 1-68; Failure Mode: 2

Circumferential cracks on both ID and OD.

O-Ring No. 1-69, 1-70; Failure Mode: 1, 2

Deep radial and circumferential cracks on OD.

Test Run No. 8: 275°F, 0.1 Watts/Ft^2 Ultraviolet

O-Ring No. 1-71, 1-76; Failure Mode: 1

Deep radial crack across OD.

O-Ring No. 1-72; Failure Mode: 1, 2

Deep radial cracks across OD. Hairline circumferential cracks at OD mold line.

O-Ring No. 1-73; Failure Mode: 1, 2

Radial fracture; very deep circumferential cracks at OD mold line.

O-Ring No. 1-74; Failure Mode: 1, 2

Deep radial and circumferential cracks.

O-Ring No. 1-75; Failure Mode: 1, 2

Deep radial and circumferential cracks at OD.

O-Ring No. 1-77; Failure Mode: 1

Radial fracture; two deep radial cracks across OD.

O-Ring No. 1-78; Failure Mode: 1, 2

Several deep radial and circumferential cracks.

O-Ring No. 1-79; Failure Mode: 1, 2

Deep radial crack, connected to network of deep circumferential cracks at OD mold line.

O-Ring No. 1-80; Failure Mode: 1, 2

Deep radial cracks connected to deep circumferential cracks.

Test Run No. 9: 275°F, 0.2 Watts/Ft^2 Ultraviolet

O-Ring No. 1-81; Failure Mode: 2

Deep circumferential cracks at OD.

O-Ring No. 1-82; Failure Mode: 1, 2

Radial fracture; slight circumferential cracks at OD.

O-Ring No. 1-83; Failure Mode: 1, 2

Deep radial crack on OD; slight circumferential cracks.

O-Ring No. 1-84, 1-85; Failure Mode: 2

Deep circumferential cracks on ID and OD.

O-Ring No. 1-86; Failure Mode: 1, 2

Network of deep circumferential cracks on entire surface which cross mold line periodically. One moderately severe radial crack.

O-Ring No. 1-87; Failure Mode: 2

Deep circumferential cracks on ID. Several lesser circumferential cracks on OD.

O-Ring No. 1-88; Failure Mode: 1, 2

Deep circumferential cracks on OD. Radial fracture.

O-Ring No. 1-89; Failure Mode: 1

Deep radial crack on OD.

O-Ring No. 1-90; Failure Mode: 1, 2

Deep radial crack on OD; connected to network of deep circumferential cracks on OD.

APPENDIX V PHYSICAL TEST METHODS

This appendix contains a description of the physical test method used in the life tests conducted on each of the four parts included in the study program.

APPENDIX V-1 PHYSICAL TEST METHOD (SWITCHES)

The switch test setup is schematically shown by Figure V-1. The test setup had provisions for testing two switches simultaneously. A four lobe cam was used to provide the mechanical movement that displaced the roller leaf actuator and in turn operated the switch plunger. The test samples were mounted on the fixture and the necessary wiring connection made. The overtravel was measured by optical means and the necessary mechanical adjustment of switch position made to achieve the desired overtravel condition of .005, .010 or .015 inches. The mechanical adjustment was made by moving the switch mounting plate toward the cam to increase the overtravel or away from the cam to reduce the overtravel. Overtravel is defined as the additional plunger movement measured after the normally open contact circuit has been completed.

The electrical load was applied to the normally closed contact of the switch. This load was established by using one resistor in series with the power source for the 5 amp test condition. The addition of a second resistor in parallel with the original resistor accomplished the 10 amp load, and a third resistor connected in parallel provided the 15 amp load.

The rotational speed of the cam was adjusted by a variable speed drive to provide the desired actuation rates of 70, 150 or 300 cycles per minute.

Electrical impulse counters were connected to the normally open contacts of each switch and were used to record the number of switching cycles. Miss detectors were used to monitor both the normally open and the normally closed switching function. At the time of a switch malfunction the miss detector opened the circuit to the drive motor and triggered the failure indicator to show which switch had the failure or miss. All testing was conducted at normal room ambient temperature (65°F to 80°F). The switch test loads were obtained using 120 volts ac and a 1000 watt load bank. The cam provided a switching duty cycle of approximately 70% on and 30% off for the normally closed contact.

The following items of test equipment were utilized to provide the setup and test data:

Item	Instrument Accuracy	Data Measurement
Gaertner Scientific Co. Optical Measuring Device Serial # 1295P	±.0001 inch	Contact Overtravel

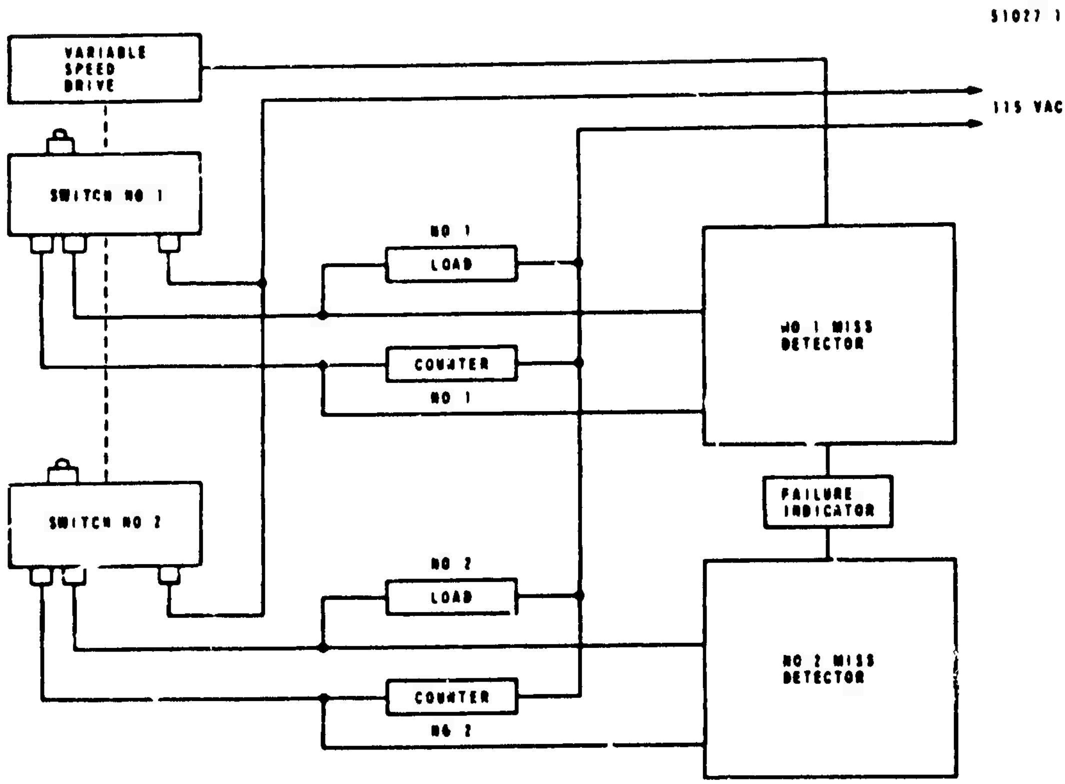

Figure V-1. Schematic for Snap-Action Switch Test Method

Item	Instrument Accuracy	Data Measurement
Chatillon Gage Cat. #509-250 Spring Scale	±2 grams	Operate and release force measurement
Triplet Meter	±3%	Contact Resistance
Weston Ammeter and Current Transformer H8984 H93789	±.65%	Switch load current

The test procedure utilized in the performance of these tests is given in the following paragraphs:

General - These tests shall be conducted at normal room temperature (65°F to 80°F) under controlled environmental conditions.

Installation - Remove switch from sealed protective cover and install mechanically in test fixture and check for performance as switch. Adjust overtravel to proper condition for test cell requirement by adjusting switch mounting plate in reference to cam lobe.

With power off, make electrical connections to the normally open (load) normally closed (counter), and common contacts (power). Connect the load banks to provide the proper test current.

5 amps - Single load bank
10 amps - Two load banks wired in parallel
15 amps - Three load banks wired in parallel

Data Recording - Set counters to zero. Fill in values for test cell conditions and measure and record the following initial data:

Contact resistance
Operate force
Release force
Contact overtravel

Turn on power and adjust drive for proper switch actuation speed as specified for the test cell in process.

Set miss detectors and remove detector bypass connection.

Allow test to proceed until interrupted by miss detector. Record first miss, repeat initial measurements, and record data on data sheet including counter reading.

If specified by test cell requirements, restart and rest miss detectors and repeat above procedure for second and third miss data.

Upon completion of the number of misses specified by the test cell requirement, the appropriate miss detector shall be bypassed and the test continued to total failure of the switch.

The switch shall then be removed from the test setup and placed in an envelope having the proper identification on the exterior.

In general, the measurement accuracy of the various parameters was controlled by the measuring instrument accuracy. Only in the cases of operate force, release force and overtravel measurements would technician or "human" accuracy contribute to the actual measurement accuracy limits. The contact resistance measurements using the Triplet meter however do not result in highly accurate measurements for this parameter.

In the case of operate force, the plunger load was increased gradually by the spring scale until it was sufficient to actuate the switch contact to the normally open position. The maximum reading of the scale was the operate force. Two or more readings were used to achieve a repeatability confidence level. Release force was measured in the same manner except that the load was gradually reduced until the switch contact returned to the normally closed position. After familiarization and practice, the technicians were able to consistently make repetitive measurements with a reading accuracy of ±2 grams.

The overtravel measurement was made with an optical instrument, consisting of a magnifying lens system with a reference cross hair, mounted to a calibrated vernier drive. The accuracy of the vernier drive was ±.0001 inch for measuring the switch overtravel limits involved. The switching cam was manually rotated until the normally open circuit was completed. The vernier was adjusted to align the cross hair with a reference on the switch plunger and the vernier dial reading was noted. The switching cam was then rotated to its peak position and the vernier was readjusted to obtain the plunger reference-crosshair relationship and the new vernier was noted. The difference in the two readings represented the switch overtravel. Through extensive familiarization and practice, the technicians were able to consistantly repeat measurements to an accuracy of ±.0002 inch. Since it was established that overtravel data would be adequate if measured to the nearest .001 inch, the effect of "human" error in this measurement became insignificant.

Actuation speed was measured by setting the variable speed control at the desired speed position and, with the test setup running, the counters were used to check the actual number of switching cycles for a 1 minute period. If necessary the speed control was readjusted and speed rechecked until the desired test condition was achieved.

Since switch current was controlled by fixed value wire wound resistors, it was decided that periodic monitoring on a daily basis would suffice. The initial setup was made by selecting 6 resistors with nearly identical resistance values and, using a motorized Variac, adjusting the voltage across one resistor until a 5 amp current was measured. The variac drive motor was then disconnected and current was checked for the two and three parallel resistor circuits for 10 amps and 15 amps respectively. A separate power line was used to minimize voltage fluctuation. The maximum error found during the test cycle was ±.15 amp.

APPENDIX V-2 PHYSICAL TEST METHOD (RELAYS)

The test method used for the study program on relays was as follows: All relays were subjected to initial screening tests at room temperature and at the life test temperature prior to the start of the cycling. The screening test parameters measured were: dc coil resistance, contact resistance, pickup and dropout voltages, operate and release times, and contact bounce. Loads were resistive with an open circuit voltage of 28 Vdc. All relay coils were energized with rated coil voltage (26.5 Vdc).

Periodically through the life cycle of each part, measurements were taken and recorded of:

- Contact resistance - by measuring the contact voltage drop at the life test current level using the voltmeter-ammeter method and by calculating resistance
- Coil resistance - using a Wheatstone bridge
- Pickup voltage - using a lamp circuit
- Dropout voltage - using a lamp circuit
- Operate time - using an oscilloscope
- Release time - using an oscilloscope
- Contact bounce - using an oscilloscope.

As the test progressed, each cycle was recorded on temperature-sensitive chart paper using a Sanborn recorder. The parts were monitored for first miss, intermittent operation, and catastrophic failure. The analyst also recorded whether the failure-to-make was on the normally open or normally closed position.

Primarily, the measurement accuracy of the various test parameters was limited only by the measuring instrument accuracy. Exceptions may have occurred due to the human factor as stated in the following test conditions.

Oscilloscope measurements of operate and release time and contact bounce may vary due to the slight parallax in the oscilloscope screen. The measurement may vary slightly depending on the technician viewing the oscilloscope.

Pickup and dropout voltage measurements may vary with different rates of voltage change. A rate of approximately 0.1 volt per second was used when approaching the critical potential.

The D.C. coil resistance measurements were made as soon as possible after the interruption of the life test cycling. The coil resistance was highest at this time, due to the temperature rise of the relays during operation, and decreased steadily until stabilized at the ambient temperature. The resistance was therefore dependent on the time lapse between the life cycle interruption and the time measurement. The measurements were made within ten seconds of the interruption and all specimens were measured in the same sequence each time to minimize variations.

The load current was controlled by variable wire wound resistors and monitored after each life cycle interruption. Regulated power supplies were used to increase stability.

All ambient temperatures above room temperature were monitored steadily until stabilized and daily thereafter.

Cycling rates were controlled by solid state devices to increase stability and monitored daily.

The test equipments used on the relay test program are listed below. The instrument accuracy limits are shown in parentheses.

Equipment List EL-5138

Oscilloscope, Tektronix, 535A	H-75865	(Sweep accuracy 1-3%)
Oscilloscope, Tektronix, 535A	H-102029	
Oscilloscope, Tektronix, 535A	H-180855	
Oscilloscope, Tektronix, 535A	H-76263	
Oscilloscope, pre-amp, Tektronix, type CA	H-77903	(Amplitude calibrator accuracy = 3%)
Oscilloscope, pre-amp, Tektronix, type CA	H-77924	
Oscilloscope, pre-amp, Tektronix, type CA	H-77907	
Oscilloscope, pre-amp, Tektronix, type CA	H-46581	

Digital voltmeter, Non-Linear Systems, V35RB,	510-03247	±1 digit in last digit)
Digital voltmeter, Non-Linear Systems, V35,	H-101977	

D.C. Ammeter, Weston, 901, 0-1-5-10A,	H-34537	(±.5%)
D.C. Voltmeter, Weston, 622, 0-30 V range,	H-47992	(±.1%)
Resistance bridge, Leeds & Northrup, No. 5305,	520-02173	(±.1%)

D.C. Power Supply, Perkin,	MR 2432-200,	H-15975
D.C. Power Supply, Perkin,	MR 2432-300,	520-00455
D.C. Power Supply, Perkin,	MR 532-15A,	520-01458
D.C. Power Supply, Perkin,	MR 532-15A,	520-01460
D.C. Power Supply, Lambda,	LA 200-03AM,	H-102291
D.C. Power Supply, Hewlett Packard,	711A,	520-00122
D.C. Power Supply, Hewlett Packard,	711A,	H-31400

Electronic counter, Hewlett Packard,	5243L,	H-180920	(±1 digit in last digit)
Electronic counter, Hewlett Packard,	523BR,	520-01571	

Square wave generator, Hewlett Packard, 211A, H-101912
Square wave generator, Hewlett Packard, 211A, H-94532
Amplifier, McIntosh, H-45201

Oven, Tenney, TMUF-100240,	520-01160
Oven, Blue M, OV-475	H-47857
Oven, Precision Scientific, Model 18,	H-41727

8 channel Recorder, Sanborn, 150, 520-00533 FECL-4608
4-D. C. Amplifiers, Sanborn, dual channel FECL-8251, 8252, 8253, 8254 model 150-2900
4 channel Recorder, Sanborn, 150, H-18648
4-D. C. Amplifiers, Sanborn, single channel H-18649, H-18650, H-18651, H-18652

Thermocouple Bridge, Rubicon, 2745, 520-02264 (±.1%)
2-Load Bank, lab. fab.
2-Relay test fixtures, lab. fab.
2-Relay cycles, lab. fab.

APPENDIX V-3 PHYSICAL TEST METHOD (O-RINGS)

Figure V-2 illustrates the method of environmental stress application. The outline represents the temperature controlled oven which was set for the required temperature stress level. The chamber was set up to simultaneously supply the three levels of ultraviolet exposure. This condition was achieved by using an opaque shield for the "no ultraviolet" level, setting the bulb-to-O-ring distance for 0.2 watt/ft^2 and providing a $\sqrt{2}$ distance-from-bulb relationship for the 0.1 watt/ft^2 and 0.2 watt/ft^2 levels. The bulb-to-O-ring distance was periodically reduced to compensate for the light output decrease associated with bulb aging.

The O-rings were installed in individual test blocks and were not removed until failure was evident. This minimized the possibility of damage by mishandling or from installation and removal. The test blocks were mounted on the pressure test fixture illustrated by Figure V-3. A hydraulic pressure of 1500 psi was applied for a period of 1 minute and then released. This cycle was repeated 3 times for each test cycle. The O-ring and test block were removed as a unit and washed with gasoline to remove the hydraulic oil. After drying, O-ring and test blocks were placed in the appropriate environment chamber. Periodically the test specimens were removed from the environment chamber, allowed to cool, pressure tested, cleaned and returned to the environment chamber. This was repeated until failure occurred.

The following items of test equipment were used in the testing procedure:

Item	Function
Tenny Oven 520-011528	Temperature environment
Dispatch Oven Serial #52517	Temperature environment
Ultraviolet Lamp G8T5	Ultraviolet environment

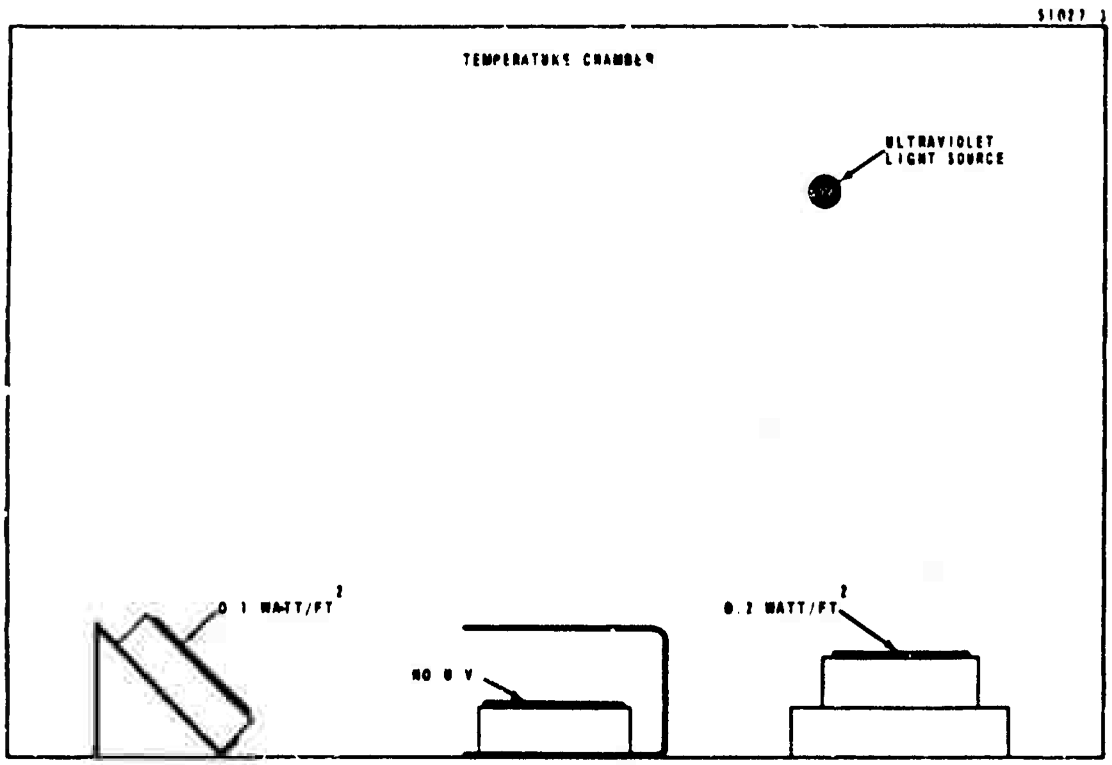

Figure V-2. O-Ring Test Method

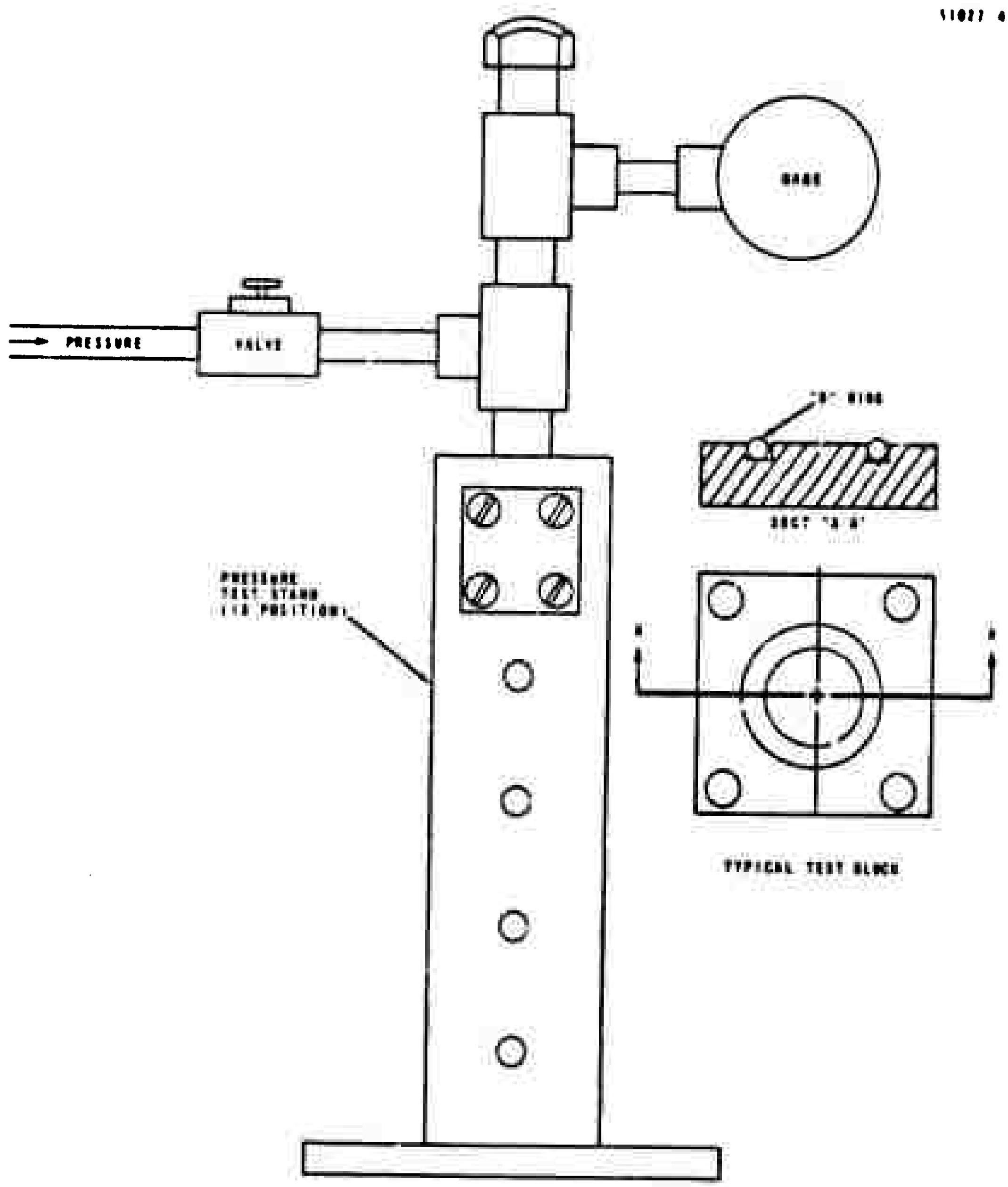

Figure V-3. O-Ring Test Fixture

Item	Function
Crosby Model AIH 1500 psi gage	Indicate test pressure
Blackhawk Model P151 Hydraulic Pump	Hydraulic Test Pressure Source

The specific steps in the O-ring test procedure are as follows:

Visually inspect O-ring for manufacturing imperfections and carefully install in test block with identification dots on the exposed surface.

Mount O-ring and test block on the pressure test fixture and raise hydraulic pressure to 1500 psi for approximately 1 minute. If O-ring passes initial pressure test, remove block and ring from test fixture, wash in pan of gasoline and carefully blot with a clear cloth until dry.

Record environmental exposure information on data sheet. Place O-ring and test block in oven and expose to the proper level of ultraviolet light.

None - Place in shield area

0.1 watt/ft^2 - set block in position 14" from bulb

0.2 watt/ft^2 - set bulb at 9.9" above O-ring

Reduce the vertical height of the bulb by 0.1" each 7 day period to compensate for bulb aging. Replace the bulb at 10 week intervals with a new bulb that has been "burned in" for 100 hours.

O-rings exposed to the 275°F environment shall be pressure tested at 24 hour maximum intervals until failure. Pressure testing shall consist of following the initial test procedure except it shall be pressurized to 1500 psi for three cycles for each test.

O-rings exposed to the 250°F environment shall be pressure tested at 48 hour maximum intervals in the same manner as the 275°F O-rings.

O-rings exposed to the 200°F environment shall be pressure tested at maximum 4 day intervals in the same manner as the 275°F O-rings.

When failure is evident, remove the O-ring from the test block, wash in gasoline, and place in an envelope having the identification information on the exterior.

APPENDIX V-4 PHYSICAL TEST METHOD (TIMING BELTS)

Figure V-4 is a schematic representation of the Timing Belt test setup. Three complete setups were in use on this program to provide a fixed load condition of 1/15 H.P., 1/8 H.P., or 1/4 H.P. Each consisted of 5 belt test positions in series between the input and load providing a total of up to

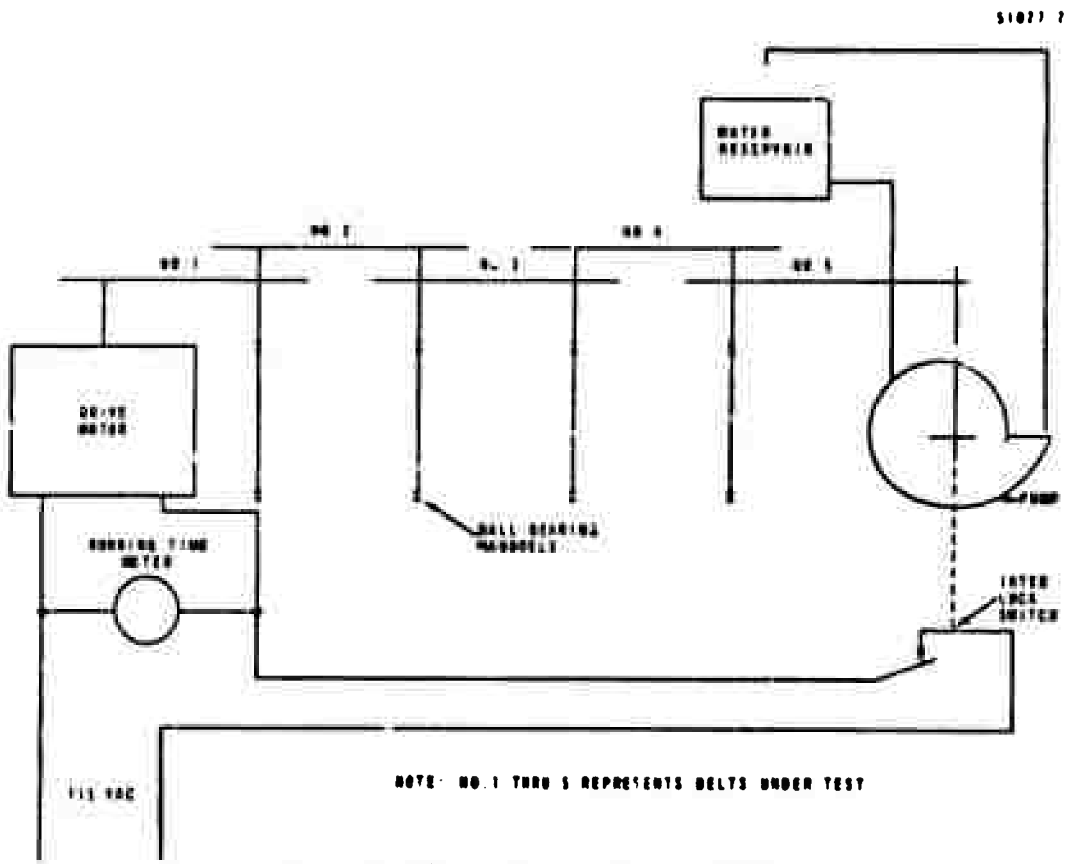

Figure V-4. Schematic of Timing Belt Test Method

15 Timing Belts undergoing tests at any one time. By installing different pairs of pulley (12, 15 or 18 tooth) on the proper load setup a combination of tests could be running simultaneously. Water pumps were utilized as driven loads. Since the tests were to run 24 hours per day including week-ends, a tac-generator connected mechanically to each pump shaft was used to open a relay in the drive motor power line at the time of a belt failure. This also interrupted the running time meter for the setup and provided the time-to-failure information. To minimize test setup failures, the 1/15 H.P. and 1/8 H.P. loads were driv by 1/4 H.P. motors while the 1/4 H.P. load was driven by a 1/2 H.P. motor. A variac was used to bring the motors up to speed gradually rather than subjecting the belts to the excessive full starting torque of the oversize motors. This also prevented "tooth jumping" during the starting cycle on the 1/4 H.P. test setup.

The following items of test equipment were used in the setup:

Item	Function
Variac General Radio Type W5MT3	Control starting torque
Tac-Generator Madison Electric Products Type M2P	Provide relay interruption of power line
Running Time Meter Aero Instrument Co. Type 61134	Indicate running time

The general test instructions are as follows:

General - These tests shall be conducted at normal room temperature (65° to 80°F) with no uncontrolled environmental conditions introduced.

Installation - Visually inspect the belt for obvious imperfections and, if none exist, install it on the proper test setup for the load environment required for the desired test cell. The installation should utilize a pair of pulleys of the proper size as indicated for the test cell. The pulley center distance must be adjusted to provide no initial belt tension and so that a light finger pressure at the center of the belt deflects it approximately 1/8". Care must be exercised to obtain parallelism between shafts and an in-line condition for the pulleys.

Enter the test conditions on the data sheet including the reading from the running time meter. Using a variac, gradually increase the voltage to the drive motor until it has been brought up to running speed.

Inspection - Twice a week, stop the setup and inspect belts for signs of cracks, wear, or other deterioration. Any indication of deterioration shall be noted on the test data sheet.

Continue the tests until belt failure occurs.

APPENDIX VI WEIBULL PLOTS OF TEST RUNS

VI-1 SNAP ACTION SWITCHES

Each of the 27 test runs, consisting of 10 switches each was plotted on Weibull probability paper (Figures VI 1 thru VI-27). The line of best fit was drawn through the plotted points based on a linear regression performed on a computer. The scales used on the cycles to failure axis were selected only for the purpose of convenience in presenting the data on the graph. Each figure is identified by the Test Run number, the level of each accelerating stress used, and also shows the Weibull shape parameter (β) and the scale parameter (α). The (α) shown on each graph is a coded value which is dependent on the time scale used. To convert the α to an uncoded state that is independent of the time scale used on the graph paper and hence is the true estimate of α, the following conversion method is used:

Suppose X is the random variable with density function:

$$f(X) = \frac{\beta X^{\beta-1}}{\alpha} e^{-\frac{X^\beta}{\alpha}}$$

$$F(X) = 1 - e^{-\frac{X^\beta}{\alpha}}$$

Now suppose X is multiplied by K, $-\infty < K < \infty$. Then the cumulative distribution function of Y, where Y = KX, is:

$$F(Y) = 1 - e^{-\frac{Y^\beta}{K^\beta \alpha}}$$

which is Weibull with beta = β and alpha = $\alpha^* = K^\beta \alpha$.

Hence, multiplying X by K has the effect of increasing α by K^β and has no effect on β.

Now suppose X is Weibull with the same density as above and a constant is added to X, i.e., $Y = X + K$, $-\infty < K < \infty$.

Then, since $X \geq 0$, $Y - K \geq 0$ and

$$F(Y) = 1 - e^{-\frac{(Y-K)^\beta}{\alpha}}$$

and Y has a Weibull distribution with the same α and β as before but with a guarantee time K introduced.

To illustrate this, observe in the Weibull plot of Test Run #1, the time scale is cycles to first miss $X10^{-5}$. The $\ln \alpha = -3.176$ and $\tilde{\alpha} = 24.05$. The value 24.05 is coded and to convert it to its actual value, the following operations are performed:

$$\tilde{\alpha}_o = \tilde{\alpha}_K \cdot K^{\tilde{\beta}}$$

$$\tilde{\alpha}_o = 24.05 \times 10^{5\tilde{\beta}}$$

$$\tilde{\alpha}_o = 24.05 \times 10^{5(4.07)}$$

$$\tilde{\alpha}_o = 53,848 \times 10^{17}$$

where

$K = 10^5$

$\tilde{\beta} = 4.07$

$\tilde{\alpha}_o$ = uncoded value

$\tilde{\alpha}_K$ = coded value

The ordinate scale on the Weibull plots, Percent Failure was plotted at the median rank values (Reference 13) for a sample size of 10. The subscript on α indicates the power of ten that the original data was divided by. The "~" over the α, β's indicates these are graphic estimates of the true α and β's.

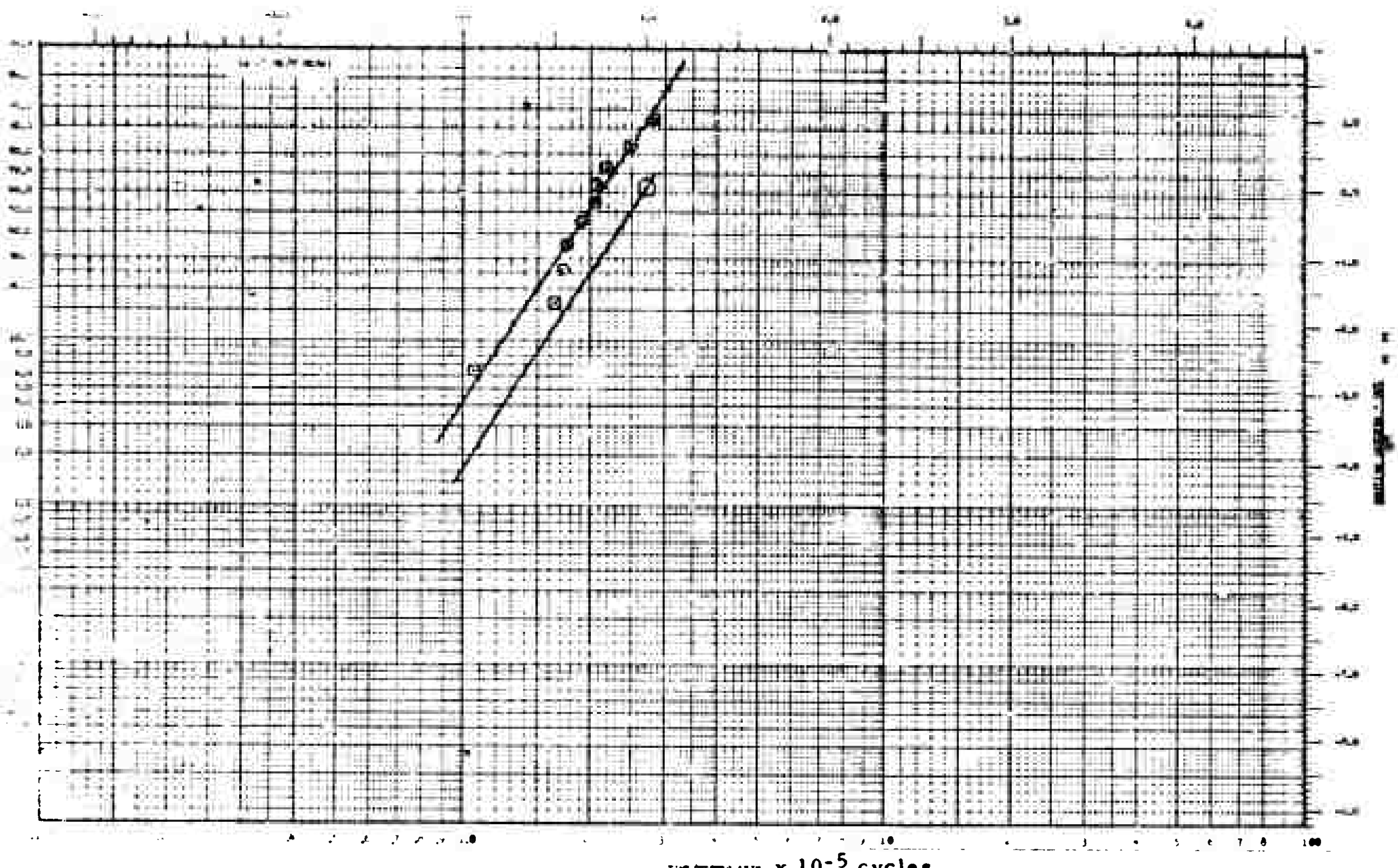

... Load - 5 amps, Contact Overtravel - .005 inch, Actuation Rate - 70 cpm, $\ln \alpha = -3.176$, $\alpha = 24.05$, $\beta = 4.07$

Figure VI-1 Switch Test Run No. 1

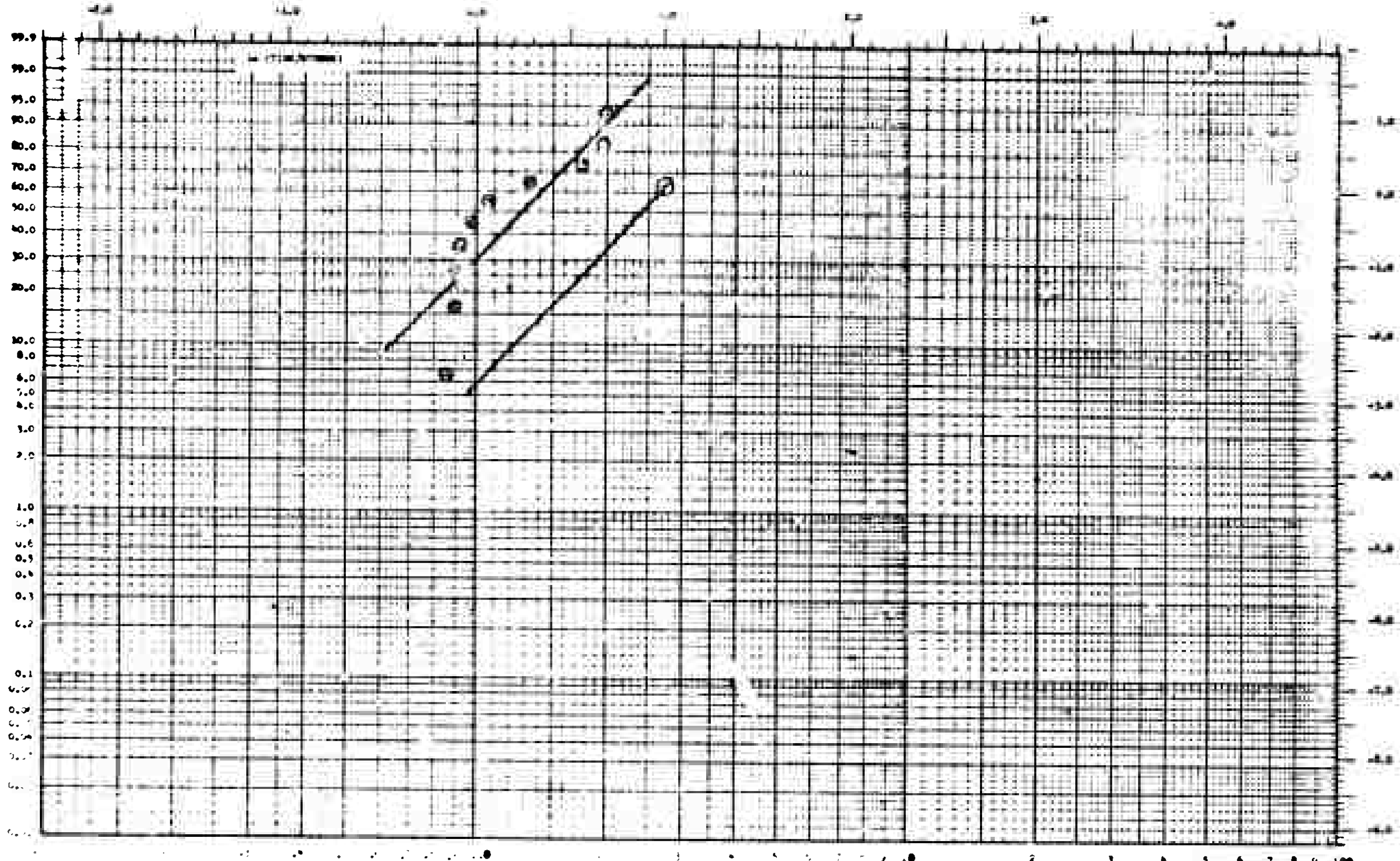

x 10^{-5} cycles

Contact Load - 5 amps, Contact Overtravel - .005 inch, Actuation Rate - 150 cpm, $\ln \alpha = -1.035$, $\alpha = 2.83$, $\beta = 2.81$

Figure VI-2 Switch Test Run No. 2

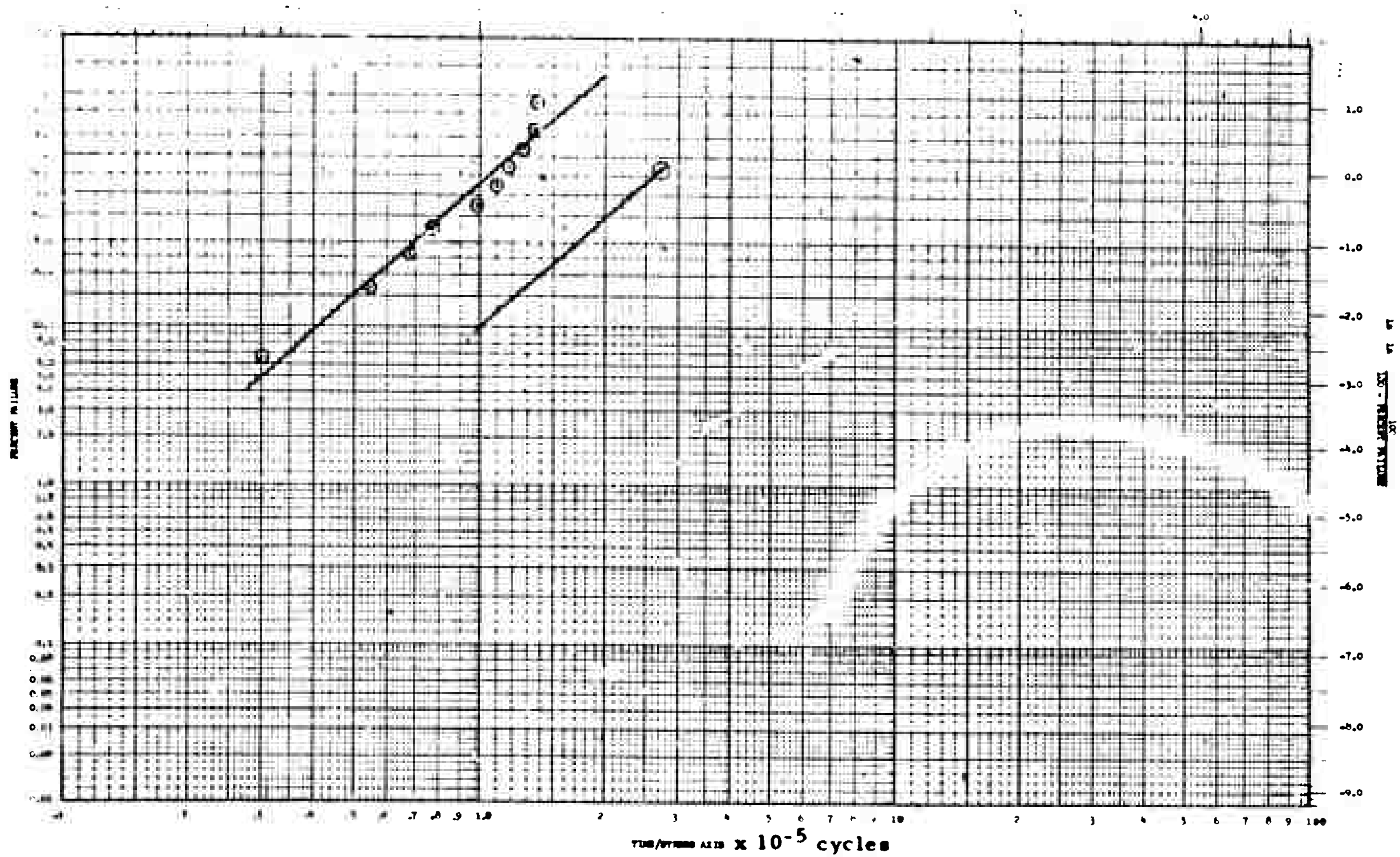

Contact Load - 5 amps, Contact Overtravel - ,005 inch, Actuation Rate - 300 cpm, $\ln \alpha = -2.05$, $\alpha = 1.23$, $\beta = 2.25$

Figure VI-3 Switch Test Run No. 3

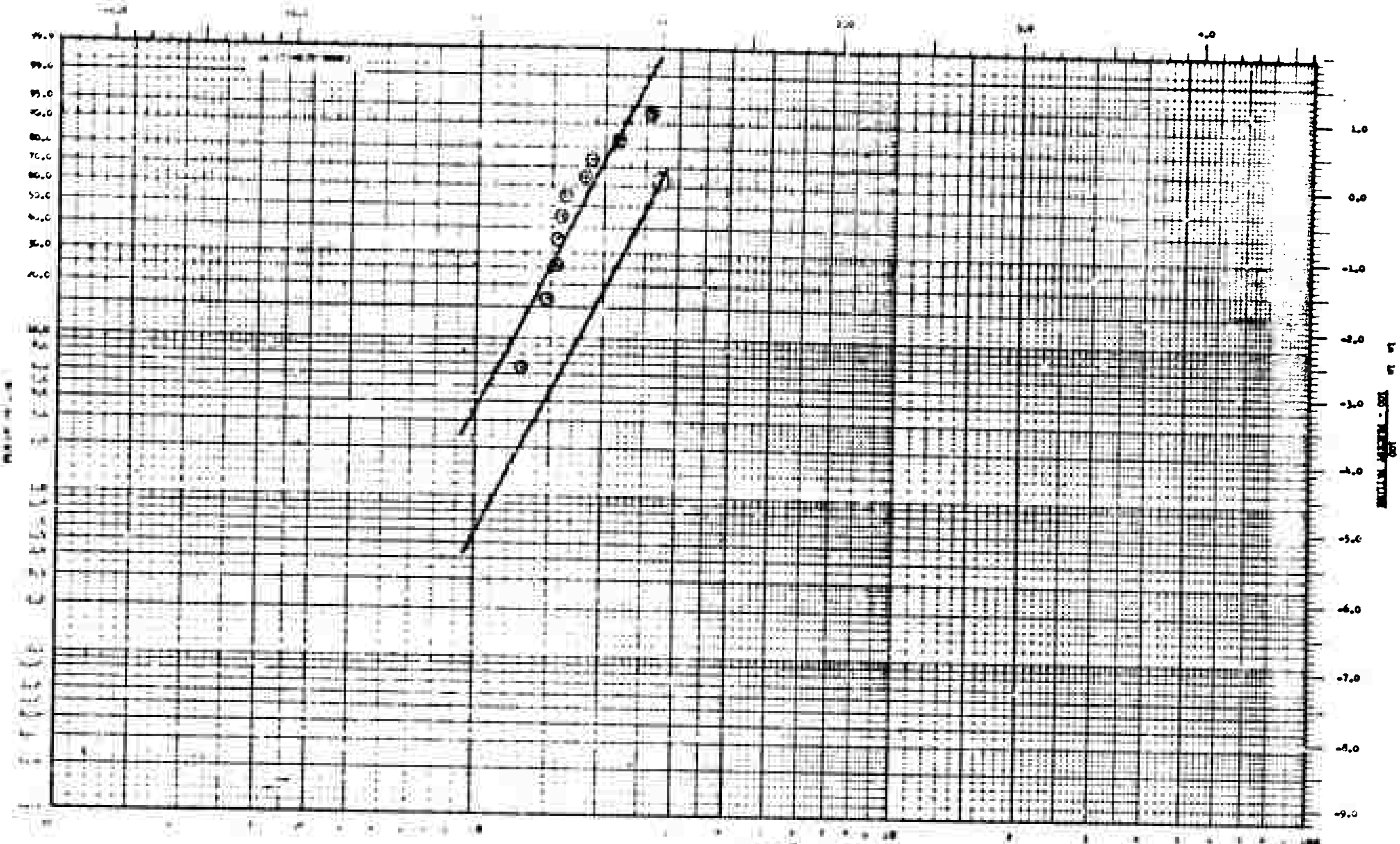

Contact Load - 5 amps, Contact Overtravel - .010 inch, Actuation Rate - 70 cpm, $\ell n\,\alpha = -3.275$, $\alpha = 26.58$, $\beta = 5.12$

Figure VI-4 Switch Test Run No. 4

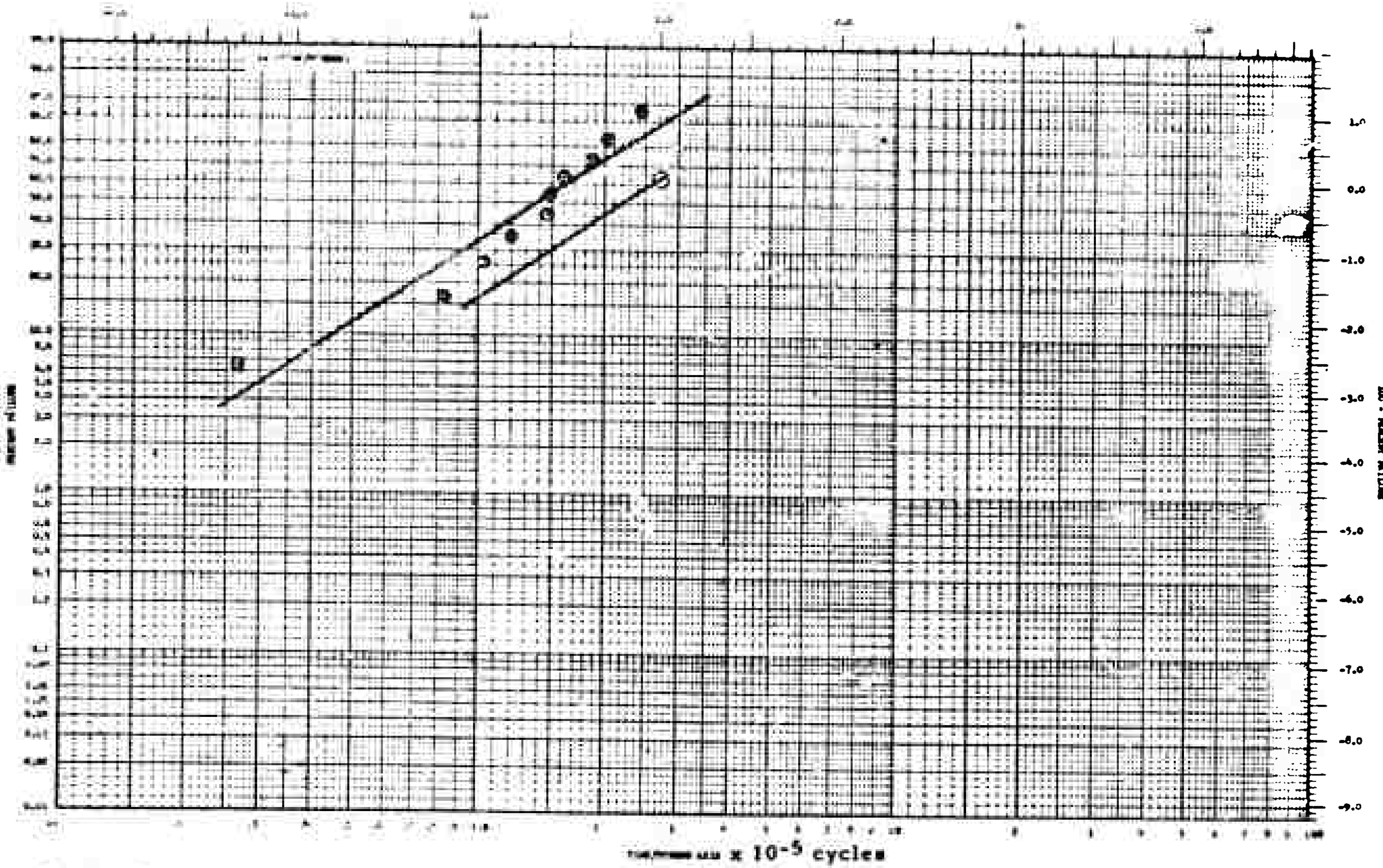

Contact Load - 5 amps, Contact Overtravel - .010 inch, Actuation Rate - 150 cpm, $\ln \alpha$ = -.898, α = 2.46, β = 1.70

Figure VI-5 Switch Test Run No. 5

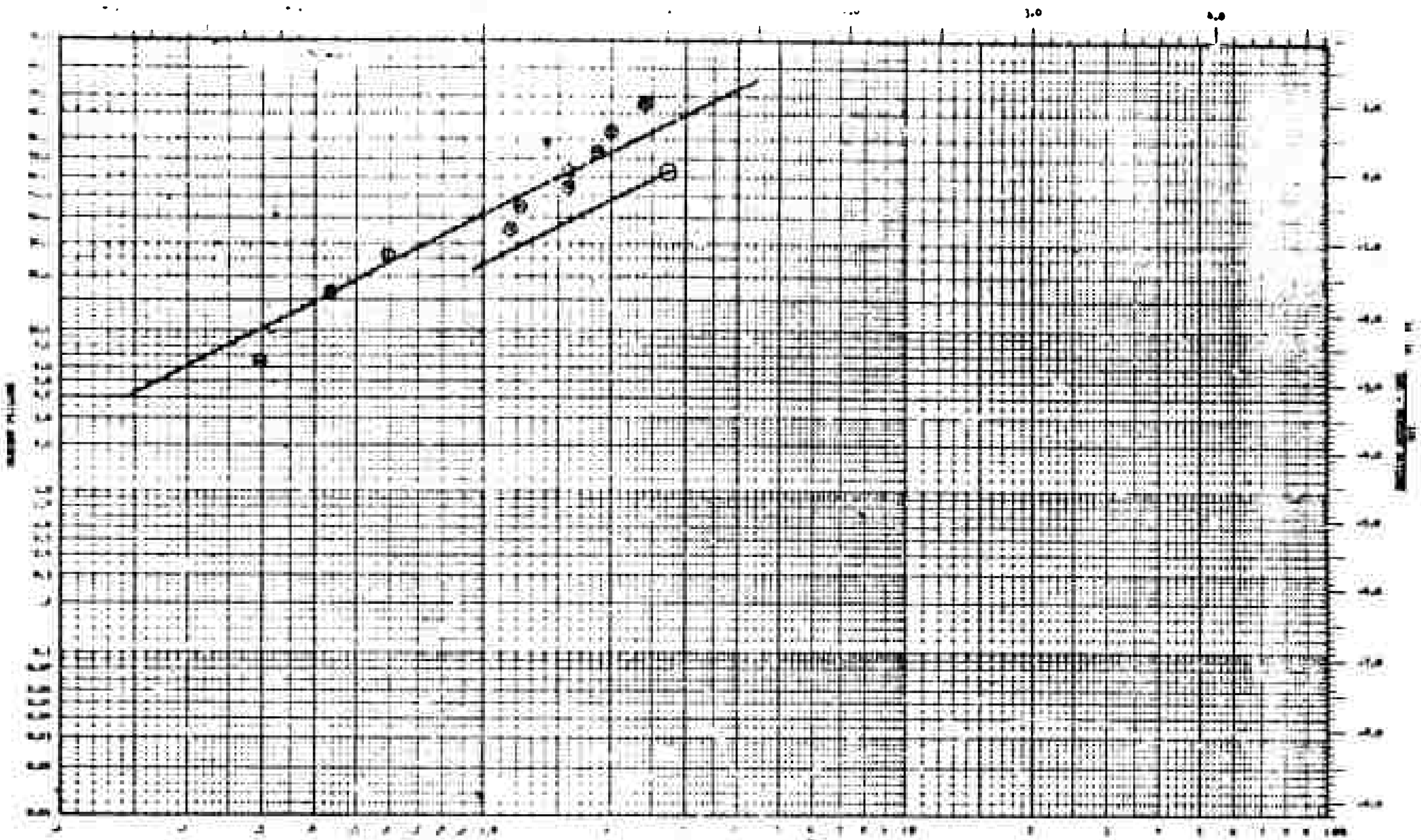

Contact Load - 5 amps, Contact Overtravel - .010 inch, Actuation Rate - 300 cpm, $\ln\alpha = -.648$, $\alpha = 1.92$, $\beta = 1.33$

Figure VI-6 Switch Test Run No. 6

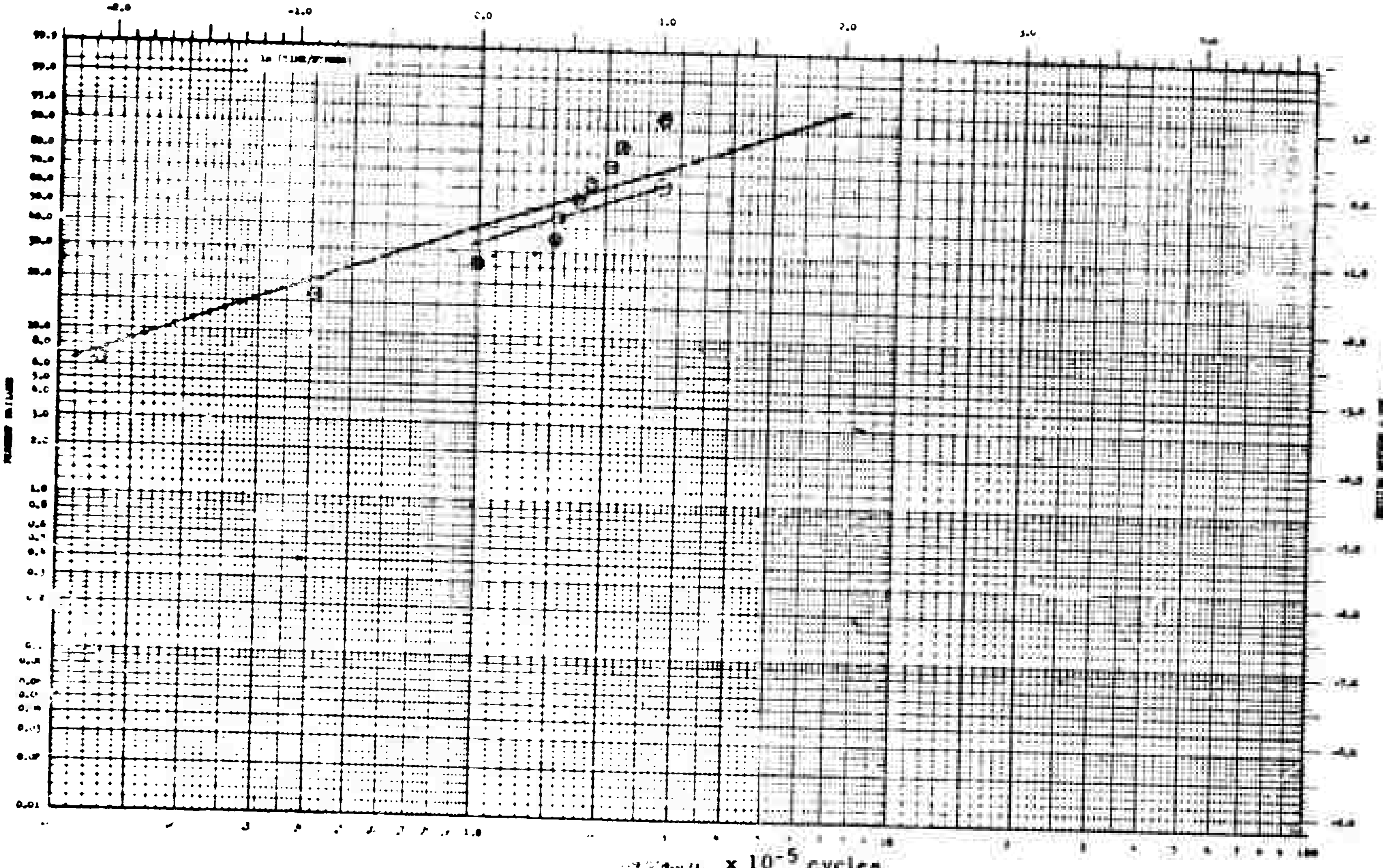

Contact Load - 5 amps, Contact Overtravel - .015 inch, Actuation Rate - 70 cpm. $\ln \alpha = -.667$, $\alpha = 1.95$, $\beta = .906$

Figure VI-7 Switch Test Run No. 7

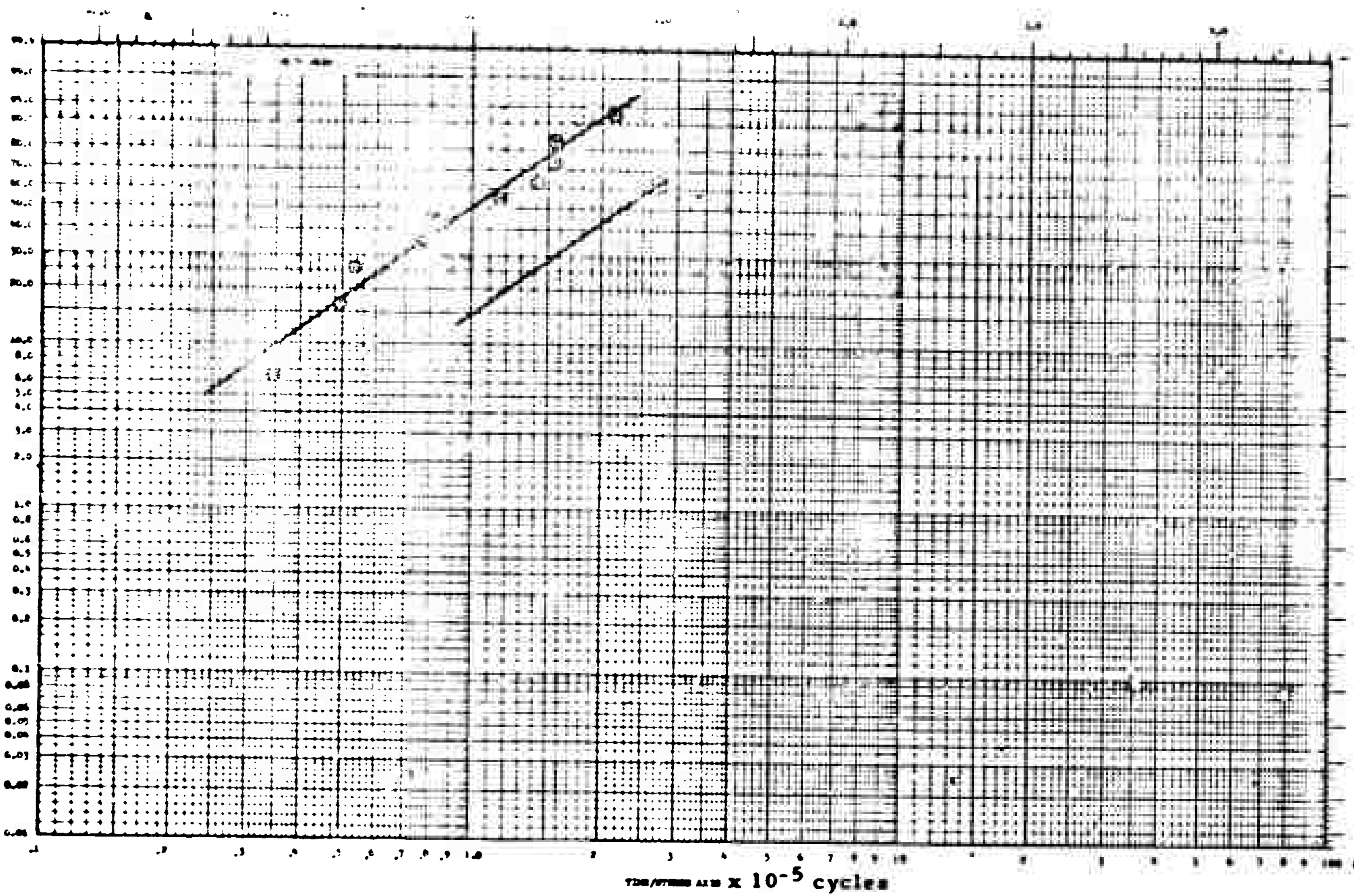

Contact Load - 5 amps, Contact Overtravel - .015 inch, Actuation Rate - 150 cpm, $\ln \alpha = -.397$, $\alpha = 1.49$, $\beta = 1.84$

Figure VI-8 Switch Test Run No. 8

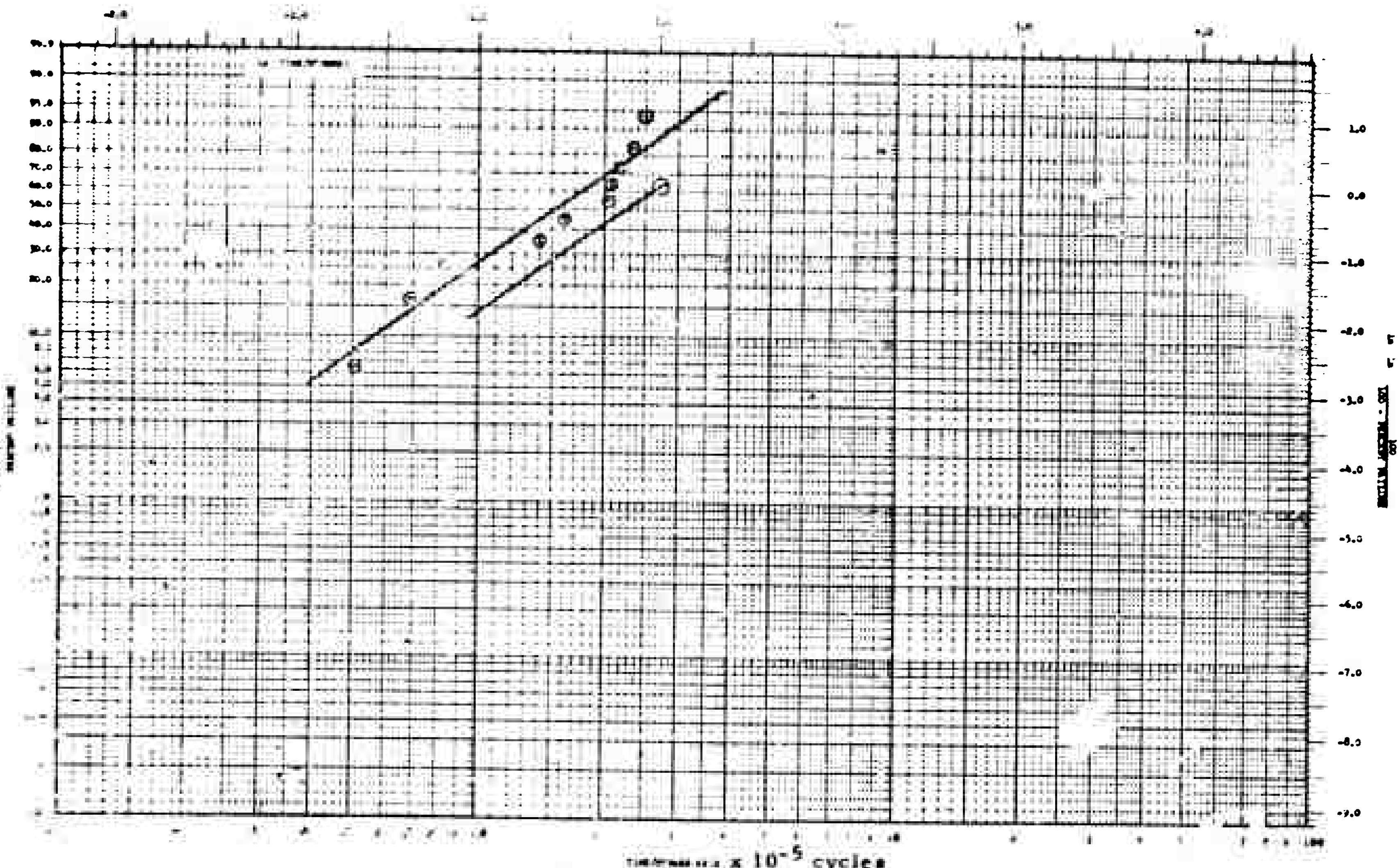

Contact Load - 5 amps, Contact Overtravel - .015 inch, Actuation Rate - 300 cpm, $\ln\alpha = -1.199$, $\alpha = 3.06$, $\beta = 1.89$

Figure VI-9 Switch Test Run No. 9

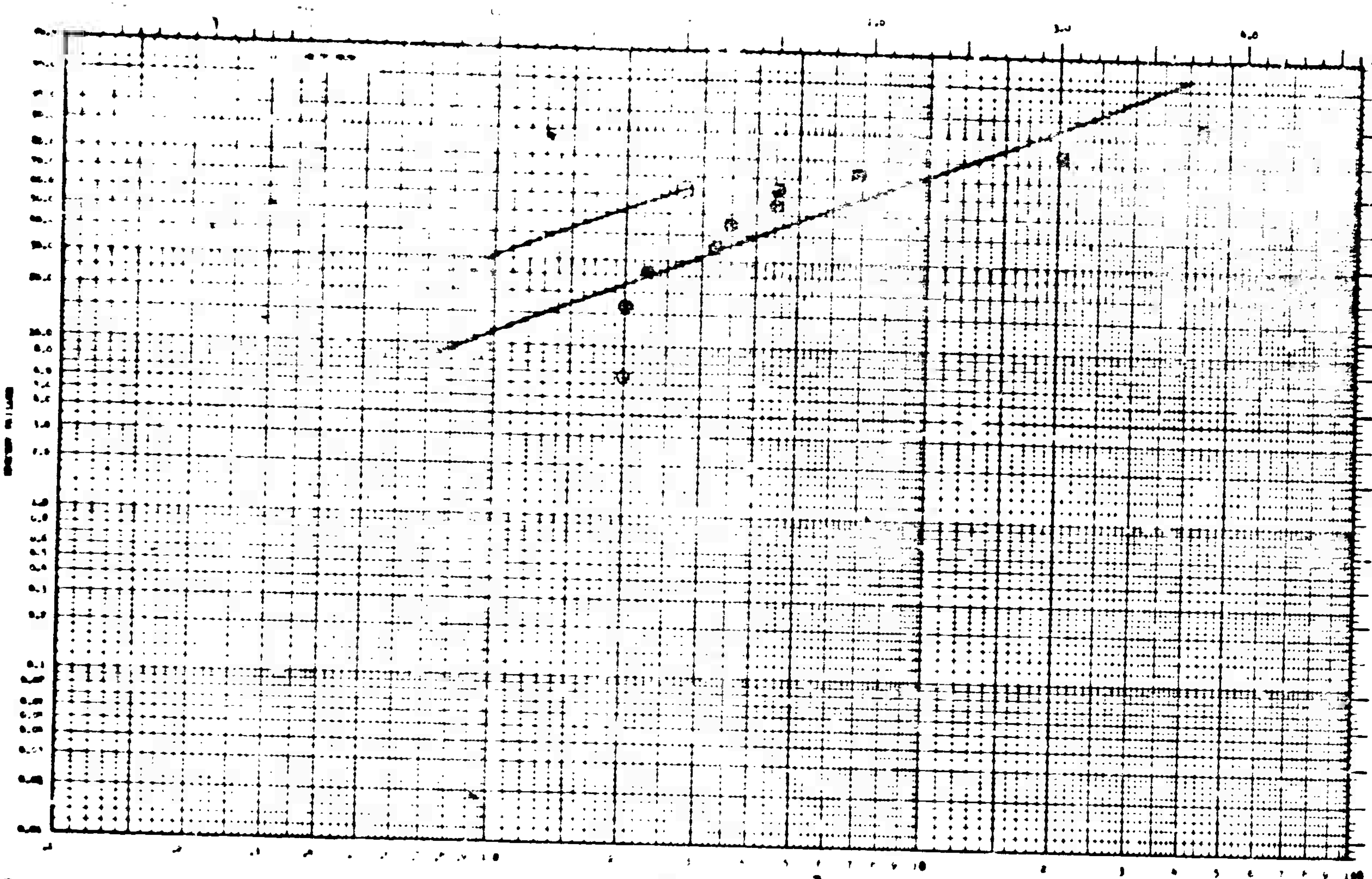

Contact Load - 10 amps, Contact Overtravel - .005 inch, Actuation Rate - 70 cpm, $\ln \alpha$ = -2.076, α = 8.00, β = 1.01

Figure VI-10 Switch Test Run No. 10

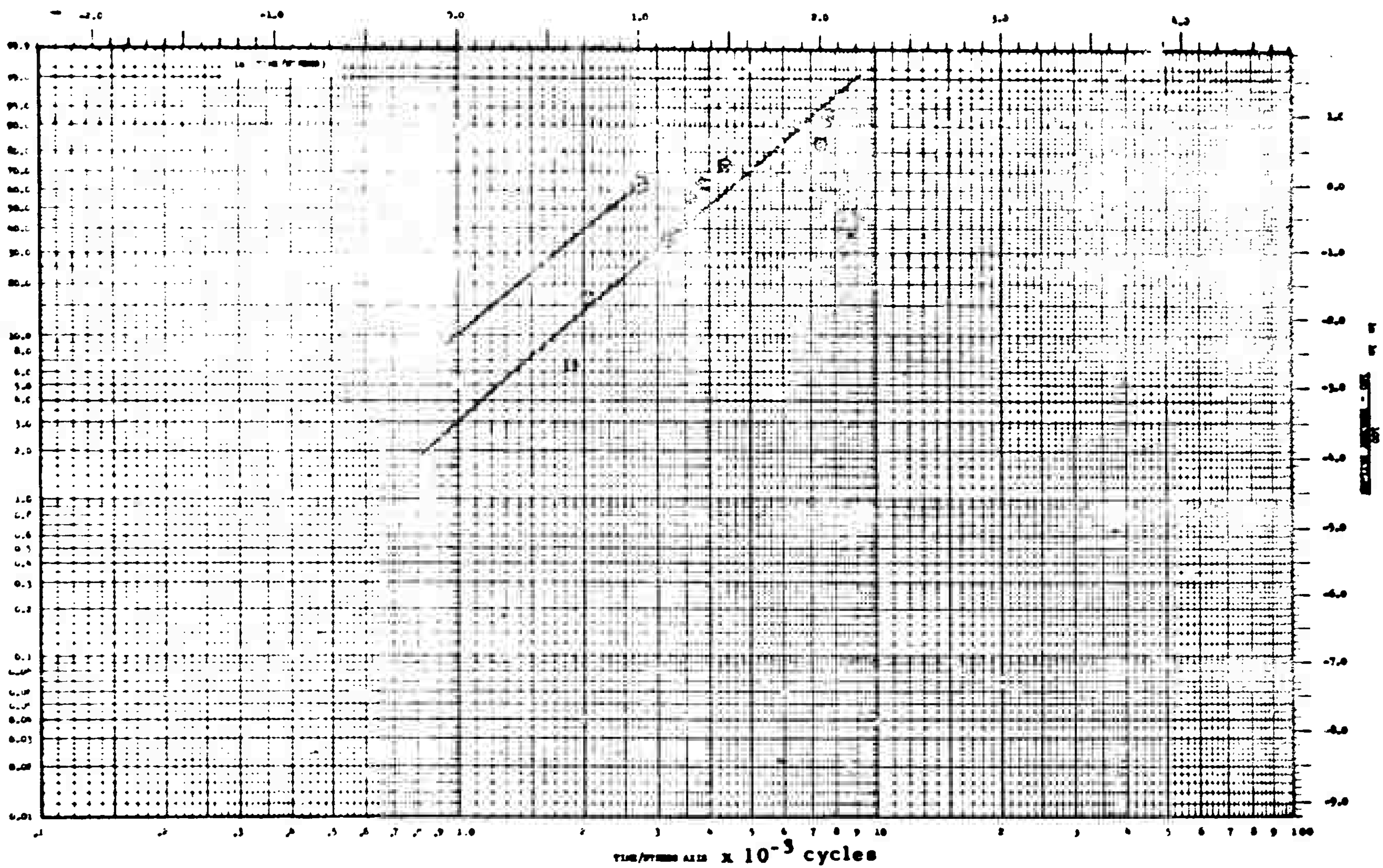

Contact Load - 10 amps, Contact Overtravel - .005 inch, Actuation Rate - 150 cpm, $\ln \alpha$ = -3.464, α = 31.82, β = 2.26

Figure VI-11 Switch Test Run No. 11

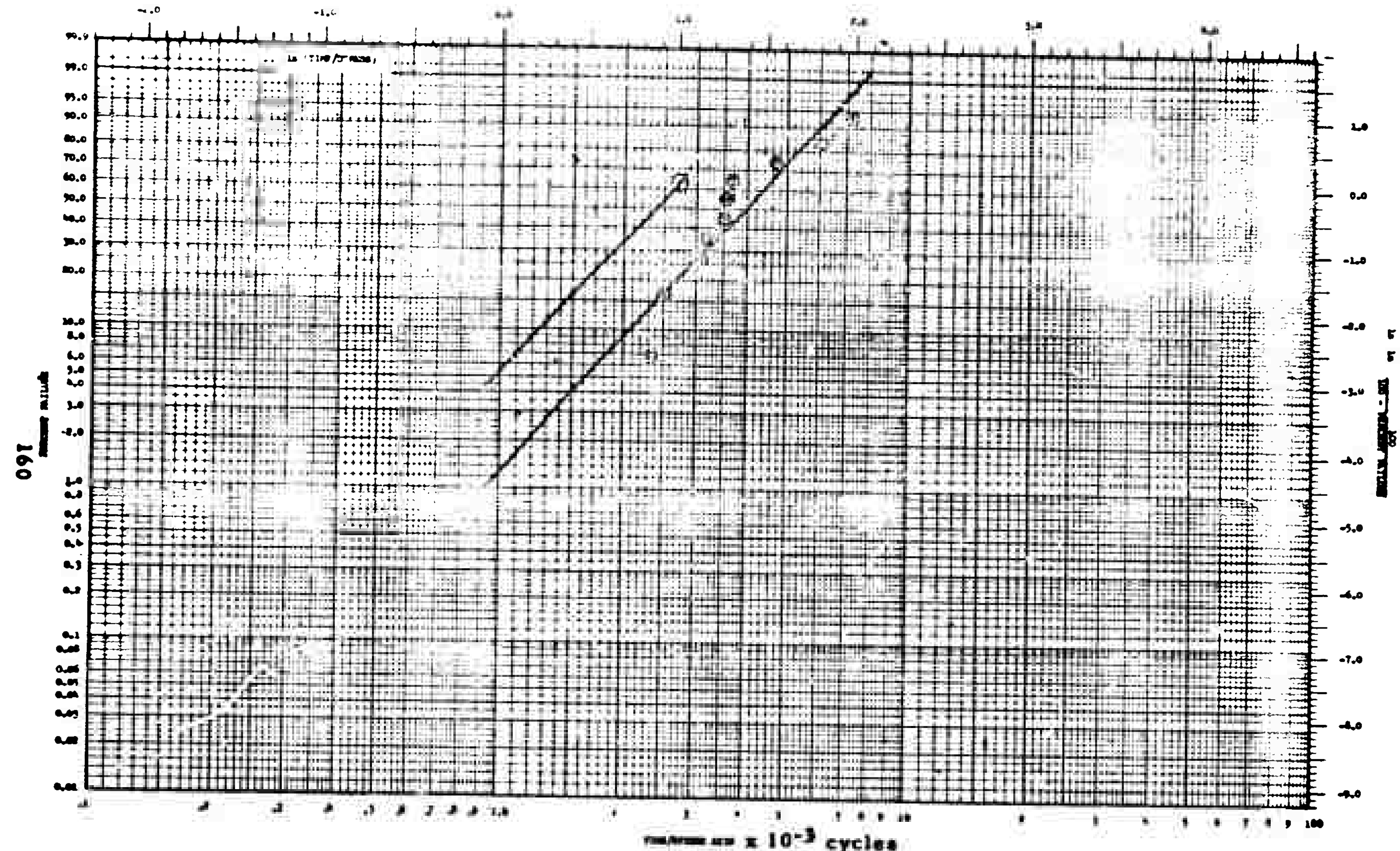

Contact Load - 10 amps, Contact Overtravel - .005 inch, Actuation Rate - 300 cpm, $\ln \theta$ = -4.373, α = 79.04, β = 2.91

Figure VI-12 Switch Test Run No. 12

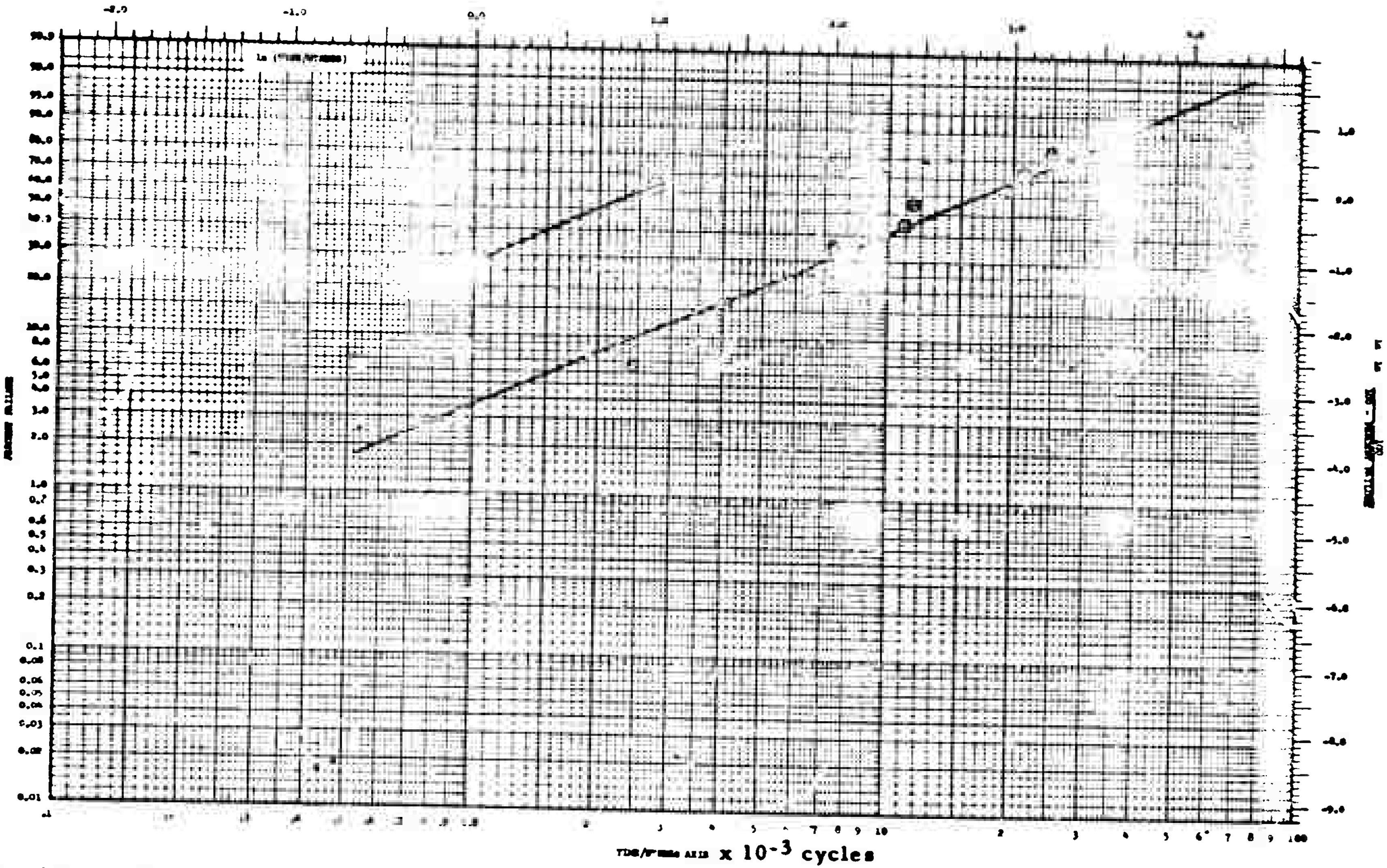

Contact Load - 10 amps, Contact Overtravel - .010 inch, Actuation Rate - 70 cpm, $\ln \alpha = -3.277$, $\alpha = 26.58$, $\beta = 1.12$

Figure VI-13 Switch Test Run No. 13

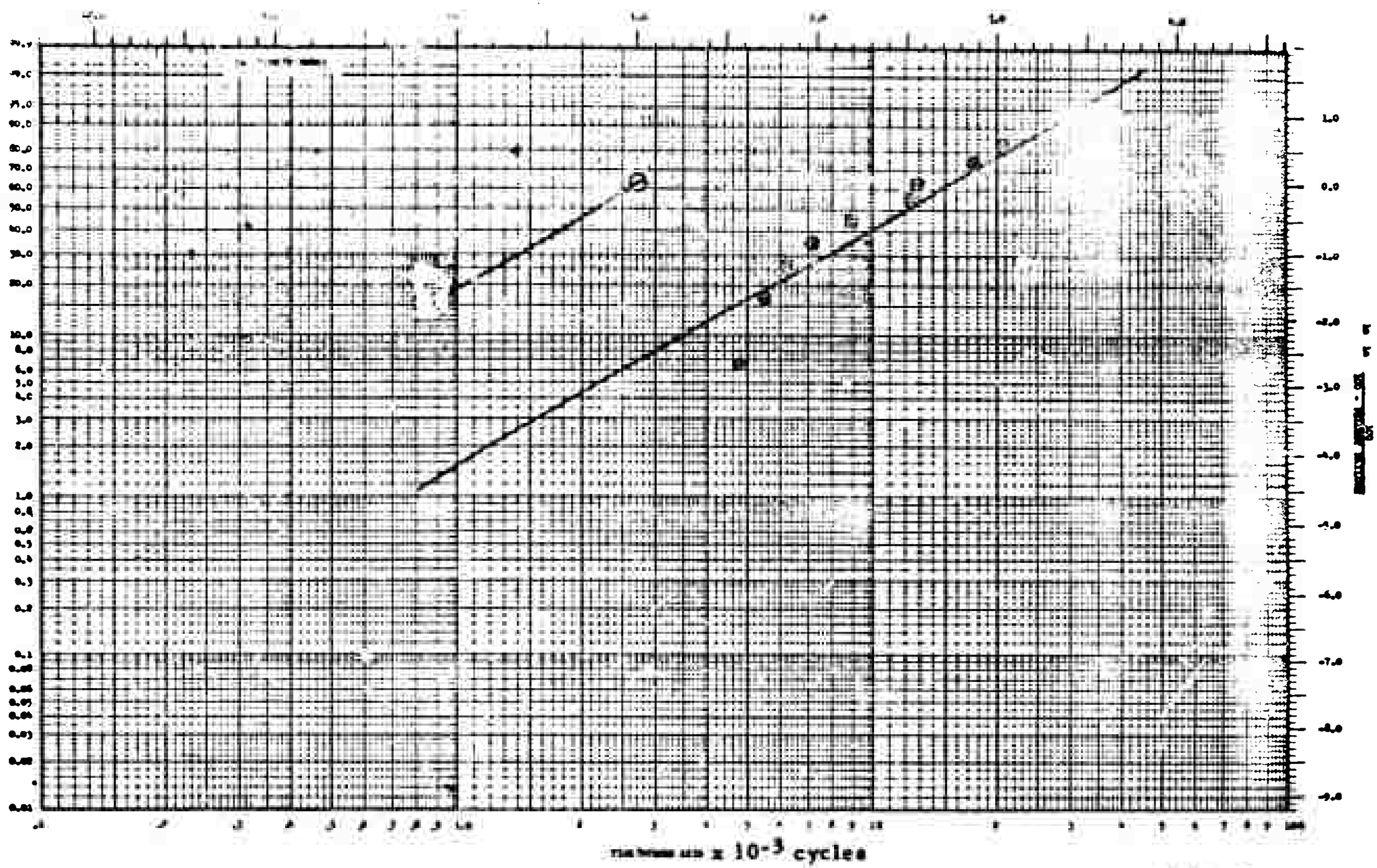

Contact Load - 10 amps, Contact Overtravel - .010 inch, Actuation Rate - 150 cpm, $\ln \alpha$ = -4.198, α = 66.69, β = 1.53

Figure VI-14 Switch Test Run No. 14

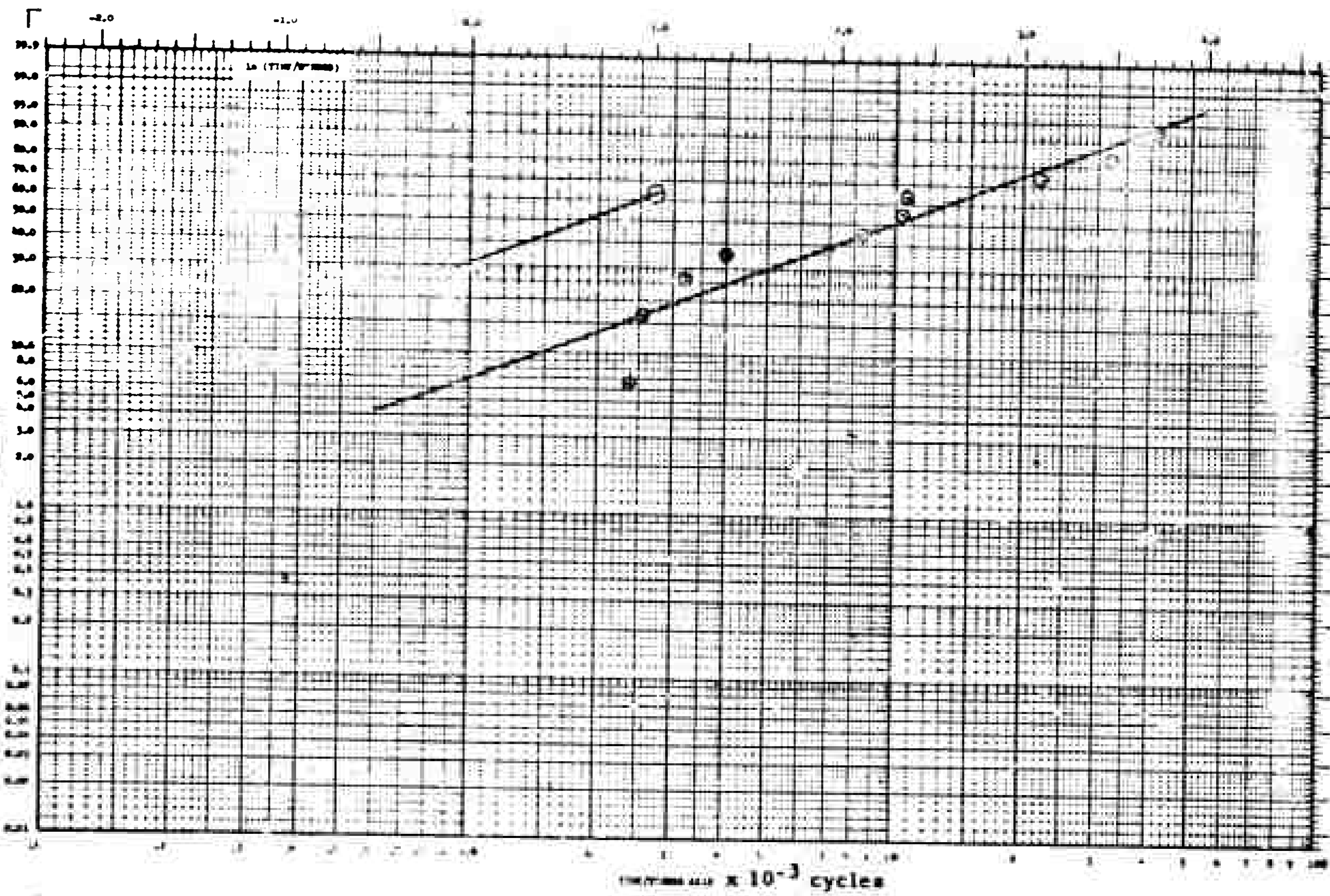

Contact Load - 10 amps, Contact Overtravel - .010 inch, Actuation Rate - 300 cpm, $\ln\alpha = -2.673$, $\alpha = 14.44$, $\beta = 1.00$

Figure VI-15 Switch Test Run No. 15

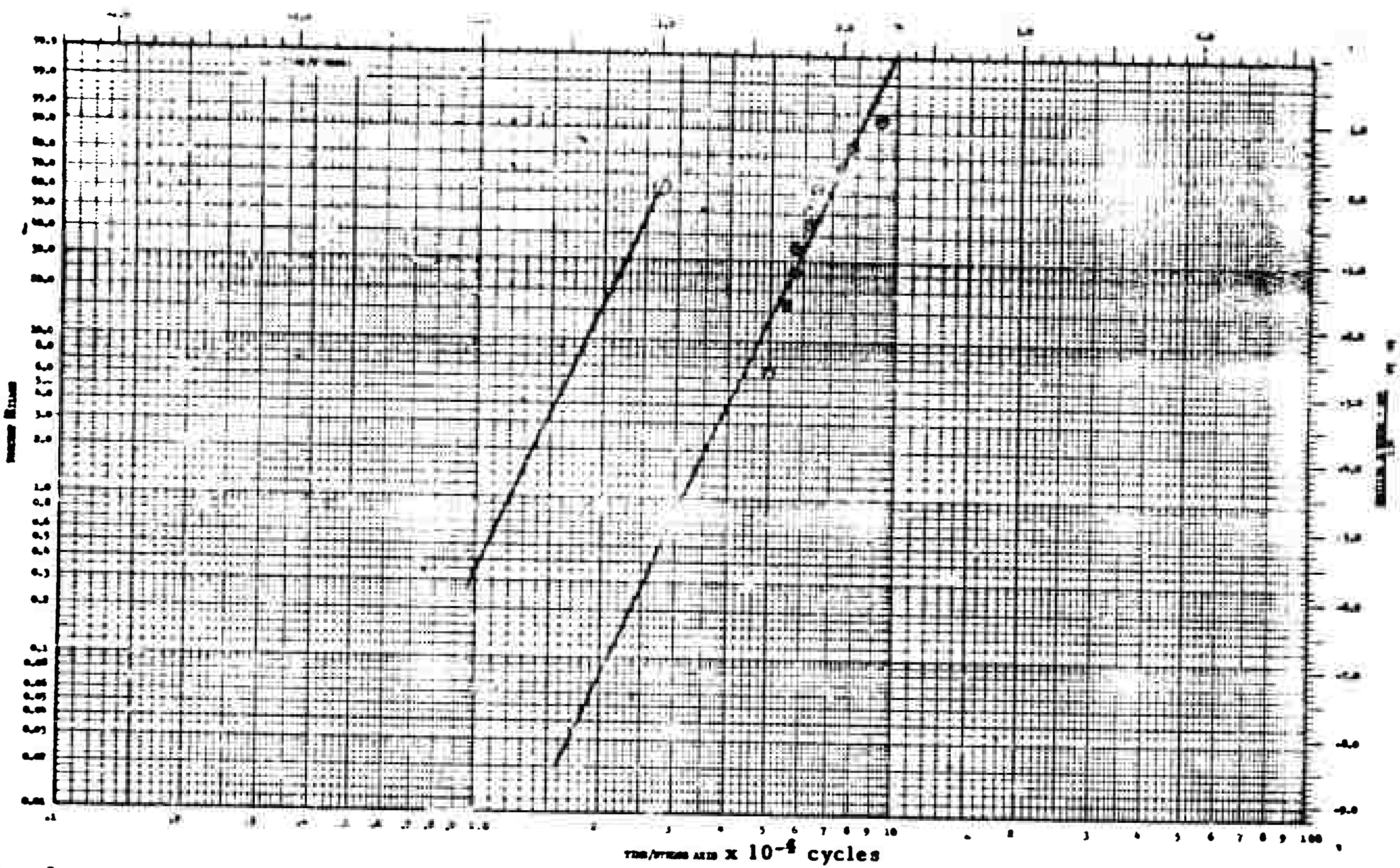

Contact Load - 10 amps, Contact Overtravel - .015 inch, Actuation Rate - 70 cpm, $\ln \alpha = -11.15$, $\alpha = 69.564$, $\beta = 5.71$

Figure VI-16 Switch Test Run No. 16

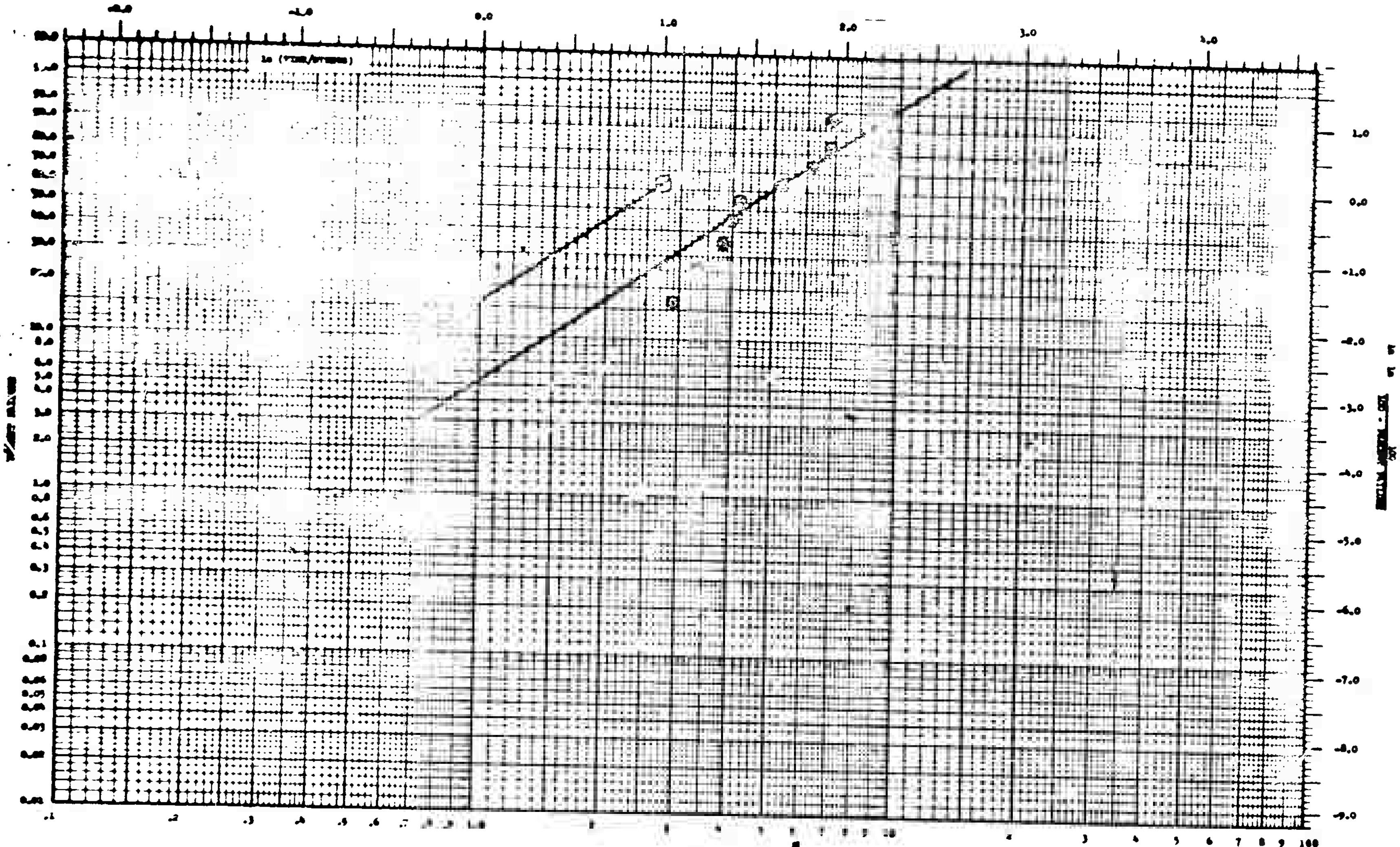

x 10^{-4} cycles

Contact Load - 10 amps, Contact Overtravel - .015 inch, Actuation Rate - 150 cpm, $\ln \alpha = -2.888$, $\alpha = 18.000$, $\beta = 1.74$

Figure VI-17 Switch Test Run No. 17

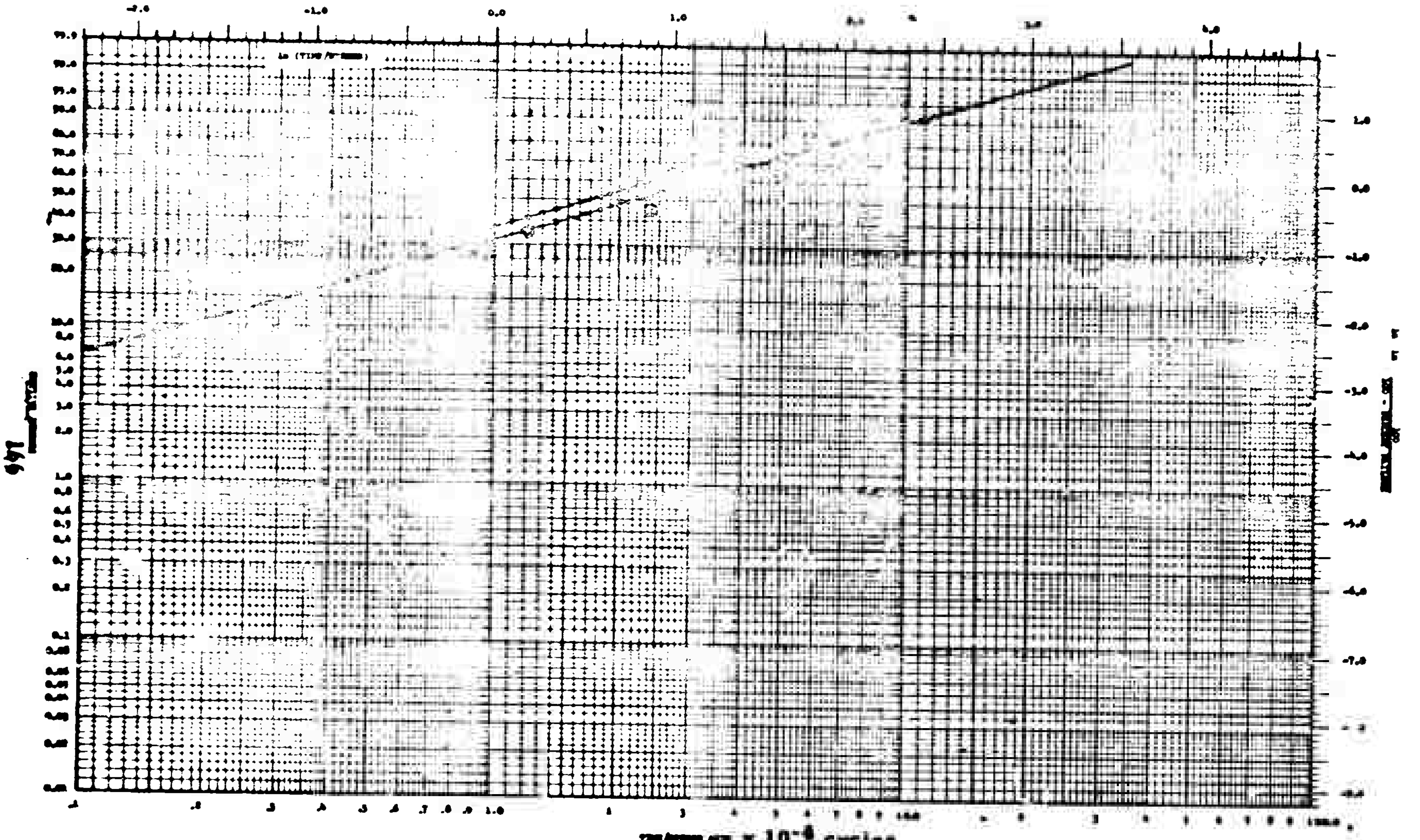

Contact Load - 10 amps, Contact Overtravel - .015 inch, Actuation Rate - 300 cpm, $\ln \alpha = -.964$, $\alpha = 2.61$, $\beta = .78$

Figure VI-18 Switch Test Run No. 18

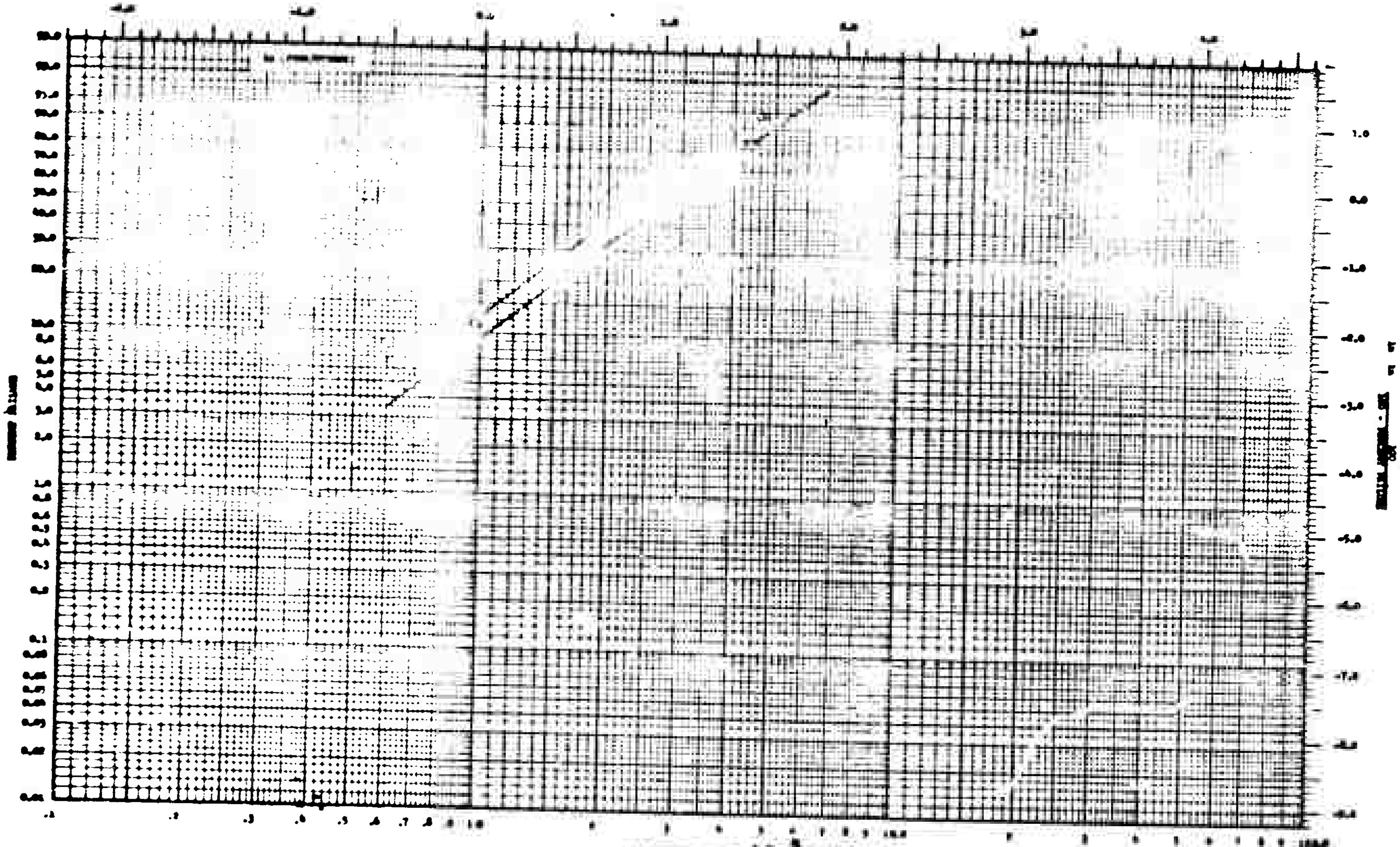

Contact Load - 15 amps, Contact Overtravel - .005 inch, Actuation Rate - 70 cpm, $\ln \alpha = -2.342$, $\alpha = 10.38$, $\beta = 2.00$

Figure VI-19 Swifth Test Run No. 19

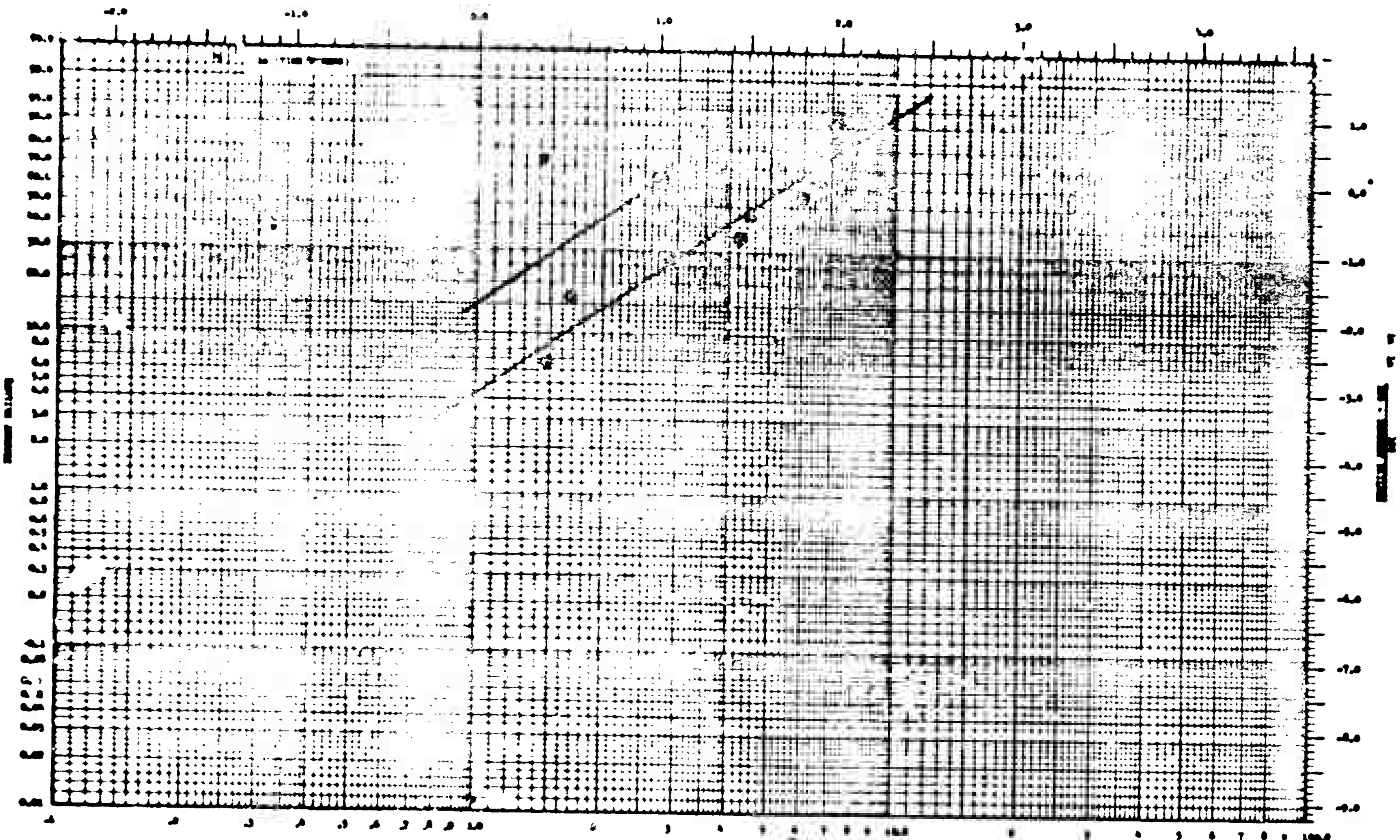

Contact Load - 15 amps, Contact Overtravel - .005 in/s, Actuation Rate - 150 cpm, $\ln\theta$ = -3.131, α = 22.87, β = 1.80

Figure VI-20 Switch Test Run No. 20

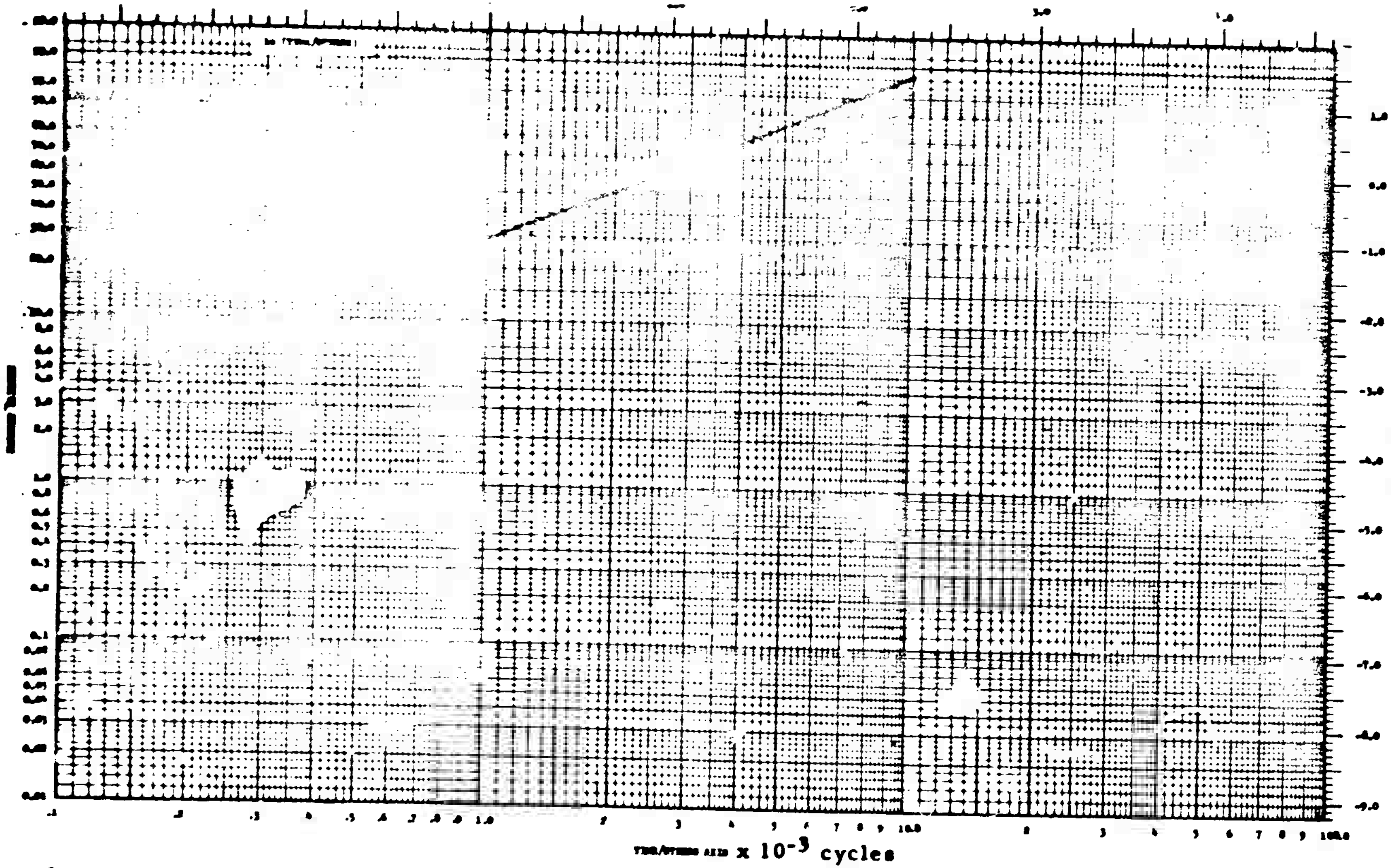

Contact Load - 15 amps, Contact Overtravel - .005 inch, Actuation Rate - 300 cpm, $\ln \alpha$ = -1.103, α = 3.00, β = 1.09

Figure VI-21 Switch Test Run No. 21

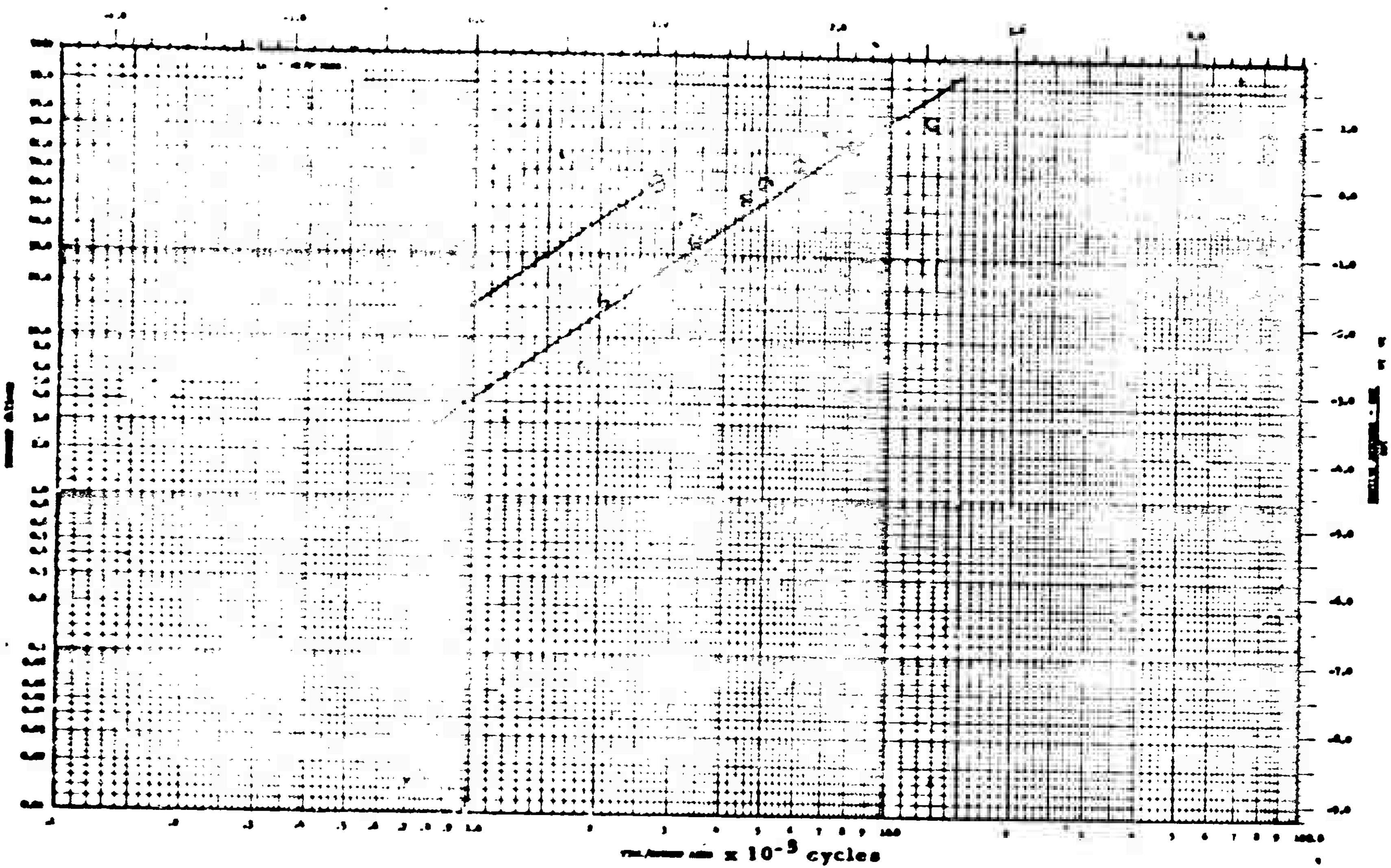

Contact Load - 15 amps, Contact Overtravel - .010 inch, Actuation Rate - 70 cpm, $\ln\alpha = -3.132$, $\alpha = 22.87$, $\beta = 1.79$

Figure VI-22 Switch Test Run No. 22

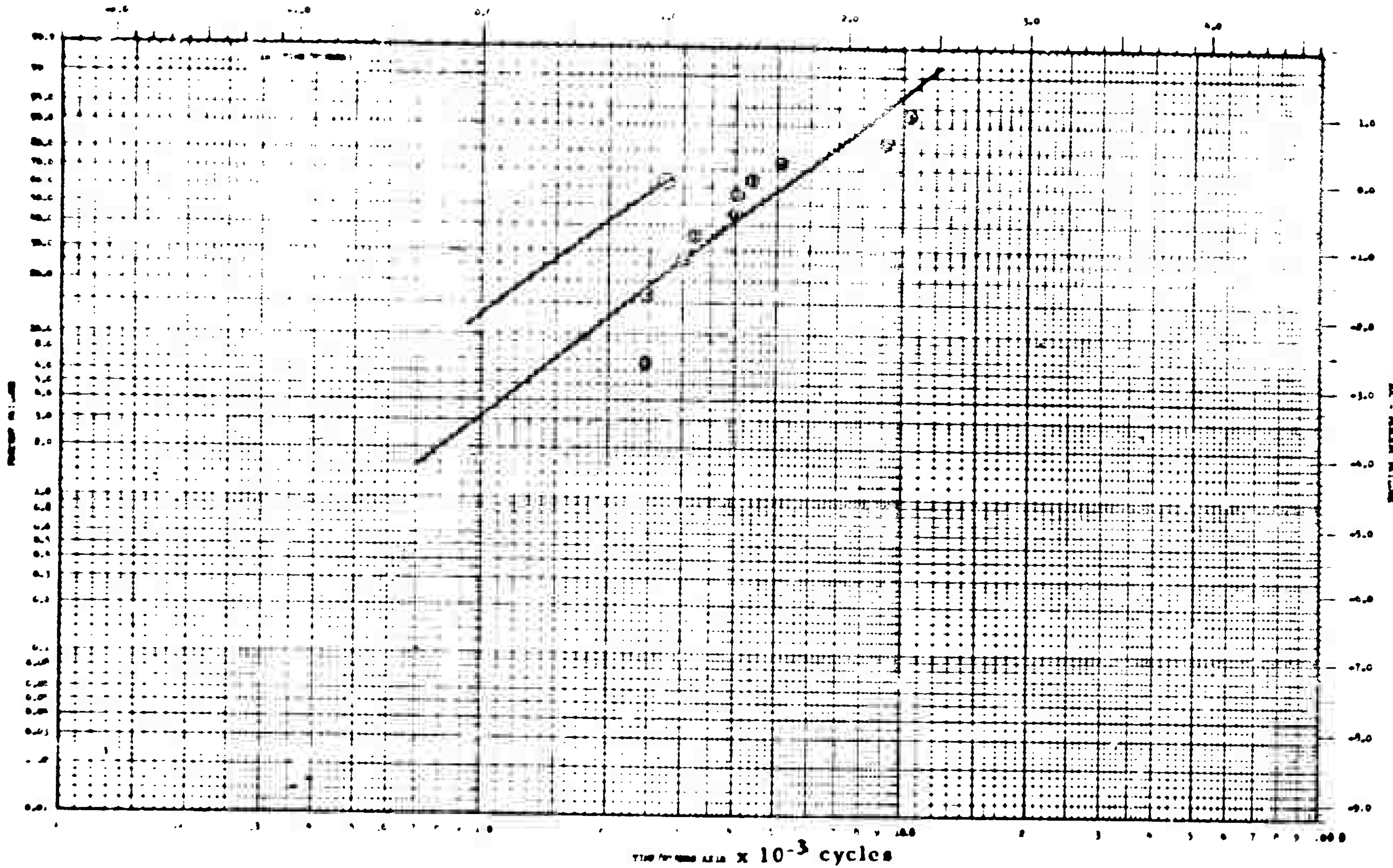

Contact Load - 15 amps, Contact Overtravel - .010 inch, Actuation Rate - 150 cpm, $\ln \alpha$ = -3.460, α = 31.87, β = 2.02

Figure VI-23 Switch Test Run No. 23

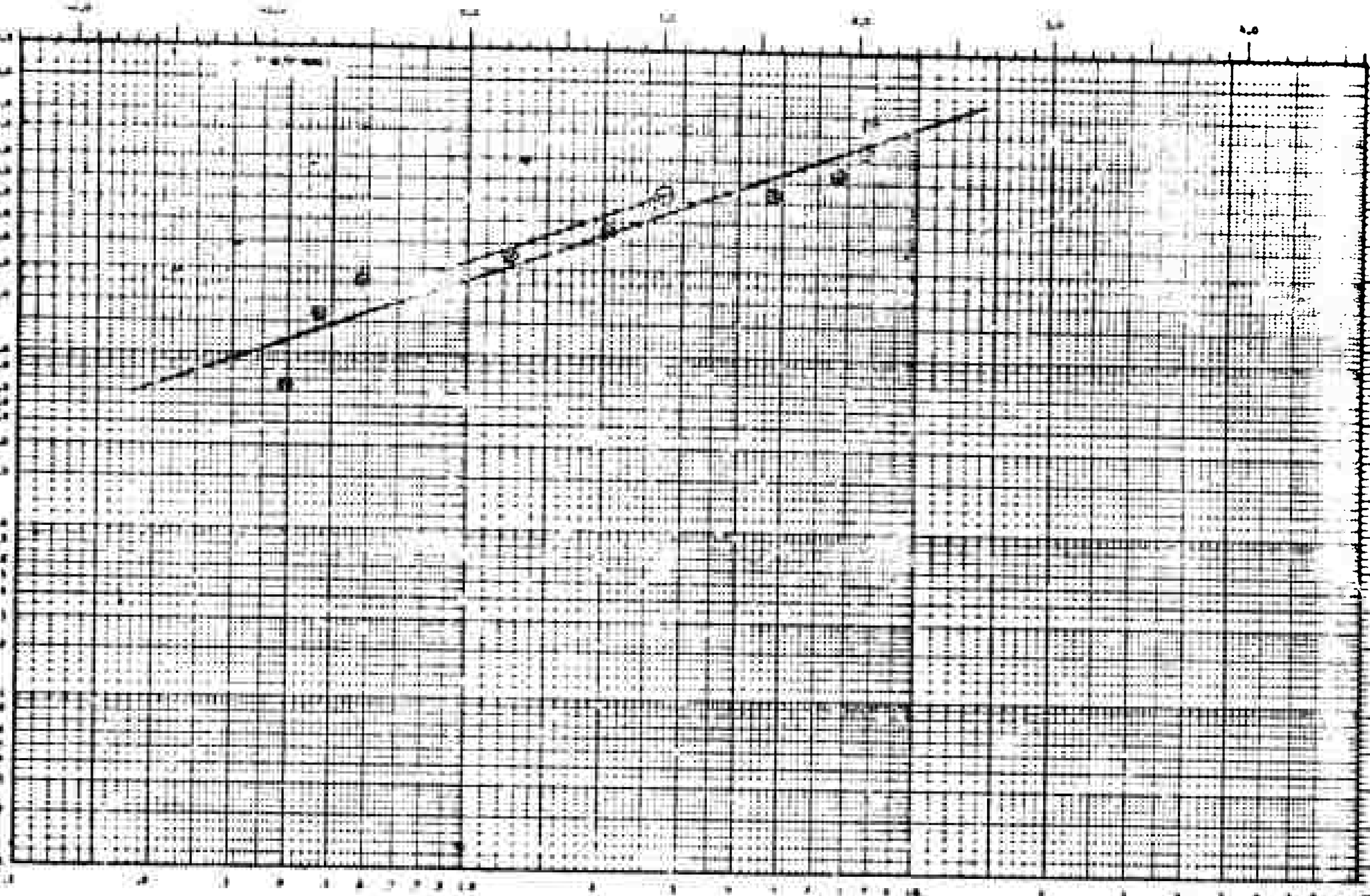

Contact Load - 15 amps, Contact Overtravel - .010 inch, Actuation Rate - 300 cpm, $\ln \alpha$ = -1.179, α = 3.25, β = .91

Figure VI-24 Switch Test Run No. 24

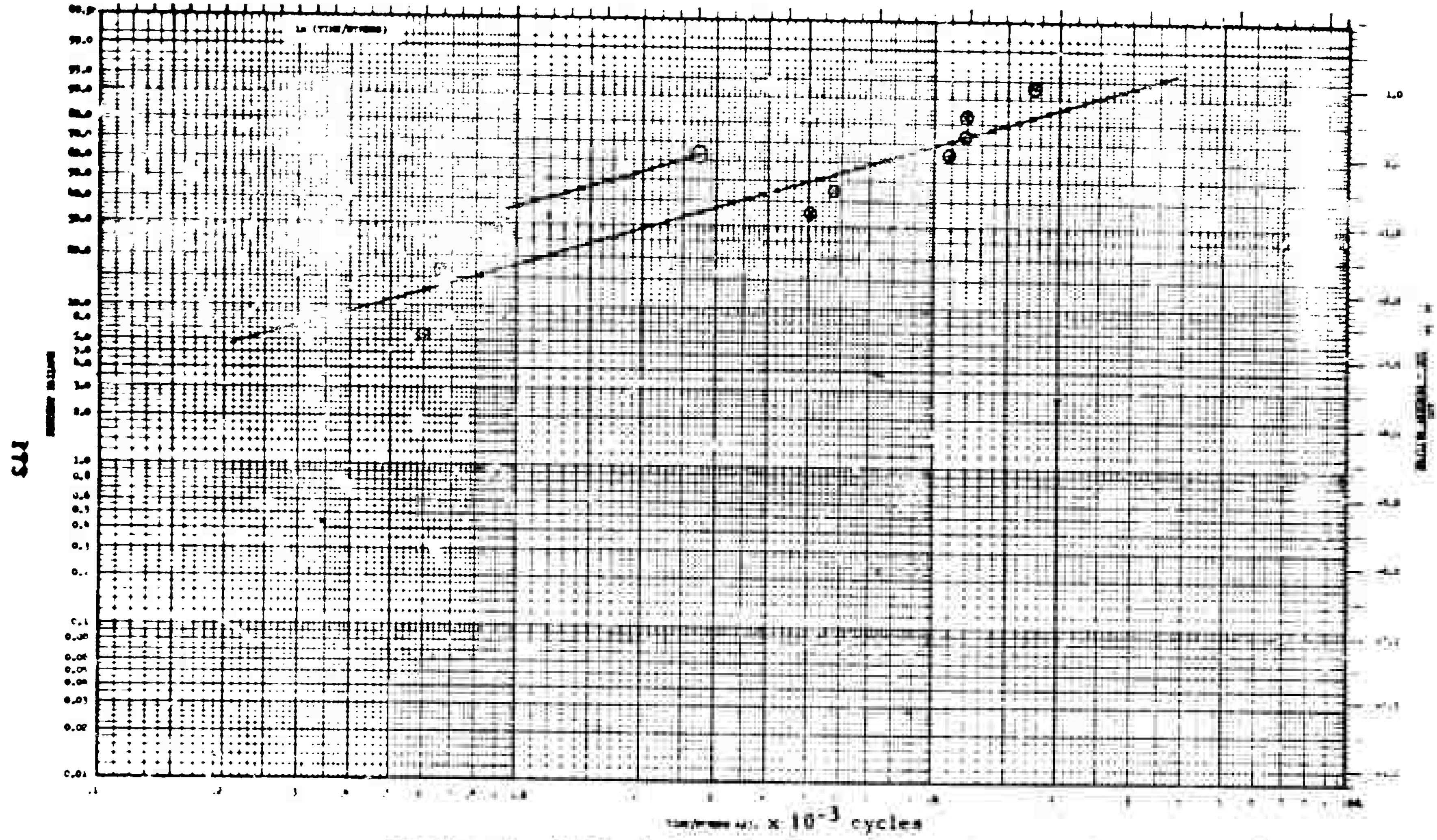

Contact Load - 15 amps, Contact Overtravel - .015 inch, Actuation Rate - 70 cpm, $\ln\alpha = -1.64$, $\alpha = 5.16$, $\beta = .77$

Figure VI-25 Switch Test Run No. 25

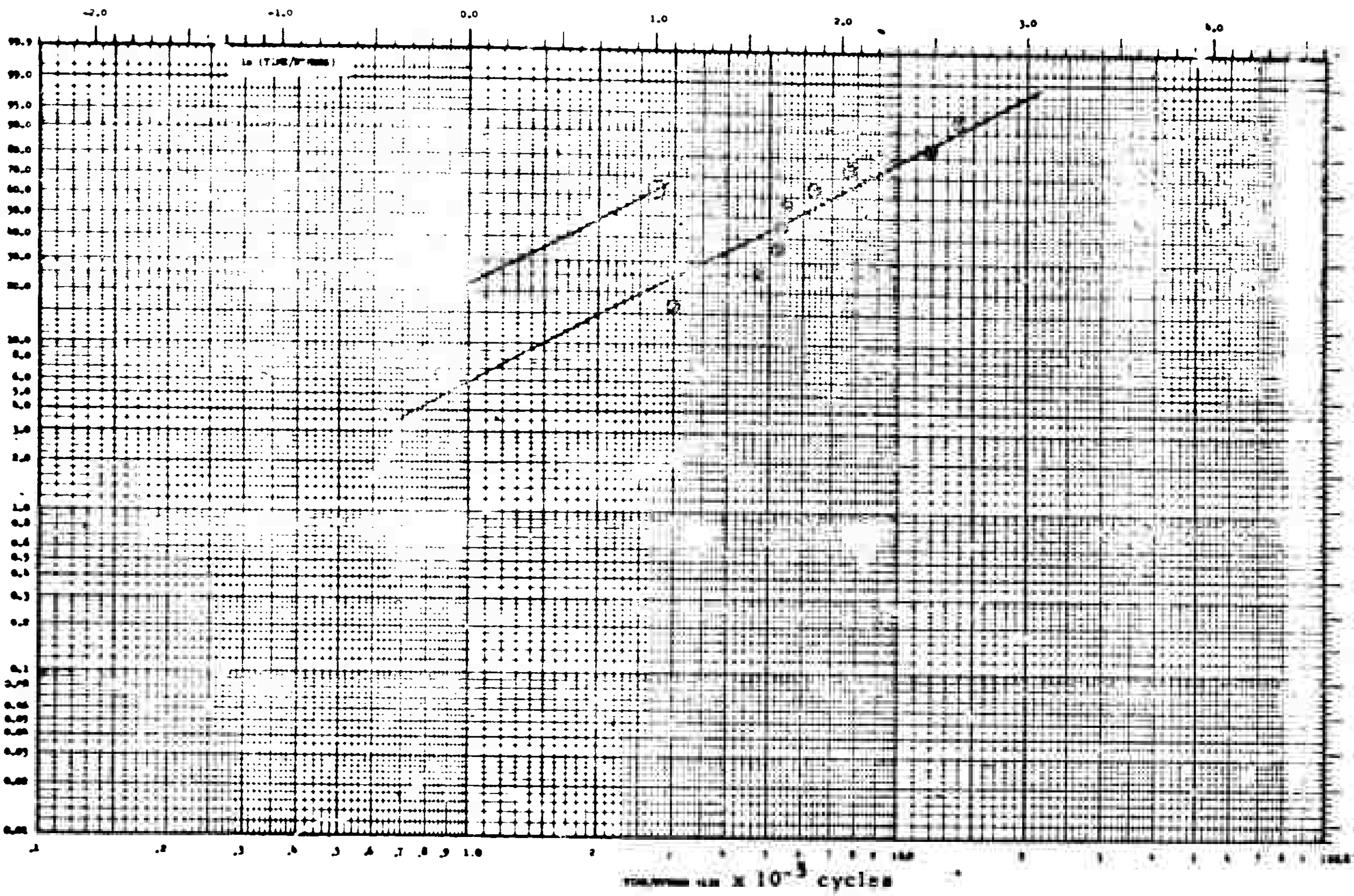

Contact Load - 15 amps, Contact Overtravel - .015 inch, Actuation Rate - 150 cpm, $\ln \alpha = -2.818$, $\alpha = 16.78$, $\beta = 1.38$

Figure VI-26 Switch Test Run No. 26

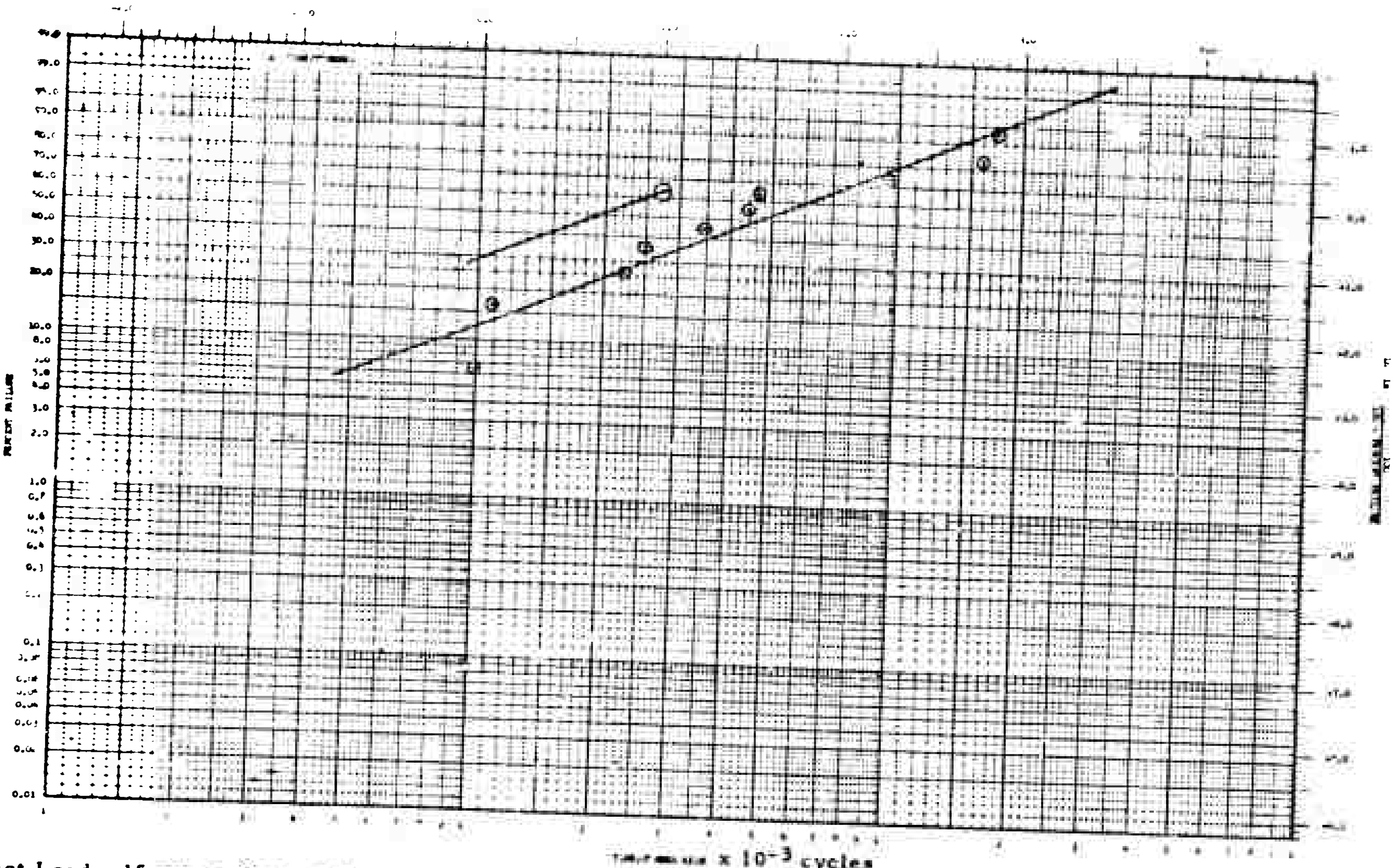

Contact Load - 15 amps, Contact Overtravel - .015 inch, Actuation Rate - 300 cpm, $\ln\alpha$ = -2.013, α = 7.46, β = 1.07

Figure VI-27 Switch Test Run No. 27

VI-2 CRYSTAL CAN RELAYS

The following charts (Figures VI-28 through VI-54) are Weibull plots of the times to failure of the relays operated at manufacturer's rated conditions (Test Run 1) and 26 other test runs employing combined accelerated stresses. Each chart displays the failure time of each relay, the detailed description of the stresses applied in combination, and the calculated Weibull shape (β) and scale (α) parameters.

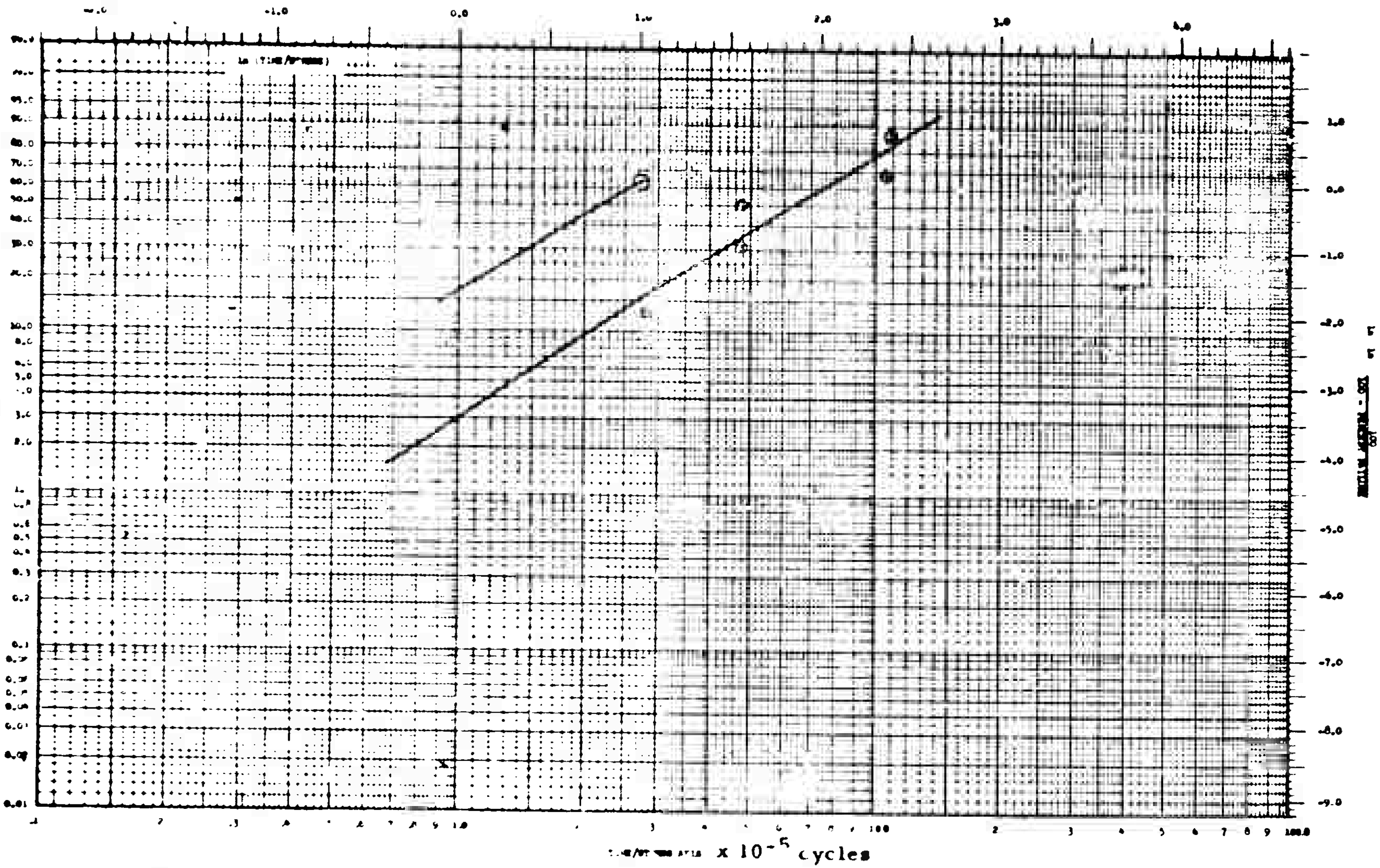

Contact Load - 3 amps, Temperature - 25°C, Actuation Rate - 1 cps, $\ln \alpha = -3.482$, $\alpha = 32.46$, $\beta = 1.68$

Figure VI-28 Relay Test Run No. 1

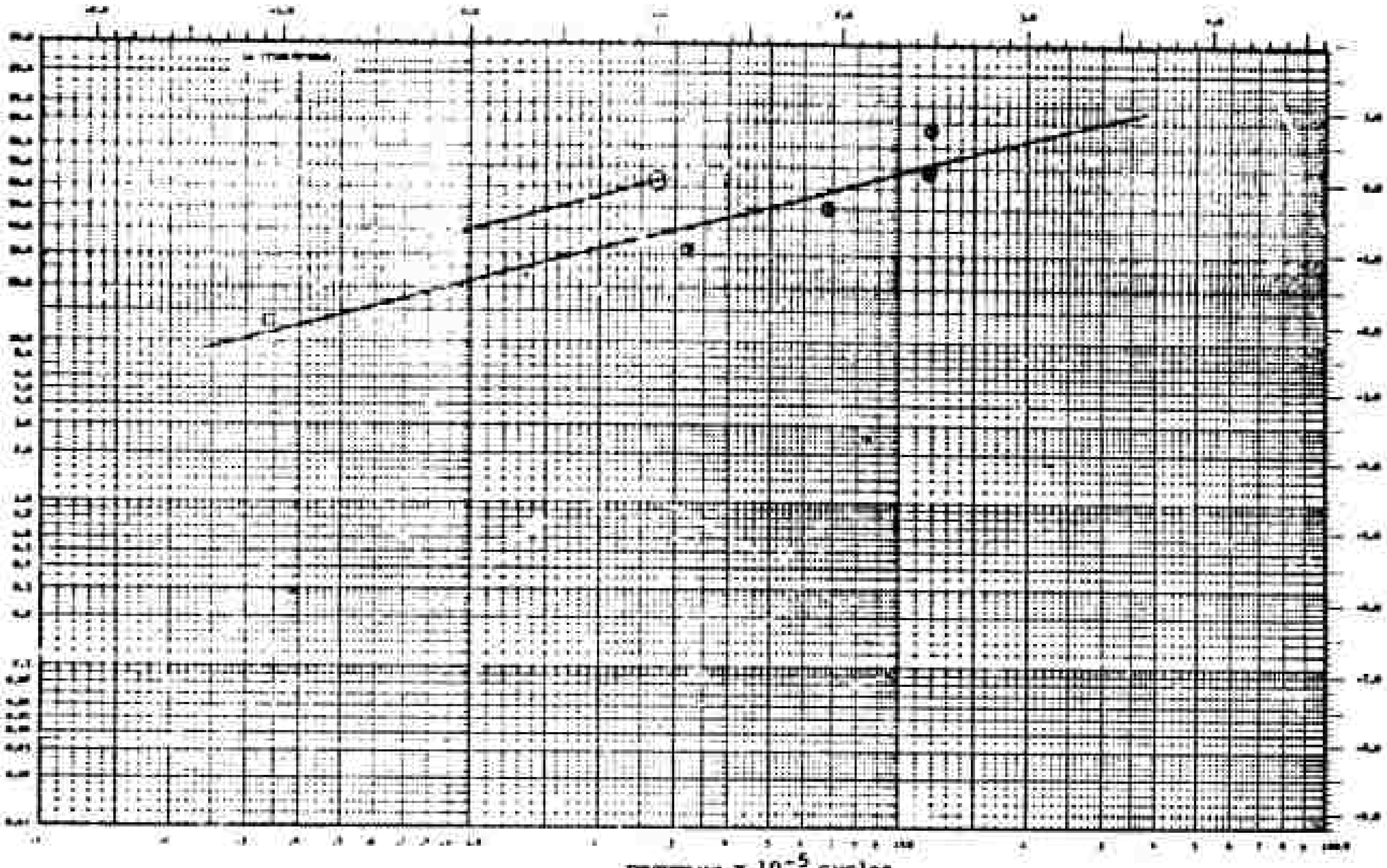

Contact Load - 3 amps   Temperature - 100°C, Actuation Rate - 1 cps, $\ln \alpha = -1.405$, $\alpha = 4.10$, $\beta = .66$

Figure VI-29 Relay Test Run No. 2

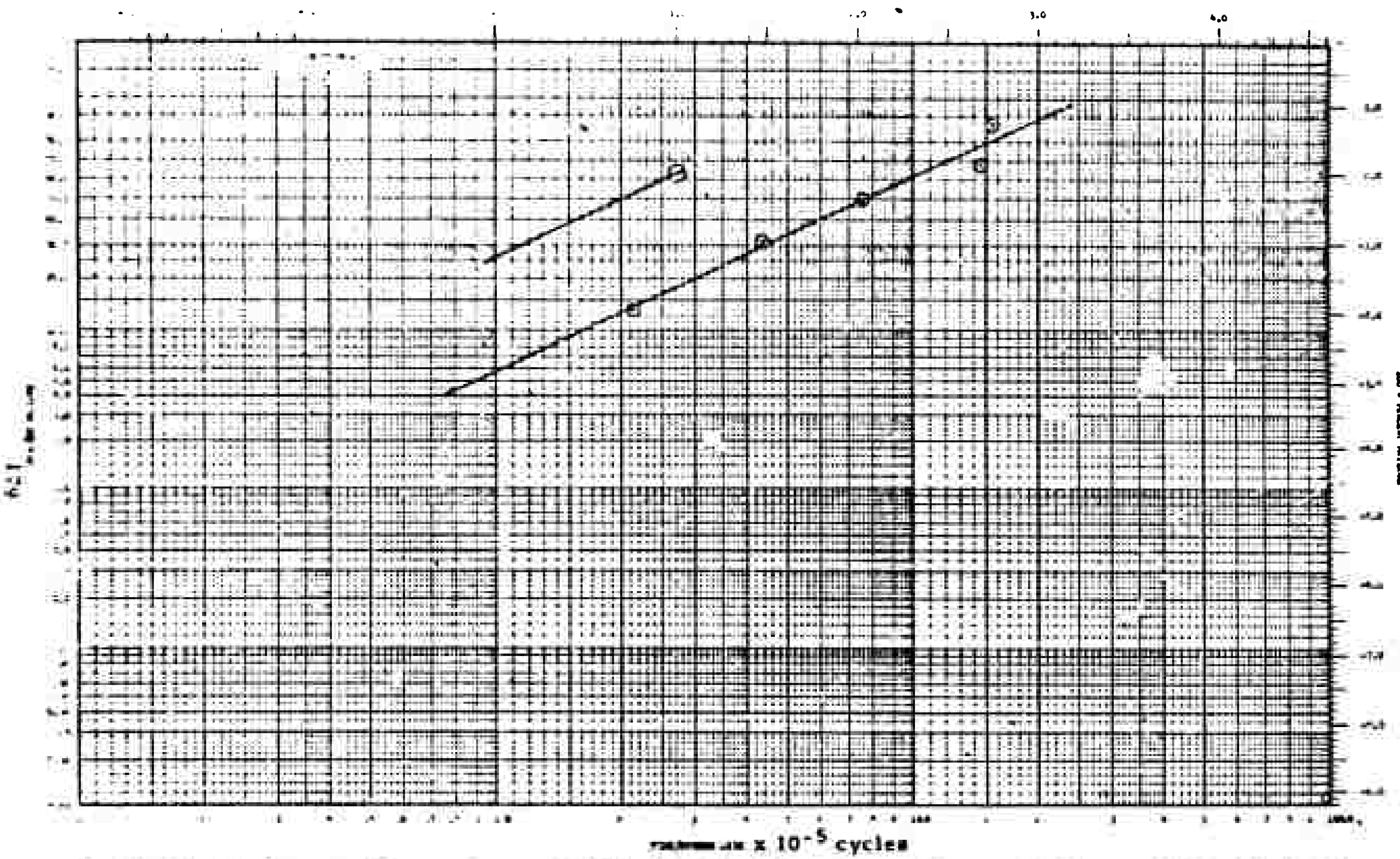

Contact Load - 3 amps, Temperature - 150°C, Actuation Rate - 1 cps, $\ln \alpha = -2.835$, $\alpha = 17.12$, $\beta = 1.21$

Figure VI-30 Relay Test Run No. 3

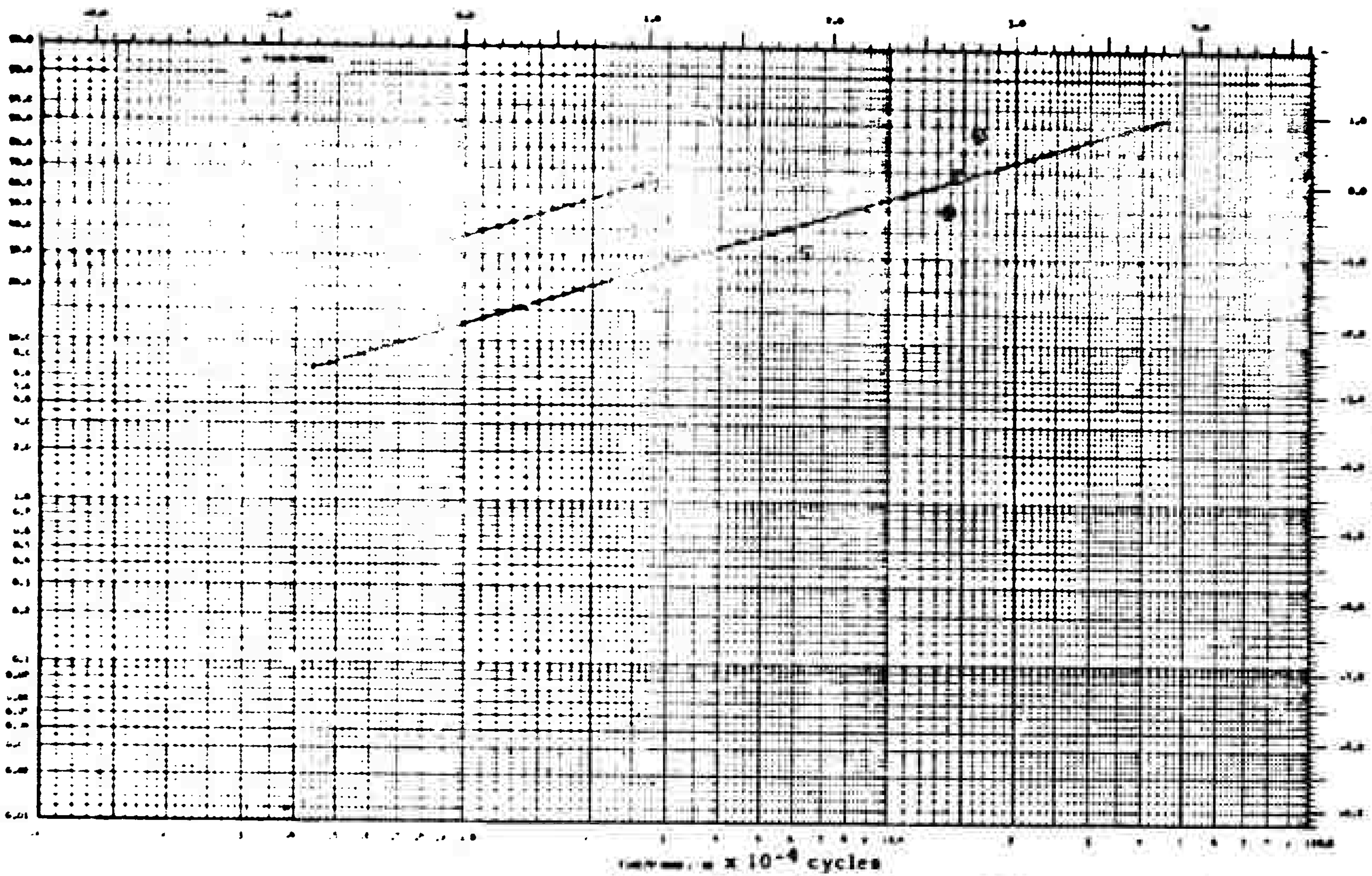

Contact Load - 6 amps, Temperature - 25°C, Actuation Rate - 1 cps, $\ln \alpha = -2.024$, $\alpha = 7.54$, $\beta = .78$

Figure VI-31 Relay Test Run No. 4

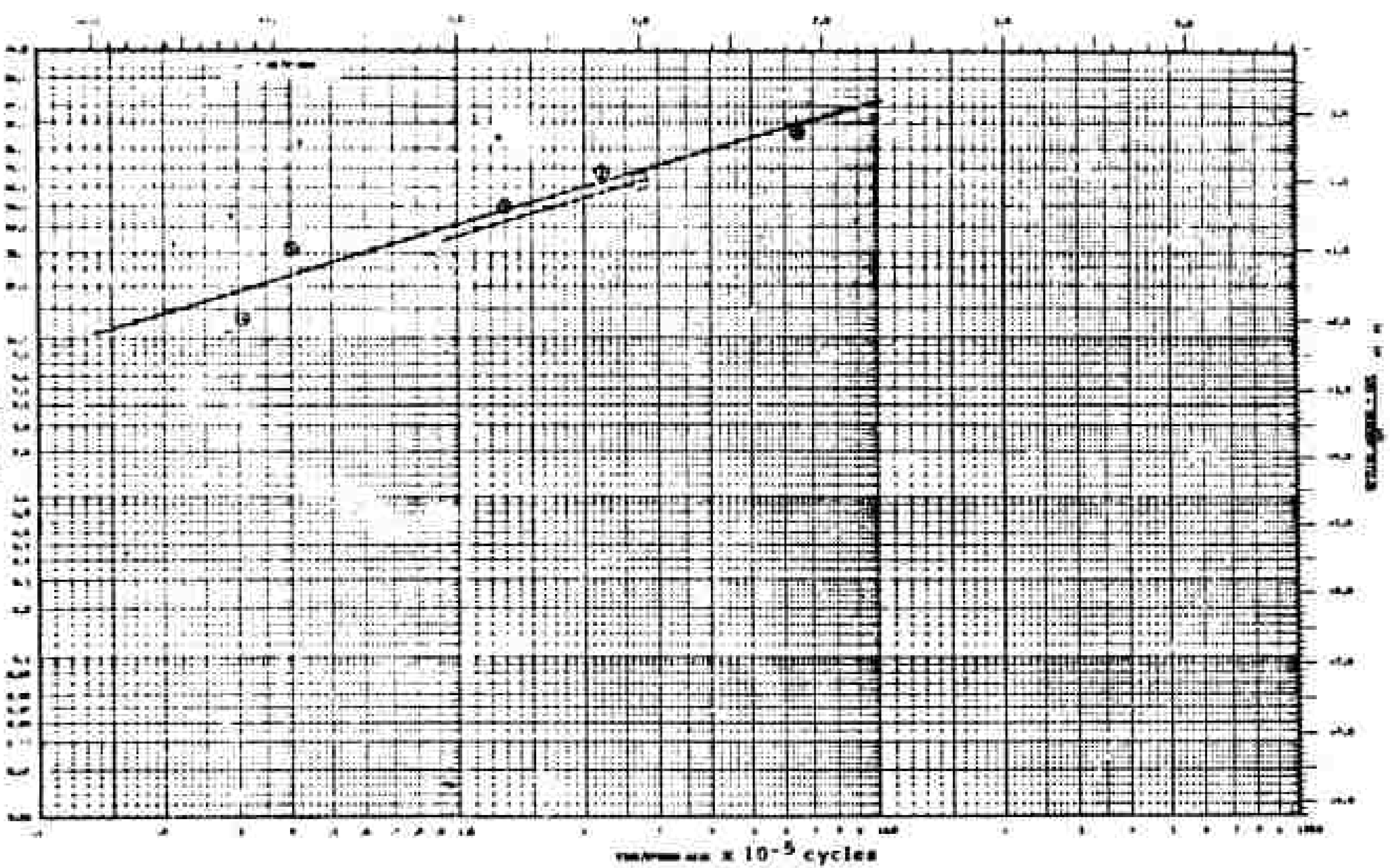

Contact Load - 6 amps, Temperature - 100°C, Actuation Rate - 1 cps, $\ln \alpha$ = -.627, α = 1.88, β = .79

Figure VI-32 Relay Test Run No. 5

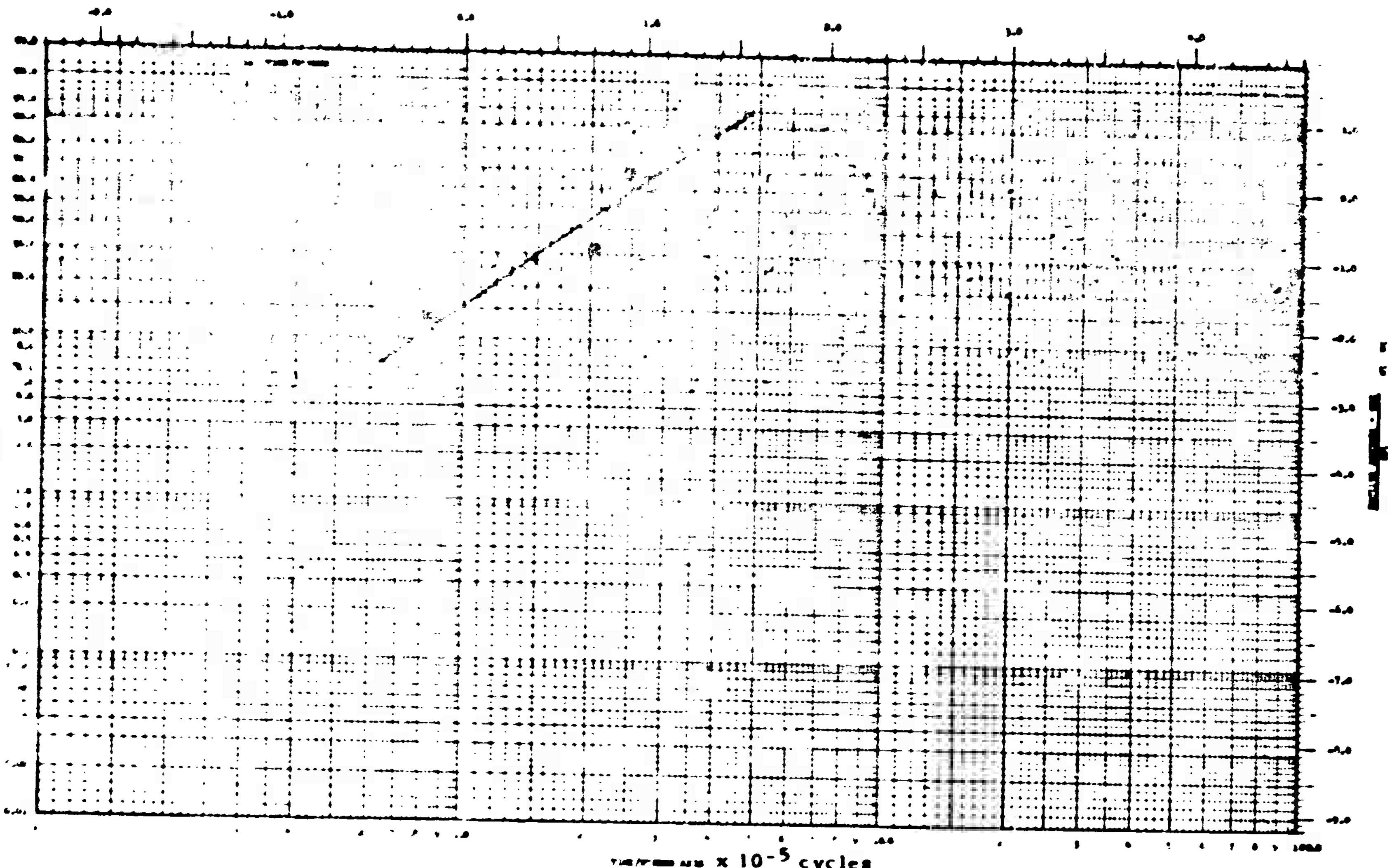

Contact Load - 6 amps, Temperature - 150°C, Actuation Rate - 1 cps, $\ln \alpha = -1.804$, $\alpha = 6.05$, $\beta = 1.84$

Figure VI-33 Relay Test Run No. 6

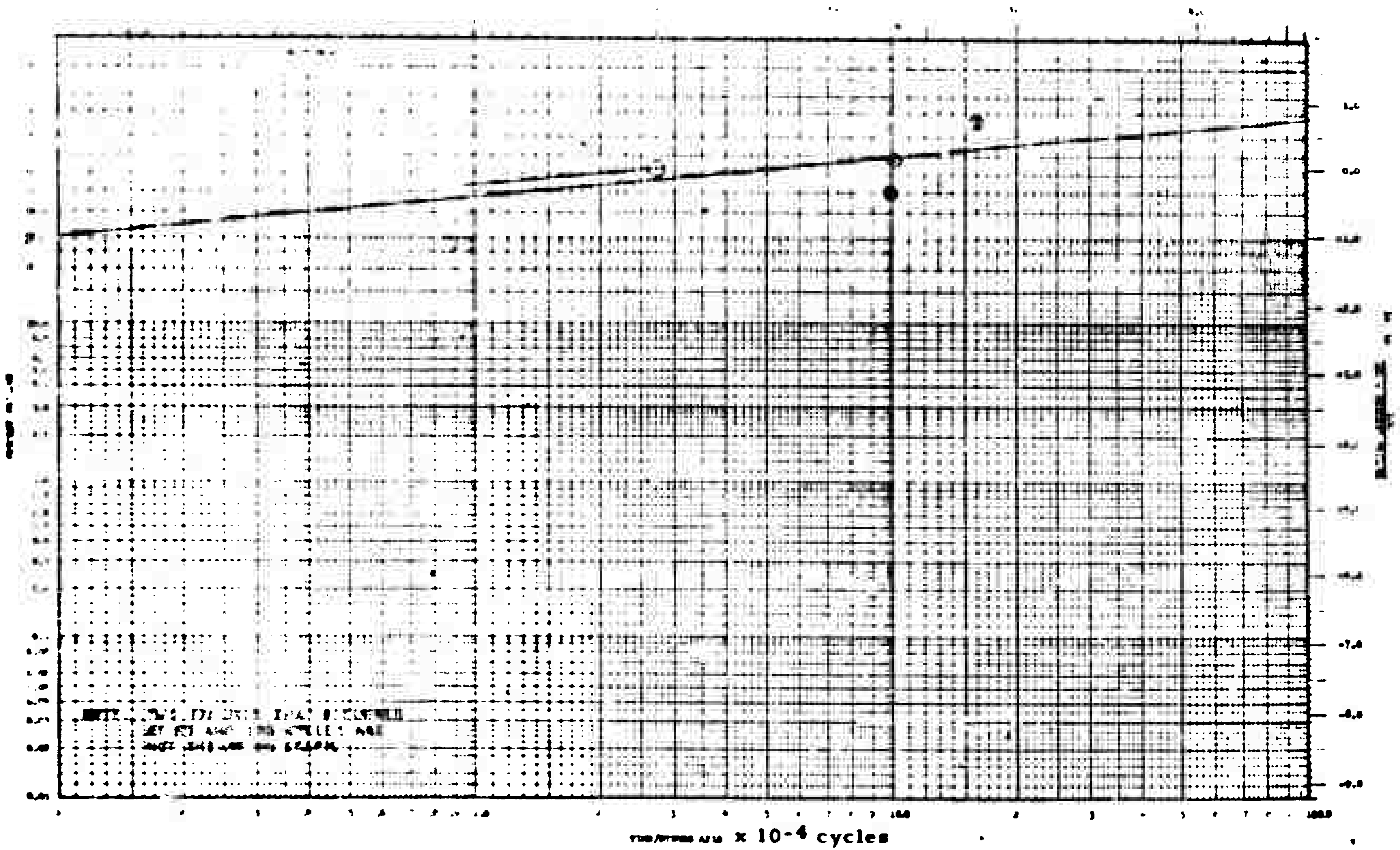

Contact Load - 8 amps, Temperature -25°C, Actuation Rate - 1 cps, $\ln \alpha = -.432$, $\alpha = 1.54$, $\beta = .25$

Figure VI-34 Relay Test Run No. 7

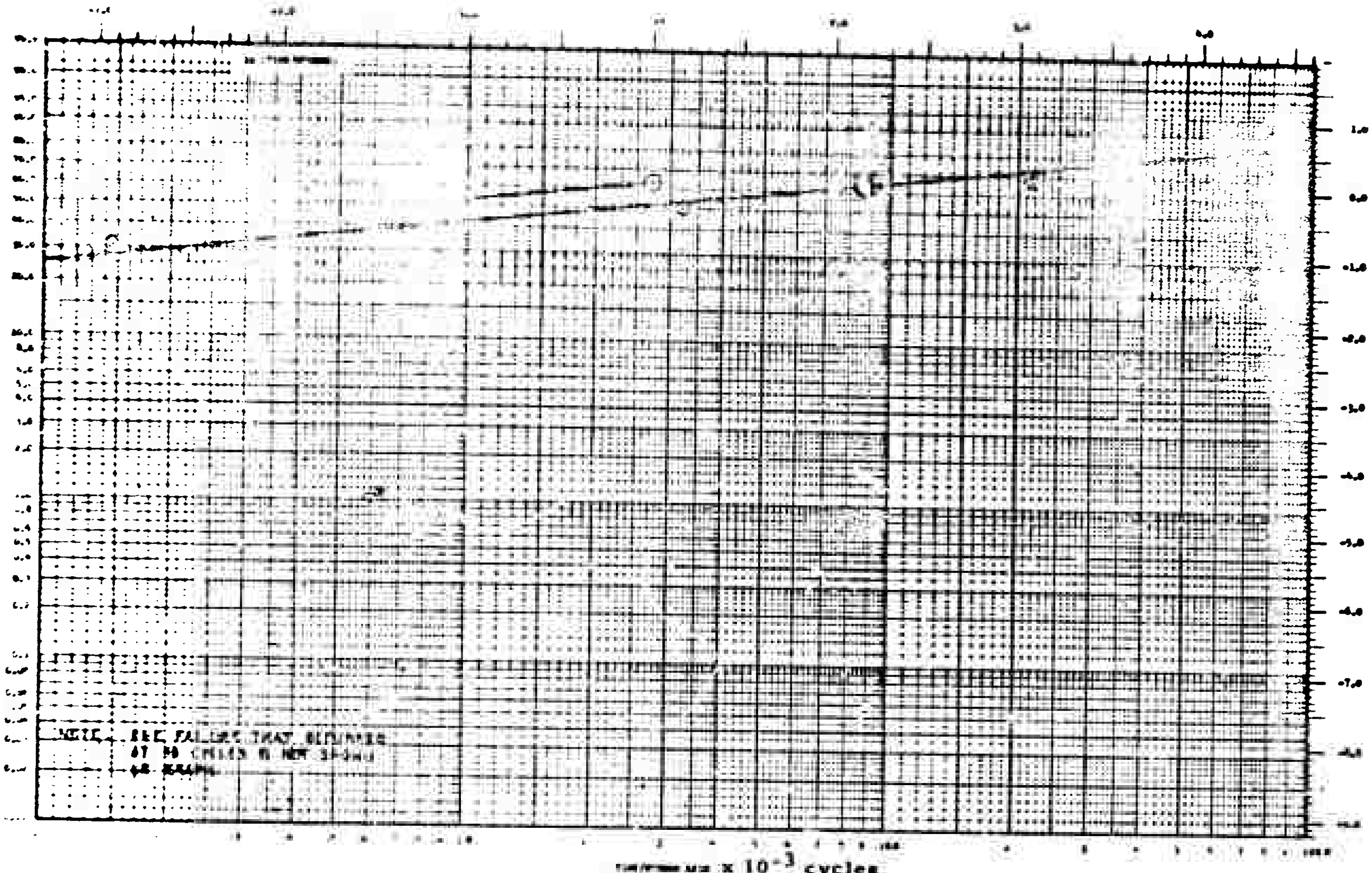

Contact Load - 8 amps, Temperature - 100°C, Actuation Rate - 1 cps, $\ln \alpha = -.594$, $\alpha = 1.80$, $\beta = .28$

Figure VI-35 Relay Test Run No. 8

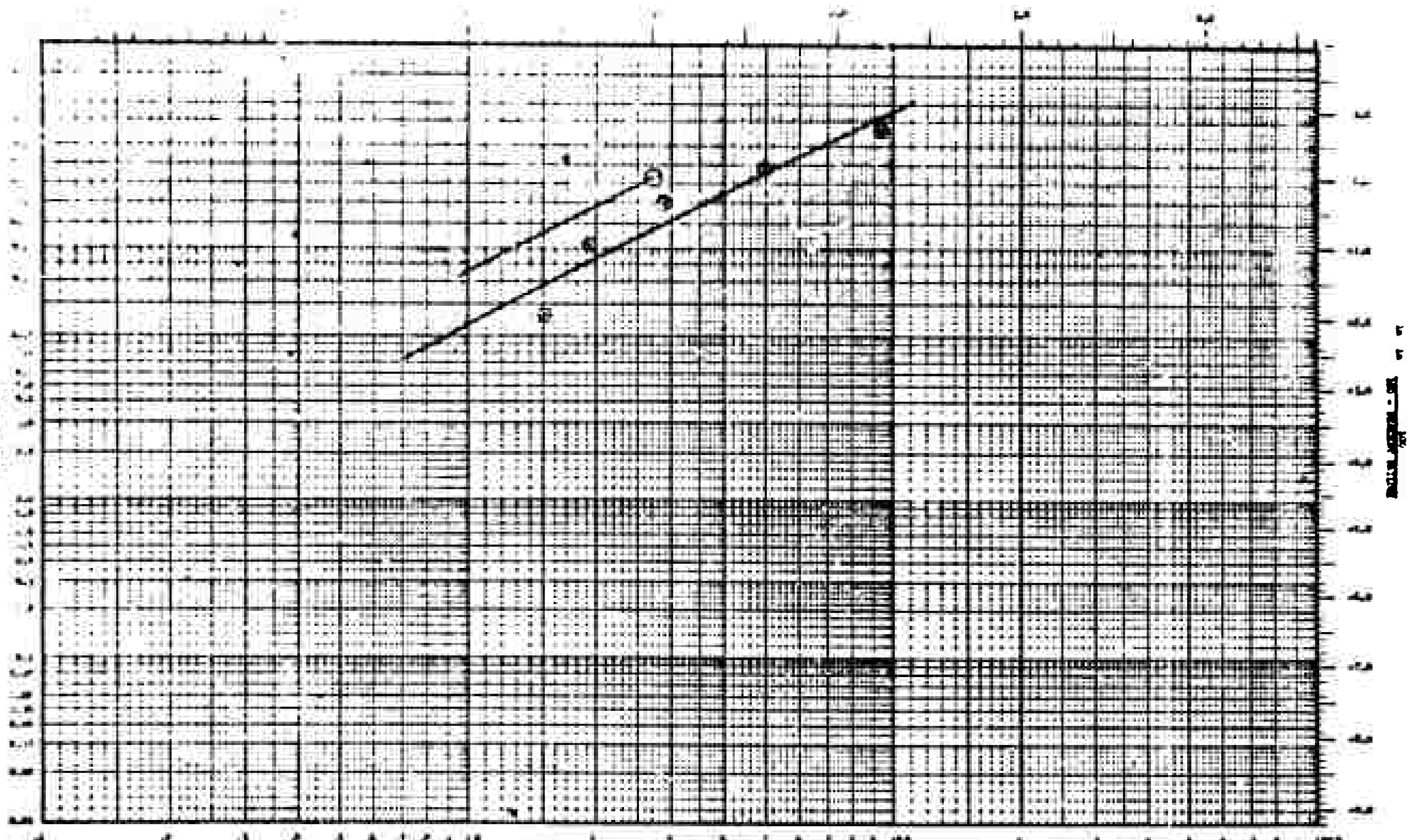

Contact Load - 8 amps, Temperature - 150°C, Actuation Rate - 1 cps, $\ln \alpha = -2.103$, $\alpha = 8.17$, $\beta = 1.35$

Figure VI-36 Relay Test Run No. 9

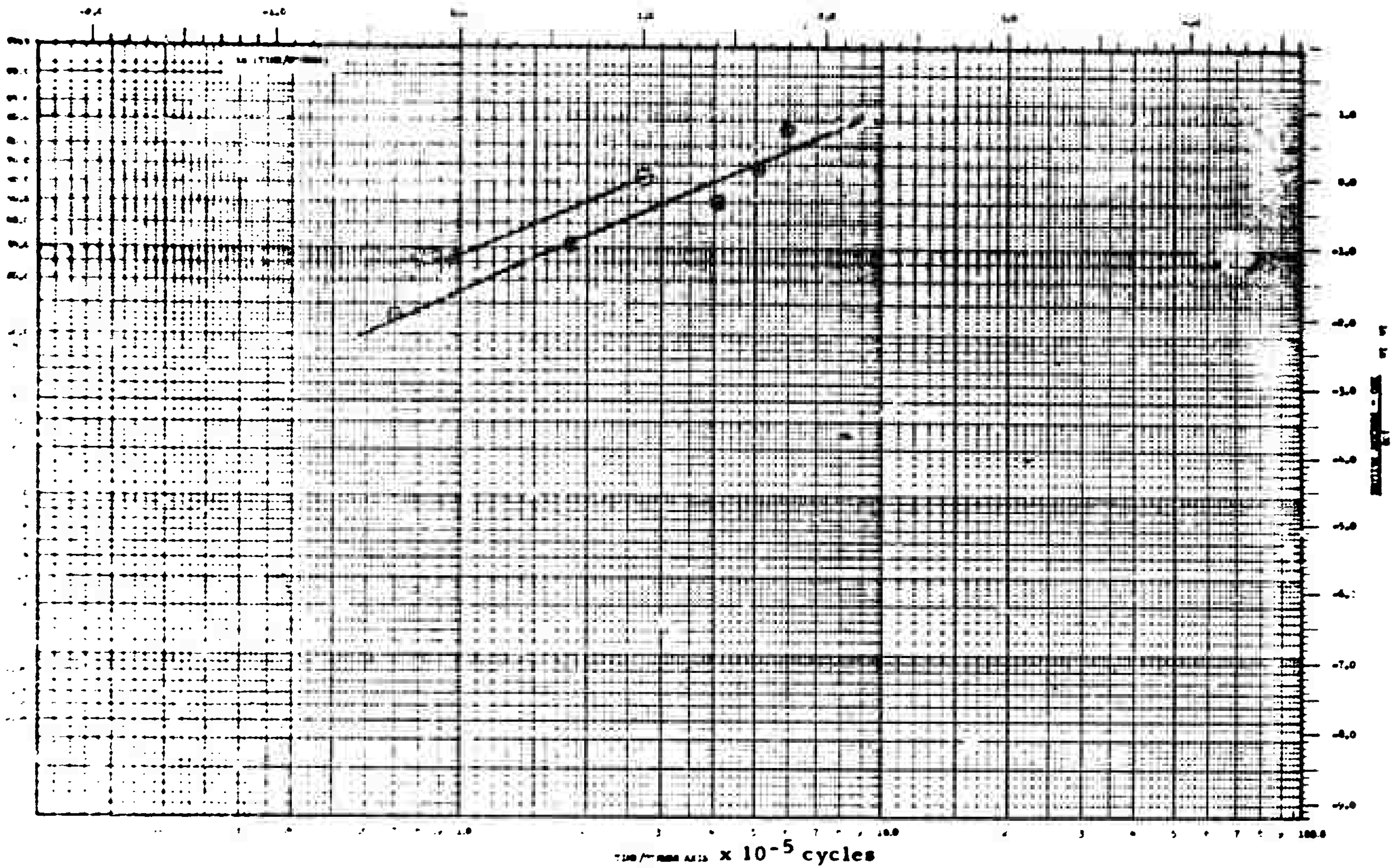

Contact Load - 3 amps, Temperature -25°C, Actuation Rate - 10 cps, $\ln \alpha$ = -1.646, α = 5.21. β = 1.14

Figure VI-37 Relay Test Run No. 10

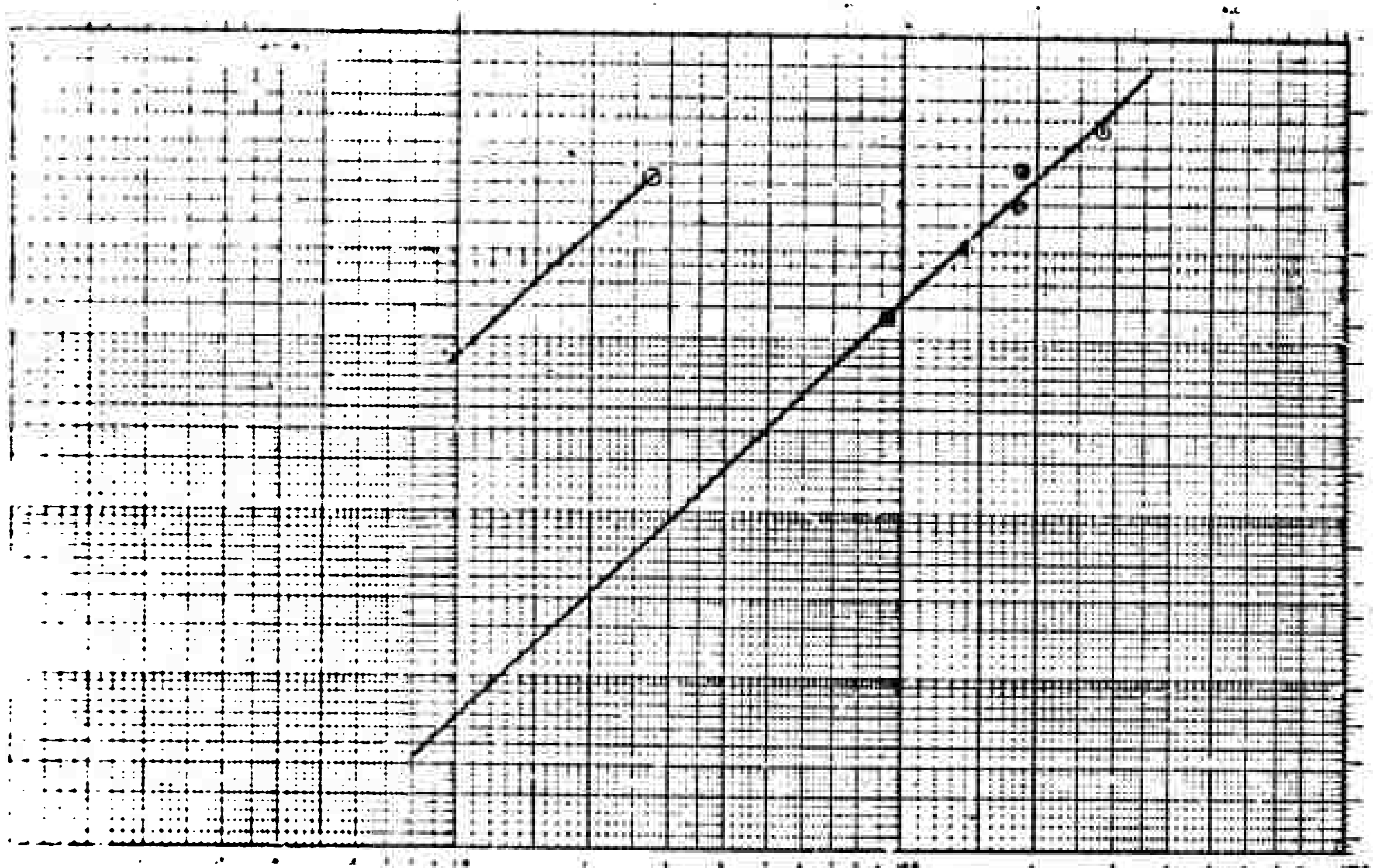

[illegible] x 10^{-5} cycles

Contact Load - 3 amps, Temperature - 100°C, Actuation Rate - 10 cps, $\ln \alpha$ = -7.472, α = 1719.9, β = 2.49

Figure VI-38 Relay Test Run No. 11

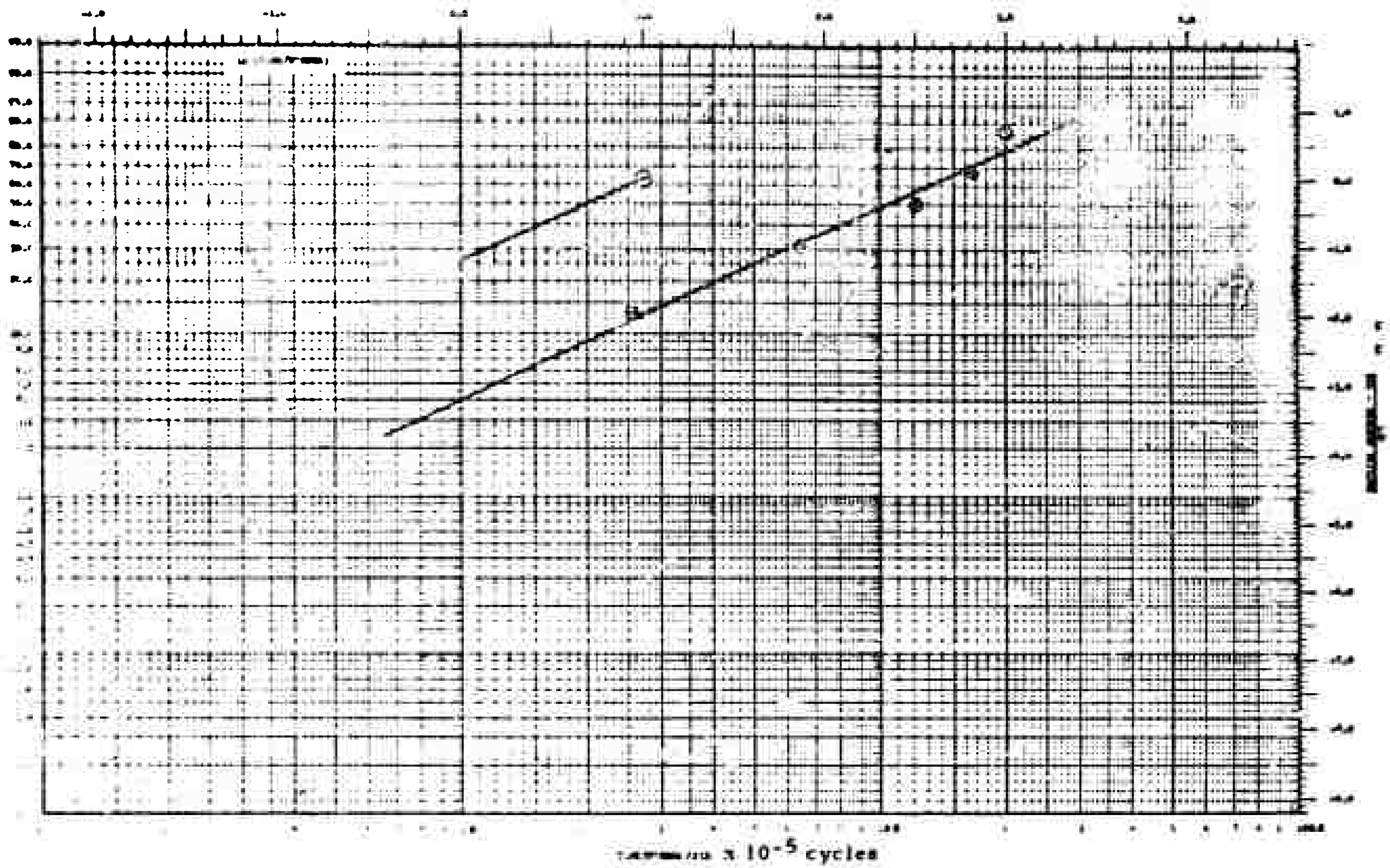

Contact Load - 3 amps, Temperature - 150°C, Actuation Rate - 10 cps, $\ln \alpha$ = -3.206, α = 24.78, β = 1.22

Figure VI-39 Relay Test Run No. 12

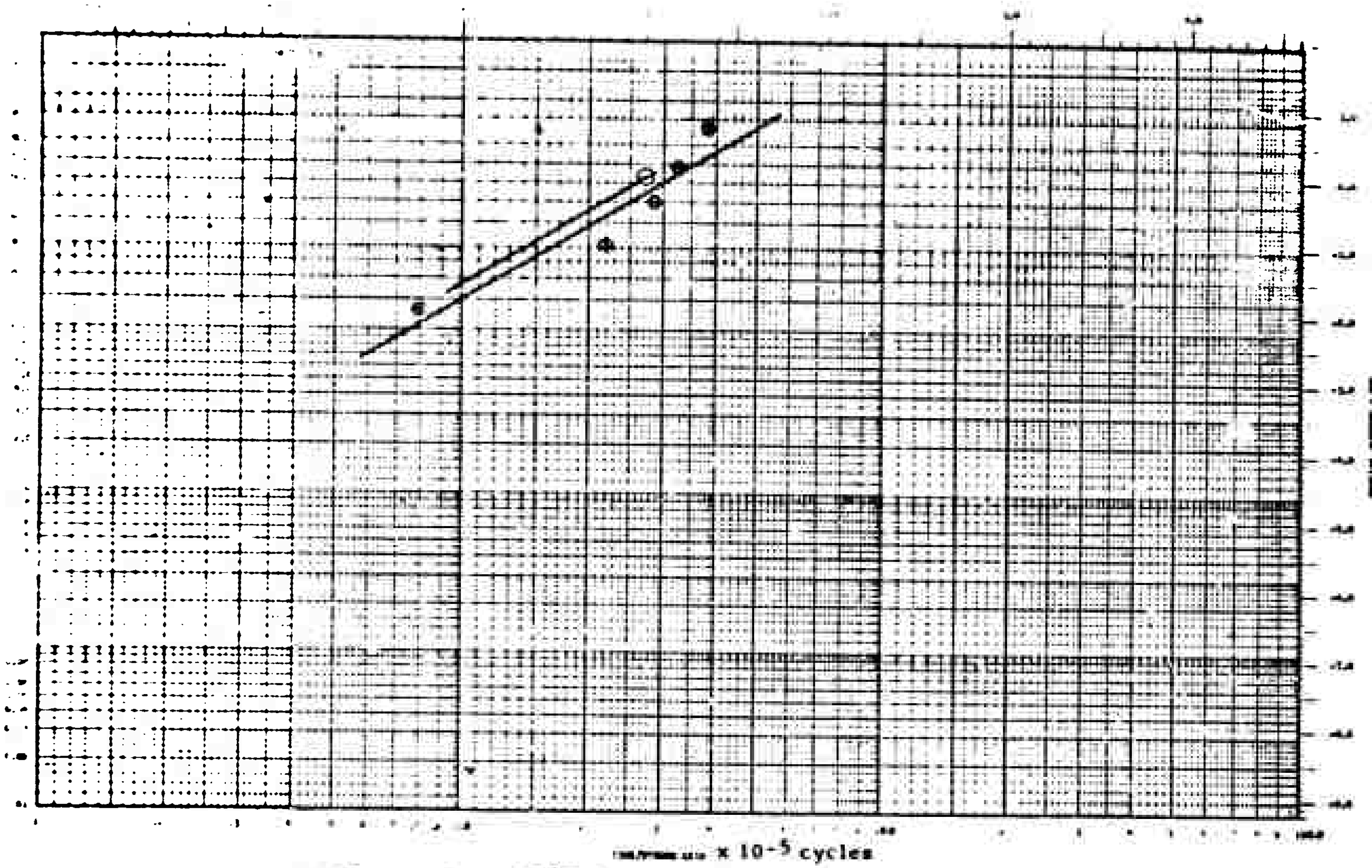

Contact Load - 6 amps, T-mperature - 25°C, Actuatior Rate - 10 cps, $\ln \alpha = -1.805$, $\alpha = 6.11$, $\beta = 1.59$

Figure VI-40 Relay Test Run No. 13

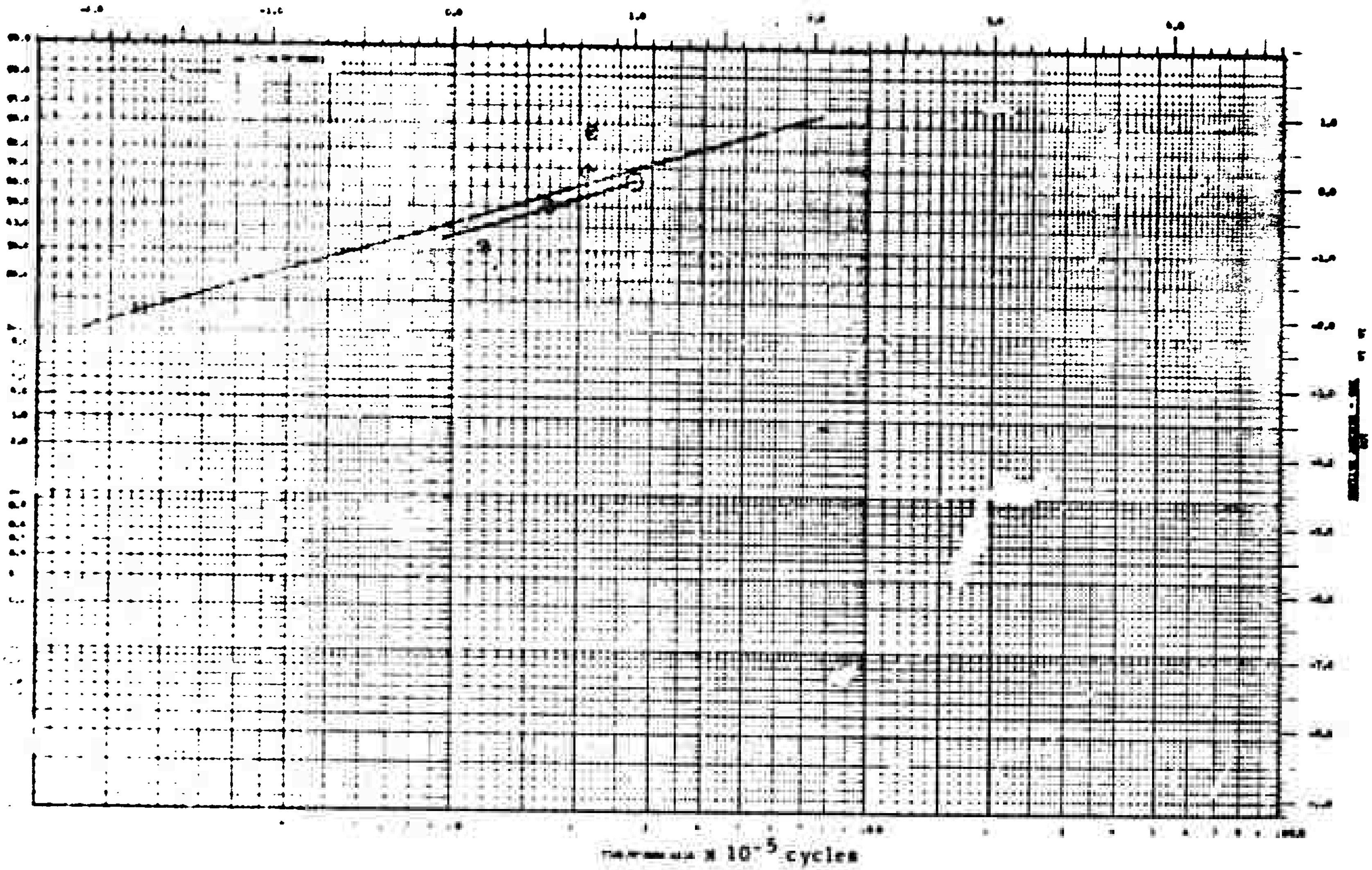

Contact Load - 6 amps, Temperature - 100°C, Actuation Rate - 10 cps, $\ln\alpha$ = -.610, α = 1.84, β = .79

Figure VI-41 Relay Test Run No. 14

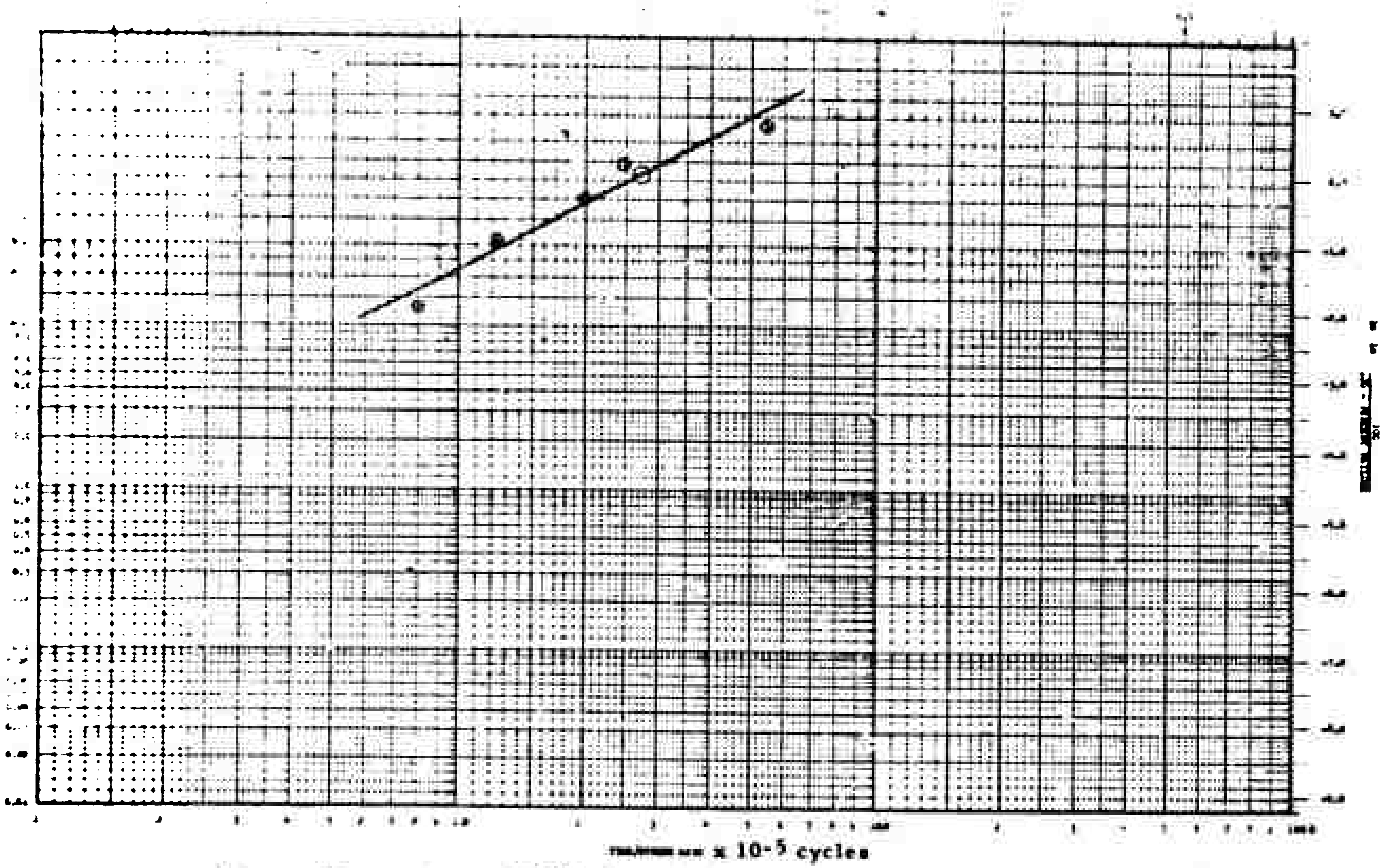

Contact Load - 6 amps, Temperature - 150°C, Actuation Rate - 10 cps, $\ln \alpha = -1.396$, $\alpha = 4.06$, $\beta = 1.39$

Figure VI-42 Relay Test Run No. 15

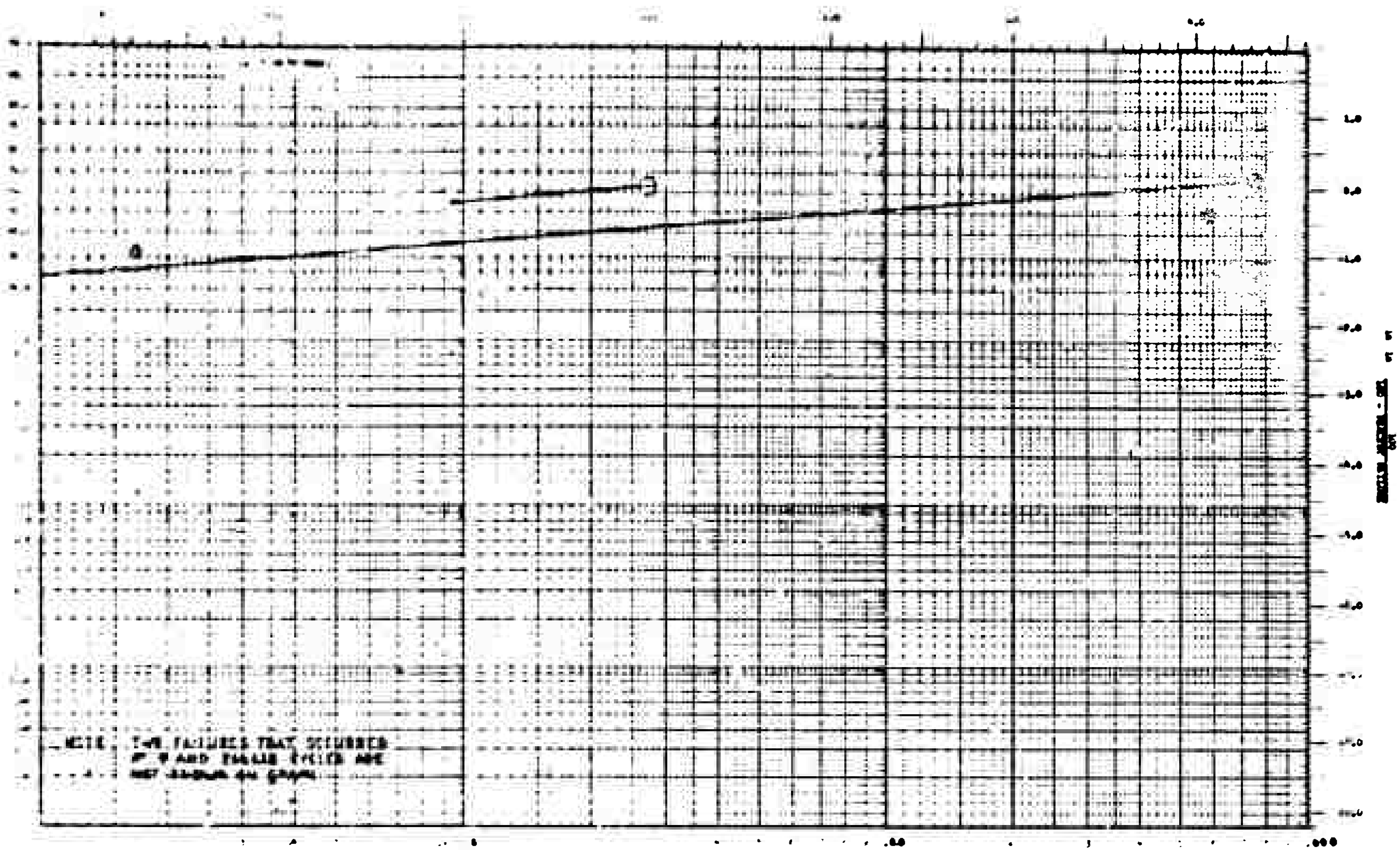

x 10^{-3} cycles

Contact Load - 8 amps, Temperature - 25°C, Actuation Rate - 10 cps, $\ln \alpha = -.820$, $\alpha = 2.27$, $\beta = .22$

Figure VI-43 Relay Test Run No. 16

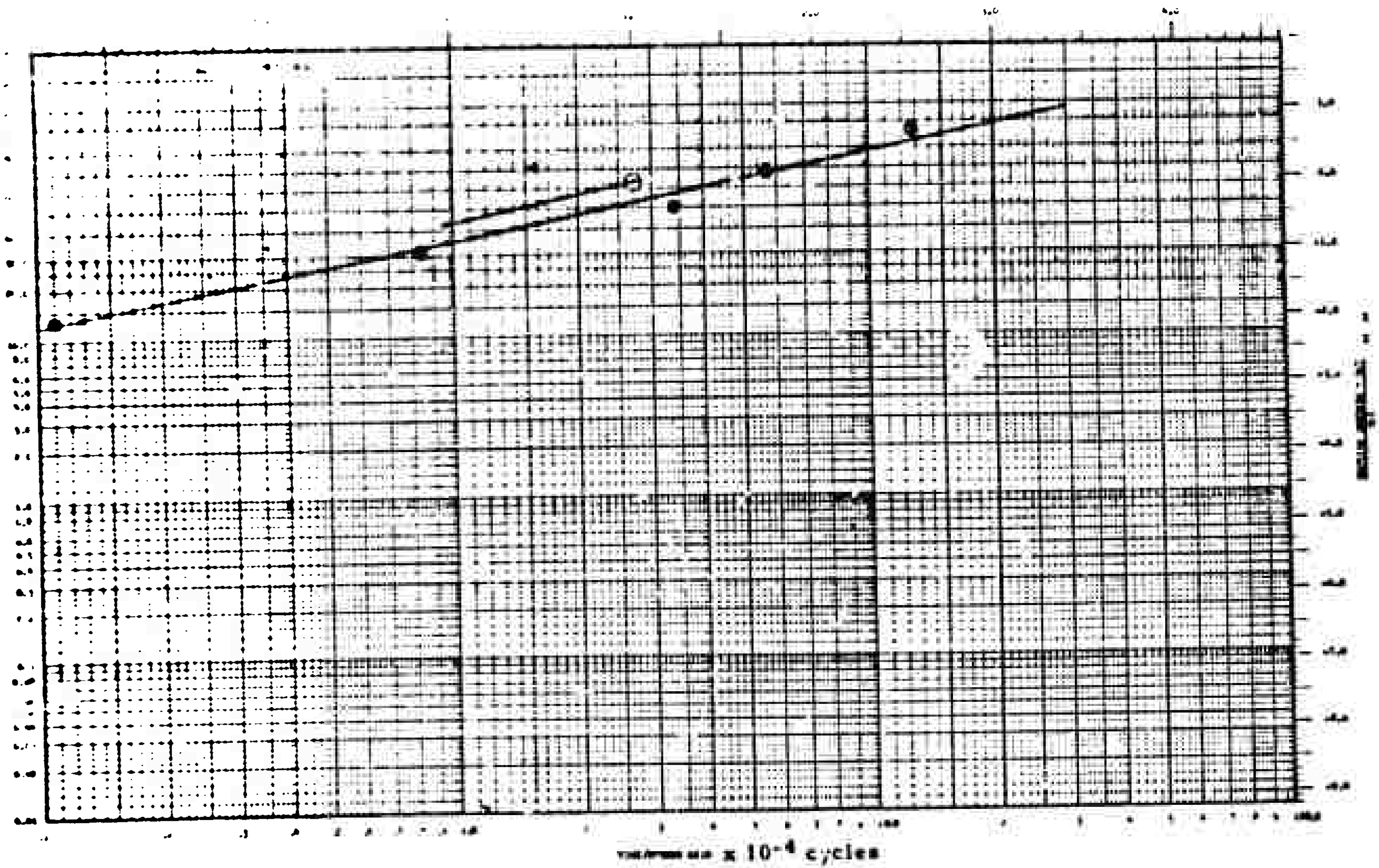

Contact Load - 8 amps, Temperature - 100°C, Actuation Rate - 10 cps, $\ln \alpha = -.836$, $\alpha = 2.32$, $\beta = .55$

Figure VI-44 Relay Test Run No. 17

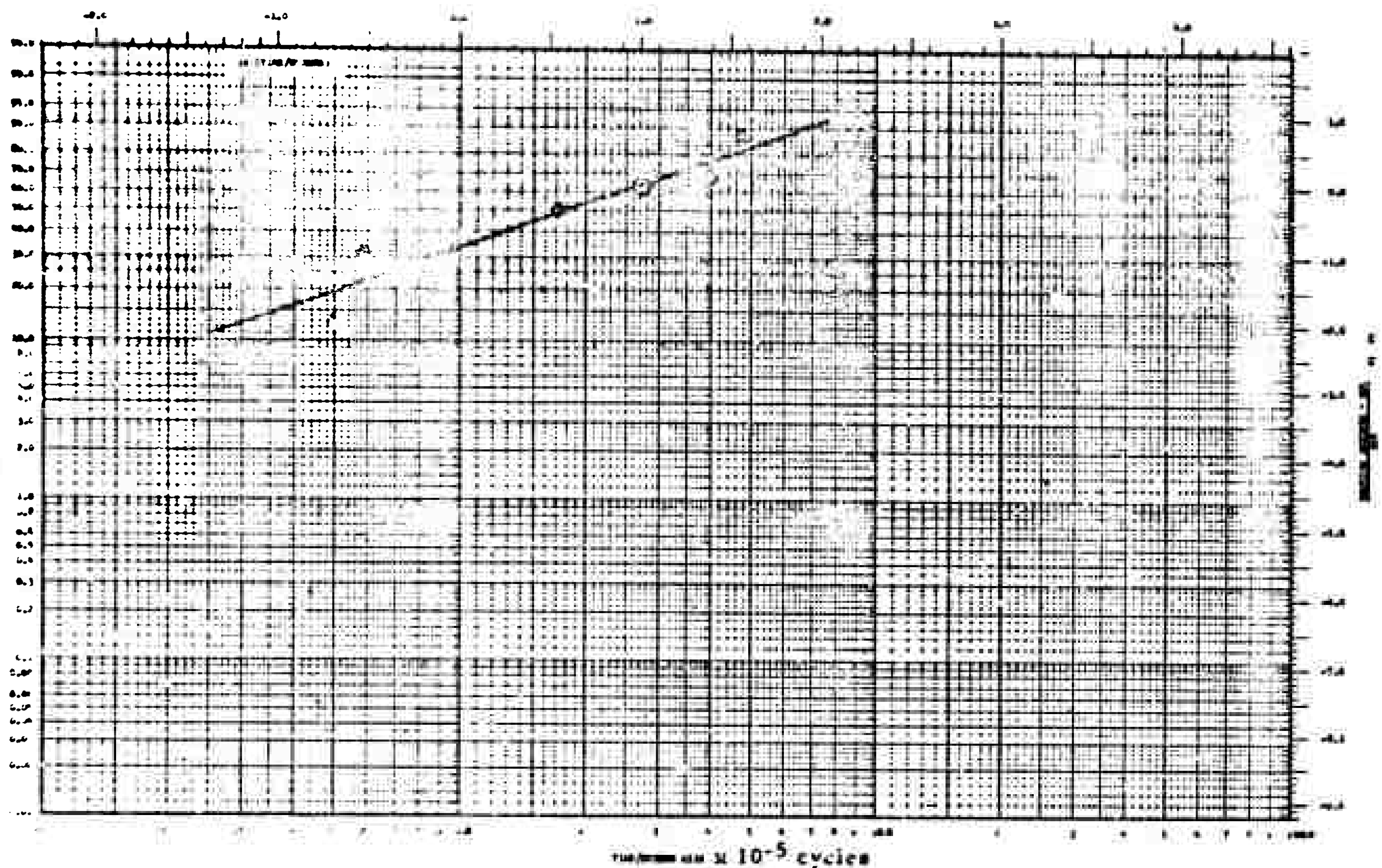

Contact Load - 8 amps, Temperature - 150°C, Actuation Rate - 10 cps, $\ln \alpha = -9.18$, $\alpha = 2.51$, $\beta = .94$

Figure VI-45 Relay Test Run No. 18

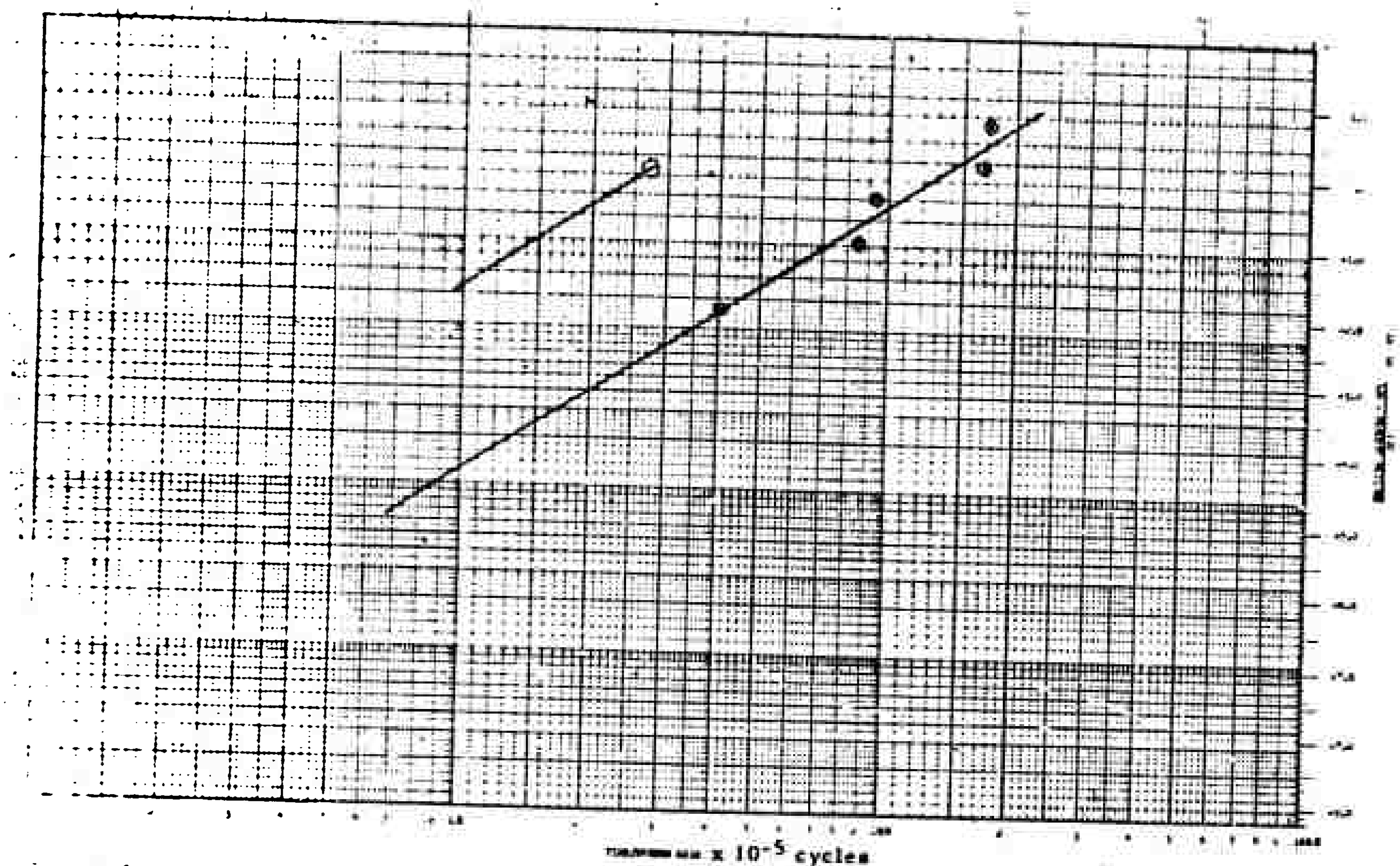

Contact Load - 3 amps, Temperature - 25°C, Actuation Speed - 30 cps, $\ln \alpha = -4.383$, $\alpha = 79.84$, $\beta = 1.70$

Figure VI-46 Relay Test Run No. 19

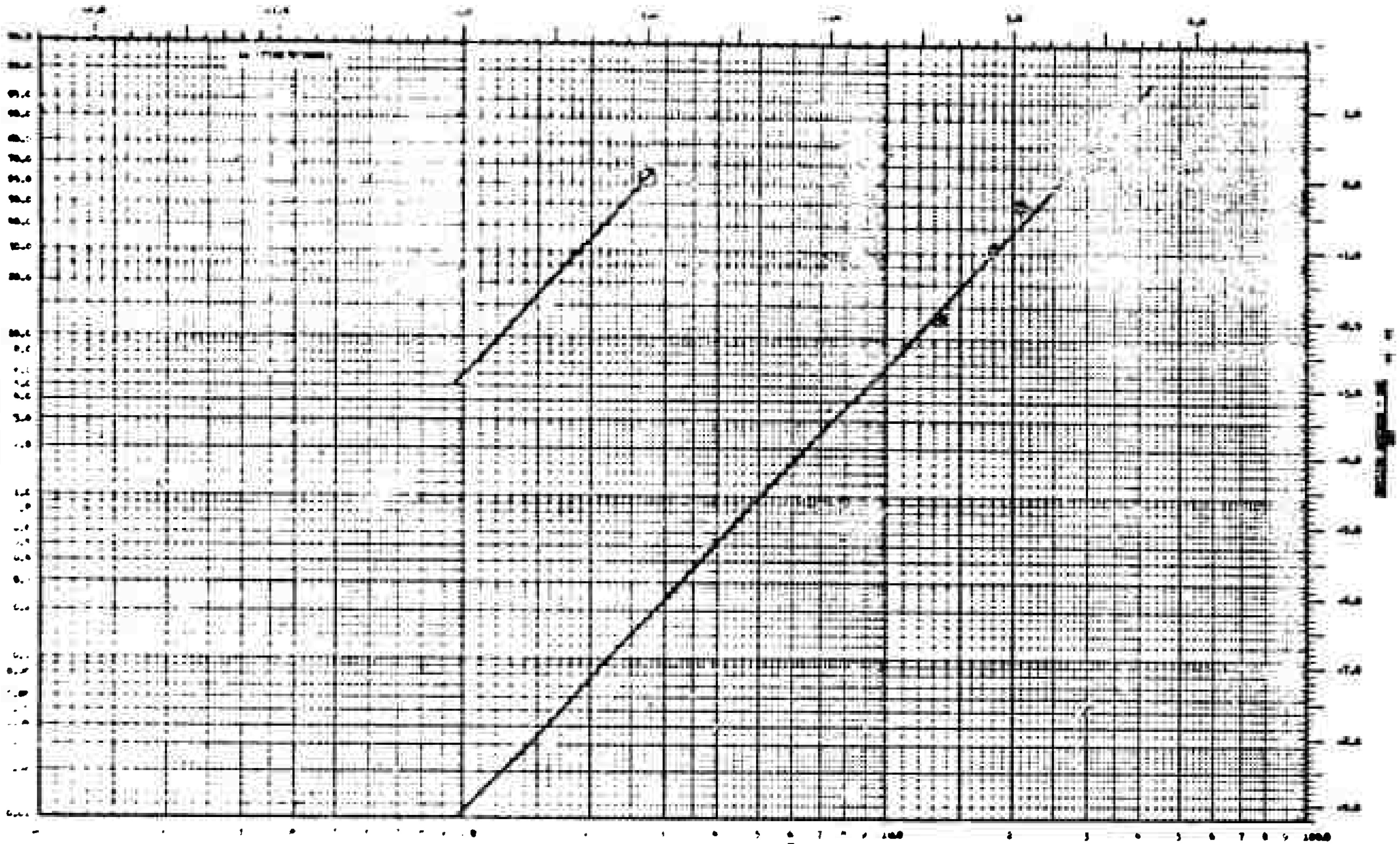

Contact Load - 3 amps, Temperature - 100°C, Actuation Rate - 30 cps, $\ln \alpha$ = -9.122, α = 8955.3, β = 2.80

Figure VI-47 Relay Test Run No. 20

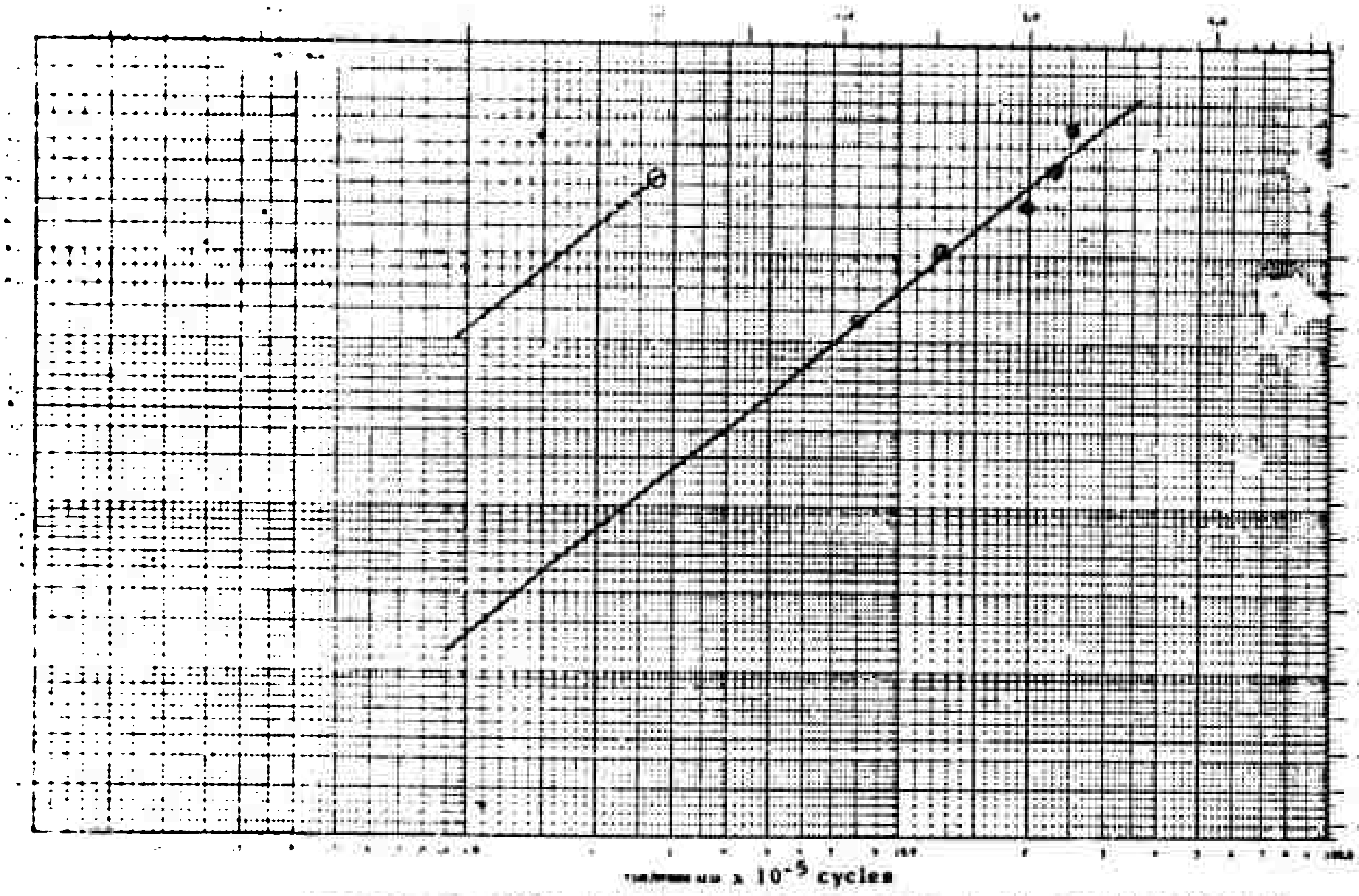

Contact Load - 3 amps, Temperature - 150°C, Actuation Rate - 30 cps, $\ln\alpha$ = -6.385, α = 601.85 β = 2.11

Figure VI-48 Relay Test Run No. 21

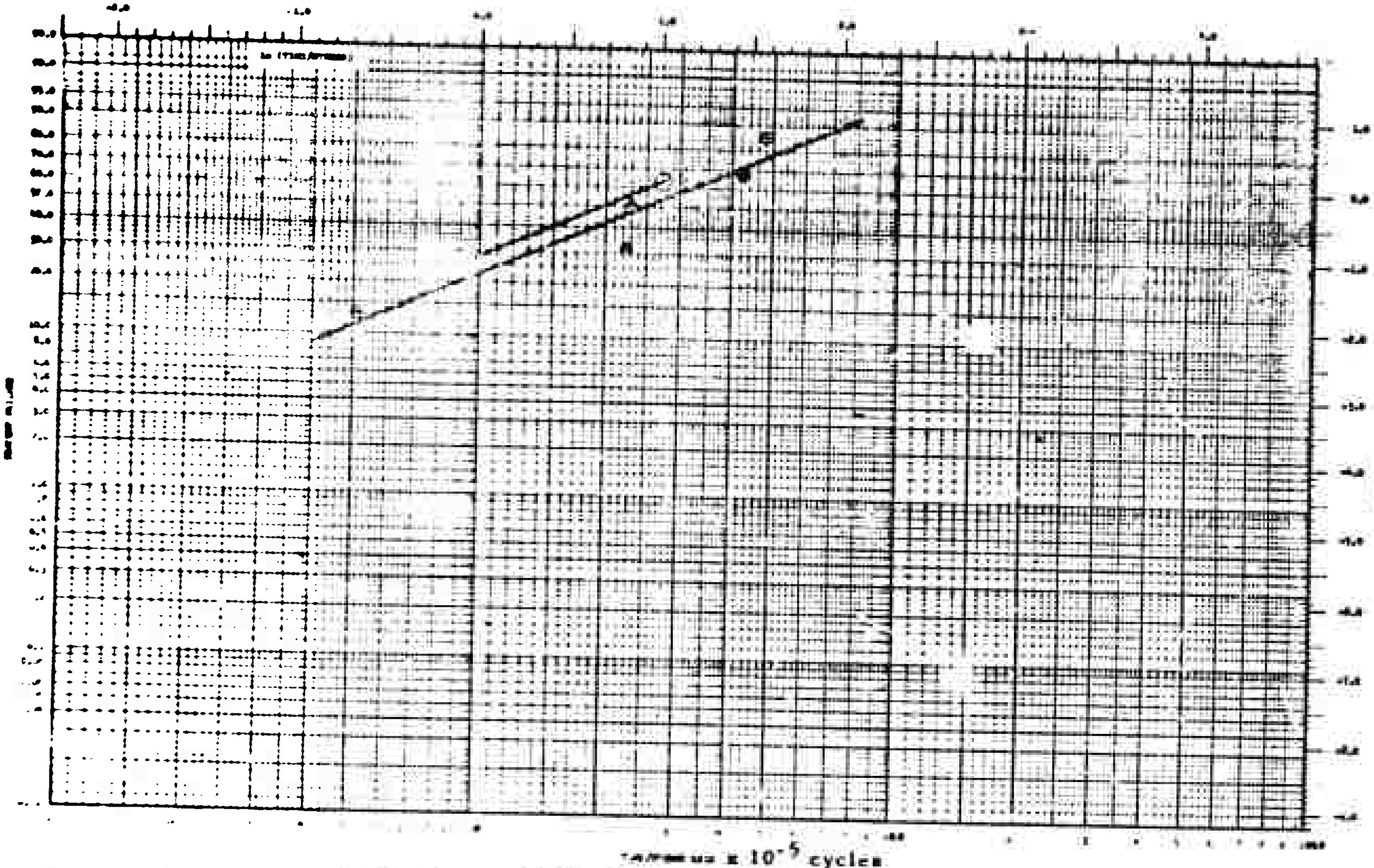

Contact Load - 6 amps, Temperature - 25°C, Actuation Rate - 30 cps, $\ln\alpha$ = -1.376, α = 3.97, β = 1.11

Figure VI-49 Relay Test Run No. 22

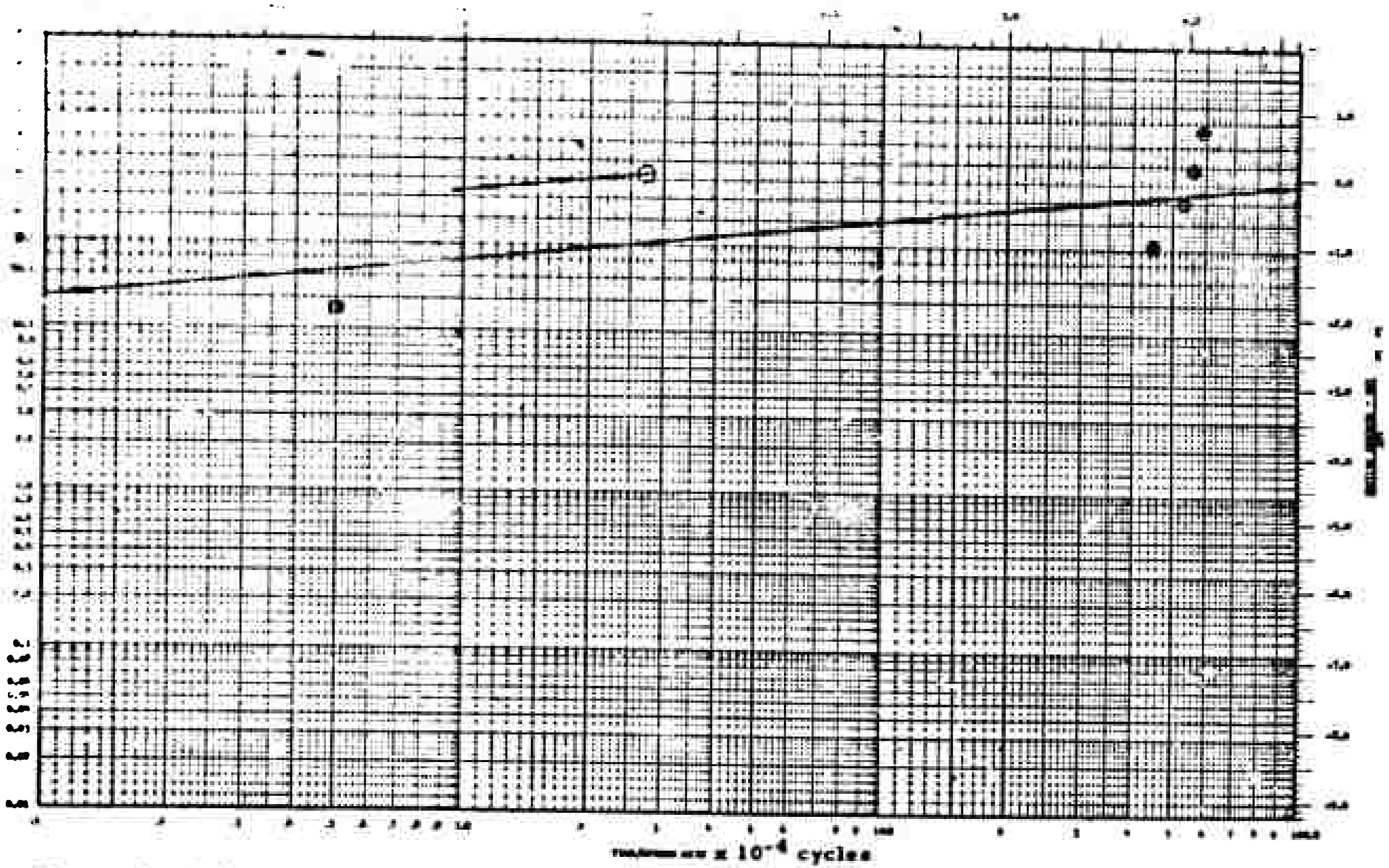

Contact Load - 6 amps, Temperature - 100°C, Actuation Rate - 30 cps, $\ln \alpha = -1.250$, $\alpha = 3.49$, $\beta = .25$

Figure VI-50 Relay Test Run No. 23

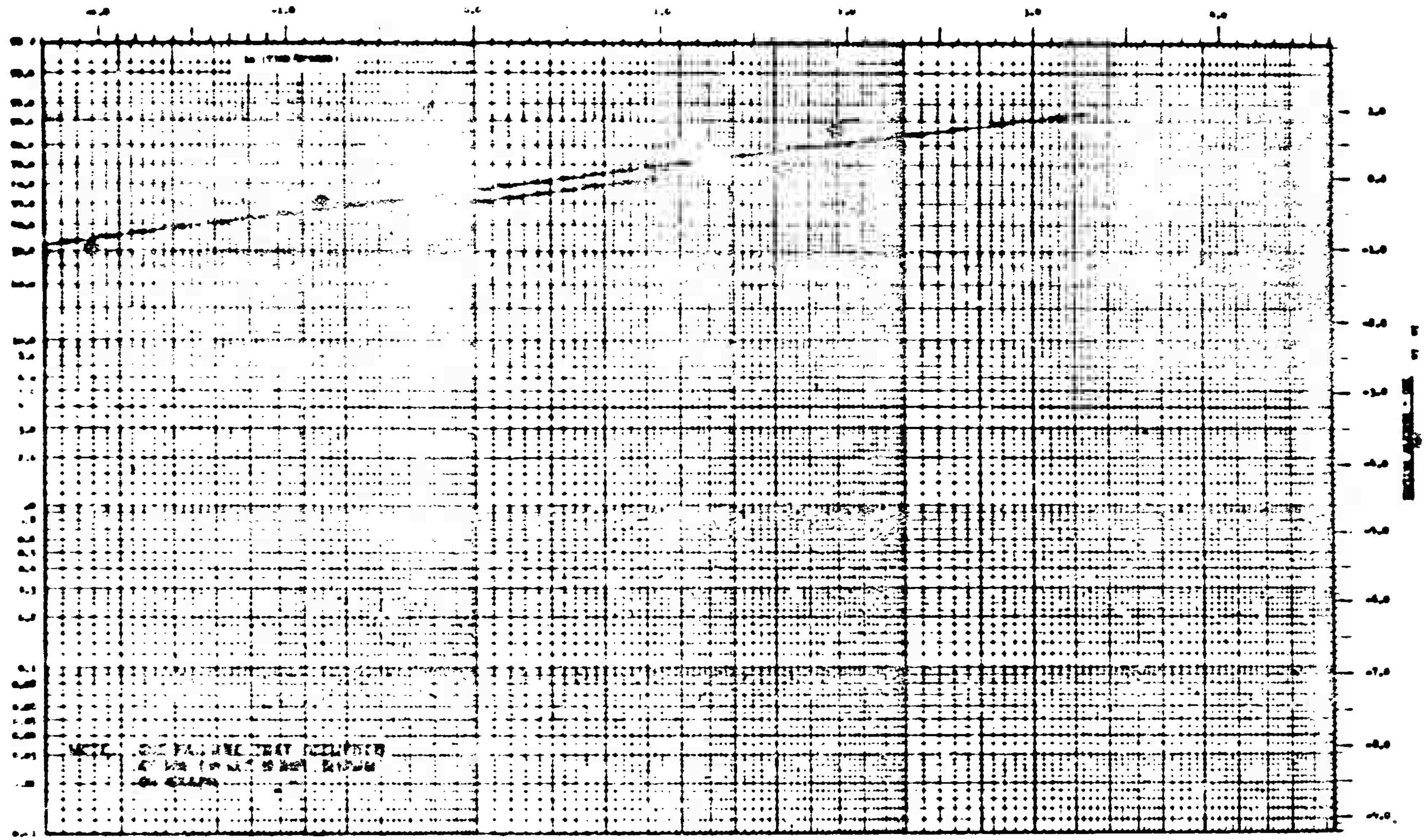

Contact Load - 6 amps, Temperature - 150°C, Actuation Rate - 30 cps, $\ln\alpha$ = -.181, α = 1.20, β = .34

Figure VI-51 Relay Test Run No. 24

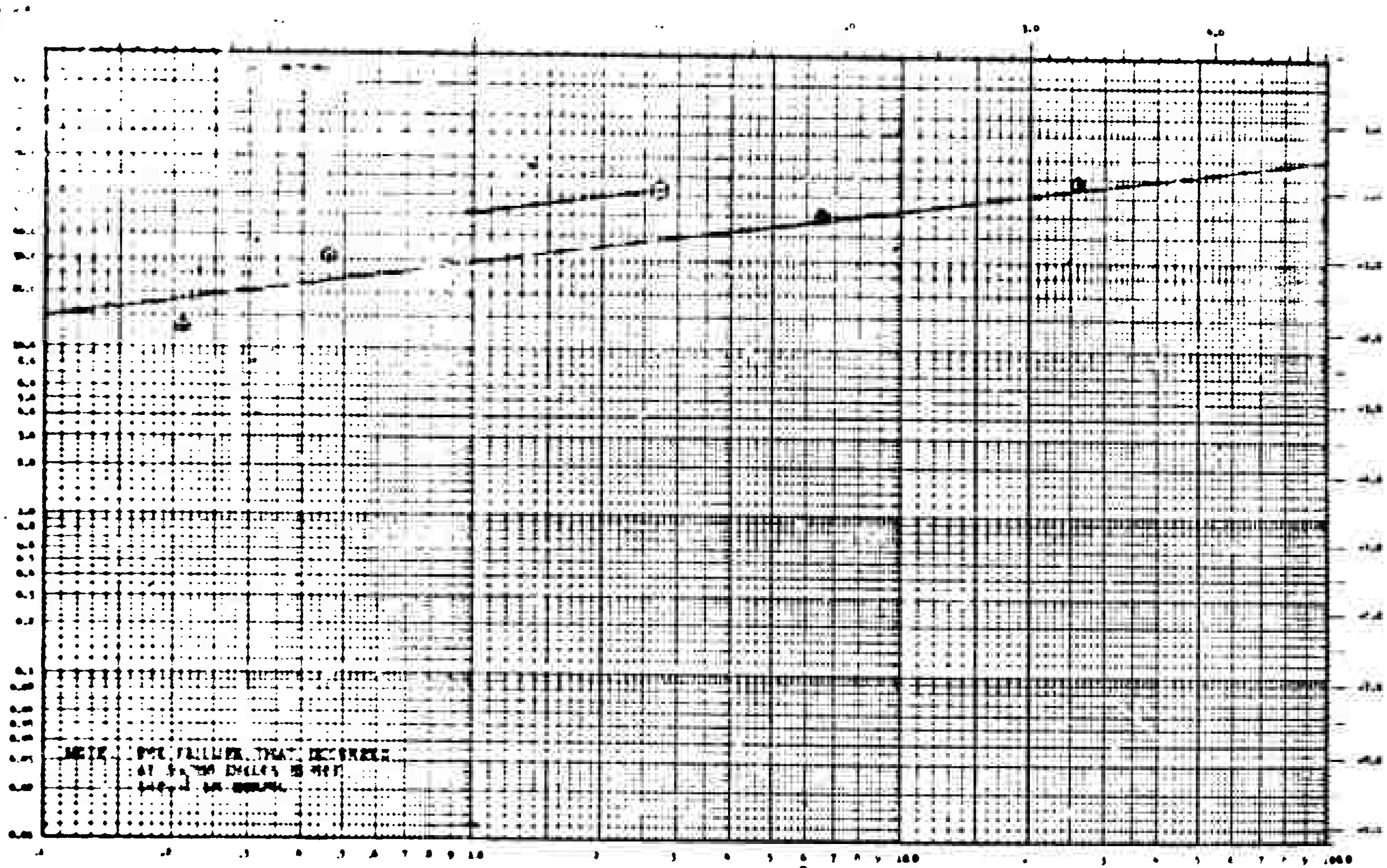

Contact Load - 8 amps, Te · perature - 25°C, Actuation Rate - 30 cps, $\ln \alpha = -1.061$, $\alpha = 2.89$, $\beta = .33$

Figure VI-52 Relay Test Run No. 25

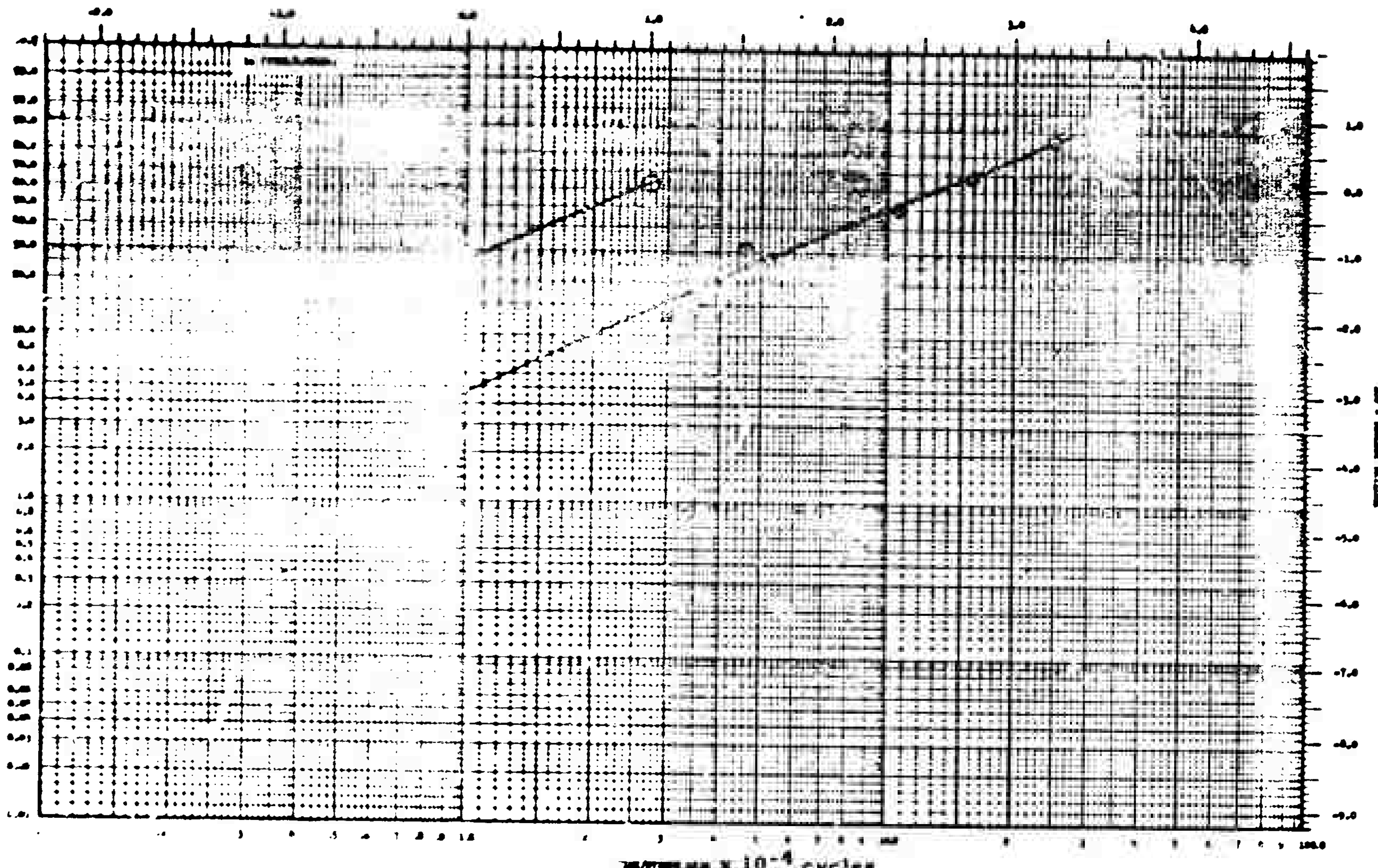

Contact Load - 8 amps. Temperature - 100°C, Actuation Rate - 30 cps, $\ell n\ \alpha = -3.060$, $\alpha = 21.33$, $\beta = 1.17$

Figure VI-53 Relay Test Run No. 26

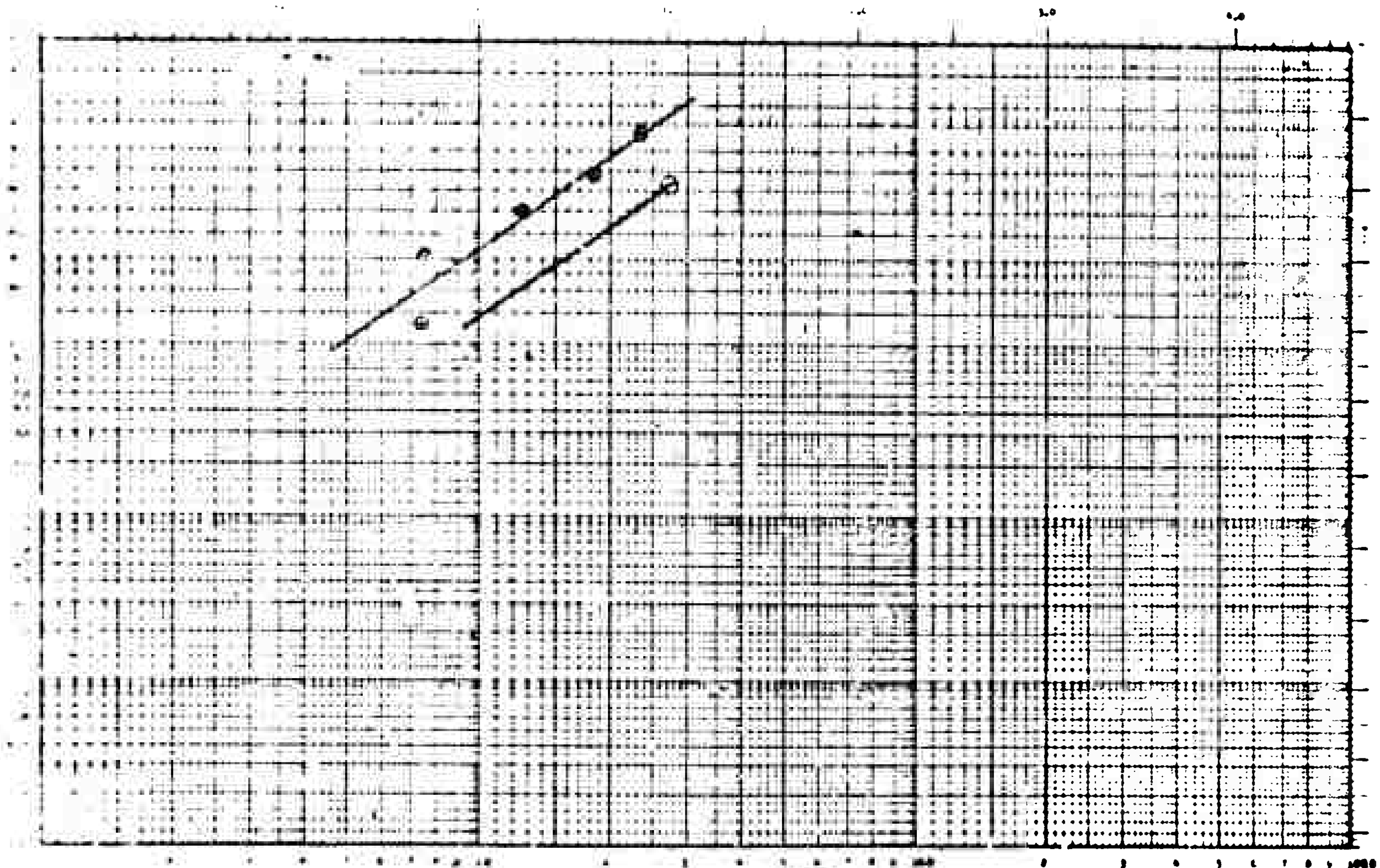

Contact Load - 8 amps, Temperature - 150°C, Actuation Rate - 30 cps, ln α = -.913, α = 2.48, β = 1.88

Figure VI-54 Relay Test Run No. 27

VI-[illegible] O-RINGS

The following charts (Figures VI-55 through VI-63) are Weibull plots of each of the 9 test runs on O-rings. Ten parts were tested at each set of combined stresses and the line of best fit was drawn through them using the method of least squares.

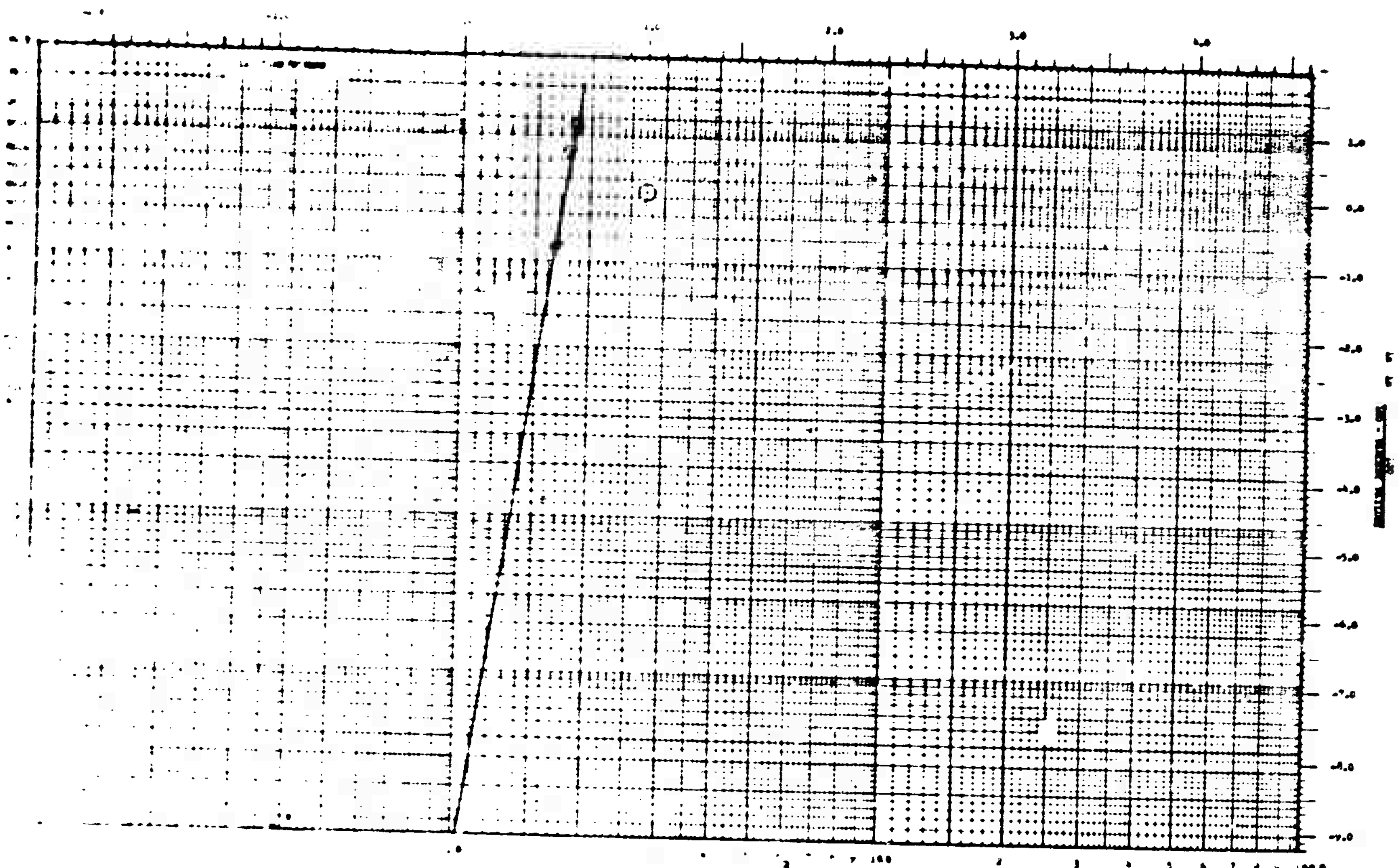

x 10^{-3} hours

Temperature - 200°F, Ultraviolet - none, $\ln \alpha$ = -9.906, α = 19.930, β = 17.75

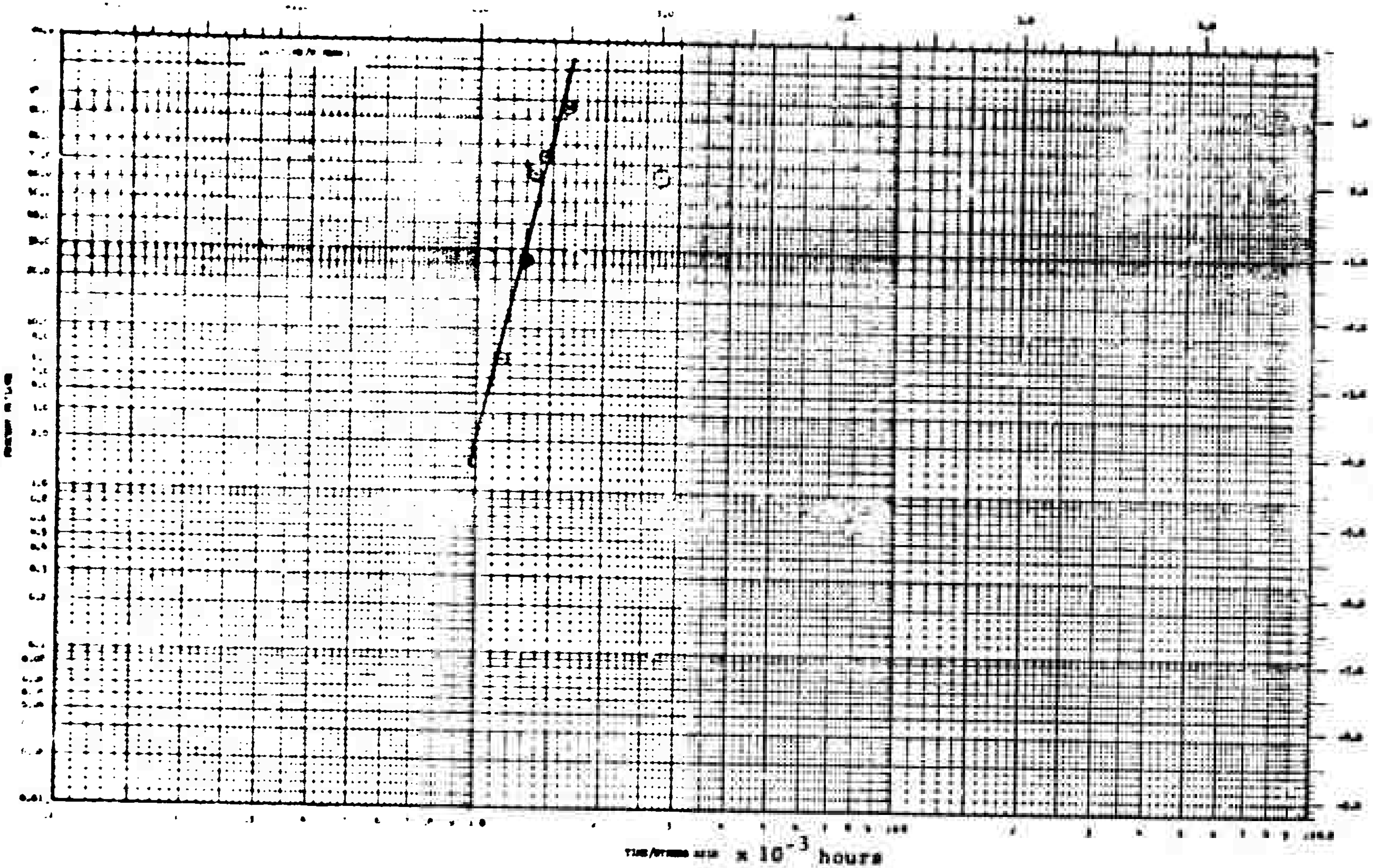

Temperature - 200°F, Ultraviolet - 0.1 watts/sq.ft., $\ln \alpha$ = -3.879, α = 48.424, β = 10.71

Figure VI-56 O-Ring Test No. 2

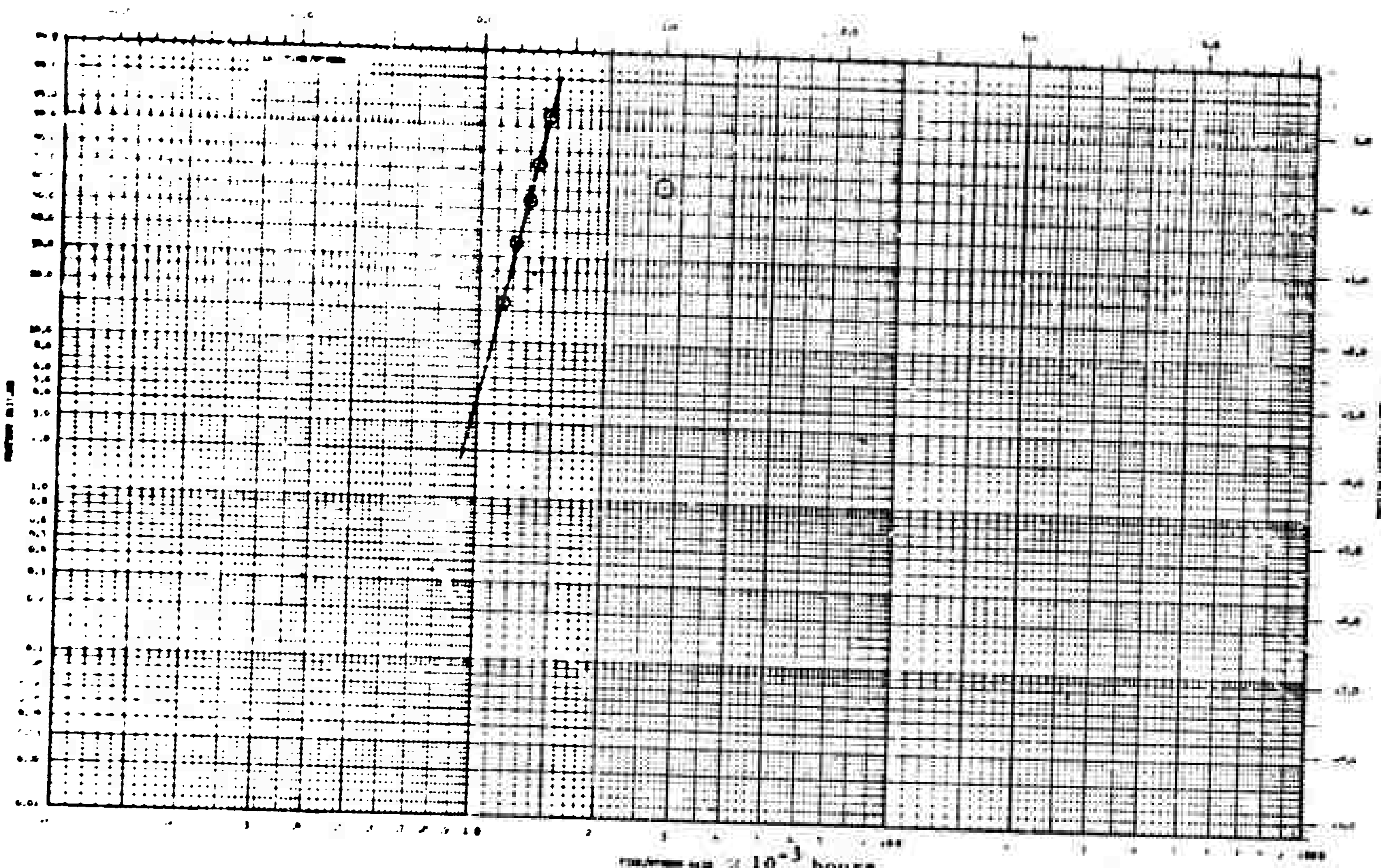

Temperature - 200°F, Ultraviolet - 0.2 watts/sq.ft., $\ell n \alpha = -3.115$, $\alpha = 22.646$, $\beta = 11.01$

Figure VI-57 O-Ring Test No. 3

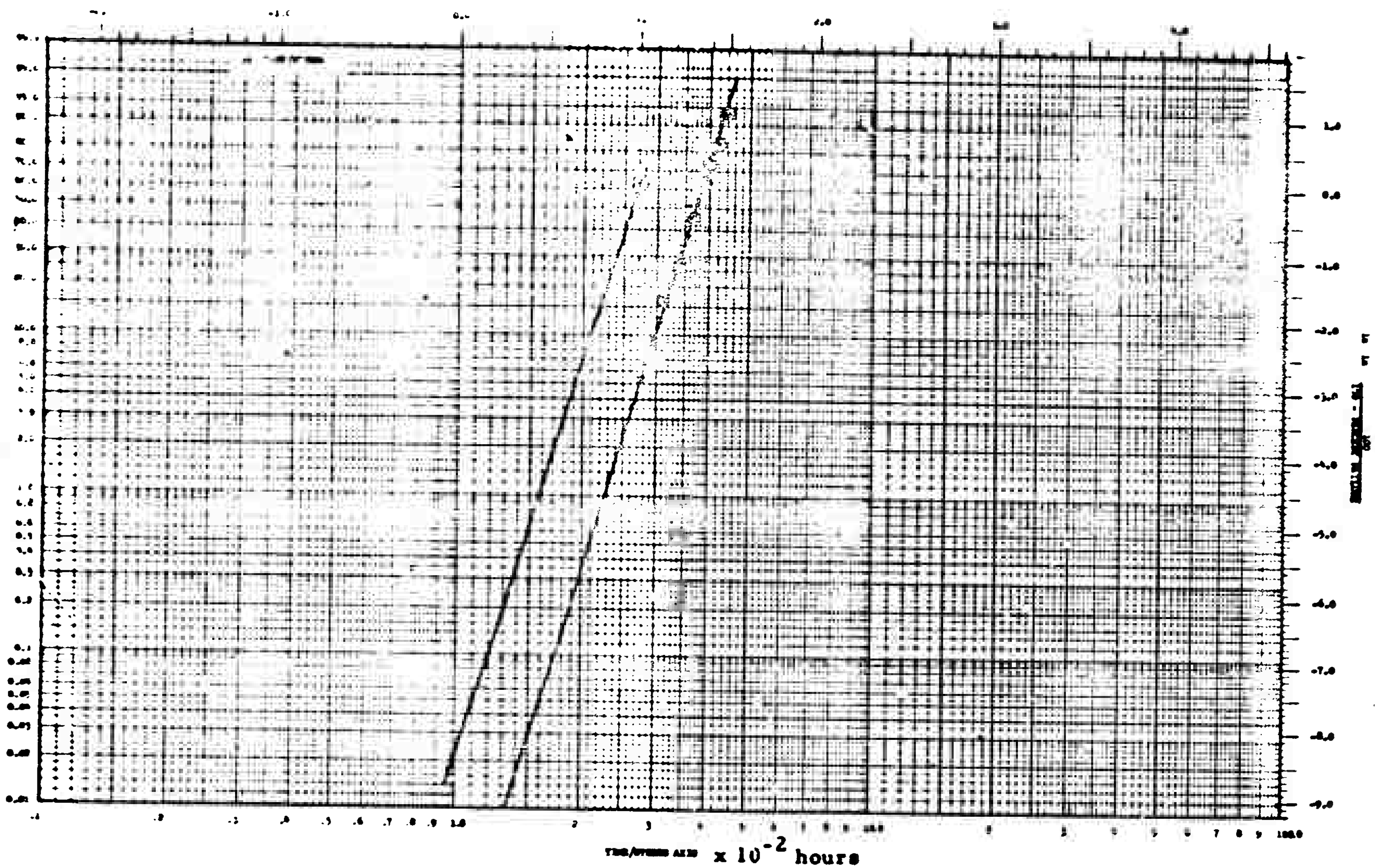

Temperature - 250°F, Ultraviolet - none, $\ln \alpha$ = -11.539, α = 102,740, β = 8.459

Figure VI-58 O-Ring Test No. 4

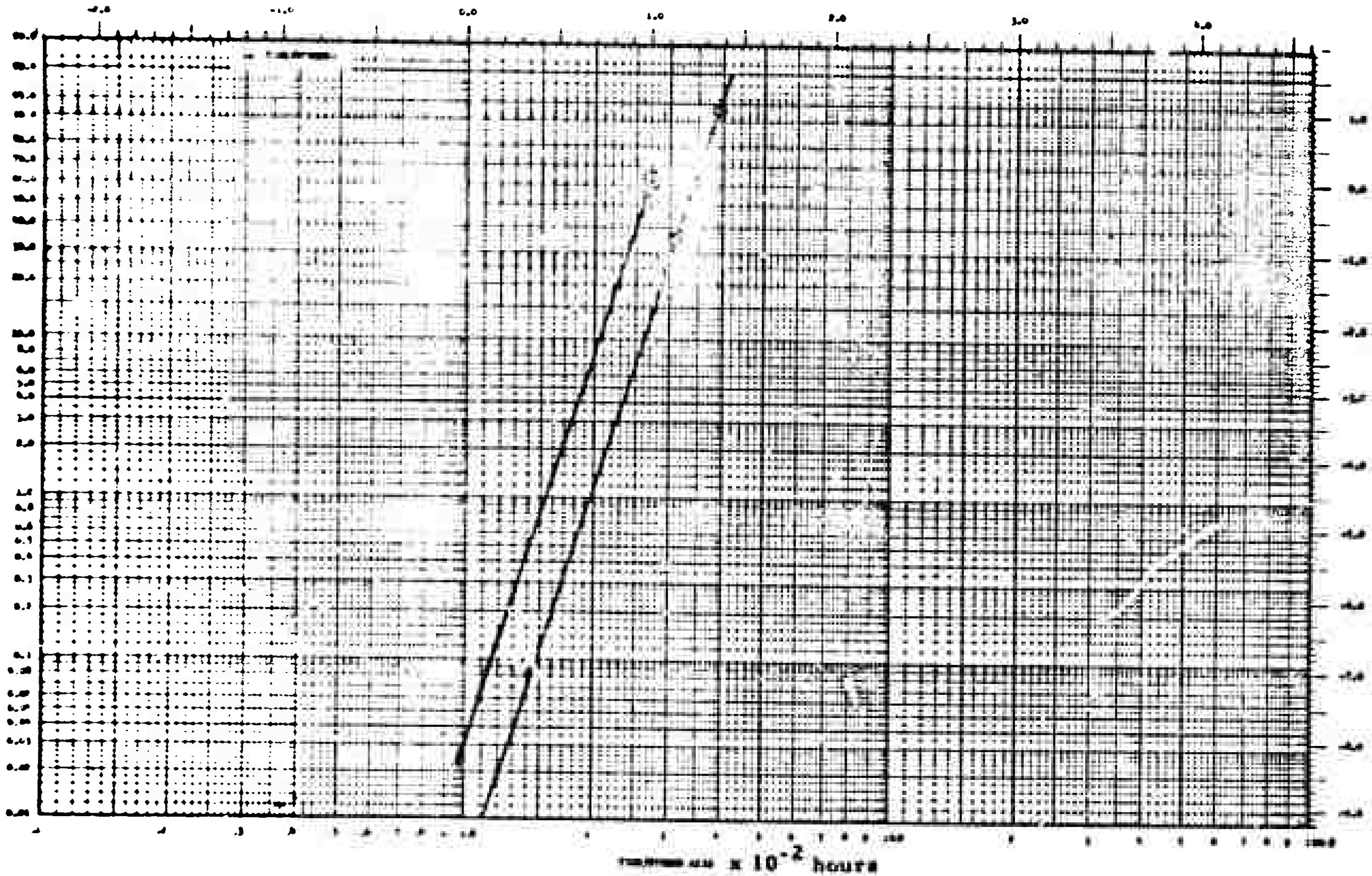

Temperature - 250°F, Ultraviolet - 0.1 watts/sq.ft., $\ln \alpha$ = -10.141, α = 25,330, β = 8.123

Figure VI-59 O-Ring Test No. 5

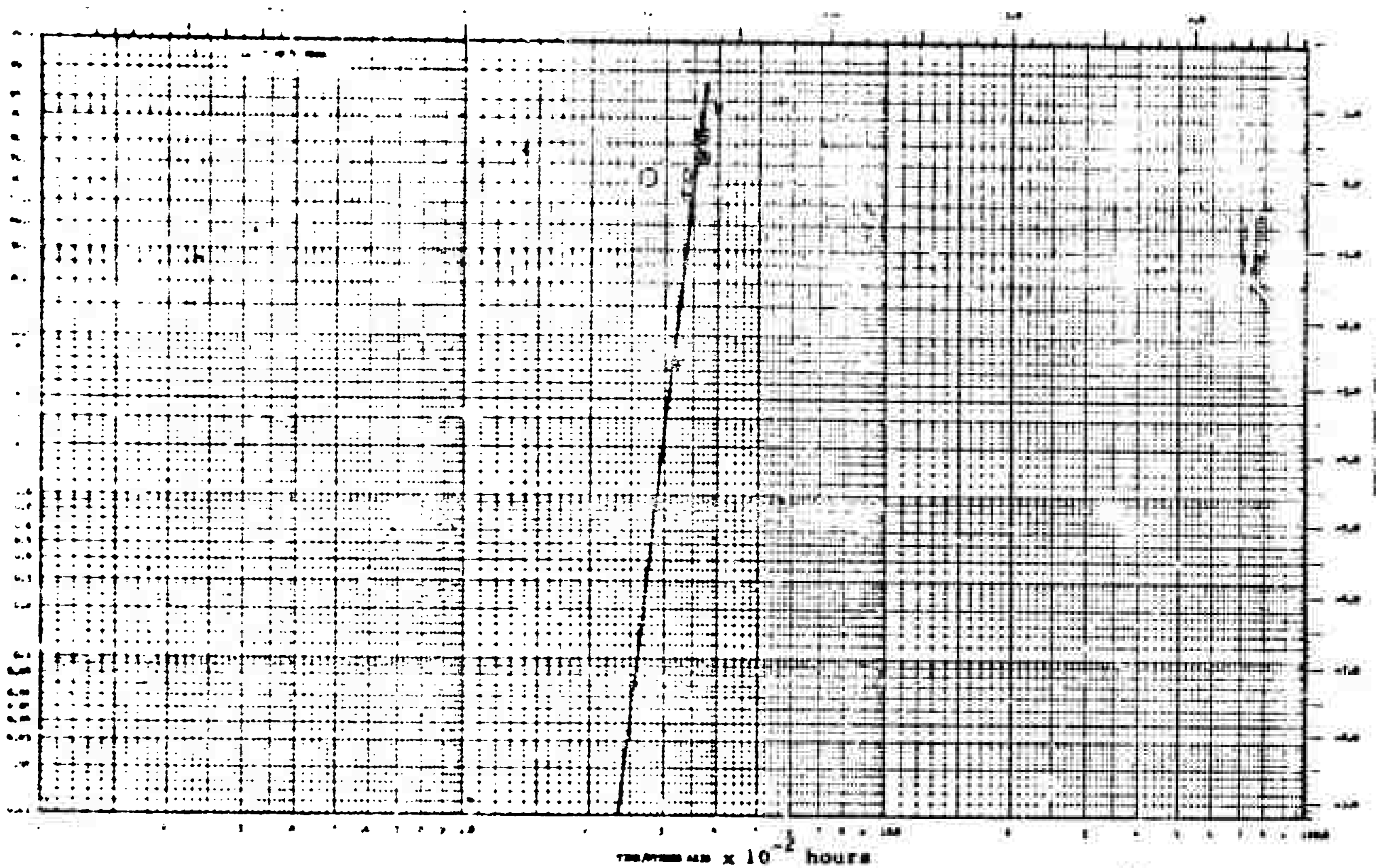

Temperature - 250°F, Ultraviolet - 0.2 watts/sq.ft., $\ln \alpha = -28.468$, $\alpha = 2.314 \times 10^{12}$, $\beta = 22.459$

Figure VI-50 O-Ring Test Run No. 6

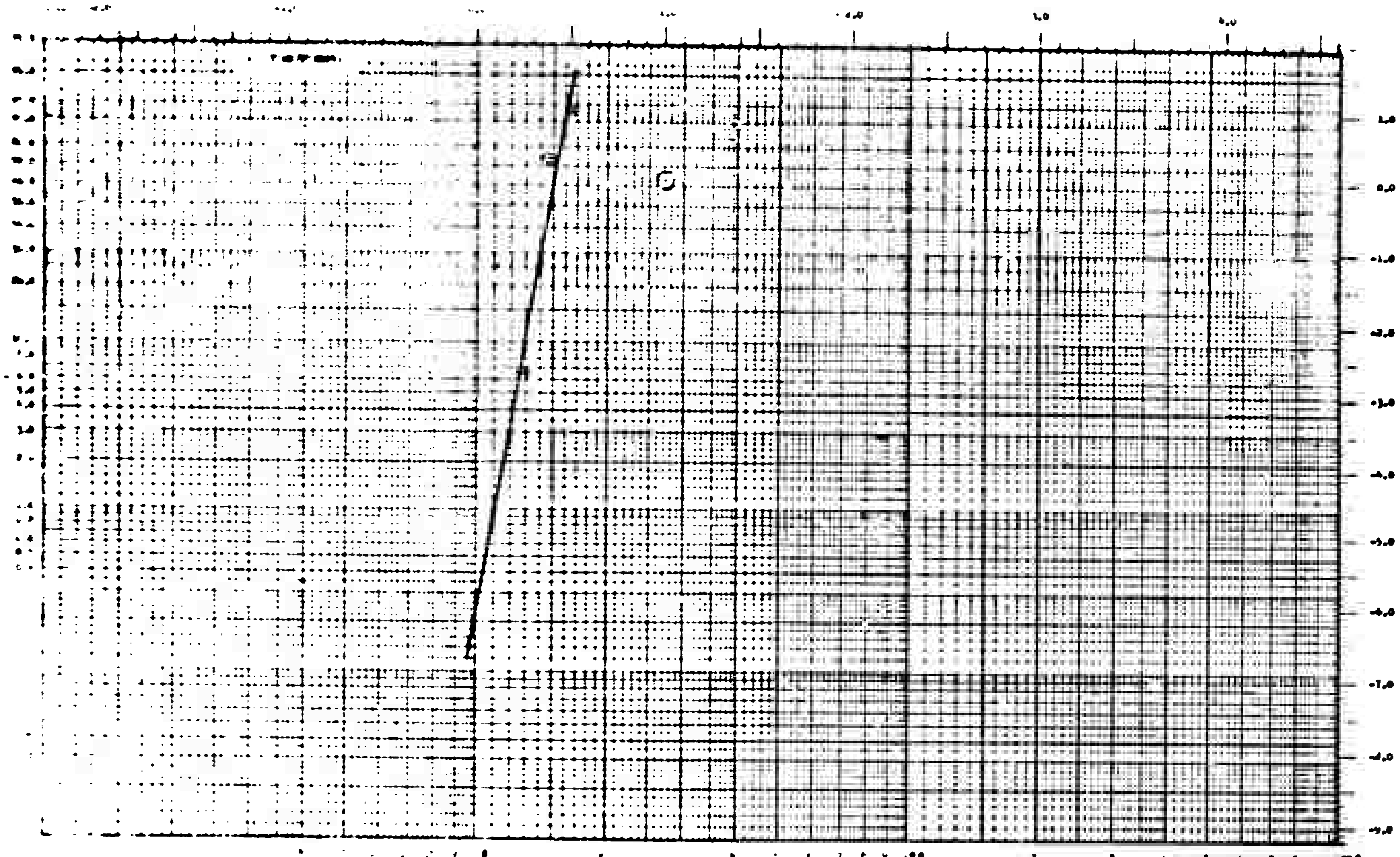

Temperature - 275°F, Ultraviolet - none, $\ln \alpha$ = -6.019, α = 403.43, β =14.68

Figure VI-61 O-Ring Test Run No. 7

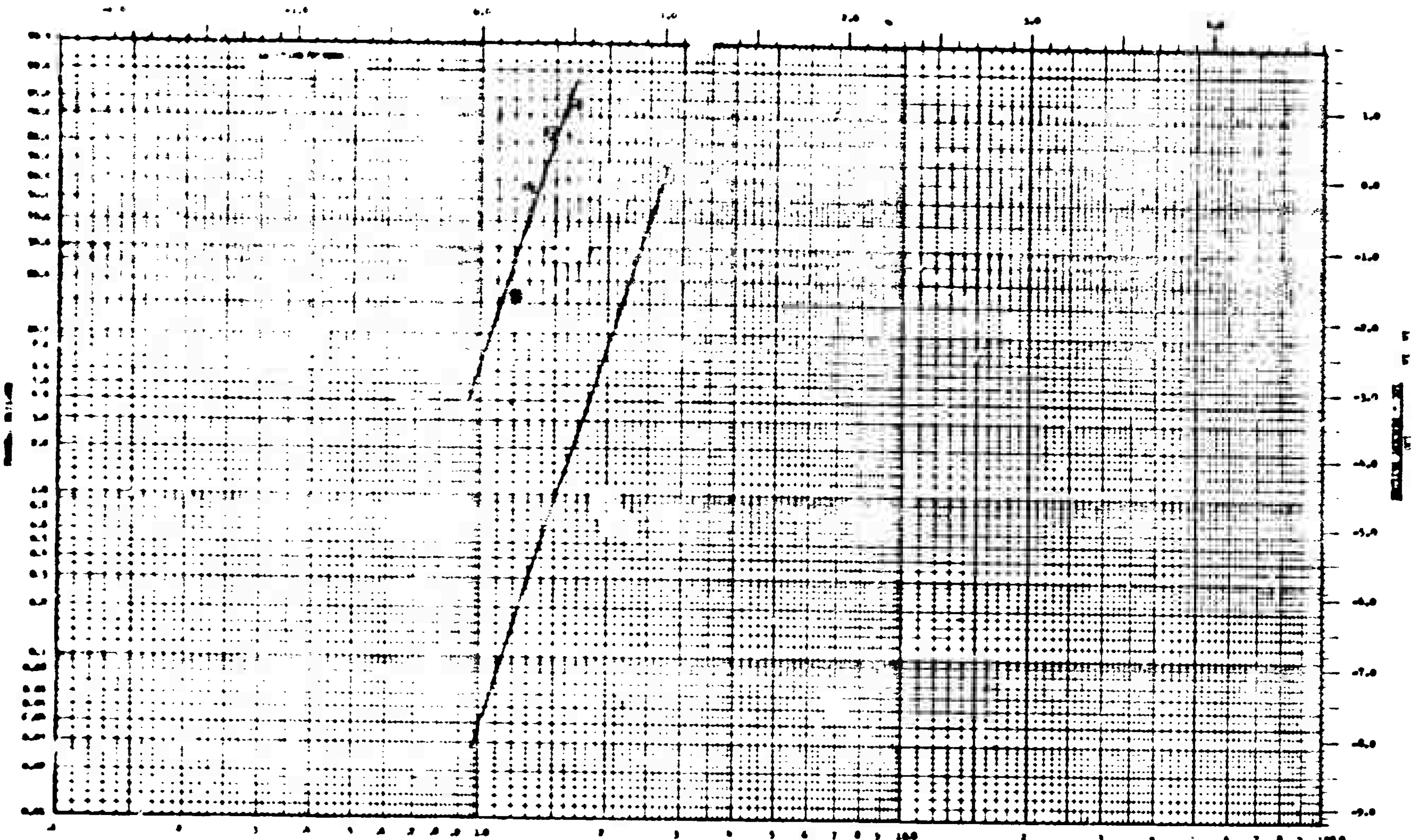

x 10^{-2} hours

Temperature - 275°F, Ultraviolet - 0.1 watts/sq.ft., $\ln \alpha = -2.735$, $\alpha = 15.487$, $\beta = 7.943$

Figure VI-62 O-Ring Test Run No. 8

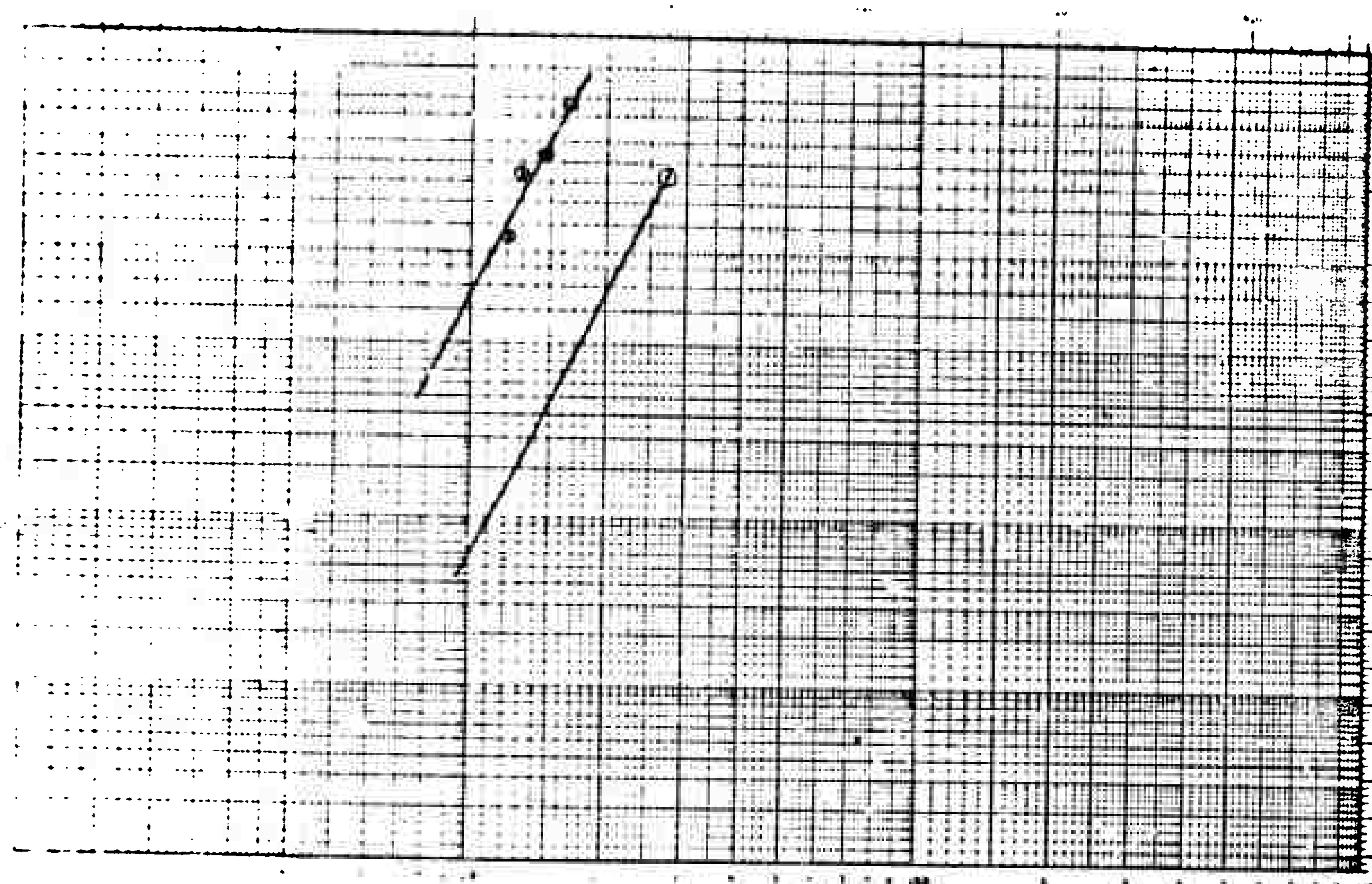

Temperature - 275°F, Ultraviolet - 0.2 watts/sq.ft., $\ln \alpha = -1.6$, $\alpha = 4.95$, $\beta = 5.166$

Figure VI-63 O-Ring Test Run No. 9

APPENDIX VII CONFIDENCE LIMITS FOR WEIBULL PARAMETERS

The use of a least squares straight line to estimate the parameters of the Weibull distribution yields confidence limits for α and β, the parameters of the Weibull:

$$\ln \ln \left[\frac{1}{1-F(x)}\right] = \log\left(\frac{1}{\alpha}\right) + \beta \log x$$

the slope of the straight line, say, b is then equal to β and the intercept of the straight line say a is such that

$$a = \log\left(\frac{1}{\alpha}\right) = -\log \alpha$$

so that

$$e^{-a} = \alpha$$

By the usual techniques in setting confidence limits for the true values of the slope and intercept, confidence limits for β are obtained directly by using b, the std error of estimate, σ_y, and the t distribution. Confidence limits for α are obtained by using a, the std error of estimate, the t distribution and the relation:

$\alpha_{.025} = e^{-a_{.975}}$ and decoding the upper and lower limits.

eg (test run #6 switches)

$$a_{.975} = a + t_{.025} \frac{S_{xy}}{\sqrt{10}}$$

$$= -.285$$

$$a_{.025} = a - t_{.025} \frac{S_{xy}}{\sqrt{10}}$$

$$= -1.011$$

hence

$$\alpha_{.025} = e^{-(-.285)} = 1.336$$

$$\alpha_{.975} = e^{-(-1.011)} = 2.746$$

but these confidence limits are for α based on the random variable $\left(\frac{\text{actual life}}{10^5}\right)$ thus for actual data

$$\alpha_{.025} = 1.336 \times (10^5)^{1.33} = 5.970 \times 10^6$$

$$\alpha_{.975} = 2.746 \times (10^5)^{1.33} = 1.226 \times 10^7$$

$$\beta_{.975} = b + t_{.025} \frac{S_{xy}}{\sigma_y \sqrt{n}} \; .$$

$$= 1.33 + .325$$

$$= 1.655$$

$$\beta_{.025} = 1.33 - .325$$

$$= 1.005$$

APPENDIX VIII MATHEMATICAL MODELS

VIII-1 The derivation of the model 1 proposed in section 4.3 is given below.

The instructions on how to return to normal conditions, given some future test at similar accelerated conditions as in this report is now obtainable for model 1. Based on the assumptions clearly:

$$\beta_A = \beta_N$$

so that (A-1)

$$\beta_N^* = \beta_A^*$$

and since from (6)

$$\alpha_A = c^{\beta_N} \alpha_N = c^{\beta_A} \alpha_N$$

$$\longrightarrow \alpha_N = \frac{\alpha_A}{c^{\beta_A}}$$

$$\longrightarrow \tilde{\alpha}_N^* = \frac{\tilde{\alpha}_A^*}{c^{\hat{\beta}_A^*}} \qquad \text{(A-2)}$$

where

$$c = \left(\frac{\alpha_A}{\alpha_N}\right)^{1/\beta_N} = \left(\frac{\alpha_A}{\alpha_N}\right)^{1/\beta_A}$$

and c is estimated from this report by

$$\tilde{c} = \left(\frac{\hat{\alpha}_A}{\hat{\alpha}_N}\right)^{1/\hat{\beta}} \qquad \text{(A-3)}$$

where $\hat{\beta}$ is an estimate of β based on a combination of $\tilde{\beta}_A$ and $\tilde{\beta}_N$.

VIII-2 The derivation of the algorithm for model 2 is as follows (see Section 4.4)

Since

$$\beta_N = d\beta_A$$

then

$$\hat{\beta}_N = \hat{d}\hat{\beta}_A$$

and hence

$$\hat{\beta}^*_N = \hat{d}\hat{\beta}^*_A \qquad \text{(A-4)}$$

Since

$$\alpha_N = \frac{\alpha_A}{c^{\beta_N/d}}$$

then

$$\hat{\alpha}_N = \frac{\hat{\alpha}_A}{\tilde{c}^{\tilde{\beta}_N/\tilde{d}}}$$

and hence

$$\tilde{\alpha}^*_N = \frac{\hat{\alpha}^*_A}{\tilde{c}^{\tilde{\beta}_N/\tilde{d}}} \qquad \text{(A-5)}$$

VIII-3 The derivation of the algorithm of model 3 of section 4.5 is given below. As in that section it is assumed that the physical law is such that: g(x) is always the same, i.e., $g(x) = g^*(x)$ where g(x) is the TFC for this report and $g^*(x)$ is the TFC for a future accelerated test. Then:

$$g(x) = \left(\frac{\alpha_A}{\alpha_N}\right)^{1/\beta_A} x^{\beta_N/\beta_A} = \left(\frac{\alpha^*_A}{\alpha^*_N}\right)^{1/\beta^*_A} x^{\beta^*_N/\beta^*_A} = g^*(x) \qquad \text{(A-6)}$$

$$\Rightarrow \frac{1}{\beta_A}\log\left(\frac{\alpha_A}{\alpha_N}\right) + \frac{\beta_N}{\beta_A}\log x = \frac{1}{\beta^*_A}\log\left(\frac{\alpha^*_A}{\alpha^*_N}\right) + \frac{\beta^*_N}{\beta^*_A}\log x$$

this is a straight line in log x hence if equality is to hold for all x (more than x is all that is needed) it must be that:

$$\frac{1}{\beta_A} \log\left(\frac{\alpha_A}{\alpha_N}\right) = \frac{1}{\beta^*_A} \log\left(\frac{\alpha^*_A}{\alpha^*_N}\right)$$

and

$$\frac{\beta_N}{\beta_A} = \frac{\beta^*_N}{\beta^*_A}$$

so that

$$\beta_N = \beta^*_A \frac{\beta_N}{\beta_A} \qquad \text{(A-7)}$$

and hence

$$\tilde{\beta}^*_N = \tilde{\beta}^*_A \frac{\tilde{\beta}_N}{\tilde{\beta}_A} \qquad \text{(A-8)}$$

Inspecting equation (A-4) of section VIII-2 and noting that from (13) of 4.2

$$\tilde{d} = \frac{\tilde{\beta}_N}{\tilde{\beta}_A},$$

it can be seen the algorithm for $\tilde{\beta}^*_N$ is the same as the model of section 4.2. Similarly (A-6) implies

$$\left(\frac{\alpha_A}{\alpha_N}\right)^{1/\beta_A} = \left(\frac{\alpha^*_A}{\alpha^*_N}\right)^{1/\beta^*_A}$$

$$\alpha^*_N = \frac{\alpha^*_A}{\left(\frac{\alpha_A}{\alpha_N}\right)^{\beta^*_A/\beta_A}} \qquad \text{(A-9)}$$

and hence

$$\alpha_N^* = \frac{\alpha_A^*}{\left(\frac{\alpha_A}{\alpha_N}\right)^{\beta_A^*/\beta_A}} = \frac{\alpha_A^*}{\left(\frac{\alpha_A}{\alpha_N}\right)^{\beta_N^*/\beta_N}} \qquad \text{(A-10)}$$

and from section 4.2 (A-5, 13, 14)

$$\alpha_N^* = \frac{\alpha_A^*}{c^{\beta_N^*/d}} = \frac{\alpha_A^*}{\left(\frac{\alpha_A}{\alpha_N}\right)^{\beta_N^*/\beta_N}} \qquad \text{(A-11)}$$

which is the same as (A-10).

VIII-4 The proof that the TFH (defined in 4.6) and the TFC (defined in 4.5) are never identically equal is given below.

If

$$f(x) = \left(\frac{\alpha_A\beta_N}{\alpha_N\beta_A}\right)^{1/\beta_A - 1} x^{\frac{\beta_N-1}{\beta_A-1}} = \left(\frac{\alpha_A}{\alpha_N}\right)^{1/\beta_A} x^{\beta_N/\beta_A} = g(x) \qquad \text{(A-12)}$$

then it must be that

$$\frac{1}{\beta_A - 1}\log\left(\frac{\alpha_A\beta_N}{\alpha_N\beta_A}\right) + \left(\frac{\beta_N-1}{\beta_A-1}\right)\log x = \frac{1}{\beta_A}\log\left(\frac{\alpha_A}{\beta_A}\right) + \frac{\beta_N}{\beta_A}\log x \qquad \text{(A-13)}$$

these are straight lines in log x and if equal for more than one x their slopes and intercepts must be identical, hence

$$\frac{\beta_N}{\beta_A} = \frac{\beta_N - 1}{\beta_A - 1} \qquad \beta_A \neq 1 \qquad \text{(A-14)}$$

$$\Rightarrow \beta_N = \beta_A$$

From (A-14) and (A-13) then the intercepts must satisfy

$$\frac{1}{\beta_A - 1} \log\left(\frac{\alpha_A}{\alpha_N}\right) = \frac{1}{\beta_A} \log\left(\frac{\alpha_A}{\alpha_N}\right) \qquad \text{(A-15)}$$

$$\Rightarrow \frac{1}{\beta_A - 1} = \frac{1}{\beta_A}$$

$$\Rightarrow \beta_A - 1 = \beta_A \quad \underline{\text{provided } \alpha_A \neq \alpha_N} \qquad \text{(A-16)}$$

and this equation has no solution in the field of real numbers. If $\alpha_A = \alpha_N$ and $\beta_A = \beta_N$ (a trivial situation) then $j(x) = g(x)$ for all x.

As an example in the exponential case ($\beta_A = \beta_N = 1$)

$$g(x) = \frac{\alpha_A}{\alpha_N} x \qquad \text{(A-17)}$$

and there is no $j(x)$ such that (A-17) is satisfied, i.e., no composition function exists. However there exists a function $j^1(t)$ such that

$$h_N(x) = j^1(x)\, h_A(x) \qquad \text{(A-18)}$$

since

$$h_N(x) = \frac{1}{\alpha_N} \text{ and } h_A(x) = \frac{1}{\alpha_A}$$

(A-18) implies that

$$\frac{1}{\alpha_N} = j^1(x) \frac{1}{\alpha_A}$$

$$j^1(x) = \frac{\alpha_A}{\alpha_N} \qquad \text{(A-19)}$$

It will be noted that $g(x) = j^1(x)$ when and only when $x = 1$.

The derivative of the algorithm of model 4 of section 4.6 based on constant TFH is given below.

$$j(x) = \left(\frac{\alpha_A \beta_N}{\alpha_N \beta_A}\right)^{1/\beta_A - 1} x^{\frac{\beta_N - 1}{\beta_A - 1}} = \left(\frac{\alpha_A^* \beta_N^*}{\alpha_N^* \beta_A^*}\right)^{1/\beta_A^* - 1} x^{\frac{\beta_N^* - 1}{\beta_A^* - 1}} = j^*(x) \qquad \text{(A-20)}$$

$$\Rightarrow \frac{\beta_N - 1}{\beta_A - 1} = \frac{\beta_N^* - 1}{\beta_A^* - 1}$$

$$\Rightarrow \beta_N^* = \frac{\beta_N - 1}{\beta_A - 1} (\beta_A^* - 1) + 1 \qquad \text{(A-21)}$$

and also that

$$\alpha_N^* = \frac{\dfrac{\alpha_A^* \beta_N}{\beta_A^*}}{\left(\dfrac{\alpha_A \beta_N}{\alpha_N \beta_A}\right)^{\beta_A^* - 1/\beta_A - 1}} \qquad \text{(A-22)}$$

hence

$$\tilde{\beta}_N^* = \frac{\tilde{\beta}_N - 1}{\tilde{\beta}_A - 1} (\tilde{\beta}_A^* - 1) + 1 \qquad \text{(A-23)}$$

and

$$\tilde{\alpha}_N^* = \frac{\dfrac{\tilde{\alpha}_A^* \tilde{\beta}_N^*}{\tilde{\beta}_A^*}}{\left(\dfrac{\alpha_A \tilde{\beta}_N}{\tilde{\alpha}_N \tilde{\beta}_A}\right)^{\tilde{\beta}_A^* - 1/\tilde{\beta}_A - 1}} \qquad \text{(A-24)}$$

where β_N^* in (A-24) is found from (A-23). It should be remembered that α_A, β_A, α_N, β_N are given in this report, so that when α_A^* and β_A^* are obtained α_N^* and β_N^* are estimable.

VIII-5 The derivative of the algorithm of model 5 of section 4.7 (CRH) is as follows.

$$K(x) = \frac{h_N(x)}{h_A(x)}$$

$$K^*(x) = \frac{h_N^*(x)}{h_A^*(x)}$$

Now

$$K(x) = \frac{\dfrac{\beta_N\, x^{\beta_N - 1}}{\alpha_N}}{\dfrac{\beta_A\, x^{\beta_A - 1}}{\alpha_A}} \text{ and } K^* = \frac{\dfrac{\beta_N^*\, x^{\beta_N^* - 1}}{\alpha_N^*}}{\dfrac{\beta_A^*\, x^{\beta_A^* - 1}}{\alpha_A^*}}$$

$$K(x) = \frac{\alpha_A \beta_N}{\alpha_N \beta_A}\, x^{\beta_N - \beta_A} \text{ and } K^*(x) = \frac{\alpha_A^* \beta_N^*}{\alpha_N^* \beta_A^*}\, x^{\beta_N^* - \beta_A^*} \qquad \text{(A-25)}$$

and (19) in Section 4.7 requires that

$$\frac{\alpha_A \beta_N}{\alpha_N \beta_A}\, x^{\beta_N - \beta_A} = \frac{\alpha_A^* \beta_N^*}{\alpha_N^* \beta_A^*}\, x^{\beta_N^* - \beta_A^*} \qquad \text{(A-26)}$$

which means

$$\log\left(\frac{\alpha_A \beta_N}{\alpha_N \beta_A}\right) + (\beta_N - \beta_A)\log x = \log\left(\frac{\alpha_A^* \beta_N^*}{\alpha_N^* \beta_A^*}\right) + (\beta_N^* - \beta_A^*)\log x$$

hence

$$\beta_N - \beta_A = \beta_N^* - \beta_A^*$$

$$\beta_N^* = \beta_A^* + (\beta_N - \beta_A) \qquad \text{(A-27)}$$

and

$$\frac{\alpha_A \beta_N}{\alpha_N \beta_A} = \frac{\alpha_A^* \beta_N^*}{\alpha_N^* \beta_A^*}$$

$$\alpha_N^* = \left(\frac{\alpha_N \beta_A}{\alpha_A \beta_N}\right) \frac{\alpha_A^* \beta_N^*}{\beta_A^*} \tag{A-28}$$

and hence the algorithms for estimating α_N^* and β_N^* are

$$\tilde{\beta}_N^* = \tilde{\beta}_A^* + (\tilde{\beta}_N - \tilde{\beta}_A) \tag{A-29}$$

$$\tilde{\alpha}_N^* = \left(\frac{\tilde{\alpha}_N \tilde{\beta}_A}{\tilde{\alpha}_A \tilde{\beta}_N}\right) \frac{\tilde{\alpha}_A^* \tilde{\beta}_N^*}{\tilde{\beta}_A^*} \tag{A-30}$$

where $\tilde{\beta}_N^*$ in (A-30) is obtained from (A-29) and $\tilde{\alpha}_A$, $\tilde{\beta}_A$, $\tilde{\alpha}_N$, $\tilde{\beta}_N$ are given this report.

VIII-6 As previously indicated the validation of the mathematical model is a task for future investigation. However in order to show how to use the algorithms associated with the various models the following examples are given for switches. The $\tilde{\alpha}_A^*$ and $\tilde{\beta}_A^*$ were assumed for sake of illustration and nothing more. They are not actual results of an accelerated test.

Suppose that in a future accelerated test:

$\tilde{\alpha}_A^* = 1,000,000$

$\tilde{\beta}_A^* = 3.06$

From this report it was learned that:

Normal conditions (test run 1) $\tilde{\alpha}_N = 53,848 \times 10^{17}$

$\tilde{\beta}_N = 4.07$

Accelerated Conditions (test run 14) $\tilde{\alpha}_A = 2,259,241$

$\tilde{\beta}_A = 1.53$

Then estimates of α_N^* and β_N^*, i.e., $\tilde{\alpha}_N^*$ and $\tilde{\beta}_N^*$ are given, by model, as follows (see Table 4-2):

Model 1: $\tilde{\beta}_N^* = 3.06$

$$\tilde{\alpha}_N^* = \frac{1,000,000}{(42 \times 10^{-1})^{-2}}$$

$$= \frac{10^6}{(1764)\cdot 10^{-34}}$$

$$\tilde{\alpha}_N^* = \frac{1}{1764\cdot 10^{-40}}$$

Model 2 & 3: $\tilde{\beta}_N^* = \left(\frac{4.07}{1.53}\right) 3.06$

$$\tilde{\beta}_N^* = 8.14$$

$$\tilde{\alpha}_N^* = \frac{1}{1764\cdot 10^{-40}}$$

Model 4: $\tilde{\beta}_N^* = \left(\frac{3.07}{.53}\right)(2.06) + 1$

$$\tilde{\beta}_N^* = 12.92$$

$$\tilde{\alpha}_N^* = \frac{(1,000,000 \times 12.92)}{3.06} \left[\frac{(2,259,241)(4.07)}{(53,848.10^{17})(1.53)}\right]^{\left(\frac{2.06}{.53}\right)}$$

$$= \frac{4,222,222}{(42 \times 10^{-17})(2.66)^4}$$

$$\tilde{\alpha}_N^* = \frac{4,222,222}{(111.7 \times 10.^{-17})^4}$$

Model 5: $\tilde{\beta}_N^* = 3.06 + (4.07 - 1.53)$ $\tilde{\beta}_N^* = 5.60$

$$\tilde{\alpha}_N^* = \left[\frac{(53,848 \times 10^{17})(1.53)}{(2,259,241)(4.07)}\right] \frac{(1,000,000)(5.60)}{(3.06)}$$

$$\tilde{\alpha}_N^* = 16,154 \times 10^{17}$$

APPENDIX IX BIBLIOGRAPHY

1. Allen, W R , Interference from Tests with Continuously Increasing Stress, Operations Research, Vol 7, 1959.

2. Beaver, R L and Best, W E , Automation of Relay Acceptance Testing, 9th NARM Symposium on Electromagnetic Relays, April, 1961.

3. Bekkedahl, J L and Maiocco, F R , Statistical Analysis of Electronic Parts Reliability Test Data, North American Aviation Company, June, 1964.

4. Bell, J E , Weibull Distribution in Reliability Analysis of Certain Electronic Components, Semiconductor Products, March, 1963.

5. Berrettoni, J N , Practical Applications of the Weibull Distribution, Industrial Quality Control, August, 1964.

6. Bessler, S , Chernoff, H. and Marshall, A W , An Optimal Sequential Accelerated Life Test, Technometrics, Vol. 4, 1962.

7. Bodamer, A., Effect of Multiload Switching on Microminiature Relay Contacts., Electronic Design News, February, 1964.

8. Bohndick, K. H. and Voelz, K., Influence of Pulley Diameter and Spindle Load on Service Life of V-Belts, Kautschuk and Gummi, Vol. 10, 1957.

9. Brownlee, K. A., Industrial Experimentation, Chemical Publishing Co., Inc., 1948.

10. Carr, L D , Relay Contact Failures, 8th NARM Symposium on Electromagnetic Relays, May 1960.

11. Cary, H. and Thomas, R. E., Accelerated Testing as a Problem of Modeling, 6th National Symposium on Reliability and Quality Control, January, 1960.

12. Chernoff, H , Optimal Accelerated Life Designs for Estimation, Technometrics, Vol. 4, 1962.

13. Chernowitz, G., Electromechanical Component Reliability, RADC TDR-63-295, May, 1963.

14. Davies, O. W , The Design and Analysis of Industrial Experiments, Hafner Publishing Company, 1954.

15. Didinger, G H , Tantalum Capacitor Accelerated Life Testing, Evaluation Engineering, Vol. 3, September/October 1964.

16. Diel, D. and Reynolds, L G., Determinate Relay Reliability, 10th NARM Symposium on Electromagnetic Relays, April, 1962.

17. Dodson, G. and Howard, B., High Stress Aging to Failure of Semiconductor Devices, Seventh National Symposium on Reliability and Quality Control, January, 1961.

18. Epstein, B., Statistical Techniques in Life Testing, AD 211 457, October, 1956.

19. Epstein, B. and Sobel, M., Life Testing, Journal of the American Statistical Association, Vol. 48, 1953.

20. Farbo, J. L., Acceptance Testing for Reliability Analysis, 11th NARM Symposium on Electromagnetic Relays, April, 1963.

21. Freira, E., and Yule, F., Correlation of Test Procedures Under Various Environments, 8th NARM Symposium on Electromagnetic Relays, May, 1960.

22. Fulton, D. W., The Reliability Analysis of Nonelectronic Components, RADC Technical Memorandum 63-2, March 1963, AD 405 871.

23. Goode, H. P. and Kao, J. H. K., Sampling Procedures and Tables for Life and Reliability Testing Based on the Weibull Distribution, Office of the Assistant Secretary of Defense, Washington, D.C., TR 3, September, 1961.

24. Groocock, J. M., Accelerated Testing and Over-stress Testing of Transistors, Electronics Reliability & Microminiaturization, Vol. 2, December, 1963.

25. Gunther, P., Life Test Sampling Plans: I, Report No. R55GL37, General Electric Co., 1955.

26. Gunther, P., Life Testing Sampling Plans: II, Report No. R55GL73, General Electric Co., 1955.

27. Gunther, P., Techniques for Statistical Analysis of Life Test Data, Report No. 56GL278, General Electric Company, 1956.

28. Hecht, B., Prediction of Failure Rate with Accelerated Life Tests, 4th National Symposium Reliability and Quality Control, 1958.

29. Hodman, G., Twelve Causes of Short V-Belt Life, Power, Vol. 93, May 1949.

30. Hoeck, D. W., Relay Parameters by the Push Button Method, 8th NARM Symposium on Electromagnetic Relays, May, 1960.

31. Jordan, J. S., Relayability Applied to Reliability, 11th NARM Symposium on Electromagnetic Relays, April 1963.

32. King, J. R., The Underlying Mechanics of Weibull Distribution Behavior, North American Aviation Company, April, 1964.

33. Leird, F. E., and Froehlich, R. C., Precision Snap-Action Switches, Machine Design, March 30, 1961.

34. Lesser, W. H., Statistically Designed Experiment of Integral Capsular Relays, AD 412351, June, 1963.

35. Lewis, S. and Cooper, J. P., Advances in Combined Environmental Testing, Environmental Quarterly, March, 1962.

36. Loeseke, C. W., Circuits for Testing Reliability of Relays, 11th NARM Symposium on Electromagnetic Relays, April, 1963.

37. Marco, S. M., Starkey, W. L. and Hornung, K. G., A Quantitative Investigation of the Factors Which Influence the Fatigue Life of a V-Belt, Journal of Engineering for Industry, February, 1960.

38. McCall, C. H., Life Testing Models, 18th ASQC Convention, May, 1964.

39. Mease, G. E., Fabrication and Acceptance Testing of Power Relay Structure, Final Report, U.S. Army Electronics Laboratory, January, 1964.

40. Miracle, K. M., Reliability of Production Relays and its Relation to Operate Phenomena, 10th NARM Symposium on Electromagnetic Relays, April, 1962.

41. Neff, G. and Young, R. W., Predicting "O Ring" Leak Rates, Research and Development, Vol. 13, October 1962.

42. Norman, C. A., V-Belt Tests at OSU Provide Surprises, Industry and Power, Vol. 58, March, 1950.

43. Pettinato, A. D. and McLaughlin, R., Accelerated Reliability Testing, 7th National Symposium on Reliability and Quality Control, January, 1961.

44. Pommerening, U. A., A Practical Guide to Contact Applications, 9th NARM Symposium on Electromagnetic Relays, April, 1961.

45. Russell, R. W., Environmental Testing of Relays at Sandia Corporation, 10th NARM Symposium on Electromagnetic Relays, April 1962.

46. Schuchard, W. F., Relay Application for Satisfactory Performance, Machine Design, August, 1957.

47. Schwartz, B. R., and Siegel, A., Relay Degradation - A New Reliability Tool, 11th NARM Symposium on Electromagnetic Relays, April, 1963.

48. Scott, J. K., and Leach, C. V., Instrumentation for Mass Relay Life Testing, 11th NARM Symposium on Electromagnetic Relays, April, 1963.

49. Steulpnagel, T. R., Comments on Aircraft Switch Testing, Applications and Industry, November, 1954.

50. Toye, Charles, Extrapolating Component Life Tests, Electro-Technology, October, 1964.

51. von Alven, W. H. and Blakemore, G. J., Reliability of Semiconductor Devices, ARINC Research Publication No. 144-6-270.

52. Welch, T. R., A Means of Improving and Proving Relay Reliability, 9th NARM Symposium on Electromagnetic Relays, April, 1961.

53. Wickstrom, H. L., Causes and Effects of Fretting Erosion on Contact Surfaces, 11th NARM Symposium on Electromagnetic Relays, April, 1963.

54. Winter, B. B., Denison, C. A., Hietala, H. J. and Greene, F. W., Accelerated Life Testing of Guidance Components, AL TDR 64-235, 30 September 1964.

55. Yanikoski, F. F., Fallacies in Life Testing, 10th NARM Symposium on Electromagnetic Relays, April, 1962.

56. Accelerated Life Testing for Space Guidance Components, TP-380, Hughes Aircraft Company, August, 1963.

57. Gilmer Timing Belt Developed, India Rubber World, Vol. 123, 1951.

58. NARM Relay Testing Procedures, Issue A, National Association of Relay Manufacturers.

59. O-Ring Manufacturers Test Markings and Imperfections, Hydraulics & Pneumatics, Vol. 15, June, 1962.

60. Test Methods for Electromagnetic Relays, NAS 728, October, 1962.

61. Twenty-Year Exposure Proves Neoprene Tough, Machine Design, 1963.

62. V-Belts and Belt Drives, Rubber Division Library, University of Akron, July, 1960.

UNCLASSIFIED

Security Classification

DOCUMENT CONTROL DATA - R&D

(Security classification of title, body of abstract and indexing annotation must be entered when the overall report is classified)

1. ORIGINATING ACTIVITY (Corporate author) Hughes Aircraft Company Fullerton, California	2a. REPORT SECURITY CLASSIFICATION UNCLAS
	2b. GROUP
3. REPORT TITLE Accelerated Reliability Test Methods for Mechanical and Electromechanical Parts	
4. DESCRIPTIVE NOTES (Type of report and inclusive dates) Final Report Dec 63 - Dec 64	
5. AUTHOR(S) (Last name, first name, initial) Yurkovsky, William; Schafer, R. E.	
6. REPORT DATE July 1965	7a. TOTAL NO. OF PAGES 228 / 7b. NO. OF REFS 62
8a. CONTRACT OR GRANT NO. AF30(602)-3268	9a. ORIGINATOR'S REPORT NUMBER(S) FR 65-10-16
b. PROJECT NO. 5519	
c.	9b. OTHER REPORT NO(S) (Any other numbers that may be assigned this report)
d.	RADC-TR-65-46
10. AVAILABILITY/LIMITATION NOTICES Releasable to DDC and CFSTI.	
11. SUPPLEMENTARY NOTES	12. SPONSORING MILITARY ACTIVITY RADC

13. ABSTRACT

This study is addressed to the development of accelerated reliability test methods for long lived mechanical and electromechanical parts. The parts studied were a subminiature snap-action switch, a crystal can relay, a mechanical seal, and a rubber timing belt. The failure times of all parts fit Weibull distributions. Failure analysis data is presented. Several mathematical models are presented as tentative representations of the failure laws operating under conditions of combined stresses. The merits of each are investigated in relation to the data generated during this study.

DD FORM 1 JAN 64 1473

UNCLASSIFIED

Security Classification

UNCLASSIFIED

Security Classification

14. KEY WORDS	LINK A ROLE	LINK A WT	LINK B ROLE	LINK B WT	LINK C ROLE	LINK C WT
Reliability Demonstration						
Statistical Analysis						
Test Methods						

INSTRUCTIONS

1. ORIGINATING ACTIVITY: Enter the name and address of the contractor, subcontractor, grantee, Department of Defense activity or other organization *(corporate author)* issuing the report.

2a. REPORT SECURITY CLASSIFICATION: Enter the overall security classification of the report. Indicate whether "Restricted Data" is included. Marking is to be in accordance with appropriate security regulations.

2b. GROUP: Automatic downgrading is specified in DoD Directive 5200.10 and Armed Forces Industrial Manual. Enter the group number. Also, when applicable, show that optional markings have been used for Group 3 and Group 4 as authorized.

3. REPORT TITLE: Enter the complete report title in all capital letters. Titles in all cases should be unclassified. If a meaningful title cannot be selected without classification, show title classification in all capitals in parenthesis immediately following the title.

4. DESCRIPTIVE NOTES: If appropriate, enter the type of report, e.g., interim, progress, summary, annual, or final. Give the inclusive dates when a specific reporting period is covered.

5. AUTHOR(S): Enter the name(s) of author(s) as shown on or in the report. Enter last name, first name, middle initial. If military, show rank and branch of service. The name of the principal author is an absolute minimum requirement.

6. REPORT DATE: Enter the date of the report as day, month, year, or month, year. If more than one date appears on the report, use date of publication.

7a. TOTAL NUMBER OF PAGES: The total page count should follow normal pagination procedures, i.e., enter the number of pages containing information.

7b. NUMBER OF REFERENCES: Enter the total number of references cited in the report.

8a. CONTRACT OR GRANT NUMBER: If appropriate, enter the applicable number of the contract or grant under which the report was written.

8b, 8c, & 8d. PROJECT NUMBER: Enter the appropriate military department identification, such as project number, subproject number, system numbers, task number, etc.

9a. ORIGINATOR'S REPORT NUMBER(S): Enter the official report number by which the document will be identified and controlled by the originating activity. This number must be unique to this report.

9b. OTHER REPORT NUMBER(S): If the report has been assigned any other report numbers *(either by the originator or by the sponsor)*, also enter this number(s).

10. AVAILABILITY LIMITATION NOTICES: Enter any limitations on further dissemination of the report, other than those imposed by security classification, using standard statements such as:

(1) "Qualified requesters may obtain copies of this report from DDC."

(2) "Foreign announcement and dissemination of this report by DDC is not authorized."

(3) "U. S. Government agencies may obtain copies of this report directly from DDC. Other qualified DDC users shall request through ________________."

(4) "U. S. military agencies may obtain copies of this report directly from DDC. Other qualified users shall request through ________________."

(5) "All distribution of this report is controlled. Qualified DDC users shall request through ________________."

If the report has been furnished to the Office of Technical Services, Department of Commerce, for sale to the public, indicate this fact and enter the price, if known.

11. SUPPLEMENTARY NOTES: Use for additional explanatory notes.

12. SPONSORING MILITARY ACTIVITY: Enter the name of the departmental project office or laboratory sponsoring *(paying for)* the research and development. Include address.

13. ABSTRACT: Enter an abstract giving a brief and factual summary of the document indicative of the report, even though it may also appear elsewhere in the body of the technical report. If additional space is required, a continuation sheet shall be attached.

It is highly desirable that the abstract of classified reports be unclassified. Each paragraph of the abstract shall end with an indication of the military security classification of the information in the paragraph, represented as *(TS), (S), (C), or (U)*.

There is no limitation on the length of the abstract. However, the suggested length is from 150 to 225 words.

14. KEY WORDS: Key words are technically meaningful terms or short phrases that characterize a report and may be used as index entries for cataloging the report. Key words must be selected so that no security classification is required. Identifiers, such as equipment model designation, trade name, military project code name, geographic location, may be used as key words but will be followed by an indication of technical context. The assignment of links, rules, and weights is optional.

UNCLASSIFIED

Security Classification